12-1-2009

Microsphere based protease assays and high throughput screening of bacterial toxin proteases

Matthew Saunders

Matthew J. Saunders
Candidate

Biomedical Science Graduate Program
Department

This dissertation is approved, and it is acceptable in quality and form for publication:

Approved by the Dissertation Committee:

Bruce Edwards Ph.D., Chairperson

Steve Graves, Ph.D.

Paul McGuire, Ph.D.

Larry Sklar, Ph.D.

Michael Wilson, Ph.D.

MICROSPHERE BASED PROTEASE ASSAYS AND HIGH THROUGHPUT SCREENING OF BACTERIAL TOXIN PROTEASES

BY

MATTHEW J. SAUNDERS

B.S., Biochemistry University of Oregon, 2002

DISSERTATION

Submitted in Partial Fulfillment of the
Requirements for the Degree of

Doctor of Philosophy

Biomedical Science

The University of New Mexico
Albuquerque, New Mexico

December 2009

ACKNOWLEDGMENTS

I would like to acknowledge and thank my research advisors Dr. Steve Graves and Dr. Bruce Edwards for their support and the effort they have put into mentorship during this project. Their continued encouragement and guidance have made this work possible and directly led to the development of my professional career. I thank them for their continued encouragement, guidance and assistance during this time.

I would like to acknowledge and express my gratitude to the National Flow Cytometry Resource at Los Alamos National Laboratory, particularly director Jim Freyer and former director John Nolan for their financial support and guidance of this project. Being a part of this organization has been a great privilege and I am thankful for the support.

I would also like to thank Dr. Larry Sklar for mentorship, laboratory space and assistance in my graduate student career. This project would not have been possible without his support and contributions.

I also thank my committee members, Dr. Paul McGuire and Dr. Michael Wilson. They have contributed a great deal toward the development of this work through their recommendations and guidance on this project. I am very grateful.

I thank my friends and family for their continued support and encouragement during this time.

MICROSPHERE BASED PROTEASE ASSAYS AND HIGH THROUGHPUT SCREENING OF BACTERIAL TOXIN PROTEASES

BY

Matthew J. Saunders

ABSTRACT OF DISSERTATION

Submitted in Partial Fulfillment of the
Requirements for the Degree of

Doctor of Philosophy

Biomedical Science

The University of New Mexico
Albuquerque, New Mexico

December, 2009

MICROSPHERE BASED PROTEASE ASSAYS AND HIGH THROUGHPUT SCREENING OF BACTERIAL TOXIN PROTEASES

by

Matthew J. Saunders

B.S. Biochemistry University of Oregon 2002

Ph.D. Biomedical Science University of New Mexico 2009

ABSTRACT

Proteases, proteins which cleave peptide bonds in other proteins, are a large and varied group of proteins which regulate a variety of physiological processes. Methodologies to study proteases are often protease specific and often differ greatly from the roles proteases play *in vivo*. *In vitro* protease assays often use peptide based substrates, which do not take into account highly specific interactions distal from the proteolytic site of peptide cleavage on protease substrates. In the work described here we have developed a microsphere based protease assay, capable of using full length protease substrates, and have successfully measured proteolytic activity via loss of fluorescence as measured by flow cytometry. This assay is capable of being used in high throughput screening for small molecule inhibitors for proteases of medical relevance. Screening of chemical libraries against the *Bacillus anthracis* Lethal factor metalloprotease and the *Clostridium botulinum* Neurotoxin type A Light Chain metalloprotease has led to the discovery of small molecule inhibitors for both of these pathogenic proteases. The compound ebselen has been shown to inhibit Botulinum Neurotoxin type A Light Chain with an IC_{50} value

in the low µM range. Additional small molecule inhibitors for Botulinum neurotoxin type A Light Chain as well as for anthrax lethal factor have also been discovered by this methodology. This work shows the potential for microsphere based protease assays in discovery of small molecule protease inhibitors and can be adapted to any protease/substrate system of interest in a multiplex setup. Additional work with these proteases has also led to the discovery of novel solution based kinetics models and shows promise to validate microsphere based protease kinetics using the same system.

Table of Contents

List of Figures

List of Tables

Chapter 1:
Introduction

1.1 Proteases as Drug Targets

Proteases are a large and diverse group of enzymes that break down other proteins through the hydrolysis of peptide bonds [1]. Current genetic analysis of the human genome predicts the existence of 500 to 600 proteases [1]. Of the approximately 400 known proteases, 14% are currently under investigation as drug targets [2]. The roles of proteases in the human body are varied, and include functions such as degradation of proteins for amino acid recycling, processing of zymogen protein precursors to active enzymes, activation of the immune system and clotting of blood through a series of protease cascades [1]. Until recently, proteases were primarily thought of as protein degrading enzymes; however, new research and understanding of the downstream results of proteolytic activities has shown that proteolytic mechanisms are highly regulated components of cellular signaling pathways. The improper regulation of specific human proteases involved in cellular signaling can lead to human diseases including inflammatory disease, thrombosis, osteoporosis, cardiovascular and neurological disorders, and increased growth and metastasis in specific cancers [1].

The study of proteases is varied and usually protease specific [3], [4]. Protease activity *in vitro* often differs greatly from their specificity and physiological effects *in vivo* [1] [3]. Numerous methods have been developed to determine optimal substrates for protease cleavage *in vitro* [3]. Such systems have been used to identify inhibitors for specific proteases of interest to human health

[1]. Proteases of clinical significance include human proteases which are improperly regulated [1], pathogenic proteases, which mediate the effects of toxins [5], and viral proteases which process viral precursor proteins controlling viral life cycles [6].

It would be advantageous to develop a high-throughput protease assay to identify small molecule inhibitors of specific proteases of interest in disease. Such an assay would also benefit from the use of full length protease substrates, because many protease/substrate interaction sites are distal from the protease cleavage site [7-10]. There is significant conservation of protease active sites amongst families of proteases, and similarities in structure and function between related proteases [11]. Therefore a platform that could simultaneously evaluate multiple proteases and protease substrates in parallel would speed the identification of selective protease inhibitors. We hypothesize that a high throughput flow cytometry assay that uses full length protease substrates and multiplex microsphere sets for parallel analysis of multiple protease/substrate combinations, could identify potentially new classes of protease inhibitors which affect protease/substrate distal interactions, as well as identify inhibitors of protease active sites.

1.2 Bacterial toxin proteases

There are several known bacterial pathogens which use proteases in their secreted two-part toxins to mediate effects upon the host during progression of infection [5]. These bacterial toxins use a cellular receptor binding protein to

deliver zinc metalloproteases inside of the cell, where they cleave their respective target proteins to exert toxic effects on the host [5]. The pathogenic bacteria *Bacillus anthracis, Clostridium tetani and Clostridium botulinum* all secrete two-part toxins consisting of a cellular receptor binding protein and zinc metalloproteases, which act intracellularly to cleave target proteins. Due to the extreme toxicity of these pathogens and their potential use as bioweapons it is highly desirable to discover specific inhibitors of the protease components of their toxins.

1.3 Bacillus anthracis infection and toxin secretion

Bacillus anthracis, the causative agent of anthrax, secretes two toxins consisting of three proteins, the cellular binding protein Protective Antigen (PA), Edema Factor (EF) and the metalloprotease Lethal Factor (LF) [12]. Both EF and LF require PA for entry into their target cells and are commonly referred to as edema toxin (ET), consisting of PA and EF, and lethal toxin (LT), consisting of PA and LF [12]. (**Fig 1.1**)

Inhalation anthrax occurs when anthrax spores are inhaled and phagocytosed into alveolar macrophages, and are carried to the lymph node where they germinate [13]. Once inside the macrophage, anthrax spores must survive and germinate, and require the production of EF and LF to do so, eventually leading to death and lysis of the cell [14]. Toxin components are produced and secreted at the spore stage [15] and by newly germinated spores in the macrophage [13, 14]. Early PA and LF expression are thought to promote

survival of emergent *Bacillus* anthracis bacteria after macrophage lysis and release into the bloodstream [13, 15, 16]; however, it has been shown that EF function is also required for survival of germinated bacteria [14].

Upon bacterial release into the bloodstream anthrax toxin has several roles in aiding bacterial survival [12]. During the initial stages of infection, after release from macrophages, sublethal doses of LT lead to cleavage of MAP kinase kinase (MKK) proteins which help bacteria survive by preventing cytokine responses [17-19], dendritic cell responses [20], and B and T cell immunity [20]. Production of ET incapacitates phagocytes and cytokine pathways as well [21, 22]. It is thought that production of these toxins shuts down the immune system and prevents immunity from fighting off anthrax infection [12]. Experimental evidence now shows that lethal toxin (LT) is required for the dissemination of the disease and subsequent lethality, while edema toxin (ET) contributes to the process, but is not required [23]. Further analysis of the molecular mechanisms of anthrax toxin, with particular focus on the lethal factor metalloprotease as a drug target are described below.

The protective antigen protein (PA), named so for its effectiveness in inducing protective immunity against anthrax, is the cellular binding protein responsible for delivery of LF and EF into the cytosol of target cells [24]. PA binds to either of the cellular based receptors tumor endothelial marker 8 (TEM8) [25] and capillary morphogenesis protein 2 (CMG2) [26]. PA is proteolytically activated by members of the furin-like protease family after binding to cellular receptors [24]. Removal of a N-terminal 20 kDa piece of PA leaves the remaining 63 kDa protein

bound to the cellular receptor. Receptor bound PA63 then oligiomarizes to form a ring shaped heptameric complex, capable of binding three molecules of LF or EF competitively [24]. These PA/LF/EF complexes are endocytosed, and under low pH conditions the PA63 heptamer forms a pore through which LF and EF enter the cytosol [24], where they are enzymatically active. Although not a receptor for PA itself, recent studies have shown that low density lipoprotein receptor-related protein 6 (LRP6) is also required for cellular uptake of oligiomerized PA bound to LF and/or EF [27].

The Edema Factor protein is a calcium and calmodulin dependent adenylate cyclase and causes increased levels of cyclic AMP (cAMP), which inhibits neutrophil chemotaxis, phagocytosis, superoxide production and microbicidal activity [28]. Animal models have shown that edema toxin (PA and EF) is non-lethal, although it does cause edema upon subcutaneous administration [28]. In monocytes and macrophages EF affects cytokine production, particularly decreased TNFα release, while increasing interleukin 6 production [28]. Edema toxin inhibits T-cell proliferation and cytokine production. Although edema toxin is not necessarily associated with *Bacillus anthracis* lethality, it does weaken the host immune system significantly to promote anthrax pathogenesis.

1.4 The Bacillus anthracis lethal factor

The *Bacillus anthracis* Lethal Factor is a 90 kDa protein consisting of a N-terminal PA binding domain, a large central domain and a C-terminal

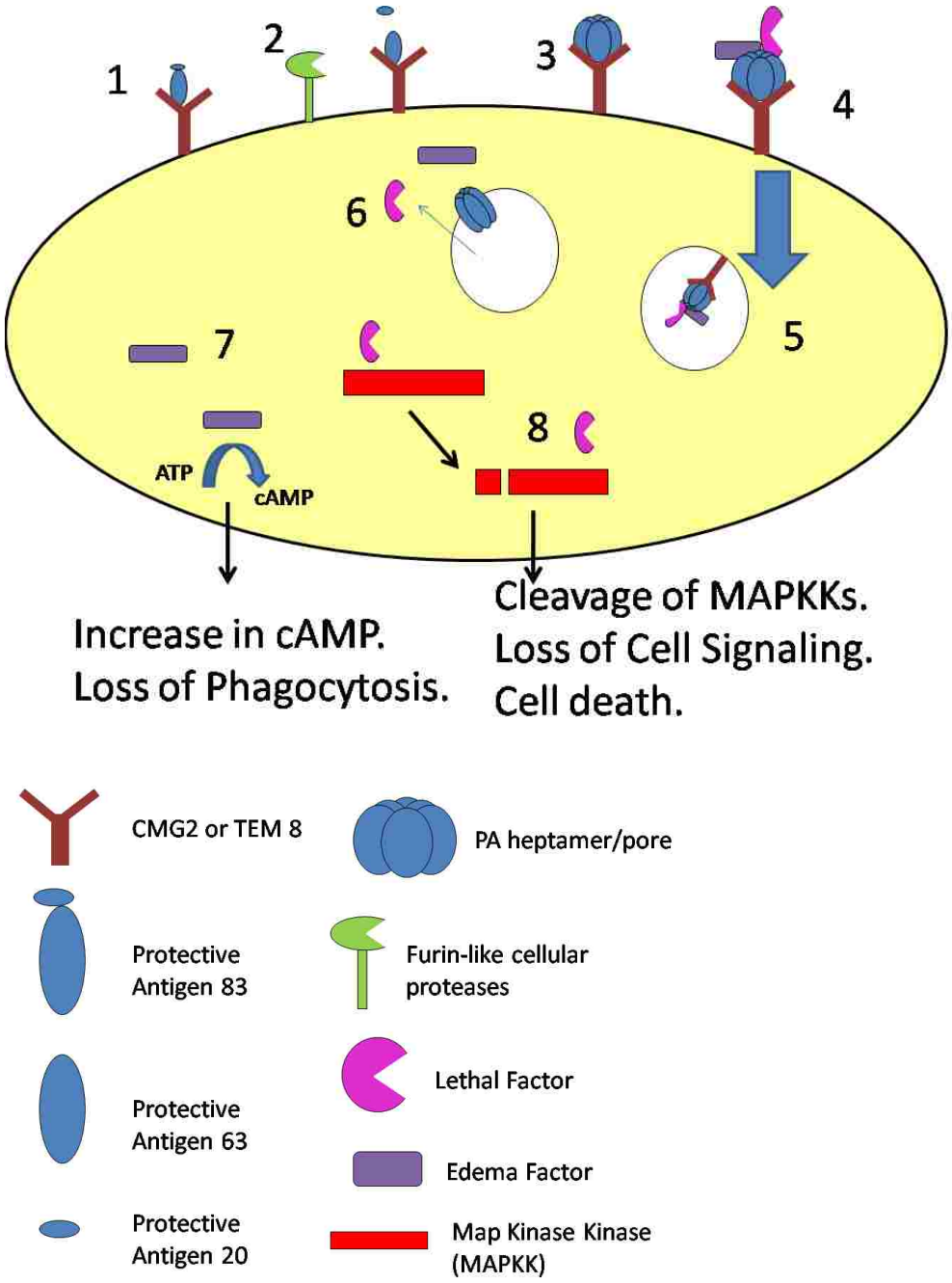

Figure 1.1 Lethal Toxin Protective antigen binds to cellular receptors CMG2 or TEM8 on macrophages or dendritic cells (1). PA 83 is cleaved by furin-like cellular proteases to give PA63 (2). PA63 forms a heptamer (3) and binds lethal factor (LF) or edema factor (EF) (4). The complex is endocytosed (5) and the PA 63 heptamer forms a pore through which LF and EF are translocated into the cytosol (6). Edema factor causes increased cAMP (7) leading to loss of phagocytosis. LF cleaves Map Kinase Kinase (MKK) proteins (8) leading to loss of cellular signaling and cell death.

metalloprotease domain with a HExxH Zn^{2+} binding domain [29]. LF specifically cleaves the family of Map Kinase Kinases (MKK) near their N-terminus [7, 18, 30], which prevents phosphorylation and activation of mitogen activated protein kinases (MAPKs). LF cleaves all of the family of MKKs, except for MKK5, and shuts down the ERK, JNK and p38 signaling pathways leading to immune system response and activation [28]. Analysis of LF cleavage sites of MKKs reveals conserved features including a cluster of basic residues three to five residues upstream of two or more aliphatic residues [28]. The consensus cleavage site of the MKK family by Lethal Factor has been identified to contain a motif of BBBB-H-^H----- where B is a basic amino acid, H a hydrophobic acid, the dash is any amino acid, and the ^ indicating the cleavage site [31]. These residue characteristics of the LF cleavage site are conserved among all of the MKKs and are important for efficient proteolysis of the MKKs [30, 32, 33]. The MKKs also contain an identified distal interaction site for LF near their C terminus [7, 8]. This C-terminal lethal factor interacting region (LFIR) is conserved amongst all of the MKKs [8], which may account for the high specificity of LF for the MKKs. *In vitro* experiments with recombinant MKK1 have shown that mutations in the C-terminal LFIR abolish the ability of LF to cleave MKK1 [8]. Biochemical analysis has also shown that full length MKKs are cleaved much more efficiently than peptides which span the cleavage site alone [8, 33].

LT is known to act upon numerous cell types of the immune system, impairing the function of neutrophils and monocytes [34, 35], T cells [36, 37], and B cells [38]. Although LT affects all of these cell types through mechanisms

involving MKK cleavage, there are two main cell types involved in the immune response which it directly kills, dendritic cells and macrophages [39]. Macrophages uptake lethal factor by PA binding and translocation to the cytosol (**Fig. 1.1**), where MKKs are cleaved. Although the MKKs are the only verified substrate of LF, no direct connection between MKK cleavage and cell death has been established [40]. Recent work by Boyden and Dietrich has shown that the macrophage polymorphic gene Nalp1b is the primary mediator of mouse macrophage lethal toxin susceptibility, and LT macrophage death requires caspase-1 [41]. Macrophage types which do not contain Nalp1b are resistant to LT induced death unless transfected with Nalp1b, whereupon they become susceptible to LT induced macrophage death [41]. This macrophagic cell death also requires caspase-1, which is activated in Nalp1b containing macrophages leading to cell death, but not in macrophages containing other variants of the Nalp1 paralogs [41]. It is unknown if Lethal Factor directly acts upon Nalp1b, causing caspase-1 induced cell death, or if Nalp1b activates caspase-1 due to intracellular stress caused by LF cleavage of the MKKs [40]. Regardless of the direct mechanism, inhibition of LF will prevent macrophage cell death.

Dendritic cells are also affected by lethal toxin, although the role of LF on dendritic cells is unclear [39]. Immature dendritic cells circulate in the peripheral tissue and take up antigens, which they present to naïve T cells in the lymphoid organs after maturation [42]. Dendritic cells are also the most efficient antigen presenting cells in the immune system [39]. Studies by Reig et al., using bone marrow derived dendritic cells in several different genetic variants of mice, have

shown that lethal toxin can induce two separate death inducing pathways in dendritic cells [39]. One pathway is dependent on Nalp1b and caspase-1, leading to rapid cell death independent of cell maturity; the other pathway is independent of caspase-1 and only effective in immature dendritic cells at times greater than four hours after LT exposure [39]. Another important finding in these studies is that the protective effect of mature dendritic cells in the caspase-1 independent pathway occurs downstream of MKK cleavage [39]. Much work still needs to be done to separate the pathways in dendritic cell and macrophage death in different genetic backgrounds.

In summary, current literature shows that Lethal Factor, and its specific delivery to these cell types by PA, is critical to survival and germination of anthrax spores at early stages of infection, and promotes immune system evasion and specific cell death at later stages of the disease. LF is thought to play a central role in anthrax toxicity, primarily due to these reasons [43]. Because of the high biothreat potential of inhalation anthrax there is much interest in finding novel LF protease inhibitors as a potential treatment for inhalation anthrax.

Anthrax is listed as a category A biothreat agent by the Center for Disease Control [44]. Anthrax has been weaponized and used in numerous cases dating back as far as World War 1 [44]. Numerous deaths worldwide have occurred due to weaponized anthrax use and accidental exposure [44]. The somewhat recent postal service anthrax terror of 2001 caused 11 cases of inhalational anthrax

which led to 5 fatalities and highlights the need for fast-acting preventative drugs for inhalational anthrax treatment [44].

1.5 Tetanus toxin

Clostridium tetani neurotoxin (TeNT) is another two part toxin with a cellular binding protein heavy chain of 100 kDa which delivers a 50 kDa light chain (TeNTLC) zinc metalloprotease inside of neurons. Tetanus toxin binds to and enters peripheral motor neurons and travels by retrograde transport to the central nervous system, crosses transynaptic gaps and enters inhibitory neurons [45]. The TeNTLC crosses into the cytosol of inhibitory neurons from endocytic bodies and acts intracellularly to prevent inhibitory interneuron vesicle release [45]. Cleavage of vesicle-associated membrane protein-2 (VAMP-2) on the surface of pre-synaptic vesicles by the tetanus neurotoxin light chain in inhibitory interneurons leads to a block of gamma-aminobutyric acid (GABA) and glycine release which elicits spastic paralysis [45].

Studies on TeNT light chain, and the closely related botulinum neurotoxin type B light chain, which also cleaves VAMP-2 at the same peptide bond in different neuron types [46], reveal extensive substrate/protease recognition domains distal from the protease cleavage site on VAMP-2. Deletion and mutational studies on VAMP-2 show that mutations in amino acid residues 41-51 result in a much reduced cleavage rate by TeNTLC compared to wild type VAMP-2 [46]. Mutations in this region had a greater effect on VAMP-2 cleavage than mutations in amino acids 70-80 adjacent to cleavage site itself located

between residues 76 and 77 [46]. VAMP-2 residues 82-87, C-terminal to the VAMP-2 cleavage site, were also shown to be important for VAMP-2 cleavage by TeNTLC [46]. Particularly interesting is the fact that the closely related botulinum neurotoxin type B light chain (BoNTBLC), which cleaves VAMP-2 at the same peptide site, has entirely different distal recognition sites than TeNTLC [46]. The distal interaction sites of both proteases are different than the original SNARE motifs described by Rossetto et al., hypothesized to be important in protease/substrate recognition [9].

These studies show distal recognition elements of tetanus toxin light chain are important for protease/substrate specificity and substrate recognition. Tetanus is a often a fatal disease with death occurring by heart or respiratory failure [47], however, due to large-scale vaccination and availability of vaccines, the disease has dramatically declined [48], and is not considered to be of particular interest in drug discovery. Instead, much focus is currently being placed on drug discovery for the closely related botulinum neurotoxins.

1.6 Botulinum Neurotoxins

The *Clostridium botulinum* neurotoxins, like tetanus toxin and anthrax lethal toxin, are two part toxins. These neurotoxins are of seven types, A-G, all of which target the molecular machinery of docking and vesicle fusion in neurotransmitter release [49,50], the loss of which can lead to flaccid paralysis and death [51]. They are expressed as 150 kDa polypeptides and processed by proteases into a 100 kDa heavy chain and a 50 kDa light chain, which are linked

by a disulfide bond [52]. The 100 kDa heavy chain targets gangliosides and neuron specific receptors on the presynaptic membrane of motoneuron nerve endings [49], and the 50 kDa light chain zinc metalloprotease acts intracellulary in neurons to cleave SNARE proteins, which form complexes required for pre-synaptic vesicle fusion. Cleavage of SNARE proteins in pre-synaptic motoneurons leads to a loss of acetylcholine release into neuromuscular junctions, and leads to flaccid paralysis due to lack of muscle contraction [53]. These toxins are some of the most deadly substances known to man [53].

The heavy chains of botulinum neurotoxins (BoNTs) have been shown to bind to polysialoganglioside lipids on the neural cell membrane, but require a protein receptor for internalization [49]. The heavy chain (HC) of botulinum neurotoxin types A and C bind specifically to the family of synaptic vesicle receptor proteins SV2 isoforms A, B and C while BoNT type E heavy chain only binds to SV2 A and B [54, 55]. BoNT serotypes B and G have been shown to bind strongly to synaptotagmin I and synaptotagmin II [49]. The dual binding requirement for these receptors and specific lipids by the BoNTs is thought to account for their ability to enter pre-synaptic nerve terminals with high specificity [54].

Upon binding to their specific receptors and polygangliosides, BoNTs are endocytosed in vesicles forming endosomal compartments. The light chain must then exit these endosomal compartments to the cytosol in order to act upon their specific SNARE proteins. Once inside of endosomal compartments the low pH causes the light chain protease to undergo a conformational change where

previously buried hydrophobic residues and domains are on the outside of the molecule [56]. The reducing environment of the endosome also causes the disulfide bond between the chains to separate. The light chain then translocates through the heavy chain, which forms a pore through the endosomal compartment membrane once the disulfide linkage to the light chain is reduced. Once in the cytosol, the light chain re-folds to its active state where it can act upon its substrate SNARE proteins [56] (**Fig. 1.2**).

The targets of botulinum neurotoxins, the SNARE (soluble NSF attachment protein receptor) proteins are bound to pre-synaptic vesicles and membranes. SNAREs are attached by either a transmembrane region, as seen with the SNARE proteins synaptobrevin (VAMP) to the pre-synaptic vesicle and syntaxin to the pre-synaptic membrane, or via post-translational palmitoylation on cysteine residues and attachment to pre-synaptic membranes, as seen with SNAP-25 [57, 58]. Depolarization of the neuron by action potentials and calcium influx causes the calcium binding protein synaptotagmin to initiate SNARE protein complex formation of VAMP, SNAP-25 and syntaxin into a colied coil structure, leading to membrane fusion and release of acetylcholine from acetylcholine containing vesicles into the synaptic cleft of the neuromuscular junction [52, 59].

The SNARE proteins are mostly unstructured in the absence of their binding partners but form a highly stable structured coiled-coil helical structure once they come into contact after neural depolarization, mostly due to hydrophobic packing [60-64]. Formation of the low energy coiled-coil SNARE

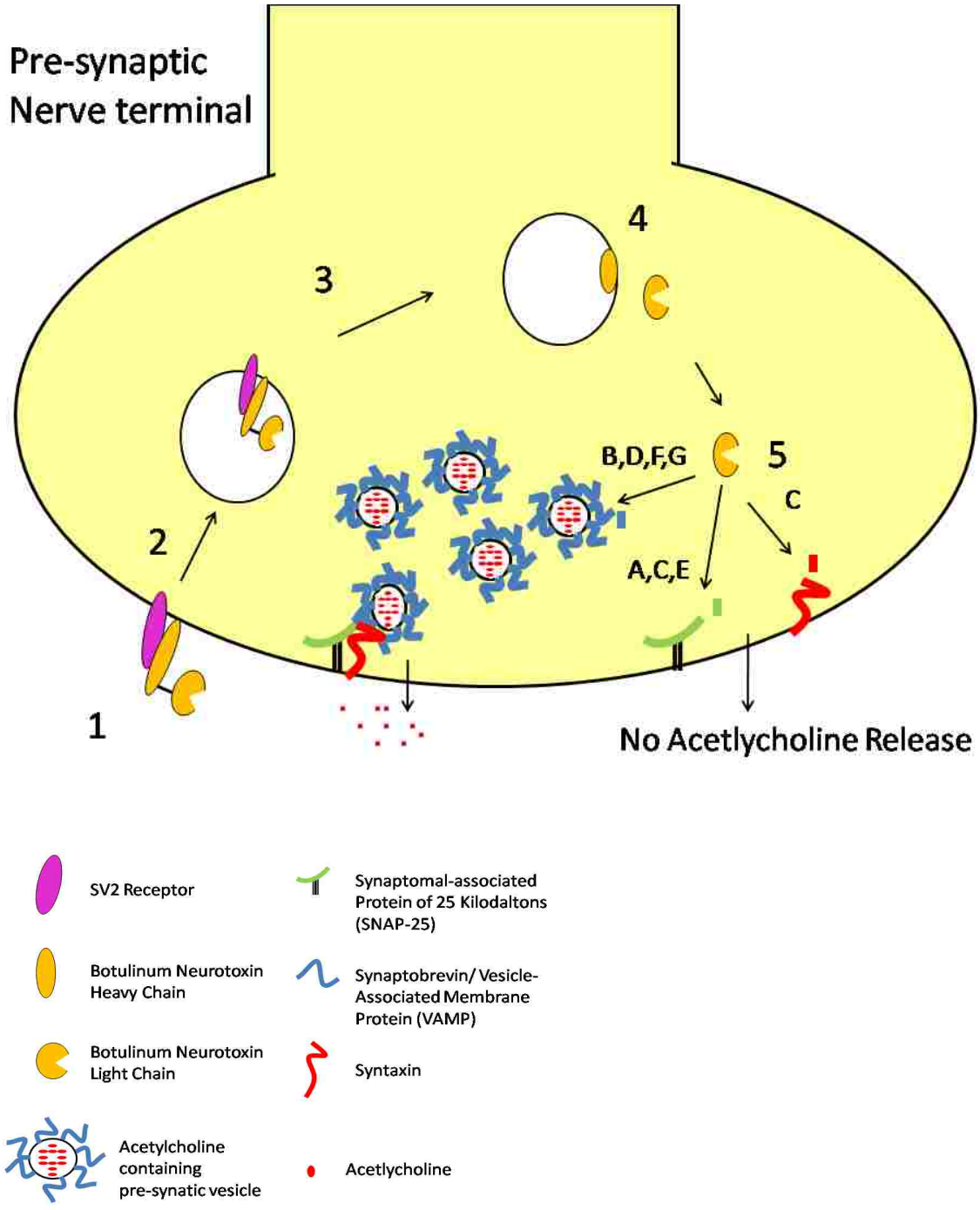

Figure1.2 Botulinum neurotoxin (BoNT) binds to the SV2 receptor on pre-synaptic nerve terminal via the heavy chain (1) and is internalized (2). The change in endosomal pH (3) causes the heavy chain to form a pore and translocate the light chain protease into the cytosol of the neuron (4). The Light chain protease cleaves specific SNARE proteins causing loss of acetylcholine release. Light chains of serotypes A, C and E cleave SNAP-25 while serotypes B, D, F and G cleave VAMP/synaptobrevin. Serotype C alone cleaves syntaxin as well as SNAP-25.

complex by the three SNARE proteins is thought to counter the energetic penalty of bringing phospholipids head groups from separate membranes together and makes membrane fusion of these separate membranes energetically favorable [52, 65]. SNARE complex formation is crucial for neural exocytosis of pre-synaptic vesicles and release of acetylcholine into neuromuscular junctions [49, 52]. The cleavage of any of the SNARE proteins by botulinum neurotoxins leads to a loss of acetylcholine release in neuromuscular junctions and the flaccid paralysis seen in botulism, as well as death by respiratory failure [49]. BoNT light chains are some of the most selective proteases known [52]. The enzymatic mechanism of the BoNTLC Zn^{2+} metalloproteases is thought to be similar to other Zn^{2+} metalloproteases [66, 67]; however, recognition of SNARE proteins by BoNTLC proteases is very specific and structurally based [67]. The BoNT light chains do not recognize a specific consensus cleavage site in the SNARE proteins, or even have defined requirements for side chains near the sissile bond [68].

1.7 Botulinum Neurotoxin type A Light Chain Recognition of SNAP-25

Early work with the SNARE proteins identified several commonly shared 10 amino acid motifs distal from the BoNT LC cleavage sites on the SNARE proteins [9]. These sequences, termed the SNARE motif, consist of the amino acid consensus sequence of XHBBXHBXHP, where X is any residue, H is a hydrophobic residue, B is a basic residue and P is a polar residue, and are proposed to form an α helical wheel conformation. Two of these SNARE motifs are found on synaptobrevin (VAMP), the SNARE substrate for BoNT B,D,F and

G. These SNARE domains span the amino acids 38-47 and 62-71 and are termed V1 and V2. Two SNARE motifs are on syntaxin, the SNARE protein substrate for BoNT type C light chain, at residues 29-38 and 164-173, termed the X1 and X2 SNARE domains. There are four SNARE motifs on SNAP-25, the SNARE substrate for BoNT types A, C and E light chains, consisting of amino acid residues 21-31, 35-45, 49-59 and 145-155, termed the S1-S4 SNARE domains, respectively [9] (**Fig. 1.3**). Peptide analogues of these SNARE domains, which are soluble, were shown to inhibit their respective BoNTs and restore acetylcholine release when injected into neurons in the buccal ganglion of *Aplysia californica* [9].

The similarities in the BoNT light chain (LC) active sites indicates that the specificities of the proteases are due to sites of protease substrate interactions distal from the cleavage site [52]. Serotypes which target the same SNARE protein also cleave at different peptide bonds [9,52], which also supports the concept that distal binding or interaction sites may differentially affect cleavage. None of the BoNT LCs efficiently cleave substrate peptides less than 20-30 amino acids long. All require long stretches of the substrate for efficient cleavage [9, 68, 69], although this can be optimized for BoNTALC using amino acid combinations corresponding to the S4 SNARE motif and the protease cleavage site in SNAP-25 [70]. Deletion and truncation studies on SNAP-25 with BoNT types A and E light chains have shown that the aforementioned S4 SNARE motif contributes the most to the cleavage rate by both of these light chain proteases, with the S1-S3 binding sites promoting a smaller, yet additive rate of cleavage [71].

Binding studies with an inactive BoNTALC, mutated in the Zn^{2+} binding domain, have shown that the minimal fragment capable of binding the inactive protease is SNAP-25 146-197 [72], which includes the S4 SNARE domain and the protease cleavage site [9]. This same region, from amino acids 146-202, is also the minimal domain of SNAP-25 required for maximal cleavage [52, 73], although it is still not cleaved as efficiently as full length SNAP-25 containing all 4 of the SNARE domains [71]. While the importance of these SNARE domains for cleavage by BoNTLCs has been demonstrated, substrates lacking SNARE domains have been shown to be cleaved in high performance liquid chromatography (HPLC) based assays [74]. Thus the role of SNARE domains in BoNTLC cleavage is still being investigated. The crystal structure of BoNTALC bound to a C terminal portion of SNAP-25, consisting of amino acids 141-204 has been determined [10, 75]. In the BoNTALC /SNAP-25 interaction SNAP-25 wraps around most of the BoNTALC molecule, with extensive contact regions between the substrate and protease [10, 52] (**Fig. 1.3**).

Upon binding to BoNTALC, SNAP-25 undergoes extensive conformational changes. These changes result in formation of an α helix by residues 147-167, N-terminal to the cleavage site, which includes most of the S4 SNARE domain, and formation of a distorted β strand by residues 201-204, C-terminal to the cleavage site [10, 52]. Residues in between are mostly extended [10]. The N terminal α helix and C terminal β strand are critical for efficient substrate binding and cleavage by BoNTALC, and have been termed the α and β exosites respectively. These interactions and conformational changes place the scissile bond in close

proximity to the protease active site for enzymatic cleavage [10, 52]. The α exosite, which the crystal structure shows to form important contacts for protease and substrate re-arrangement, consisits of SNAP-25 amino acids 152 to 166. This region overlaps with a portion of the S4 domain, consisting of amino acids 145-155. Although only four amino acids of the SNAP-25 S4 domain overlap with the complexed α exosite, it has been proposed that glutamine 152 on SNAP-25 forms hydrogen bonds with lysine 356 on BoNTALC, and valine 153 on SNAP-25 is involved in hydrophobic interactions with phenylalanine 357 on BoNTALC while in complex [10]. This finding demonstrates a potential mechanism of how BoNTALC binding to SNAP-25 through the SNARE domain could cause the structural re-arrangements of BoNTALC, leading to proteolysis. These observations also explain why many substrates lacking the S4 or α exosite are not efficiently cleaved by BoNTALC.

The β exosite, consisting of methionine 202 (Met 202) on SNAP-25 and several residues on BoNTALC is present in BoNTALC substrates which do not contain the S4/α exosite yet are still cleaved by BoNTALC. These β exosite-Met 202 containing substrates include the HPLC peptides used by Schmidt et al., and may account for the findings that the SNARE domains are not required for cleavage of this substrate by BoNTALC [68]. The β exosite residue SNAP-25 Met 202 has been optimized for optimal substrate cleavage in the SNAPtide fluorescenece resonance energy transfer (FRET) peptide, available from List Biological Labs (Campbell, CA.). This peptide does not contain the S4/α exosite region of SNAP-25, yet is still efficiently cleaved by BoNTALC. Although the

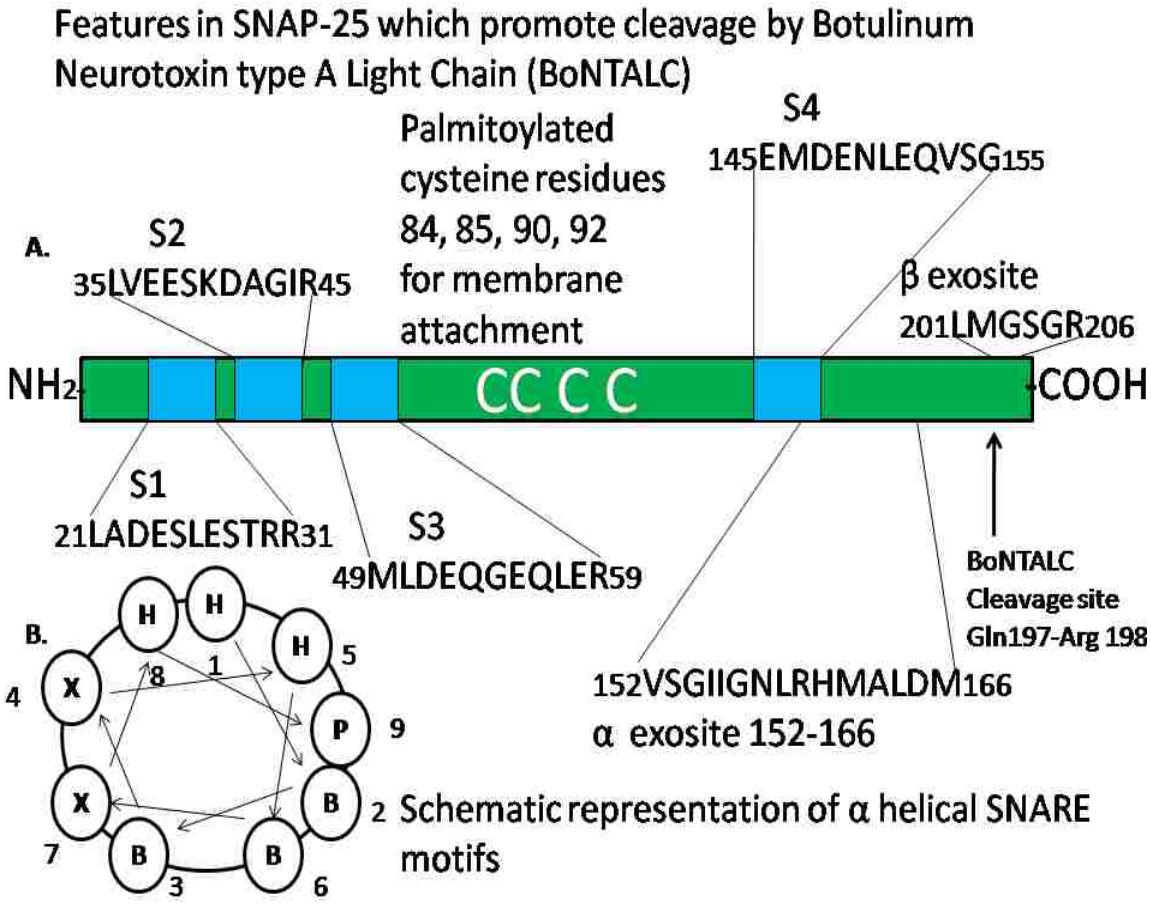

Figure 1.3 **A.** Schematic representation of regions of SNAP-25 for Boutlinm Neurotoxin type A light chain recognition and cleavage. Blue regions represent SNARE domains identified by Rosetto et al., The single letter amino acid sequences and numbering on SNAP-25 of SNARE domains and the α and β exosites identified by Breidenbach and Brunger are labeled along with the BoNTALC cleavage site. **B.** Helical representation of SNARE domains identified by Rosetto et al., and the numbering of amino acid order in the helix from N to C terminus. Letters in each position are defined by the nature of the amino acids with H being hydrophobic, B being basic, P being polar and X being any amino acid.

crystal structure shows the primary β exosite contacts between Met 202 on SNAP-25 and numerous residues on BoNTALC, it has also been shown that lysine 201 on SNAP-25 plays an important role in the β exosite as well [76], potentially forming a salt bridge with glutamic acid 257 on BoNTALC [77]. These α and β exosite regions on SNAP-25 show extensive BoNTALC/SNAP-25 contacts and either region seems to allow for specific recognition of *in vitro* BoNTALC substrates and leads to substrate cleavage.

Studies using SNAP-25 146-206, the optimal cleavage domain of SNAP-25 for BoNTALC, and SNAP-25 93-206 with mutational analysis have shown several of the domains on SNAP-25 mentioned to be important for cleavage by BoNTALC [76]. Deletion of the S4 SNARE motif, originally described by Rossetto et al.,[9], which also contains a portion of the α exosite described by Breidenbach and Brunger in the crystal structure [10], led to a five-fold reduction in cleavage [76]. This is also consistent with experiments done as part of this dissertation work, which shows an approximate five fold reduction on full length SNAP-25 cleavage by BoNTALC when the S4 SNARE domain is deleted. These studies have shown that deletion of residues 145-166, (both the S4 SNARE domain and the α exosite) renders SNAP-25 93-206 completely resistant to cleavage by BoNTALC [76].

These data suggest that the S4 SNARE domain plays a large role in SNAP-25 recognition by BoNTALC, while the α exosite (SNAP-25 residues 152-166) plays a critical role in substrate rearrangement leading to cleavage by BoNTALC [76]. Inhibitors that act at sites other than the BoTNALC active site would represent

a novel class of botulinum neurotoxin inhibitors. These regions of protease/substrate interaction therefore represent potentially important novel targets of small molecule inhibitors [78, 79].

1.8 BoNT type A in theraupeutics and cosmetics

Botulinum Neurotoxin type A has been in clinical use as a pharmaceutical agent for over 20 years, and is used to treat a variety of diseases [80]. BoNTA is considered first-line therapy in treatment of focal dystonias and hemifacial spasm [81]. It is also used for treatment of spasticity of various causes [81]. Botulinum neurotoxin type A has also been shown to treat achalasia (swallowing disorders) [82], idiopathic blepharospasm (spasms which force the eyelids shut) [81], lower urinary tract dysfunction [83], anal fissure [84], hyperhidrosis (excess sweating) [80, 85], and even habitual snoring [86] and headaches [87].

BoNTA is also widely used as a successful cosmetic agent for wrinkle reduction [80]. Botulinum Neurotoxin use in medicine has wide applications and is expected to have far broader applicability toward medical practices with molecular engineering of the toxin to extend to other applications involving delivery of enzymes or drugs to the neuromuscular junction [80].

Small numbers of patients who undergo treatments with botulinum neurotoxin type A experience adverse effects. Complications associated with BoNTA treatment include excessive weakness of treated muscles, weakness of neighboring muscles, suppression of neighboring salivatory or lacrimal gland function and immunological resistance [81]. A recent study of 266 patients treated

with BoNTA for spasticity revealed that several patients showed clinical symptoms of toxin spread with muscular weakness, four of whom displayed increased jitter in muscles distant from the site of injection. One patient had denervation with no sign of reinnervation in muscles distal from the site of injection [88]. A child with cerebral palsy showed severe respiratory complications and stridor with accompanying sickness after BoNTA treatments aimed at controlling spasticity [89]. Reports to the FDA on nearly 100,000 patients showed adverse effects in 0.6% of patients treated with BoNT, with 0.1% of cases reporting serious adverse effects [80]. Adverse effects included dyspagia (n=23), dry mouth (n=15), myasthenia (n=9), and dyspepsia (n=1) [80, 90]. Other reported effects included vomiting, asthenia, constipation, and visual effects [80].

Small molecule BoNTALC inhibitors would therefore be desirable for interventions related to accidental misuse and adverse effects. It has also been proposed that small molecule activators which increase the catalytic efficiency of BoNTALC might be useful to minimize BoNTA doses and increase clinical efficiency [91, 92]. A high throughput screening (HTS) assay which is capable of identifying BoNTALC activators as well as inhibitors could therefore lead to extended pharmacological applications of BoNTA.

No approved pharmacological therapies exist for botulinum neurotoxin poisoning [79]. Countermeasures for the neurotoxin consist of administration of equine origin antibodies, which can cause serious side effects, and have a short window of application [79]. In the specialized case of infant botulism, caused by colonization of the large intestine by *Clostridium botulinum*, a human anti-sera

treatment has been approved for use in patients less than 1 year of age [93]. Once BoNTs enter the neural cell, antibody neutralization strategies are ineffective [79]. It is thought that as little as one molecule of BoNTALC in the pre-synaptic nerve terminal can completely abolish acetylcholine release.

Botulinum toxins are the cause of three varieties of human botulism: food borne botulism, wound botulism and intestinal botulism [94]. In the U.S. half the cases of food bourne botulism are caused by BoNTA, with the other half divided between serotypes B and E [94]. Amongst wound botulism cases, approximately 80% result from serotype A and 20% from serotype B [94]. BoNT serotypes C and D have no recognized role in food-borne botulism cases [94]. Naturally occurring food-borne botulism is usually not fatal; however, symptoms can last from several days to several months. Recovery occurs when the BoNT LC protease inside of pre-synaptic nerve terminals is degraded, allowing newly synthesized SNARE proteins to re-activate membrane fusion and acetylcholine release [94]. There are currently no pharmaceutical treatments for food or wound borne botulism. Therapies consist of waiting until the degradation of the LC protease occurs. Prophylactic treatment with antibiotics is used to prevent secondary infections. In severe cases artificial respiration devices can be used to prevent death by respritory failure [94]. Death from food or wound bourne botulism usually occurs because of badly controlled infection and prolonged toxin secretion [94]. Advances in hygiene and food processing have mostly eliminated food borne botulism as a major public health concern [52]; however, small numbers of

outbreaks still occur in the U.S, most commonly associated with home-canned vegetables [95].

1.9 Terrorist Threat of Botulinum Toxins.

The U.S. CDC has classified Botulinum neurotoxin as one of the six highest risk threats for bioterrorism. Botulinum neurotoxin type A is the deadliest of the seven serotypes with a lethality approximately 10^{11} times greater than cyanide [96], with a lethal dose of approximately 1 ng/kg body weight [97]. Unlike anthrax lethal toxin poisoning, botulinum neurotoxins do not require the infection and germination of the bacteria which produce them, making the purified toxin itself a biothreat agent [94]. *Clostridium botulinum* spores are easily found in the environment, and it is relatively easy to produce crude neurotoxin preparations [94]. Neurotoxin alone, purified from bacteria and inhaled or ingested is sufficient to cause the toxic effects resulting from neurotoxin inhibition of neuromuscular junctions. Botulinum toxins are readily absorbed through either respiratory or oral routes, with the lethal dose dependent on the grade of purity [94].

While it does take sophisticated microbiological laboratory equipment and techniques to purify BoNTs, and their aerosolization requires formation of a small enough particle size to reach the alveoli of the lungs, botulinum neurotoxins have been successfully implemented as weapons [94]. The largest historical case of botulinum neurotoxins as weapons was found in Iraq, after the 1991 Persian Gulf war, where inspection teams found over 19,000 L of purified botulinum toxin, with 10,000 L loaded onto military weapons [94]. This amount of BoNT is theoretically

three times as much as would be required to kill the entire human population by BoNT inhalation. Iraq had also weaponized more botulinum neurotoxin than any other biological agent [94].

1.10 Lethal Factor and BoNTALC Inhibitors and HTS methodology.

Due to the high biothreat potential of both *Bacillus anthracis* and *Clostridium botulinum,* there is a great deal of interest in finding small molecule inhibitors of the protease components of the toxins produced by these bacteria. The current and expanding use of Botulinum neurotoxin type A as a pharmaceutical and cosmetic agent and the potential for overdose and adverse effects makes the light chain protease a target of interest for novel inhibitors as well. Assays capable of identifying compounds which give enhanced BoNTALC activity as well as inhibition are particularly desirable because of the potential for development of new BoNTA pharmaceuticals. Currently, numerous high throughput screening (HTS) methodologies are used for identification of lead compounds for both anthrax lethal factor and BoNTALC protease inhibitor development. Many of these methods, however, do not address the extended substrate interaction sites distal from the protease cleavage sites, which have been shown to be important in protease/substrate recognition and could potentially lead to development of new classes of inhibitors targeting protease/substrate binding. A summary of existing assays for LF and BoNTALC are listed in Table 1.1

Table 1.1 Bacterial toxin protease assays for LF and BoNTALC.

Assay	Description	HTS amenable?	Capable of using Full Length Substrates?	Comments
FRET based	An optimized protease cleavage site is used with a fluorescence resonance energy transfer fluorophore pair at each end. Cleavage leads to a loss of FRET.	Yes, by fluorescence readings	No, spatial requirements of FRET make large substrates difficult or impossible to use.	Most commonly used protease assay for bacterial toxins. Optimized substrates for both LF and BoNTALC are commercially available. Not multi-plexable
Cell based	Cell lines expressing receptors for toxin internalization are used in a viability assay with whole toxin. Macrophage or dendritic cells are used for LF, neural cell lines are used for BoNTs	Yes, by cell viability assay.	Yes, natural substrates in cells are analyzed for cleavage, typically by Western blot.	Has the advantage of assaying for membrane permeability as well as inhibition by test compounds. The disadvantage is that it requires the use of entire toxin for LF and BoNTA, requiring BSL3 laboratory facilities.
Mass spectroscopy	Substrates for protease absorbed to mass spec matrix, incubated with protease and inhibitor compounds and analyzed by MALDI-TOF Has been used for detection of BoNTALC but not HTS.	Yes, with specialized MALDI-TOF equipment and data analysis	Yes, could potentially use full length substrates. To date no LF assay or screening studies have reported use of such substrates however.	Assay has the potential to use full length protease substrates. Non-fluorescence based, ruling out false positive results due to fluorescent compounds. Cost of mass spec equipment and data analysis is extensive. Not multi-plexable
^{19}F NMR	Cleavage of ^{19}F peptide substrate leads to a change in the ^{19}F chemical environment which can be detected by NMR.	Yes, with ^{19}F NMR equipment	No, must be able to specifically label substrate with ^{19}F next to the protease cleavage site. No available methodologies to do this with full length proteins	Only done for LF. Requires ^{19}F NMR equipment and data analysis. Adaptation to full length protease substrates would be very difficult or impossible. Not multi-plexable
High Performance Liquid Chromatography (HPLC)	HPLC analysis of peptide substrates is used to screen compounds which inhibit cleavage of substrates.	Yes, by size analysis using HPLC	No, requires large amount of substrate for analysis. Peptides can be synthesized in large amounts, purification of full length proteins would be difficult in quantities.	Peptide substrates for BoNTALC do not include SNARE domains or α exosite. Include residues of β exosite which makes cleavage possible. No distinct advantage over existing FRET based methods. Not multi-plexable
Virtual binding/computer modeling in silico methods	Computer screening of binding pockets and active sites of proteases, or chemical space of known protease inhibitors are modeled and analyzed against models of chemical compounds to suggest potential inhibitors	No, must know chemical compound structure & chemical signatures to model them. Cannot test against complex libraries without this information	No, does not use substrates at all, only modeling. Modeling of full length substrate and protease mechanism would be complex and require additional knowledge of mechanism.	Chemicals which resemble known BoNTALC inhibitors have been discovered this way through virtual screening of known chemicals. Must be verified by additional assays.

Animal models (mouse models)	Test compounds are introduced into mice by water, feed or injection followed by whole toxin poisoning . If inhibitor works animal lives longer, if not animal dies at the same time as animal with no chemical compounds introduced into system	No.	N/A	Typically used as follow up assay for discovered inhibitors which have passed in vitro and cell based tests. Requires animal testing protocols and BSL3 facilities to work with whole toxin. Will give valuable information about efficiency of inhibitors in vivo.
Seven serotype BoNTLC GFP based assay.	Hines et al., have created a GFP based substrate which includes SNAP-25 residues 127-206 with exosite binding site S4, fused to VAMP amino acids 1-94. Will detect cleavage of all seven serotypes by release of GFP into solution and fluorometirc analysis of solution.	Yes, by fluorometric analysis of solution in 96 well plates	Yes, already contains important recognition and cleavage sites for each BoNTLC serotype. Could potentially fuse SNAP-25, syntaxin and VAMP together with C terminal GFP but would be difficult to express and purify.	Can be used in HTS for each BoNT LC serotype. Must be run independently however, and not in multiplex because each serotype will cleave the substrate and will not be distinguishable. Not multi-plexable, to screen all seven serotypes seven screens must be performed.
Absorbance methods	Similar to FRET where p-nitroanilide-coupled peptides of the LF consensus cleavage sequence are used and light absorbance measured.	Yes, by absorbance values of p-nitroanilide-coupled cleaved or un-cleaved peptides	No, spatial requirements are similar to FRET based assays.	Developed for HTS of LF by Tonello et al., . No distinct advantage to FRET based methods. Not multi-plexable
Chemiluminescent antibody binding	MKKS are purified as GST fusion proteins and bound N terminally to glutathione coated plates. LF and test compound are added and incubated followed by wash steps to remove non-bound material. ECL conjugated antibodies specific to the C terminal of MKK are bound and chemiluiminescence measured. Cleaved proteins give no signal, uncleaved proteins give signal	Yes, requires wash steps, antibody binding and ECL development though.	Yes, does used full length MKK1	Developed for LF cleavage detection, could easily be adapted to BoNT LC cleavage using full length protein substrates. Requires wash steps, antibody binding and ECL development which increases screening time. Not multi-plexable.

1.11 Lethal Factor High Throughput Screening and Inhibitor Identification.

Lethal Factor inhibitors and high throughput screening have had a great deal of attention and development since the anthrax letter scares of 2001. A FRET based assay, derived from the lethal factor consensus cleavage site of the MKKs of KKKKVLPI^QNAATD, with ^ representing the cleavage site, was developed for use in high throughput screening [31]. Using mixture-based peptide libraries based upon the LF cleavage sequence and Edmund degradation protein sequencing, Turk et al. were able to identify the optimized LF substrate LF15, with the sequence of RRKKVYPY^PMETIA [33]. Neither the consensus sequence used in FRET assays nor the LF15 substrate contain the C terminal distal binding element identified to be important for efficient MKK cleavage [8]; however, their optimized cleavage site sequence allows them to be cleaved efficiently in FRET based peptide assays[31, 33]. Currently, there are several peptide based FRET substrates available from multiple sources. List Biological Laboratories (Campbell, CA.) offers the MAPKKide substrate, and Calbiochem (San Diego, CA.) offers three distinct LF FRET substrates. All of these LF substrates are based upon consensus MKK cleavage sites and have been optimized for efficient cleavage by LF and use in high throughput screening assays. Chemical structures and affinity values of current LF inhibitors are listed in Appendix 1 in the order they are discussed here. HTS methodologies for LF inhibitor discovery along with advantages and disadvantages are summarized and discussed in Table 1.1.

Early LF inhibitors were based upon the consensus cleavage site of the Map Kinase Kinases (MKKs) as well [98]. By modifying these peptides with hydroxamates, known to be Zn^{2+} chelators, even tighter binding LF inhibitors were derived. One particular competitive hydroxylamine peptide inhibitor of LF, termed IN-2-LF, was found to have a K_i value of 1 nM [98]. The LF consensus sequence, and the derived inhibitor IN-2-LF, contain a strongly basic sequence of amino acids [31, 98], a feature of peptides able to cross cell membranes [99]. Experiments with lethal toxin infected macrophage cell lines RAW264.7 and J774.A1 showed that μM amounts of IN-2-LF were able to protect against MKK3 cleavage and macrophage cell death in a dose dependent manner [98]. Currently, IN-2-LF is considered the most potent LF inhibitor and is commercially available for research purposes. Peptide inhibitors are generally cleared from the bloodstream relatively quickly and typically do not make ideal drugs for human use, which highlights the need for small molecule inhibitors.

The discovery of several aminoglycoside inhibitors of LF was made by high throughput screening of a library of 3,000 compounds using the same FRET methodology [100]. The commonly used antibiotic neomycin B was found to have inhibitory activity toward LF with a K_i value of 7 nM, while three other aminoglycoside compounds had K_i values of 14.1 nM, 14.4 nM and 28.5 nM [100]. Using the structure of neomycin B and modifying a primary alcohol, Fridman et al., [101] synthesized a series of twelve aminogylcoside based inhibitors, with K_i values against LF of 0.2-13 nM, among the highest affinity LF inhibitors reported to date. Not only did these compounds inhibit LF, but they also showed

significant antibacterial activity against the Sterne strain of *Bacillus anthracis*, which lack the bacterial capsid but produce lethal toxin. The mechanism antibacterial activity of these compounds is most likely due to ribosomal binding and inhibition of protein synthesis [101]. These antibacterial neomycin derivatives are of particular interest in anti-anthrax treatment due to their dual activity of inhibition of LF coupled with antibiotic properties.

Due to the structural complexity of neomycin B, which renders it unattractive as a drug target, the structurally simpler neamine was used as a lead compound for LF inhibitors [102]. Neamine itself was found to be a weak inhibitor of LF [102]; however, guanidinylated-2,5- dideoxystreptamine derivatives of neamide showed Ki values from 65 nM to 30.6 μM in the FRET based MAPKKide assay [102]. These derivatives were also designed to have increased cell permeability and bio-availability [102]. The neamine derivatives polyamine spermine inhibited LF with a Ki of 900nM in a the FRET based assay [43]. Despite the good *in vitro* performance and the features designed to increase bio-availability, neamide derivatives were shown to have relatively poor bioavailability and potential toxicity [43].

Another group used an optimized FRET peptide to screen the NCI diversity set library, a collection of 1,990 compounds, and validated against false positives using a HPLC based assay with the same consensus peptide [103]. Three compounds had LF Ki values of 500 nM, 4.1 μM and 4.9 μM, and were shown to have no inhibitory activity against several other proteases [103]. A crystal structure of LF complexed with the most potent inhibitor found in this screen,

NCS 12155, showed several important molecular interactions of potential importance in the design of small moleucule inhibitors against LF [103]. Unfortunately these inhibitors showed only moderate ability to protect against lethal toxin induced macrophage cell death, indicating low permeability toward the macrophage cell membrane [103].

Another strategy for LF inhibitor discovery has been to optimize identified inhibitors of other metalloproteases for use against LF [43]. One hydroxamate-containing compound, Ilomastat (GM6001) had previously been shown to inhibit human skin fibroblast collegenase and thermolysin with low nM Ki values [104]. Ilomastat (GM6001) was shown to inhibit LF cleavage of MAPKKs *in vitro*, as well as in lethal toxin treated macrophages [33]. This protective effect of GM6001 was seen even when administered three hours after lethal toxin, indicating that it was capable of penetrating cell membranes and effectively preventing LF mediated MKK cleavage *in vivo* [33, 43]. The hydroxamate-containing chemically modified tetracycline (CMT) compounds CMT-300 and CMT-308 were shown to inhibit LF cleavage of the MAPKKide FRET peptide, as well as MKK2 cleavage in lethal toxin treated human monocyte, human dendritic cells and MonoMac 6 cell lines [105]. While these hydroxamate-containing LF inhibitors show promise for treatment of anthrax toxin, and have the ability to cross cell membranes, their broad spectrum inhibition of other human proteases may make them unattractive for treatment of anthrax infection.

Using the FRET based substrate Anthrax LF protease substrate III, commercially available from Calbiochem (San Diego, CA.), to screen LF against

a 10,000 compound chemical diversity set from TimTec Inc. (Newark, DE), Schepetkin et al., were able to identify 21 compounds which inhibited LF with IC_{50} values between 0.8 μM and 11 μM [106]. These inhibitors fell into three distinct groups of carboxylic acid derivatives of 2-phenylfurans, N-phenyldihydropyrazoles and N-phenylpyrroles [106]. All of the inhibitors in these classes showed a strong correlation to the current pharmacophore model of LF inhibitors, based on the crystal structure of LF bound to the small molecule inhibitor NSC 12155 [103, 106]. These compounds were inactive when tested against other proteases such as MMP-9, porcine kidney aminopeptidase M, human pancreatic chymotrypsin, human plasma kallikrein, human neutrophil elastase and human liver cathepsin B [103]. Seven of these compounds were found to be highly specific for LF, and are being used for lead compound development and *in vivo* studies [106].

Several polyphenol compounds found in green tea extract are known to inhibit matrix metalloproteases [107]. When tested against lethal factor in a peptide based assay, using the C terminal p-nitroaniline containing peptide AcGYβARRRRRRRRRVLRpNA [98], the compounds epicatechin (EC) and epigallocatechin-3-gallate (EGCG) were found to inhibit LF activity [107]. EGCG, the more potent inhibitor, was found to be a non-competitive inhibitor, with an IC_{50} value of 97 nM [107]. In the RAW264.7 macrophage cell line, challenged with lethal toxin, as little as 10 nM EGCG was found to have a protective effect on lethal toxin induced cell death and MKK2 and MKK3 cleavage [107]. Tests on

Fisher 344 rats given circulating amounts of EGCG between 50 μM and 100 μM showed delayed death after anthrax challenge [107].

A group at the Merck pharmaceutical company used a collection of known Zn^{2+} metalloprotease inhibitors in a parallel HTS assay using both the FRET based peptide assay against LF activity as well as in a macrophage cytotoxicity assay using a murine J774A.1 cell line [108]. One lead compound, a known stromelysin and matrix metalloprotease inhibitor, was found to have a Ki value of 1.2 μM in the FRET assay and an IC_{50} value of 12 μM in the macrophage cytotoxicity assay [108]. Systematic modification of this compound yielded a compound which inhibits lethal factor with a Ki value of 54 nM as compared to Ki values against matrix metalloproteases and TACE in the low μM range [108]. This selective LF inhibitor was also found to be orally bio-available in animal models [108], and to have a protective survival effect on mice and rabbits challenged with anthrax spores [109].

Mass spectroscopy methods have been used with some success to screen for lethal factor inhibitors [110]. An 18 amino acid peptide derived from the optimized LF cleavage sequence was incubated with test compounds and LF then evaluated on a mass spectrometer [110]. Individual Matrix-assisted laser desorption/ionization time of flight (MALDI-TOF) mass spectra were taken for each sample in which cleaved peptide was easily distinguishable from uncleaved peptide [110]. A screen of 10,000 small molecules identified the hydrazone-based small molecule DS-998 [110]. Characterization of DS-998 in a solution based LF assay using the C-terminally labeled p-nitroanilide peptide Ac-NleKKKVLIP-pNA,

spectrophotometrically measuring release of p-nitroanilide, showed that DS-998 gave a Ki value of approximately 1 μM [110]. Tests of this compound against other proteases, trypsin, carboxypeptidase A and β-lactamase showed no effect at concentrations up to 100 μM [110]. Cell based follow up on J774 macrophage cell lines infected with lethal toxin showed dose dependent increased cell viability [110]. While this method shows promise, the expense and data acquisition of each compound measured separately in mass spectroscopy makes this method expensive and lower throughput than other LF screening methodologies.

An alternative screening approach that uses fluorinated peptides for NMR assays, has been used to identify potent lethal factor inhibitors [111]. ^{19}F NMR spectra were used with the fluorinated LF peptide substrate Ac-A-R-R-K-K-V-Y-P-NH-Ph-CF_3. Cleavage of this peptide changes the chemical environment of the ^{19}F nuclei due to the conversion of the amide functionality in to an amine functionality, which can be detected by ^{19}F NMR [111]. This strategy led to the identification of compound BI-9B9b, with an IC_{50} value of 140 μM [111]. Testing of derivatives of BI-9B9b in both ^{19}F NMR assays and MAPKKide fluorescence assays led to the identification of the compound BI-MFM3, with a Ki value of 0.8 μM [111]. This inhibitor was also not a non-specific metalloprotease inhibitor when tested in assays against MMP-9 and MMP-2 [111]. Further substitutions of side chains on BI-MFM3 yielded the compounds BI-1B1, BI-11B2 and BI-11B3, with BI-11B3 having a Ki value of 32 nM. All three of these compounds were also tested against lethal toxin in a RAW264.7 macrophage cytotoxicity assay and were found to have IC_{50} values between 2-5 μM [111]. This particular study shows

the reasoning behind identifying chemical scaffolds which give weak inhibition and substitution of side chains to give higher Ki values.

Crystal structure analysis of the inhibitor BI-MFM3 complexed with LF showed that its rhodanine ring is capable of interacting with the Zn^{2+} ion in the LF active site via a thiazolidinedione sulphur ion [111]. Using the MAPKKide FRET assay Johnson et al., investigated further substitution of BI-MFM3. They found that substitution of the rhodanine ring with a closely related thiazolidinedione ring or thiobarbiturate rings retained the Zn^{2+} chelating properties of the rhodanine ring while substitution with creatine moiety abolished inhibitory activity due to a loss of Zn chelation [112]. In further work by this group a subset of 14,000 chemicals was selected from the ASDI and screened in mixtures of 20 chemicals per sample using the MAPKKide FRET assay [113]. Compounds from active mixtures were then tested individually. Six compounds showed LF inhibition, two of these contained a rhodanine Zn^{2+} chelation moiety [113]. None of the six compounds inhibited MMP-2 or MMP-9 while one of the non-rhodanine containing compounds inhibited BoNTALC [113]. This latter compound was considered a lead compound for development of general inhibitors of bacterial toxins. This particular study showed mixture based screening to be a viable strategy for protease inhibitor screening. It also demonstrates that Zn^{2+} chelation moieties can be specific inhibitors for bacterial toxins and identified several new scaffold families for future development of improved anthrax lethal factor and botulinum neurotoxin type A light chain inhibitors.

One HTS screen used J774A.1 macrophage cells grown in 96 well plates, incubated with the LOPAC 1280™ library from Sigma and challenged with lethal toxin [114]. When compounds which rescued cell death were subsequently tested in the *in vitro* MAPPKide FRET assay the compound N-oleoydopamine (OLDA) was identified to have an IC_{50} value of 15 μM *in vitro* and 5 μM in cell based *in vivo* assays [114]. Cell viability was seen with up to 30 μM OLDA [114]. OLDA was shown to be a non-competitive inhibitor with a Ki value of 3 μM, and was proposed to bind Zn^{2+} through its catechol moiety [114]. Addition of hydroxyl groups to the catechol moiety led to a compound which gave a two-fold increase in inhibiton, with a Ki value of 1.7 μM [114]. Replacement of the catechol moiety with another Zn^{2+} binding hydroxamate moiety decreased the Ki to 6 μM [114]. Truncation of the oleic acid tail from OLDA showed complete loss of LF inhibition, indicating that there are significant areas of contact in the oleic acid tail and LF [115]. Switching of the double bond in OLDA from cis to trans also eliminated the ability of OLDA to inhibit LF [115]. These studies demonstrate how chemical modification of identified inhibitors can identify moieties which are important or necessary for inhibitor function.

The large amount of effort put into screening and characterization of *Bacillus anthracis* lethal factor protease inhibitors has yielded a large number of lethal factor inhibitors over the past 8 years. The assays used in HTS screening for LF inhibitors are summarized in Table 1.1 with their strengths and weaknesses discussed. The *in vitro* methodologies of these screening efforts used small optimized peptide substrates which did not contain distal C-terminal

lethal factor interacting regions [8]. *In vivo* assays using entire toxin on macrophage or other lethal toxin susceptible cell lines are capable of identifying small molecules which interact with distal binding site interactions, as well as compounds capable of crossing cell membranes to exert effects intracellularly. In the absence of viable anthrax spores, lethal toxin itself is not dangerous, although care should be taken when handling any bioagents. An assay capable of identifying small molecule inhibitors of MKK C-terminal interactions with lethal factor would be useful in identifying new classes of lethal factor inhibitors.

1.12 Botulinum neurotoxin Light Chain inhibitors and High Throughput Screening

There has recently been a great amount of interest in small molecule inhibitors of BoNTALC. The lack of potent inhibitors for BoNTALC is thought by some to be because of the deficiency and lack of reliabile high throughput assays to screen libraries of small molecules for lead compound discovery [74], [116]. Methodologies have been developed for high throughput screening of small molecule libraries for BoNTALC inhibitors, most of which do not use full length SNAP-25 containing distal protease interaction sites. A summary of these methodologies are listed in Table 1.1

Most BoNTALC HTS applications have used a relatively small FRET substrate, SNAPtide, currently available from List Biological Labs (Campbell, Ca.). The disadvantage of this lies in the absence of distal binding and interaction sites for BoNTALC on the substrate, which have been shown to be important in substrate recognition [9, 10, 76]. Beyond FRET, other assay formats

such as fluorescence anisoptropy, HPLC, and mass spectrometry have been developed [74],[117], [118]. The anisoptropy method has not been specifically optimized for BoNTALC. The mass spectrometry methodology is for detection of BoNTs, and not specifically for high throughput screening, and does not use full length substrates. Each of these approaches has the advantage of being able to use full length substrates and can, with varying degrees of difficulty, be adapted to high throughput methodologies for inhibitor screening. However, the requirement for solution based substrates and the limited number of fluorophores capable of simultaneous analysis may limit the number of substrates that can be simultaneously analyzed. Chemical structures and affinity values of discovered BoNTALC inhibitors are listed in Appendix 2 in the order they are discussed here. The HTS assays used for discovery of these inhibitors along with their advantages and disadvantages are summarized in Table 1.1.

BoNTLC inhibitors are of two distinct categories, peptide based inhibitors and small organic molecules, some of which have been shown to stably bind to the protease and inhibit catalytic actions [91]. Six amino acid peptides, mimicking the BoNTALC cleavage site with cysteine resudies replacing the P_1 or P_2 sites N-terminal to the cleavage site, were shown to inhibit BoNTALC cleavage with Ki values of 2 μM in a HPLC based assay [119]. Replacing the cysteine molecule in these peptides with other sulfhydryl containing compounds resulted in inhibitors with Ki values as low as 270 nM [74]. A modified peptide inhibitor based on the SNAP-25 cleavage site, 2-mercapto-3-phenylpropionyl-RATKML, was shown to have Ki values of 300 nM [74]. The crystal structure of BoNTALC bound to

inhibitory peptides has been used to design tetrapeptides that bind BoNTALC more efficiently. RRGC, RRGL, RRGI and RRGM, had Ki values of 157 nM, 660 nM, 786 nM and 845 nM, respectively, in assays measuring the cleavage of a 17mer SNAP-25 based peptide [120]. Peptide based inhibitors generally have poor lifetimes *in vivo* and low bioavailability and do not make optimal drugs [91]. Some peptide inhibitors also have no internalization mechanism for entry into cells, and cannot act on the protease once it has been internalized inside of neuromuscular junctions.

Another strategy for inhibiting BoNT LC is the use of metal chelators. One approach was to couple a Zn^{2+} binding hydroxamate to amino acids in the BoNTALC peptide cleavage site between SNAP-25 Gln 197 and Arg 198. L-arginine hydroxamate gave much better inhibition than L-glutamine hydroxamate [116]. These findings were consistent with earlier studies in which the arginine residue at the P1' position was shown to be more critical for BoNTA cleavage of SNAP-25 than the P1 glutamine residue [68, 70]. Using L-arginine hydroxamate derivitaves, a competitive inhibitor with a Ki values of 60 μM was discovered [116]. 4-chlorocinnamic hydroxamate, had an IC_{50} value of 15 μM [121]. Chloro-substituted derivitaves of these hydroxamate-based inhibitors yielded a small molecule inhibitor 2,4,dichlorocinnamic hydroxamate with a Ki value of 300 nM [121].

Virtual screening of 2.5 million compound profiles against the crystal structure of BoNTALC led to the discovery of a competitive hydroxamate-containing compound which gave Ki values of 12 μM [122]. By changing a single

hydrogen atom in this compound, the resulting Ki value was improved to 3.8 µM. [123]. Other screening approaches used virtual binding of the potent peptide based inhibitor 2-mercapto-3-phenylpropionyl-RATKML (mpp-RATKML) [74] to search for potent small molecule non-peptide inhibitors from the National Cancer Institute's Open Repository [124]. Potential inhibitors from this virtual screen were followed up in a HPLC based assay with a small SNAP-25 analog peptide [74]. Four small molecule inhibitors of BoNTALC with Ki values of 3 µM, 6 µm and two with 10 µM were discovered [124]. Two of these inhibitors were found to be neurotoxic, while a third was unable to enter neurons [124]. The compound NSC240898, with a Ki value of 10 µM, was found to have a protective effect upon BoNTA induced SNAP-25 cleavage when 20 µM of the compound was incubated with chick neurons [124]. These particular studies highlight the potential for small molecule inhibitors for treatment of BoNTA poisoning even after BoNTALC internalization into neurons.

In an effort to screen for inhibitors of all seven serotypes of BoNT light chains using substrates which include LC distal interaction sites, Hines et al., have created a GFP based substrate which includes SNAP-25 residues 127-206 with exosite binding site S4, fused to VAMP amino acids 1-94 [125]. This substrate is covalently coupled through a C terminal cysteine residue to maleimide-activated 96 well plates, and proteolytic activity is analyzed by release and diffusion of GFP into the solution of the well. [125]. This assay was used to screen 528 natural product extracts from plants, invertebrate marine organisms and fungi against BoNT types A, B and E light chains, where 30 extracts were found

to contain serotype specific inhibitors of BoNT light chains [125]. Further characterization of these extracts is currently underway.

The S4 SNARE motif on SNAP-25, which includes the recently discovered α exosite, plays a critical role in BoNTALC substrate recognition, along with several amino acids C-terminal of the protease cleavage site, termed the β exosite [10]. This discovery led Eubanks et al., to hypothesize that small molecule libraries containing compounds known to inhibit protein-protein interactions may lead to the discovery of novel inhibitors of BoNTALC [79]. A collection of small molecule libraries with the potential of disrupting protein-protein interactions, consisting of 66,000 compounds, was screened against BoNTALC, using the SNAPtide FRET based assay. This led to the discovery of 12 small molecule inhibitors with IC_{50} values ranging from 1-90 μM [79]. Of the twelve compounds, seven were selected for follow up analysis in animal models based upon their ability to prevent cell death in Neuro-2a cells [79]. Two of these compounds showed extension of time of death in a mouse model of BoNT infection; NA-A1B2C10, and the previously discovered 2,4-dichlorocinnamic hydroxamate [79]. Interestingly, neither of these molecules showed any zinc chelation motifs [79]. These compounds are being proposed for combination therapies for BoNTA poisoning, along with compounds which may target other mechanisms of LC action or compounds which target other steps in BoNTA poisoning. [79]

One group investigated the properties of rhodanine derivatives as potential inhibitors against both the anthrax lethal factor protease as well as

botulinun neurotoxin type A light chain, and found numerous promising lead compounds [126]. In tests against the human proteases MMP-2 and MMP-9 these compounds were shown to be highly selective for toxin proteases and not metalloproteases in general [126]. These inhibitors were screened and tested using FRET peptides for LF, BoNTALC and MMP-2 and MMP-9, none of which contained important distal interactions sites discussed earlier. The best BoNTALC inhibitor of this class was found to be a furan rhodanine derivative, with an IC_{50} value of 9.72 µM. Interestingly, this same compound had an IC_{50} value of 1.09 µM for the *Bacillus anthracis* lethal factor as determined in a separate assay. While this work has shown great promise for developing selective inhibitors of LF and BoNTALC in the low µM range [126], an assay format capable of screening all of these protease/substrate combinations in parallel, and of using substrates containing distal interaction elements would save time and potentially identify novel inhibitors that act distal to the protease active site or substrate cleavage site.

1.13 Botulinum Neurotoxin type A Light Chain activators

Due to the use of BoNTA as a therapeutic, not only is there interest in discovery of small molecule BoNTALC inhibitors to treat undesirable side effects, but small molecules which increase activity of the BoNTALC protease are also of potential interest. It is thought that discovery and optimization of BoNTALC activators would be valuable in minimizing BoNTA dosage and increasing BoNTA clinical efficiency [92]. One group currently involved in discovering BoNTALC

inhibitors has recently discovered a small molecule scaffold which increases BoNTALC catalytic activity through an apparent reduction in the Km of the BoNTALC [92]. Due to the high use of BoNTA as a pharmaceutical and cosmetic agent, discovery of activators of BoNTALC will most likely be a field of great interest in small molecule high throughput screening.

1.14 Present Studies

In the work described here we have created a microsphere based flow cytometry multiplexable protease assay, capable of using multiple full length substrates at once which can be used in high throughput screening for protease drug targets. This assay has identified a novel inhibitor of Botulinum Neurotoxin type A Light Chain, which we have further characterized, and two potential Lethal Factor inhibitors. This assay has the capability of identifying small molecules which block protease/substrate protein interactions distal to the cleavage site as well as molecules which target the protease active site. This assay also has the potential for discovery of small molecule activators as well as inhibitors. Protease substrates used in this assay are also capable of being used in solution based assays to characterize kinetics of protease cleavage.

Chapter 2.
Goals and Overview of this Work

The goal of the work described here is the development of a microsphere based flow cytometry protease assay for site specific proteases for use in high throughput screening (HTS) as well as in kinetics assays. These assays would have advantages over current HTS assays in that they would be capable of using full length protease substrates, containing distal protease/substrate interaction sites instead of peptides mimicking protease cleavage sites alone used in current fluorescence based energy transfer (FRET) assays. The use of such assays in conjunction with the HyperCyt flow cytometry screening system at the University of New Mexico Center for Molecular Discovery would allow for cost effective screening of proteases of medical relevance in a time effective manner. Assays using full length protease substrates could also potentially identify new classes of specific protease inhibitors which interfere with protease/substrate interactions instead of inhibition of highly conserved protease active sites.

The studies in Chapter 3, published in *Cytometry part A* [127], describe the development of microsphere based protease assays using the proteases Factor Xa and the *Bacillus anthracis* Lethal Factor. In this publication we have shown specific proteolytic activity for microsphere based substrates for both of these proteases using a loss of fluorescence assay via C-terminal green fluorescent protein (GFP). We have also shown inhibition of both of these proteases by known inhibitors in this assay using the HyperCyt flow cytometry system. While full length protease substrates were not used in these studies, we have shown

the feasability of microsphere based flow cytometry assays and the ability to detect inhibition by known inhibitors of these proteases.

Adaptation of these microsphere based protease assays to use full-length protease substrates was performed for the *Bacillus anthracis* Lethal Factor and *Clostridium botulinum* neurotoxin type A light chain bacterial metalloproteases. Both of these proteases are current targets of interest in HTS and are active components of bacterial toxins. The Lethal Factor protease targets Map Kinase Kinase proteins (MKKs), however, does not cleave natural MKKs *in vitro*. We therefore replaced the MKK Lethal Factor cleavage site in full length MKK2 with the MKK consensus cleavage site used in our published microsphere based LF assay. Due to the size of this protein we were required to use Sf9 insect cells for expression and purification, followed by *in vitro* biotinylation. We were able to show a faster rate of initial cleavage of the full length MKK by LF when compared to the cleavage site alone, although the complications of *in vitro* biotinylation led to a lower final amount of cleaved protein. Using full length SNAP-25, the substrate for the Botulinum Neurotoxin type A Light Chain (BoNTALC) protease, we were able to show specific cleavage of full length SNAP-25 from microspheres. These studies, their rationale and methods are presented in Appendix 3.

In Chapter 4 we have created a five-plex microsphere based BoNTALC assay based upon important SNARE domain deletions on SNAP-25. These experiments were designed to highlight the potential discovery of inhibitors which interfere with protease/substrate binding compared to those which target the

active site of proteases. Screening of this five-plex assay against the Prestwick chemical library, a collection of 880 off patent and bio-available compounds pre-approved for human use, yielded the discovery of ebselen, a compound which inhibits BoNTALC with an IC_{50} value in the low µM range. Ebselen was characterized in both microsphere based and FRET based assays with the results accepted for publication in the journal of *Assay and Drug Discovery Technologies.*

The success of screening our BoNTALC assay against the Prestwick Chemical Library, led us to screen our Lethal Factor protease assay against this library as well. The screening of Lethal Factor was made cost effective by the sub-cloning and purification of recombinant LF from *E. coli.* The works in Chapter 5 describe the purification of active LF and the discovery of two compounds of interest shown to inhibit LF in this screen. The compounds pirenperone and harmalol hydrochloride dehydrate have shown inhibitory activity against Lethal Factor and we are currently following up on that work to obtain IC_{50} values for both of these compounds.

A collaboration between the University of New Mexico Center for Molecular Discovery and the Torrey Pines Institute for Molecular Studies (TPIMS) has led to the screening of our BoNTALC five-plex assay against the TPIMS combinatorial library, described in Chapter 6. This library features multiple compounds per well, each mixture consisting of defined and random combinations of scaffold modifications. The use of combinatorial libraries in HTS allows millions of compounds to be screened in the length of time normally

required for thousands. The results of screening BoNTALC against the TPIMS library, as well as follow up libraries of lead compounds are described in Chapter 6. The results show several novel potential inhibitors of BoNTALC, as well as potential BoNTALC activators.

Chapter 7 of this work focuses on solution based protease assays with the aim of verifying kinetics observed in microsphere based protease assays. This chapter outlines the difficulties of using microsphere based protease assays for kinetic analysis due to the low substrate concentrations inherent in such assays. In this chapter we have developed FRET based assays using the GFP FRET acceptor dye Cy3. By labeling streptavidin with Cy3 and binding it to the N-terminally biotinylated SNAP-25 we were able to observe GFP emission quenching. Addition of BoNTALC and cleavage of GFP from the C-terminus of SNAP-25 led to an increase of fluorescence even without a FRET partner. Thus we can use an increase of fluorescence as a measure of cleaveage in a reaction that is not apparently associated with FRET. We have also developed a novel method for jump-starting cleavage reactions to enable estimates of initial rate kinetics. This involves the use of inhibitory Zn^{2+} binding to BoNTALC to allow pre-binding of the protease to substrate without cleavage. The cleavage reaction is then initiated by subsequent addition of EDTA to chelate the inhibitory Zn^{2+}. Using these novel solution based assays we hope to measure the Km and k_{cat} of BoNTALC and compare that to the ratio observed in microsphere based assays using low substrate concentrations.

Taken together, the studies here have demonstrated the application of microsphere based protease assays for use in high throughput screening in discovery of inhibitors of bacterial toxin proteases . These assays can be adapted to other proteases of medical relevance as well, with future directions and other potential proteases of interest discussed in Chapter 8. These microsphere based protease assays may also give valuable kinetic information on measurements of the protease specificity constant (k_{cat}/Km), and we have developed solution based protease assays capable of measuring these constants independently for comparison and verification of these measurements. HTS efforts on both LF and BoNTALC are on-going using this system, however, the development of and initial screening efforts of these proteases by microsphere based flow cytometry assays are described in their entirety in this dissertation.

Chapter 3.
Microsphere Based Protease Assays and Screening Application for Lethal Factor and Factor Xa

Matthew J. Saunders[1,2], Heungbok Kim[1], Travis A. Woods[1], John P. Nolan[3], Larry A. Sklar[2], Bruce S. Edwards[2], Steven W. Graves*[1]

[1] National Flow Cytometry Resource, Biosciences Division, Los Alamos National Laboratory, Los Alamos, New Mexico, 87545

[2] Cancer Research and Treatment Center, Cytometry, University of New Mexico Health Sciences Center, Albuquerque, New Mexico 87131

[3] La Jolla Bioengineering Institute, La Jolla, CA 92037

(Published in *Cytometry part A* 2006 May;69(5):342-52.)

ABSTRACT

Background: Proteases regulate many biological pathways in humans and are components of several bacterial toxins. Protease studies and development of protease inhibitors do not follow a single established methodology and are mostly protease specific.

Methods: We have created recombinant fusion proteins consisting of a biotinylated attachment sequence linked to a GFP via a protease cleavage site to develop a multiplexable microsphere based protease assay system. Using the proteases Lethal Factor and Factor Xa we performed kinetic experiments to determine optimal conditions for inhibitor screens and detect known inhibitors using the HyperCyt® flow cytometry system.

Results: We have demonstrated specific cleavage of Lethal Factor and Factor Xa substrates, optimized screening conditions for these substrates, shown specific inhibition of the proteases and demonstrated high throughput detection of these inhibitors.

Conclusions: The assay developed here is adaptable to any site specific protease, compatible with high throughput flow cytometry systems, and multiplexable. Coupled with flow cytometry, which provides continuous time resolution and intrinsic resolution of free vs. bound fluorophores, this assay will be useful for high throughput screening of protease inhibitors in general and could simplify assays designed to determine protease mechanism.

3.1 Introduction

Protease activity is critical to the action of several two part bacterial endotoxins including Tetanus Toxin, Botulinum Toxin and Anthrax Lethal Toxin (LT). These toxins use a cellular receptor binding protein to deliver a zinc dependent metalloprotease into the cell, where it cleaves key host proteins to exert toxic effects on the host [5]. The metalloprotease for lethal toxin is the lethal factor protease (LF), which specifically cleaves the Map-kinase-kinase (MAPKK) family of proteins at an N-terminal cleavage site MAPKK family of proteins that is required for efficient cleavage by LF [30, 128]. Subsequent studies demonstrated that LF cleaved most MAPKKs, and confirmed the presence of a C-terminal distal element required for efficient cleavage [7, 8]. Distal binding elements have also been demonstrated in the substrates for Botulinum Toxin proteases [129].

The threat of bioterrorism has driven increased interest in high throughput screening (HTS) approaches to detect LF inhibitors [130]. Such HTS assays use fluorescence energy transfer (FRET), absorbance, electrochemiluminecscence (ECL) assays, and mass spectrometry of arrayed peptides [31, 98, 110,131, 132]. FRET studies using small peptides demonstrated 100 fold faster cleavage of a consensus cleavage sequence (derived from MAPKK cleavage sites) compared to natural sites [31]. Using FRET peptides, small molecule inhibitors with K_i's ranging from 0.5 µM to 7 nM have been isolated [100, 103]. Absorbance methods using p-nitroanilide-coupled peptides in HTS screens were used to select the peptide inhibitor IN-2-LF [98]. Microsphere based ECL assays use streptavidin-labeled microspheres in microtiter plates to pull down biotinylated ECL-labeled

synthetic peptides and full length substrates to show LF proteolytic activity and inhibition by IN-2-LF [131, 132]. Mass analysis of unlabeled arrayed peptides on a surface has been used to detect LF activity and screen for inhibitors [110].

The nearly ubiquitous role of proteases in cell signaling and other processes has led to the investigation of a very large number of proteases as pharmaceutical targets [2]. Among the most important of these are the proteases that regulate the blood coagulation cascade. The role of this cascade in many diseases has made it a primary target for many pharmaceuticals, including protease inhibitors. For the above reasons there has been a proliferation of many protease assays, which include: chromagenic substrates to assay proteolytic enzymes in blood coagulation pathways [133], ELISA [134], scintillation proximity [135], continuous-flow approaches using FRET in solution based fluorescence measurements to detect cleavage [136], cleavage of bioluminescent proteins linked to the surface of microtiter plates [137], and microtiter plate fluorescent assays using FRET labeled substrates [138].

The above assays resolve into homogenous solution-based approaches that optically detect the cleavage of a small substrate (*e.g.* a FRET peptide, an optically active analog, etc…) or surface based approaches that detect cleavage by the loss of a label from a surface. Solution based approaches are simple but suffer from the spatial limitations of FRET, hindering use of large substrates. This complicates screens for inhibitors that target interactions between the protease and distal elements found in many protease substrates. Surface based approaches have the advantage that they enable studies of full length substrates

and can conceivably detect inhibitors that target events distant from the cleavage site. The potential for flow cytometric analysis of protease assays on microsphere surfaces was first demonstrated using the relatively non-specific protease Gelatinase B to cleave adsorbed gelatin (non-specifically labeled with fluorescein) from the surface of microspheres [139]. This approach took advantage of flow cytometry's capability to resolve free vs. bound molecules on a microsphere surface for protease assays [139].

In this work, we use the directed attachment of protease substrates to microsphere surfaces to develop and optimize protease assays for Lethal Factor and Factor Xa activity. Lethal Factor was chosen as a target as it has a clear need for a HTS approach that can detect the interaction of distal elements. Factor Xa was chosen for its important role in the blood coagulation cascade, its availability and to provide a control protease for the LF assay. Using these proteases, we demonstrate protease assays with multiplex microsphere sets to perform cleavage assays with two substrates simultaneously and to provide controls for the reaction. Additionally, we performed assays to detect known inhibitors and adapted this assay to a high throughput flow cytometer based screening system (HyperCyt®), which (in combination with suspension microarrays) could potentially screen millions of compounds per day for protease inhibition [140, 141 , 142].

3.2 Materials and methods

3.2.1 Materials

Pin-Point Vector plasmids and Softlink Streptavadin resin were purchased from Promega (Madison, WI). BL21 (DE3) pLys cells were obtained from Novagen (Madison, WI). Chloramphenicol, IN-2-LF and Antithrombin III were obtained from Calbiochem (San Diego, CA) Quickspin miniprep kits were from Qiagen (Valencia, CA). Amicon Ultra 15 filters were from Millipore (Billerica, Mass, USA). Recombinant Lethal Factor was from List Biological Laboratories (Campbell, CA). Factor Xa was from Roche (Indianapolis, IN). Flow cytometry Pink multiplex streptavidin coated microspheres (SVFA-2558-6K) and Rainbow standards (RCP-30-5) were from Spherotech (Libertyville, IL). EGFP standards were from BD Biosciences (Palo Alto, CA).

3.2.2 Plasmid construction and sub-cloning

The Xa-sub plasmid was created by cutting the EGFP from Clontech's pEGFP-N2 using BamH1 and Not1 and pasting it into Promega's PinPoint Xa-1 [143] and for this purpose was named the Xa-sub expression plasmid. The LF-sub plasmid was created from the Xa-sub plasmid by inserting a synthetic DNA insert encoding (KKKKVLPILNAATD) in frame into the Sac I and Hind III sites which also removed the Xa site. The Factor Xa cleavage site was removed in this process. Plasmids were sequenced to confirm construction.

3.2.3 Purification of biotinylated GFP protease substrates.

Transformed BL21 pLys cells were grown overnight at 37℃ in 2ml TB cultures containing 50 µg/ml carbenicillin and 34 µg/ml chloramphineocol and transferred to 200 ml TB with 40 µM biotin, 50 µg/ml carbenicillin and 34 µg/ml

chloramphenecol and grown at 37℃ to an OD600 between 0.4 and 0.8. Cultures were induced using 100 µM isopropyl-beta-D-thiogalactopyranoside (IPTG) and grown at 30℃ overnight in a shaking incubator. Cells were spun at 10,000 x g for 15' @ 4℃, suspended in lysis buffer (50mM tris-HCl 1mM EDTA 100 mM NaCl pH 8.3) and frozen. Frozen cells were thawed on ice. 1 mg/ml lysozyme was added while stirring for 20 minutes. 1 mg/ml deoxycholic acid was added with stirring for an additional 10'. Lysates were sonicated and then centrifuged at 10,000 x g for 15' @ 4℃. The supernatant was centrifuged again in new tubes under the same conditions. The supernatant was purified over a 5 ml Softlink streptavadin resin column according to the manufacturer's instructions. Elution fractions that contained protein (detected by UV light absorbance) and that were visibly green in color were combined into a 12-15 ml pool. The entire sample was inserted into an Amicon Ultra-15 30,000 Mw cutoff filter and spun at 1800 x g for 20' @ 4℃. The flow through was discarded and an additional 10 ml of PBS was mixed with the sample and re-spun. This process was repeated 15 to 20 times to remove free biotin. The sample was concentrated to 0.5 ml. Protein concentration was determined using A280 measurements of the protein [144].

3.2.4 Titrations and saturation point GFP/microsphere number determinations

The LF-sub was used on multiplex microsphere P.9 and the Xa sub was used on microsphere P.11 obtained from the streptavidin coated Pink multiplex

flow cytometry particle kit (see above). 0.25 nM to 50 nM of each reporter was incubated with its corresponding microsphere. Plots of reporter concentration vs. mean microsphere fluorescence enabled a fit of the data to a hyperbolic curve plus linear function [145]. From this fit, the amplitude represents the maximum specifically bound fluorescence, which can be converted to mean numbers of molecules of GFP per microsphere through the use of fluorescence standard curves. The K_Ds of both LF-sub and Xa-sub (~10 nM) were obtained from the hyperbolic fit (data not shown). Using this as a guide, single point measurements with 50 nM substrate protein concentration were also used to estimate the amplitude of the maximal specifically bound fluorescence [146]. Single point measurements were done using 5 µl of microspheres ($5x10^5$) plus 50 nM GFP substrate in a 500 µl total volume of PBS. Analysis was done in triplicate with a triplicate set blocked with 2 µM free biotin for both proteins. Non-specific binding of substrate on the blocked microspheres was subtracted from mean FL1 fluorescence values of the saturated microspheres to obtain specific fluorescence.

To obtain numbers of molecules per microsphere the fluorescence values from the above measurements were converted to mean equivalent soluble fluorophore (MESF) values using a fluorescence standard curve correlated to GFP number per microsphere. This standard curve was created by correlating the fluorescence of Spherotech rainbow standards (Libertyville, CA) to numbers of EGFP per microsphere using EGFP standardized microspheres (BD biosciences, Palo Alto, CA). This was performed in a five step process. First, we

measured the fluorescence of each of the EGFP standard microspheres in FL1 of the FACScan as described above. Second, we used these values to create a standard curve between the number of EGFP molecules on the surface and FL1 fluorescence. Third, we measured the fluorescence in the FL1 channel of the FACScan of each of the Rainbow microspheres. Fourth, we correlated the measured fluorescence of the Rainbow standard microspheres to numbers of EGFP molecules on the surface of a microsphere using the standard curve from the second step. Fifth, we used these correlated values to create a standard curve generated from the fluorescence of the Rainbow microspheres. Through the use of identical FACScan settings for all measurements and carefully stored Rainbow microspheres that were always drawn from the identical stock, we were able to create a low cost accurate method of estimating the number of EGFP molecules on the surface of a microsphere. Importantly, the use of Rainbow standard microspheres made it economically feasible to quantify all samples in a HTS screen. This approach of correlating a general fluorescent microsphere set to a quantifiable standardized microsphere set has been discussed previously [147]. However, for work presented here, it must be noted that GFP is highly sensitive to its environment (pH, salt, etc…) and can also change fluorescence from one fusion construct to another. Variations in the environment and fusion type can lead to a change in GFP fluorescence. Therefore, the quantifications presented here are strictly estimates. However, these estimates are sufficiently accurate to provide excellent quality control throughout the work presented here.

3.2.5 Binding and washing of microspheres.

Spherotech Streptavidin coated Pink multiplex microspheres (10^8/ml) numbers 9 and 11 were added to PBS and biotinylated GFP substrate individually to a final volume of 500 µl with GFP substrate concentrations between 25 and 35 nM. Microspheres were incubated at room temperature on a rotator covered from light for 1 hour or at 4℃ for up to 6 hours. After incubation microspheres were centrifuged in an eppendorf microcentrifuge model 5115C at 13,800 x g for 2 minutes. Supernatant was removed and the microsphere pellet was suspended in 500 µl of PBS. This process was repeated three additional times to remove all soluble substrate. Bead types were combined, centrifuged at 13,800 x g, then suspended in appropriate protease reaction buffer and aliquotted into identical volumes. Individual aliquots were brought up to 500 µl with appropriate protease buffer for each experiment. Microsphere concentrations ranged from 250,000 to 5,000,000 per 500 µl sample in individual experiments. HyperCyt analysis used 20 µl samples containing between 5,000 and 15,000 microspheres per sample. All samples contained approximately equal amounts of each multiplex microsphere bound to substrate.

3.2.6 LF protease assays and inhibition by known inhibitors

Bacillus anthracis Lethal Factor was suspended at 1 mg/ml (10.5 µM) in 50% glycerol or 7% DMSO in PBS. The LF was divided into 20 µl aliquots and frozen at -20℃. To perform protease assays, 18 µl of LF (to a final concentration of 365 nM) was added to 500 µl of microspheres. Microsphere concentrations ranged from between 250,000 and 1,500,000 microspheres/ml of microsphere 9

bearing LF-sub and between 250,000 and 1,500,000 of microsphere 11 bearing Xa-sub in LF buffer (50 mM HEPES, 100 mM NaCl pH 7.4), and were incubated at room temperature during cleavage reactions. Exceptions to protease concentrations were the LF enzyme titration reactions, in which different amounts of LF were added to achieve increasing LF concentrations as indicated in Fig. 3.4. Exceptions to buffer conditions were the pH assays where the pH of each reaction were as indicated in Fig. 3.3 and exceptions to the microsphere range concentrations listed were the microsphere number titrations where the microsphere number was varied as described in Fig. 3.5. Lethal Factor inhibitor IN-2-LF was suspended in 5% acetic acid to a 504 µM stock solution according to manufacturer's instructions. Inhibition reactions were done in 500 µl volumes by adding the IN-2-LF from the serial dilutions of the stock solution diluted in PBS to final concentrations between 1 and 10,000 nM. Samples were analyzed at time points on a FACScan flow cytometer with photomultiplier tube (PMT) settings of forward scatter (FSC) E01/9.25, log side scatter (SSC) at 150V, log FL1 fluorescence at 700V , and log FL2 fluorescence at 600 V. Individual bead populations were doubly gated both on size (FSC and SSC) as well as fluorescence values FL2. Samples were taken for 30 seconds on High flow rate (nominally 1 µl/s) or 5,000 size-gated events. FL1 fluorescence was collected with a 560 nm dichroic long pass filter and through a 530/30 nm bandpass filter on the FL1 channel. FL2 fluorescence was collected through the 560 nm dichroic long pass filter and through a 585/42 nm bandpass filter on the FL2 channel.

3.2.7 Factor Xa protease assays and inhibition by known inhibitors

Factor Xa was suspended at 1 mg/ml in 7% dimethylsulfoxide (DMSO) and 93% phosphate buffered saline (PBS) buffer. Factor Xa reactions were carried out by adding 10.85 µl of factor Xa (to create protease assays with a final concentration of 488 nM Factor Xa) to 500 µl final volume of microspheres. Between 150,000 and 2,500,000 multiplex microspheres of each substrate in Xa buffer (50 mM Tris-HCl, 100 mM NaCl, 1 mM $CaCl_2$, pH 7.4) were used in these reactions at room temperature. Exceptions were the Xa enzyme titration reaction, in which different amounts of factor Xa were added to achieve increasing Xa concentrations (data not shown), the pH assays where the pH of each reaction was as indicated in Fig. 3.3. For inhibition reactions, antithrombin III was suspended in distilled water at 1 mg/ml and added to the samples to final concentration of 1 µM before addition of the protease. Flow cytometry analysis was as described for the LF protease assays

3.2.8 HyperCyt analysis

Microspheres were bound and washed as described above using 19 ul/well for 24 wells of each sample from sample preparations listed above. Lethal factor inhibitor (In-2-LF, suspended in 5% acetic acid) was added to wells 2, 4, 6, 8, 10, 14, 16, 18, 20, and 22 to a final concentration of 1.5 µM. Factor Xa inhibitor, Antithrombin III, was added to a final concentration of 1 µM to wells 3 ,4, 7 ,8 ,11 , 15, 16, 19, 20, 23. LF was added to wells 1-11 and 13-23 at a final concentration of 525nM, Xa was added to wells 25-35 and 37-47 at a concentration of 575 nM. Reaction buffers were as for the manual reactions

described above. The plate was incubated at room temperature on a plate rotator for 2 hours to keep the microspheres in suspension [148]. The plate was run on the HyperCyt system for 1 second/well (2 µl pickup) on 100 ms time resolution with the same FACScan settings described above. To resolve time bin based data produced by the HyperCyt system, the data were analyzed with with IDLQuery software, which was written by BE using the IDL programming language (RSI research systems Inc. Boulder, CO) and applied as described in previous work [142].

Percent inhibition of protease activity was calculated as 100 x (MFI_{test} – MFI_{min})/(MFI_{max} – MFI_{min}) in which MFI_{max}, MFI_{min} and MFI_{test} were the median green fluorescence intensities of beads in the absence of protease or inhibitors, the presence of protease alone and in the presence of the combination of test inhibitors plus protease, respectively. This calculation was made independently for each combination of protease and matching substrate bead set. Typically, 1000 or more beads in each set were assessed in each well and data for 4 separate analysis runs were averaged for graphical purposes.

3.3 Results

3.3.1 Creation of microsphere based substrates for protease assays

We created reporter proteins containing three domains: the attachment domain (biotinylation sequence), the cleavage domain, and enhanced green fluorescent protein (EGFP) as the fluorescent reporter domain (**Fig. 3.1A**) The LF reporter protein contained the consensus cleavage site (KKKKVLPIQLNAATD)

derived using FRET peptides [31] and was termed LF-sub. The factor Xa reporter protein contained the known factor Xa cleavage site (IEGR) and was dubbed Xa-sub. The expressed proteins were attached to streptavidin coated microspheres to allow for protease binding and substrate cleavage (**Fig. 3.1B**). By titrating increasing concentrations of reporter proteins onto microspheres we routinely estimated maximum specific binding of approximately 3 x 10^5 LF-sub molecules per microsphere and 6 x 10^5 Xa-sub molecules per microsphere (data not shown). The differences could be due to differing amounts of free biotin in each preparation, which could effectively block free binding sites on the microsphere, or in variations in fluorescence efficiency between the reporter proteins.

To ensure as little free reporter protein in our cleavage reactions as possible, we bound reporter proteins just above the K_D (25 nM) and we washed bound microspheres three times. This resulted in approximately 1.2 x 10^5 LF-sub and 3 x 10^5 Xa-sub molecules per microsphere. The three wash steps resulted in a microsphere loss of approximately 50%, which was estimated by coulter counting after washing (data not shown). Experimental substrate concentrations were correspondingly corrected for this loss. These wash steps were necessary, as free reporter protein would complicate measurements by serving as a sink for protease activity in solution. All experiments in this work used the Streptavidin Pink multiplex microsphere kit from Spherotech (Libertyville, IL). LF-sub was bound to microsphere 9 and Xa-sub was bound to microsphere 11 from this kit. These microspheres were used simultaneously in each protease reaction by multiplexing them based on differing orange fluorescence intensity.

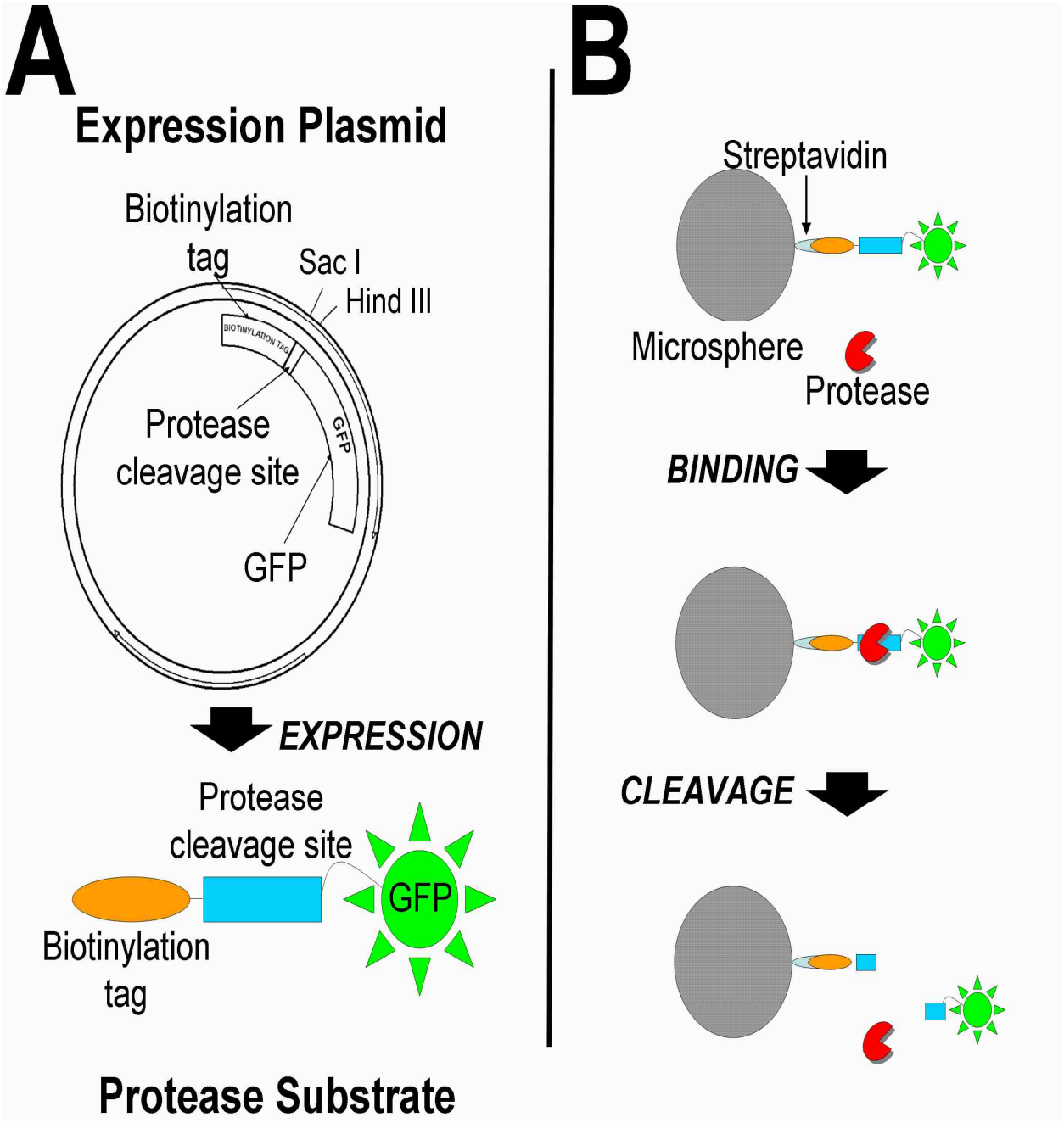

Figure 3.1. A. Expression plasmid and diagram of a substrate protein showing relevant domains. **B.** Conceptual diagram of attachment of substrate protein to a streptavidin coated microsphere, binding of a relevant protease and the subsequent cleavage step.

3.3.2 Protease cleavage assays

LF cleavage was initiated by the addition of LF to a 365 nM final concentration to a mixture containing both microsphere types. Reactions were performed at room temperature. Fluorescence was measured just prior to addition of LF (time 0) and at 1, 2, 3 and 4 hours after LF addition. Fluorescence of each microsphere type at each time was normalized to the time zero of each microsphere type and plotted as a function of time. The decrease of fluorescence on microspheres bearing LF-sub without a concurrent decrease of fluorescence on microspheres bearing Xa-sub demonstrates specific cleavage by LF of LF-sub (**Fig. 3.2A**). Factor Xa cleavage was initiated by the addition of Xa to 488 nM. The results were normalized and plotted as for the LF reaction. In similar fashion, the decrease of fluorescence on Xa-sub microspheres without a concurrent decrease of fluorescence on the LF-sub microspheres demonstrates specific cleavage by factor Xa of the Xa-sub substrate (**Fig. 3.2B**). In both cleavage reactions (**Figs. 3.2A and B**) a small decrease in the non-specific substrate as a function of time is seen. This small decrease in fluorescence of non-specific substrate bearing microspheres could be caused by small levels of non-specific cleavage, photobleaching, GFP denaturation, and/or slow dissociation of the substrate from the surface of the microsphere. Additionally, both cleavage reactions do not go to completion (**Figs. 3.2A and B**). Extended incubation (16 hours) demonstrates that cleavage can reduce fluorescence to approximately 25% of initial value (data not shown). The inability to achieve

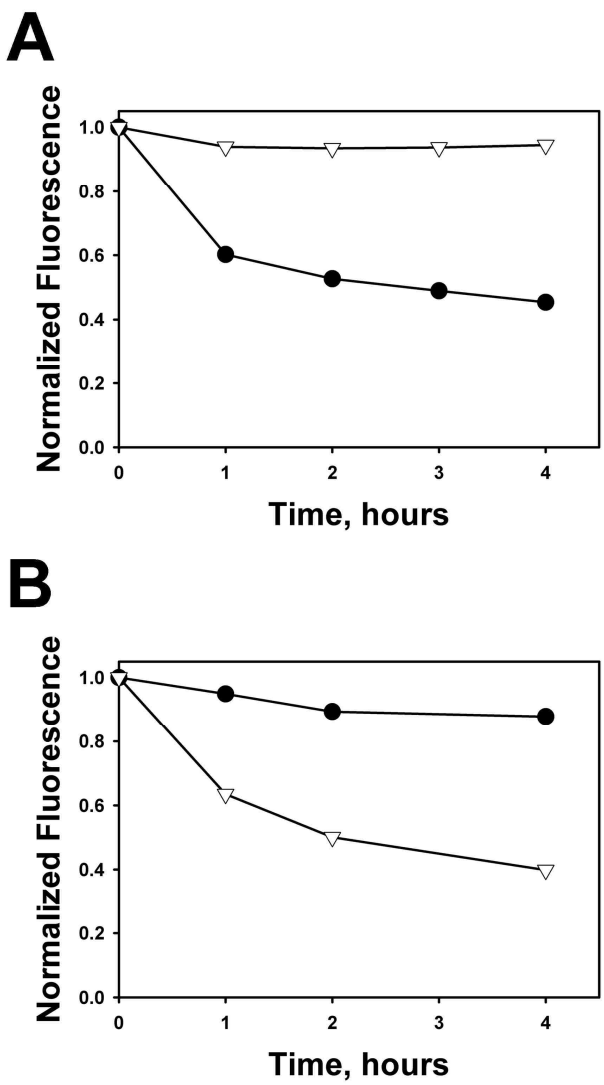

Figure 3.2. A. Normalized fluorescence as a function of time where time zero is the addition of LF to a final concentration of 365 nM to microspheres bearing lethal factor substrate (circles) or factor Xa (triangles). Mean microsphere fluorescence data were normalized to the mean microsphere fluorescence before protease addition. **B.** Normalized fluorescence as a function of time where time zero is the addition of Factor Xa to a final concentration of 488 nM to microspheres bearing lethal factor substrate (triangles) or factor Xa substrate (circles). Fluorescence normalized as in A.

100% cleavage could be the result of potential inaccessibility of some cleavage sites to the protease, time dependent loss of protease activity and/or adherence of cleaved product to the surface of the microsphere.Effects of pH on LF activity have been shown previously for solution based substrates [148]. To determine if our assay showed similar pH effects we performed room temperature cleavage assays at pHs between 5 and 10 using LF at 365 nM and Factor Xa at a final concentration of 488 nM. To correct for decreased GFP stability and reduced fluorescence as a function of pH, we performed the reactions with both microspheres bearing LF-sub and Xa-sub and normalized the fluorescence resulting from the LF-sub microspheres against the fluorescence of the Xa-sub microspheres for experiments assaying LF. Xa-sub fluorescence was normalized against the LF-sub in the same way for Xa experiments. Analyzed in this fashion, the primary contributor to the loss of normalized fluorescence was specific protease cleavage, not pH driven GFP perturbations. The results of these experiments are plotted in Figures 3.3A and 3.3C. These experiments demonstrated that LF had optimum cleavage between pHs of 6.5 to 7 and was relatively pH insensitive in pHs between 6.0 and 8.5 (**Fig. 3.3B**). Factor Xa demonstrated optimum cleavage at pH 7.4 and was relatively pH insensitive in pHs between 6.5 and 9.0 (**Fig. 3.3D**).

3.3.3 Protease and substrate concentration dependence

In the initial work presented here, we are starting the reaction through the addition of the protease. In our experimental conditions we provided the

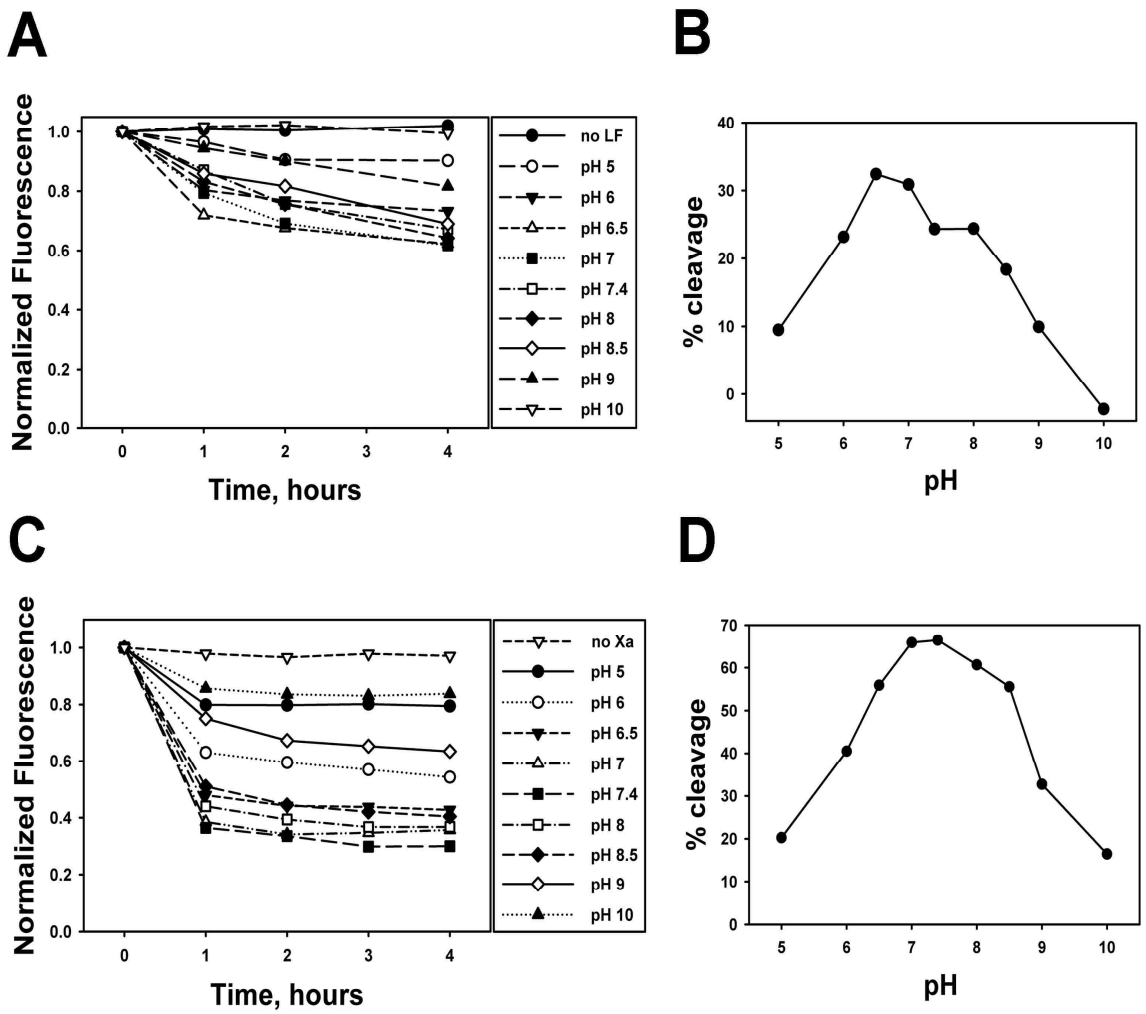

Figure 3.3. Normalized fluorescence vs. time for lethal factor and Factor Xa cleavage assays through a pH range from 5 to 10. **A.** 365nM Lethal factor was used in protease cleavage assays at the pHs indicated and normalized fluorescence was measured as a function of time. To obtain normalized fluorescence, fluorescence was first corrected for the pH effects on GFP by dividing the mean fluorescence of microspheres bearing LF-sub by the mean fluorescence of microspheres bearing Xa-sub at the same time point. These results were then normalized by dividing each time point by the result of the 0 time point to give normalized fluorescence. In this way the effects of pH on GFP fluorescence could be minimized in our measurements and only fluorescence loss due to proteolytic events are represented. **B.** 488nM Xa was used in protease cleavage assays at the pH's indicated and normalized fluorescence was measured as a function of time. Normalized fluorescence was determined in analogous fashion to A. **C and D** show the normalized % cleavage vs. pH after 2 hours of protease assays containing LF and Factor Xa, respectively.

substrate at approximately 478 pM concentrations and LF at concentrations varying from 10 to 1000 nM. The concentration of surface bound reporter protein as a function of time was plotted (**Fig. 3.4A**). As expected, increasing concentrations of LF led to increasing rates of cleavage. These experiments show that it is necessary to use above 100 nM LF in the assay to obtain a GFP fluorescence decrease above background, which results in a decay of approximately 15% in 4 hours (**Fig. 3.2A**). Increasing concentrations of LF in the reaction result in increased cleavage rates that can result in >60% cleavage after 4 hours when 1000 nM LF is present (**Fig. 3.4**). Increasing concentrations of LF do not result in a linear increase in the amount of cleavage (**Fig. 3.4**). This saturation effect suggests that increasing concentrations of LF result in faster binding of LF to the LF-sub, which causes the cleavage step (instead of LF binding) to begin limiting the maximum cleavage rate. This has been observed for other microsphere based enzyme reactions [149]. The relatively high concentrations of LF required to achieve this saturation suggest that the affinity between LF and our substrate is relatively low. A similar concentration dependence and saturation effect for Factor Xa was also found (data not shown). The relatively low affinities for both of these proteases suggest that improvements in the fusion protein by using full length substrates or smaller fluors could improve the screening assay by improving affinity between the protease and the substrate, which would reduce the amount of protease needed in the screening reaction. Nevertheless, the titration of increasing concentrations of protease allowed us to select an optimal concentration of protease to use in

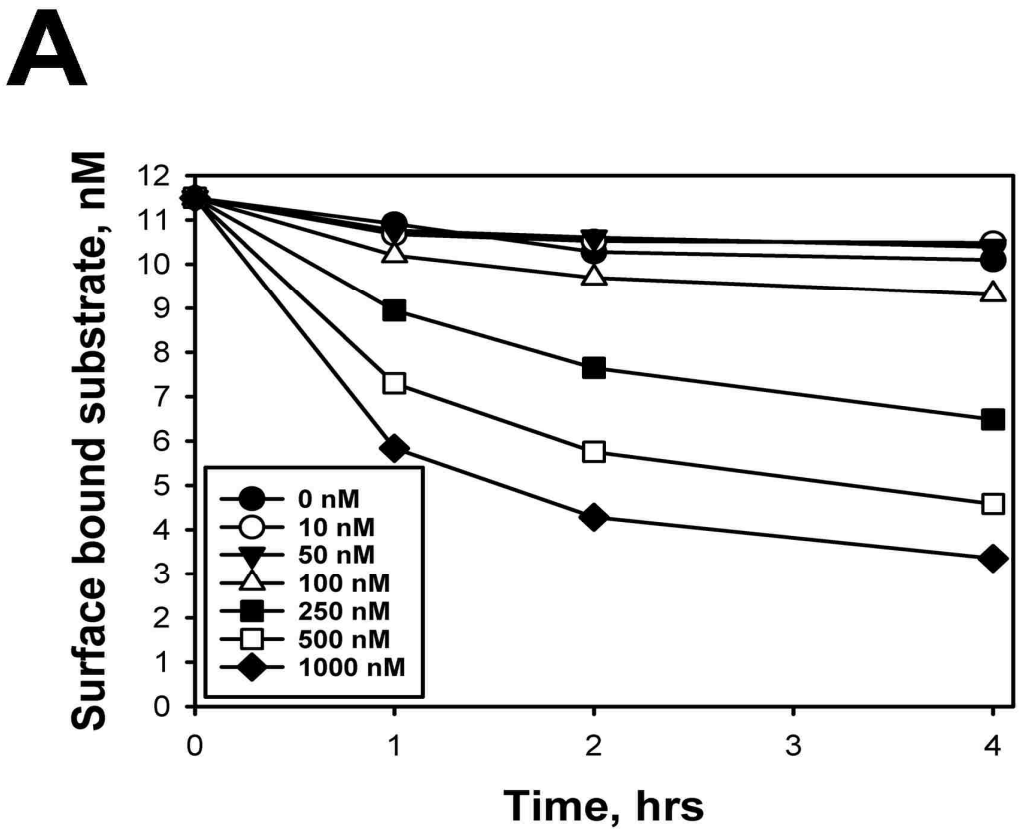

Figure 3.4. Normalized fluorescence vs. time for LF activity assays with increasing concentrations of LF as indicated in the legend (nM concentrations). Fluorescence values were normalized as described in Figure 3.2A.

the screening assays. LF-sub bound microspheres were used between 10^4 and 10^7 microspheres per ml in protease assays containing 365 nM LF. The rate of cleavage did not significantly increase as a function of increasing microsphere concentrations (**Fig. 3.5**). This minimal change as a function of increasing microsphere is most likely a result of low substrate concentrations (2×10^{-12} to 2×10^{-9} M LF-sub for these numbers of microspheres). These low concentrations are expected to be well below the K_D for LF binding. Increasing substrate concentrations further is complicated by the extremely high microsphere density required.

3.3.4 Lethal Factor and Factor Xa inhibiton

We performed a titration of increasing concentrations (1 nM to 10 μM) of the known LF inhibitor IN-2-LF into LF protease assays. This set of experiments clearly demonstrates inhibition of the cleavage of LF-sub from the surface of the microsphere (**Fig. 2.6A**). It is possible that some inhibition of cleavage activity could have been due to potential pH changes resulting from the 5% acetic acid used to make the IN-2-LF stock solution. However, inhibition is seen at concentrations as low as 100 nM and near complete inhibition seen at 250 nM IN-2-LF (**Fig. 2.6A**). These represent greater than 2000 fold dilutions (to a final concentration of <0.025% acetic acid) of the stock solution into a buffered solution. Furthermore, addition of acetic acid at the same concentration without the addition of inhibitor did not affect the cleavage reaction (data not shown). Therefore, inhibition is not likely to be a result of pH changes and most likely the effect of the increasing concentrations of IN-2-LF. We detected inhibition at

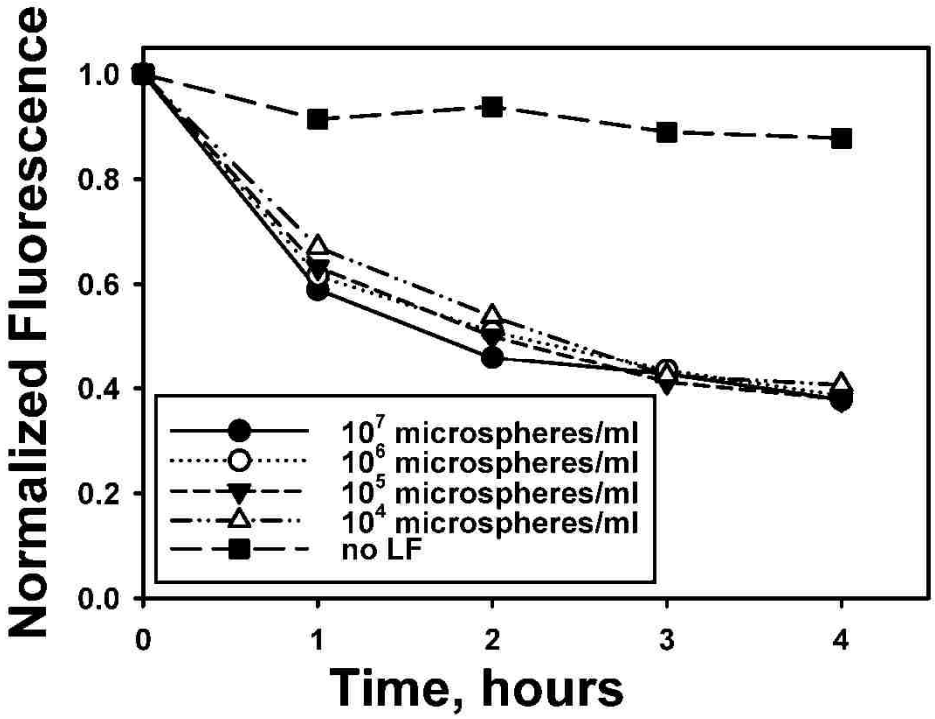

Figure 3.5. Increasing concentrations of microspheres (as indicated in the legend) bearing LF-sub were used in the LF protease assay and normalized fluorescence vs. time for each assay was plotted. Fluorescence was normalized as described in figure 3.2A.

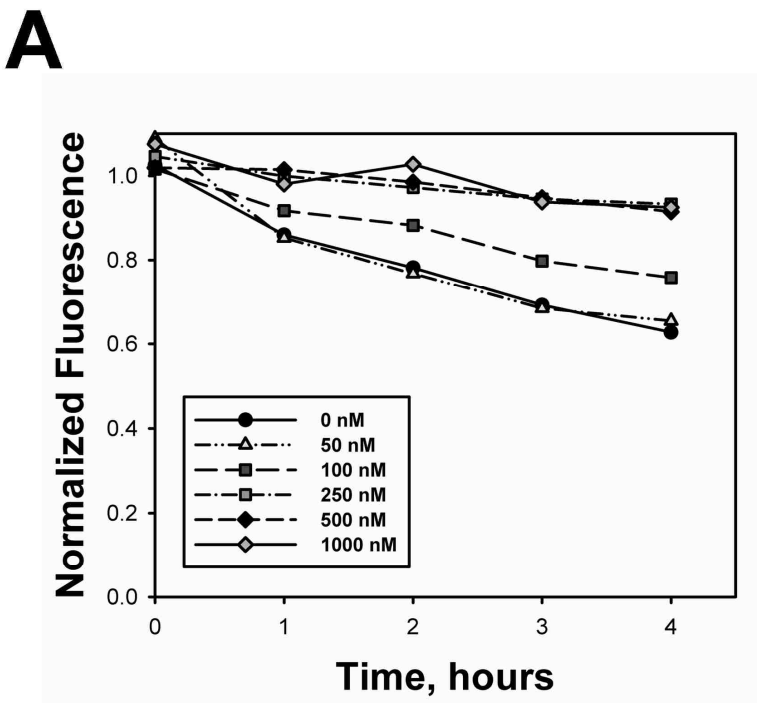

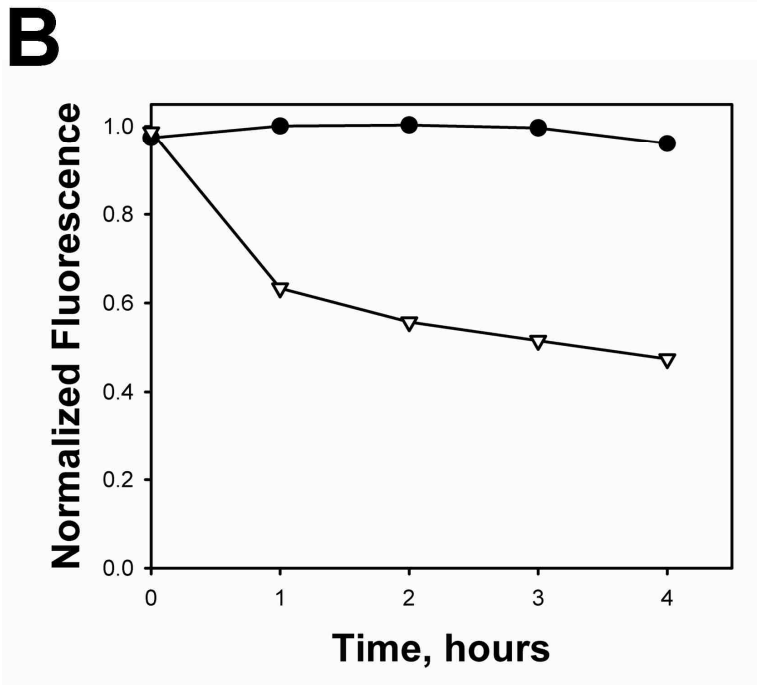

Figure 3.6. A. Inhibition of Lethal Factor by IN-2-LF. LF at 365 nM was used in protease assays with increasing concentrations of of IN-2-LF as indicated in the legend. Fluorescence was normalized as in Figure 3.2A. **B.** Factor Xa was used in protease assays at 488 nM with (circles) and without (triangles) 1 μM antithrombin III. Fluorescence was normalized as in Figure 3.2B.

approximately 100 nM, which is consistent with other measurements using different methods [150]. Factor Xa cleavage reactions were performed with and without 1 μM of the Factor Xa inhibitor antithrombin III, which almost completely inhibited cleavage (**Fig. 3.6B**).

3.3.5 High throughput screening (HTS) protease assays with the HyperCyt® platform.

To assess performance of the protease assays under HTS conditions, LF and Factor Xa were added to microspheres bearing LF-sub and Xa-sub in protease reactions performed in microtiter plate wells that also contained no inhibitor, IN-2-LF, anti-thrombin III or both inhibitors. After incubation for 2 hrs at room temperature in a rotating particle suspension system, which has been described previously [142], beads from each well were sampled at 40 wells per minute and analyzed using the HyperCyt® platform (**Fig. 3.7**). This experiment allowed us to clearly resolve inhibition of LF cleavage by IN-2-LF on LF-sub bearing microspheres and inhibition by anti-thrombin of Xa cleavage on Xa-sub bearing microspheres. Four replicate experiments using this approach (6-8 replicate wells per experiment), demonstrated that LF activity was inhibited by IN-2-LF by an average of 74 ± 5% (mean ± SD) as compared to only 16 ± 4% inhibition mediated by anti-thrombin (**Fig. 3.8**). In the parallel Factor Xa protease assays, anti-thrombin inhibited Xa-sub cleavage 82 ± 4%. Unexpectedly there was an apparent enhancement of Xa protease activity in the presence if IN-2-LF (Fig. 6, 43 ± 2% stimulation). Additionally, a reduction in inhibition was seen in

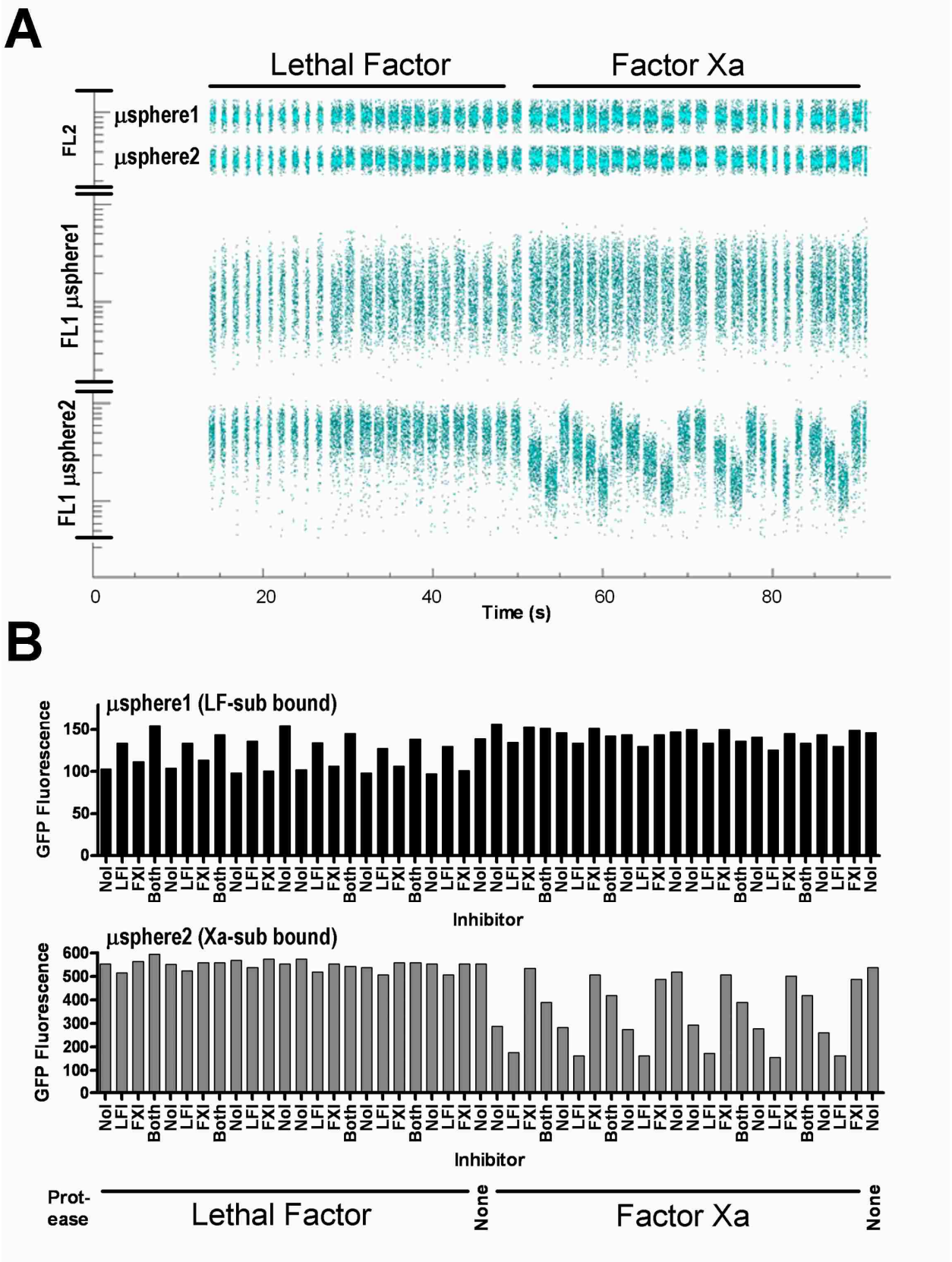

Figure 3.7. (previous page) High throughput protease assay sample from a 96 well plate. A. Time-resolved fluorescence analysis of two microsphere sets, µsphere1 and µsphere2, each present in 48 wells of a 96 well plate. From left to right along the time axis each vertical column of discrete data clusters represents fluorescence data from a single well. Wells 1-23 contained Lethal Factor, wells 25-47 contained Factor Xa and wells 24 and 48 were protease free. Sets µsphere1 and µsphere2 were coated with GFP-tagged substrates for Lethal Factor and Factor Xa, respectively. Top series: The microsphere sets were distinguished by distinct levels of fluorescence intensity in the FL2 fluorescence channel. Middle series: GFP fluorescence intensity distribution of µsphere1 microspheres in the FL1 fluorescence channel (analysis gated on µsphere1 FL2 fluorescence). Bottom series: GFP fluorescence intensity of µsphere2 in the FL1 fluorescence channel (gated on µsphere2 FL2 fluorescence). B. Bar graphs of the median GFP fluorescence intensity of µsphere1 (top – bars in black) and µsphere2 (bottom – bars in gray). Each bar represents results from a single well. Wells containing IN-2-LF an inhibitor of Lethal Factor are labeled LFI, antithrombin III an inhibitor of Factor Xa are labeled FXI, wells containing both inhibitors were labeled Both, and wells without inhibitor were labeled NoI. These wells were run in the presence of either Lethal Factor, Factor Xa or no protease (None) as indicated by the labels below the bar graphs.

Factor Xa assays when both IN-2-LF and anti-thrombin were used together as opposed to anti-thrombin III alone. This further suggests that the addition of IN-2-LF is enhancing factor Xa cleavage. This enhancement was evident with or without normalization to correct for possible pH effects (described in Fig. 3 legend) resulting from the IN-2-LF diluent (acetic acid). We have also confirmed the stimulatory effects of IN-2-LF addition of Xa cleavage using manually mixed samples (data not shown). Therefore, the mechanism of this potential enhancement requires further study.

3.4 Discussion

We have demonstrated a novel flow cytometry system capable of measuring specific protease activity in a multiplex system with implications for

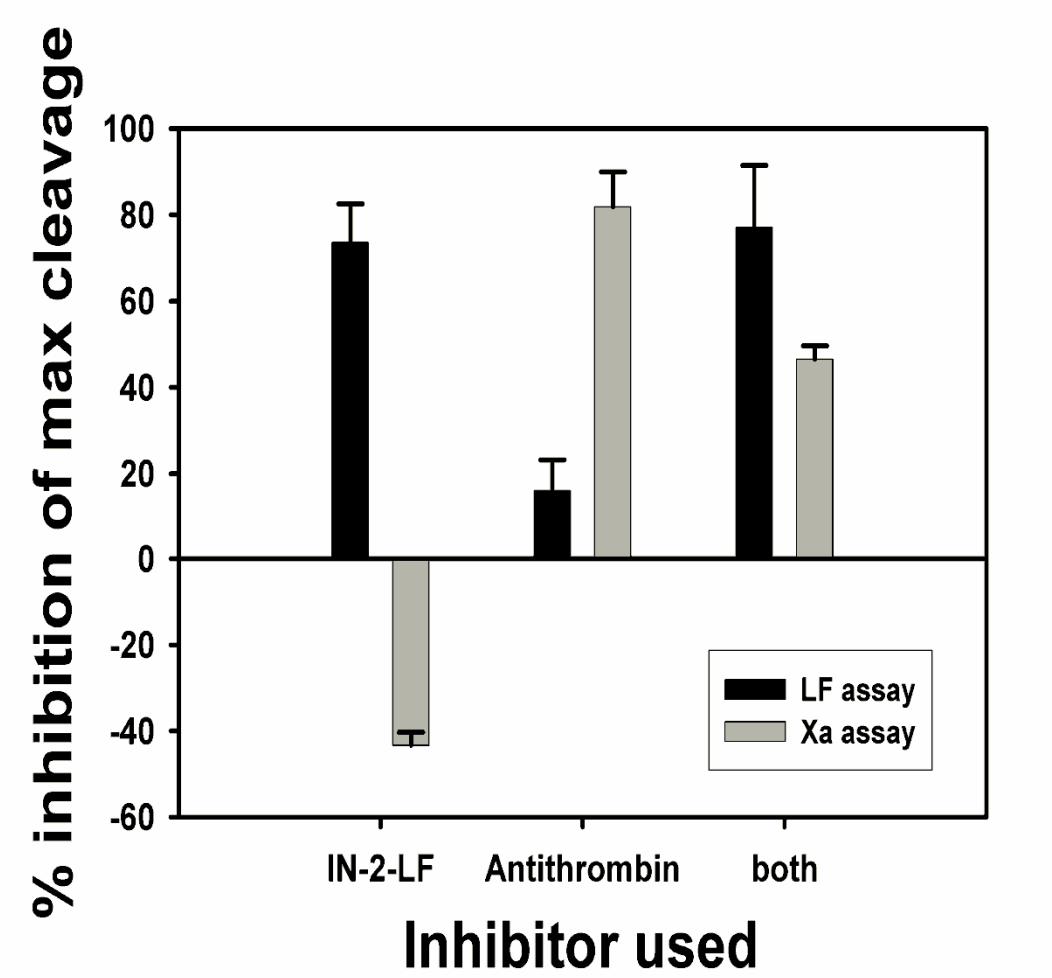

Figure 3.8. Inhibition of both LF and Factor Xa using the HyperCyt screening system. 24 wells containing both microsphere bound substrates were co-incubated with no inhibitor(6 wells of each assay), LF inhibitor IN-2-LF(6 wells of each assay), Xa inhibitor (6 wells of each assay) Antithrombin III (6 wells of each assay) or both(4 wells of each assay) were screened with each protease. Two control wells with no protease for each reaction were used for measuring GFP stability. % inhibition is the % difference between the no inhibitor samples and the no protease samples. Error bars are set on two standard deviations (95% confidence) of the experimental data values for four independent samples of the same reaction plate.

inhibitor screening for proteases. In this simplified model system we have shown specific cleavage for two different proteases of different classes: the *B. anthracis* Lethal Factor, a bacterial pathogen metalloprotease important in anthrax infection, and factor Xa, a human serine protease involved in blood clotting pathways. We have also optimized this system with regards to enzyme concentration, pH and microsphere concentration. Finally, we have used known inhibitors of these proteases in our model and the HyperCyt® HTS system [141, 142] to show the feasibility of this system to perform pharmaceutical screening for protease inhibitors.

The combination of continuous kinetic resolution, multiplex ability and high throughput capability of flow cytometry gives this assay some distinct advantages over other previously used protease assays in both the measurement of activity able to evaluate up to twelve individual substrates in the same reaction, eliminating the experimental variability of performing twelve separate experiments and allowing a built in negative control that can also be used to normalize data varying in pH or other chemical environments which may affect GFP (or other reporter molecule) fluorescence. This approach could also be of value to screen for inhibitors across a set of proteases simultaneously. We have demonstrated this concept using a binary set of proteases (**Fig. 3.7, Fig. 3.8**). Extension of this concept to proteases involved in disease states could allow simultaneous target inhibition and potential side effect screens. With other multiplex microsphere sets, experiments with up to one-hundred substrates could be attained. Additionally, this system is surface based and has the option of

using full length protein substrates, which will be used in extending our studies to full length substrates to evaluate the contributions of MAPKK distal element [7, 8]. Inclusion of substrates with the distal element could be greatly beneficial in the creation of a screening assay to detect LF inhibitors. The screening applications using the HyperCyt® system also use small amounts reagents to minimize screening costs. HyperCyt®, combined with our protease assay system, will enable us to screen for inhibitors of LF and other medically relevant proteases in a low cost high-throughput fashion. Inhibition of LF itself has been implicated to be a better pharmaceutical target than the LF Protective antigen interaction [145], which is currently under intense investigation as a pharmaceutical and second generation vaccine target [151].

Of course, as with any screening system, there are some potential weaknesses to this approach. First, our approach does not require separation steps, but it will require the attachment of an extrinsic fluorophore via chemical conjugation or the use of fluorescent fusion proteins. These additions can potentially affect the activity screen and care must be taken to verify that activity remains at a level that allows detection of inhibitors. Alternative approaches such as gel separation or mass spec can be extremely tedious, require the use of extremely expensive instrumentation, and have limited throughput. Second, the use of microspheres limits the concentration of substrate in most cases to the nM range. This will require that the affinity of the protease for the substrate be suitably tight or the use increased concentrations of the protease. Thus, high affinity substrates must be engineered, which can lengthen assay development

time, or increased enzyme concentrations must be used, which will increase assay cost. This complication is largely true of any surface based approach. The solution based approaches (*e.g.* FRET) can drive the reaction with low affinity substrates simply by the addition of large amounts of substrate (also increasing assay cost) but, as described above, are limited in their ability to observe interactions distal to the cleavage site. Additionally, future improved substrates will be necessary to minimize the potential of false negatives due to high enzyme concentrations and care will always have to be taken to make sure that inhibitor additions do not change buffer conditions to the point where false positives may occur. However, even with the above complications, the high assay throughput, assay flexibility and ability to screen full length substrates will make multiplex microsphere based assays using the HyperCyt® system a highly competitive platform for protease inhibitor screens.

This ease of monitoring substrate cleavage combined with the continuous kinetic resolution provided by flow cytometry suggest that kinetic mechanism studies using this microsphere based method will also be valuable and we are planning to use this assay format to separate kinetic steps of binding, catalysis, enzyme release and re-binding involved in LF protease activity to help understand each process in more detail. Initial work here demonstrates that LF has relatively low affinity for the microsphere bound substrate (**Fig. 3.4**), which is consistent with observations of other groups that report >2 µM K_m values for a variety of optimized synthetic peptides [150]. We also observed that our assay had a very slow cleavage rate taking hours to go to completion (**Fig. 3.4**), which is

clearly slower than what other groups have observed using FRET peptides [31] [150]. The poor affinity and slow observed cleavage rate could be the result of several factors including a suboptimal substrate (*e.g.* it lacks the distal binding element and it has a large fluorophore attached), steric effects at the surface of the microsphere and suboptimal reaction temperatures. Future studies will use full length substrates, alternative fluorophores, high resolution flow cytometry kinetic approaches [152]. and more advanced temperature control approaches [153] to investigate these issues.

Some of the above potential uses and advantages of flow cytometry based protease assays were noted in gelatinase B studies, where gelatin was non-specifically labeled using FITC and adsorbed onto polystyrene microspheres followed by digestion with gelatinase, which resulted in the loss of microsphere associated fluorescence [139]. All reactions were performed in single-plex and separate reactions of microspheres were used for negative controls and inhibitor demonstrations. In the work presented here, we have developed a new approach whereby we use oriented attachment of the protease substrate along with interchangeable cleavage sites to create a general system to study any site specific protease. Additionally, we have optimized these assays for further use in screening and kinetic studies. Furthermore, we have performed the first multiplex protease assays by flow cytometry and demonstrated their advantages and use in high throughput screening assays. We anticipate this work will be the basis of both future screening and kinetic studies for the proteases shown here as well as many other proteases.

3.5 Acknowledgements

The authors would like to thank Siyoung Lee for technical work and preliminary work on protease assays, La Verne Gallegos-Graves and Rhiannon Nolan for plasmid subcloning and technical work, Alina Deshpande for LF technical mechanism discussion and reviewing of literature, Hong Cai for technical assistance, and Susan Young for technical assistance on the HyperCyt® screening system in the University of New Mexico Flow Cytometry Shared Resource. This work was funded in part by the National Flow Cytometry Resource NIH/NCRR 2P41RR001315, by the NIH Screening Center Grant to UNM and by Joint Science and Technology funding from Los Alamos National Labs to UNM.

Chapter 4.
High Throughput Multiplex Flow Cytometry Screening for Botulinum Neurotoxin type A Light Chain Protease Inhibitors

Matthew J. Saunders[1,2,3], Steven W. Graves[2,3], Larry A. Sklar[1], Tudor I. Oprea[1,4] and Bruce S. Edwards[1]

[1]University of New Mexico Center for Molecular Discovery and Department of Pathology. Albuquerque, NM

[2]The Center for Biomedical Engineering, Department of Chemical and Nuclear Engineering, University of New Mexico Albuquerque, NM.

[3]The National Flow Cytometry Resource , Los Alamos National Laboratory, Los Alamos, NM

[4]University of New Mexico Division of Biocomputing, Department of Biochemistry and Molecular Biology, Albuquerque, NM

(Accepted for publication in *Assay and Drug Development Technologies)*

Abstract

Given their medical importance proteases have been studied by diverse approaches and screened for small molecule protease inhibitors. Here we present a multiplexed microsphere based protease assay that uses high throughput flow cytometry to screen for inhibitors of the light chain protease of Botulinum Neurotoxin type A (BoNTALC). Our assay uses a full-length substrate and several deletion mutants screened in parallel to identify small molecule inhibitors. The use of multiplex flow cytometry has the advantage of using full length substrates, which contain already identified distal binding elements for the BoNTALC, and could lead to a new class of BoNTALC inhibitors. In this study we have screened 880 off patent drugs and bio-available compounds to identify Ebselen as an in vitro inhibitor of BoNTALC. This discovery demonstrates the validity of our microsphere-based approach and illustrates its potential for high throughput screening for inhibitors of proteases in general.

4.1 Introduction

Proteases regulate many biological pathways, including: blood clotting and immune system activation [4], bacterial toxins [2], metastasis [154], viral life cycles [6], among many others. For these reasons, a large number of proteases are currently under investigation as pharmaceutical targets [2]. Within the larger set of proteases, pharmaceutical development for the BoNTALC is of interest due its role in natural disease [94] its potential role in biothreat scenarios, and increasing use as a pharmaceutical [155], which increases the potential for both accidental and intentional misuse [156].

The Botulinum neurotoxin type A light chain protease (BoNTALC), which is delivered to the cell via the toxin heavy chain, is a Zn^{2+} metalloprotease that specifically cleaves synaptosome-associated protein of 25 kilodaltons (SNAP-25), causing paralysis and death [51]. SNAP-25 contains potential conserved sites of protease interaction, termed the SNARE motif at four positions. Three N terminal SNARE motifs, S1 (residues 21-31), S2 (residues 35-45), S3 (residues 49-59) are present , and the S4 SNARE motif (residues 145-155) is located near the cleavage site [9]. Activity assays strongly suggest that S4 contains a preferred SNARE interaction site and is required for specific BoNTALC activity [71, 72]. The importance of the S4 site was confirmed via identification of the α exosite in the co-crystal structure between SNAP-25 and BoNTALC [10], which contains many contacts between the two proteins and overlaps the S4 SNARE motif. These observations, taken together, have led to a generally accepted mechanism: BoNTALC first binds to the α exosite of SNAP-25, corresponding to the S4 site,

which creates a conformational change in BoNTALC, and leads to proteolytic cleavage of SNAP-25 [10, 79]. Furthermore, the co-crystal structure indicates that BoNTALC has close contacts at many positions in the substrate beyond the α exosite. [10]. Thus, use of the full length SNAP-25 substrates, in the context of the proposed mechanism, makes its use highly desirable in screening assays.

Despite the desirability of full-length substrates, most BoNTALC screening assays use small peptides and FRET to monitor cleavage [116, 125]. The potential for discovery of inhibitors that interfere with BoNTALC-SNAP-25 interaction at the α-exosite has been suggested but have yet to be discovered [9, 12, 13]. Such inhibitors could be highly desirable as they would not likely be competitive inhibitors, which could reduce their potential for toxicity as BoNTALC contains the highly conserved Zn^{2+} metalloprotease active site found in many human proteases [157, 158]. Alternatively, cleavage of fluorescently labeled proteins from a surface offers the ability to use full length protease substrates. Among the several assays of this type, microsphere based protease assays are particularly compelling as protease activity can be measured via the loss of a fluorescent protein from the surface of the microsphere, which is performed very simply on a flow cytometer due to its inherent ability to discriminate fluorescent molecules bound to the surface vs. those in solution [127, 140]. Flow cytometry also enables simultaneous analysis of multiple substrates in the same sample via use of distinct microsphere populations for each substrate, each distinguished by differing amounts of internal fluorescence intensity.

In this work, we have we have developed a set of fluorescent SNAP-25 substrates that are attached to a multiplex set of microspheres and measured BoNTALC activity by loss of microsphere associated fluorescence as monitored by flow cytometry. We have validated the use of this assay for high-throughput screening of protease inhibitors by implementing it on the HyperCyt® high throughput flow cytometry screening system [127, 141, 159] to rapidly screen a small molecule library of chemical compounds.

4.2 Materials and Methods

4.2.1 Reagents

Hepes hemisodium salt, sodium chloride, PBS carbenicillin, chloramphenicol, biotin, DTT, IPTG, Tris base, Tween 20, BSA and ebselen were obtained from Sigma-Aldrich corporation (St. Louis, MO). BoNTALC and the SnapTide FRET peptide were obtained from List Biological Labroatories (Campbell, CA). Softlink streptavidin resin was obtained from Promega Corporation (Madison, WI). Streptavidin coated pink particle kit was obtained from Spherotech corporation.(Lake Forest, IL). Amicon Ultra-15 filters were purchased from Millipore (Billerica, MA). TB was purchased from Fisher scientific (Pittsburg, PA). Restriciton enzymes and ligase was obtained from New England Biolabs (Ipswich, MA). DNA oligionucleotides were synthesized by IDT (Coralville, IA) and, Operon (Huntsville, AL). 96 well plates were obtained from ISC BioExpress (Kaysville, UT). QIAprep spin miniprep kit was purchased from

Qiagen (Hilden, Germany). 8 ml glass econo-columns were obtained from BIO-RAD Laboratories (Hercules, CA).

4.2.2 Construction of biotinylated substrate plasmids

Protease substrate plasmids were based on the Promega PinPoint biotinylation tag vectors with enhanced green fluorescent protein cloned at the C terminus of the open reading frame as described previously [127].The negative control plasmids Xa sub and LF substrate were created as described previously[127].(The SNAP-25 GFP plasmid was created by restriction digest of the Xa sub plasmid with (BamH1 and Sac1) and ligation of a SNAP-25 PCR product from a SNAP-25 clone plasmid obtained from Open Biosystems (Huntsville, AL) using the primers CCACCGAGCTCATGGCCGAAGACGCAGACAT and GTGGGCGGATCCGCC CACTTCCCAGCA and digested with Sac1 and BamH1, into the Xa sub plasmid between the biotinylation tag and EGFP. The binding site deletion plasmids SNAP-25 ΔS1-S3 and SNAP-25 ΔS4 were created by whole plasmid PCR of the SNAP-25 full length plasmid with PCR primers flanking the binding sites of interest containing an Apa1 restriction site and ligated together. SNAP-25 ΔS1-S3 was created using the primers GAGCTAGGGCCCGTCGAAGAAGGCATGAACC and CCAATCGGG CCCCTGGTCAGCCCTTCGCTGCA. SNAP-25 ΔS4 was created using the primers GGGCCCATCATCGGGAACCTCCGT and GGGCCCATTTTCTCGGGCATCATTTG

The SNAP-25 Δ S1-S4 plasmid was created by using the SNAP-25 ΔS1-S3 plasmid and the primers GACTACACGCGTGGCATCATCGGGAACCTCCGTCACATGGCCCTGGA and GACTCAACGCGTATTTTCTCGGGCATCATTTGTTACCCTGCGGATGAAGCC G, digesting with Mlu1 and ligating the plasmid ends together. The LF15 optimized Lethal Factor cleavage sequence was cloned by digesting the Xa sub plasmid with Sac1 and HindIII and using the 5' phosphorylated DNA oligionucleotides of sequences CAGAAGAAAGAAGGTTTATCCATATCCAATGGAAACCATTGCTGGTCA and AGCTTGACCAGCAATGGTTTCCATTGGATATGGATAAACCTTCTTTCTTCTG GAGCT. Plasmid ligations were transformed into calcium competent SCS1 *E. coli,* minipreps were done with a Qiagen QIAprep miniprep kit and were sequenced to confirm correct sequences.

4.2.3 Expression and Purification of Biotinylated Protease Substrates.

Calcium competent BL21 (DE3) pLys S *E. coli,* transformed with plasmids of interest were grown overnight in 3 ml of TB media containing 50 µg/ml of carbenicillin and 34 µg/ml chloramphenicol then transferred to 200 ml of TB containing 50 µg/ml of carbenicillin and 34 µg/ml chloramphenicol and 40 µM biotin and grown at 37ºC to an opitcal density at wavelength 600 between 0.6 and 0.8. Cultures were then induced using 100 µM of IPTG and grown at 30ºC overnight in a shaking incubator. Cells were spun down at 10,000 xg for 10

minutes on a a Beckman Avanti J-301 centrifuge at 4ºC, suspended in lysis buffer (50 mM Tris-HCl, 1 mM EDTA, 100 mM NaCl, pH 8.3) and frozen at -20ºC.

Frozen cells were thawed on ice and sonicated on Branson Sonifier 250 model sonicator for 10 minutes on pulse setting, then centrifuged at 13,000 x g for 30 minutes at 4ºC. Soluble fractions were then poured into fresh centrifuge tubes and centrifuged at 13,000 x g for 30 minutes at 4ºC. The supernatant was then pumped with a peristaltic pump over a 8 ml glass Bio-Rad econo-column containing 5 ml of Softlink streptavidin resin at a flow rate of 1 ml/min at 12ºC. The column was washed with 200 ml of PBS containing 1 mM DTT, to prevent crosslinking of cysteine rich molecules, at a rate of 1 ml/min. The column was then filled with 6ml of PBS with 1 mM DTT and 5 mM biotin and let set for 30 minutes before elution with the same buffer. Elution fractions were collected and combined into a 12-15 ml pool. 4 ml fractions of this pool were centrifuged in an Amicon Ultra-15 30,000 Molecular weight cutoff filter for 10 minutes at 4,000 xg at 4ºC and condensed into 500 µl fractions. The remaining purified protein from the 12-15 ml pool was added and this was repeated until the entire elution pool was in a volume of 500 µl to 1 ml. 4 ml of PBS with 1 mM DTT was added to the Amicon Ultra-15 Mw 30,000 cutoff filter and centrifugation was repeated to remove free biotin, this process was repeated 20 times to remove as much free biotin as possible. 1-2 ml of purified protein was then dialyzed against 2L of 50 mM HEPES, 100 mM NaCl for 4 hours for two rounds of dialysis. Sodium azide was added to a concentration of 0.02% to prevent bacterial growth. Purified

proteins were stored at 4ºC. Protein concentrations were determined using A280 spectroscopic measurements and calculated extinction coefficients.

4.2.4 Binding biotinylated substrates to streptavidin microspheres

Spherotech streptavidin coated pink particle kit microspheres were used with the following protease substrate GFP protein molecules. The P.01 microsphere was incubated with SNAP-25 ΔS1-S4. P.05 was incubated with the Lethal Factor consensus substrate to be used as a negative control. P.07 was incubated with SNAP-25 ΔS4. P.09 was incubated with SNAP-25 full length and P.11 was incubated with SNAP-25 ΔS1-S3. 50 µl of microspheres at a stock concentration of 10^8 microspheres/ml was used in a final volume of 500 µl of protease buffer (50 mM HEPES, 100 mM NaCl, 1 mg/ml BSA, 0.025% Tween 20, pH 7.4) with 25 to 50 nM biotinylated GFP protease substrate molecule for 1 hour at room temperature on a neutator mixing device covered from light. Microspheres and GFP substrates were centrifuged at 14,500 rpm in an Eppendorf mini-spin plus centrifuge with a F45-12-11 rotor for two minutes. The supernatant was removed by pipette while the microsphere pellets were left intact, 500 µl of protease buffer was added to the microsphere pellets and the process was repeated three times. All microsphere pellets were suspended in 200 µl protease buffer and combined into one 1 ml fraction. 3 ml of protease buffer was added to this 1 ml fraction for loading into 96 well screening plates.

For inhibition verification experiments 50 µl of microspheres were used in the same 500 µl volumes with identical wash steps and brought up to final volumes of 1 ml with 100 µl of microspheres being used in 500 µl volumes run on a

FACScan flow cytometer using 5 nM Botulinum Neurotoxin type A Light Chain (BoNTALC) protease.

4.2.5 Plate setup and incubation

For screening of the Prestwick chemical library ISC BioSystems Genemate 96 well PCR plates were used. 14 µl of the microsphere mix was added to each well of the 96 well plate by multichannel pipette. To column 1 of the plate, no test compound was added and an additional 1 µl of microsphere mix was added. Test compounds from the Prestwick library were diluted 1 to 5 in protease buffer and 1 µl of each dilution was added to a test well in the screening plate. The final concentration of test compounds in the screening plate was 20 µg/ml, or approximately 50 to 100 µM. Wells A12, B12, C12 and D12 had $ZnCl_2$ (a known inhibitor of metalloproteases) added to a final concentration of 1 mM. Final DMSO concentrations in the assay were 1%. This level of DMSO was shown not to affect the protease assay as cleavage in endpoint assays was unchanged when they contained DMSO at concentrations as high as 10% (data not shown). Test compounds from the Prestwick library were added to wells prior to BoNTALC. 5 µl of 0.01 mg/ml BoNTALC suspended in protease buffer was added to each well except wells E12, F12, G12 and H12, giving a final concentration of 5 nM BoNTALC protease. Plates were incubated at room temperature for 1 hour on a plate rotator to keep microspheres in suspension. 1 hour time points were chosen for screening in order to give maximum protease cleavage of substrate and the ability to screen plates sequentially. Substrate concentrations were determined based on the binding capacity of the streptavidin

coated microspheres used in our assay. Plates were set up in duplicate, and each copy run three times on the Hypercyt® system.

4.2.6 High Throughput Screening and Data Analysis.

High throughput screening of plates was done on the Hypercyt® high throughput flow cytometry screening system connected to a Dako Cytomation CyAn ADP flow cytometer with settings of FS Peak Gain 15, SS Log voltage 300, gain 1.0, FITC Log voltage 700, gain 1.0 and PE Log voltage 700 gain 1. Wells were sampled for 1 second with approximately 2 µl volumes aspirated, with a 1 second wash step of protease buffer between each well. Each duplicate copy of each plate was sampled three times. Data analysis was done using the IDLe Query program developed by Dr. Bruce Edwards [127]. Each of the microsphere sets were gated in the PE channel using a compensation value of PE fluorescence- 7.6% FITC fluorescence. Median green fluorescence values for each microsphere set was calculated for each well of a 96 well plate. Data was exported to Excel in spreadsheet format for further analysis. Z' values were calculated for each bead set by using the average median and standard deviation values for wells containing no protease as a positive control and wells containing no test compound as a negative control. % inhibition was calculated using the formula (100* (averaged median well fluorescence – negative control average median fluorescence/ (positive control average median fluorescence - negative control average median fluorescence)). % inhibition values were averaged for each well with data for wells containing less than 50 events or Z'

values for a particular substrate below 0.3 not used. The averaged values for each duplicate plate copy were then averaged to give an averaged % inhibition value for each compound well. Compounds which gave an averaged % inhibition value above 20% were selected for follow up work.

4.2.7 Dose Response curves for follow up compounds.

Follow up work for compounds with more than 20% inhibition was done in 500 µl volumes of protease buffer and substrate bound microspheres. 5 nM Light Chain was used with increasing concentrations of test compounds and added after running the sample for 30 seconds on the flow cytometer. Samples ranged from 1 µM test compound to 50 µM test compound with samples of 1 µM, 5 µM, 10 µM, 25 µM and 50 µM. A positive control sample with no protease was run along with a negative control with no inhibitory compound. Protease was added to each sample and incubated at room temperature while mixing on a neutator. Samples were run on a Becton Dickinson FACScan flow cytometer with 100 µl samples run on the cytometer every 30 minutes. FACScan PMT settings were FSC E00/9.25, SSC 225 log, FL1 700 log and FL2 600 log, compensation values of FL2 -12% FL1 and gates were drawn on individual bead set in the FL2 histogram plot. Percent inhibition was calculated by taking the 1 hour sample value – 1 hour no inhibitor value and dividing by the 1 hour no protease value- 1 hour no inhibitor value and multiplying by 100.

4.2.8 Inhibitor testing against LF protease

To test the specificity of the identified inhibitor against BoNTALC the LF15 GFP substrate protein was bound to Spherotech streptavidin pink particle P.07 and SNAP-25 GFP substrate protein was bound to microsphere P.11. Microspheres were bound and washed as described above. These were combined into 1 ml with 100 µl of microsphere mix being used in each sample. Sample volume of 600 µl samples of protease buffer with the desired amount of inhibitor added were used. 100 µl of sample, microspheres and inhibitor, were taken and run as a 0 minute time point on a FACScan flow cytometer. 5 nM Light Chain protease and 500 nM Lethal Factor protease were then added to tubes together to begin the assay. Samples were run on a Becton Dickinson FACScan flow cytometer as before but without compensation. Samples were run for time periods of 1 minute on low flow rate every 30 minutes Data were normalized by dividing each time point mean fluorescence values for each gated microsphere by the 0 minute value collected for that microsphere before proteases were added.

4.2.9 Detailed dose response curve for ebselen.

To get a more detailed dose response curve for the inhibitor ebselen against full length SNAP-25 GFP 50 µl of each microsphere set was used with SNAP-25 GFP bound to microsphere P.11 and LF15 GFP bound to microsphere P.07 as described above. Microspheres were washed 3 times, combined and brought up to a 1,400 µl volume. 100 µl of the microsphere mix was used in each sample in 500 µl total volumes containing amounts of ebselen in the increments of 1 µM, 2.5 µM, 5 µM, 6 µM, 7 µM, 8 µM, 9 µM, 10 µM, 12.5 µM, 15

μM, 25 μM and 50 μM. Samples were run for 30 seconds on a FACScan flow cytometer with settings described above. 5 nM LC was added after 30 seconds and data analyzed for 15 minutes on continuous run. % inhibition was calculated by using the first 60 second slopes and the equation (slope no inhibitor-slope sample)/slope no inhibitor) *100.

4.2.10 Inhibitor measurements by FRET

The SNAPtide peptide from List Biological Laboratories was used at a concentration of 5 μM in protease buffer with excitation at 490 nm and emission measured at 523 nm on a PTI fluorimeter model # LPS 220B, with the PTI monochrometer slit size of 2 nm and a stir bar continuously stirring the sample. 5 nM BoNTALC protease was added at 60 seconds of measurement and run for 10 minutes with samples containing increasing concentrations of identified inhibitor present. The 10 minute slopes of each sample were taken and converted to percent inhibition using the equation (slope no inhibitor – slope sample)/slope no inhibitor *100.

4.3 RESULTS

4.3.1 A multiplex microsphere based flow cytometry assay for BoNTALC activity

Four fusion proteins from SNAP-25 (bearing amino terminal biotinylation tags and carboxyl terminal GFP labels) were cloned, purified, and attached to a multiplex set of microspheres (**Fig. 4.1**). A substrate for *Bacillus anthracis* lethal factor protease was used as a negative control **(Fig. 4.1).** BoNTALC assays were

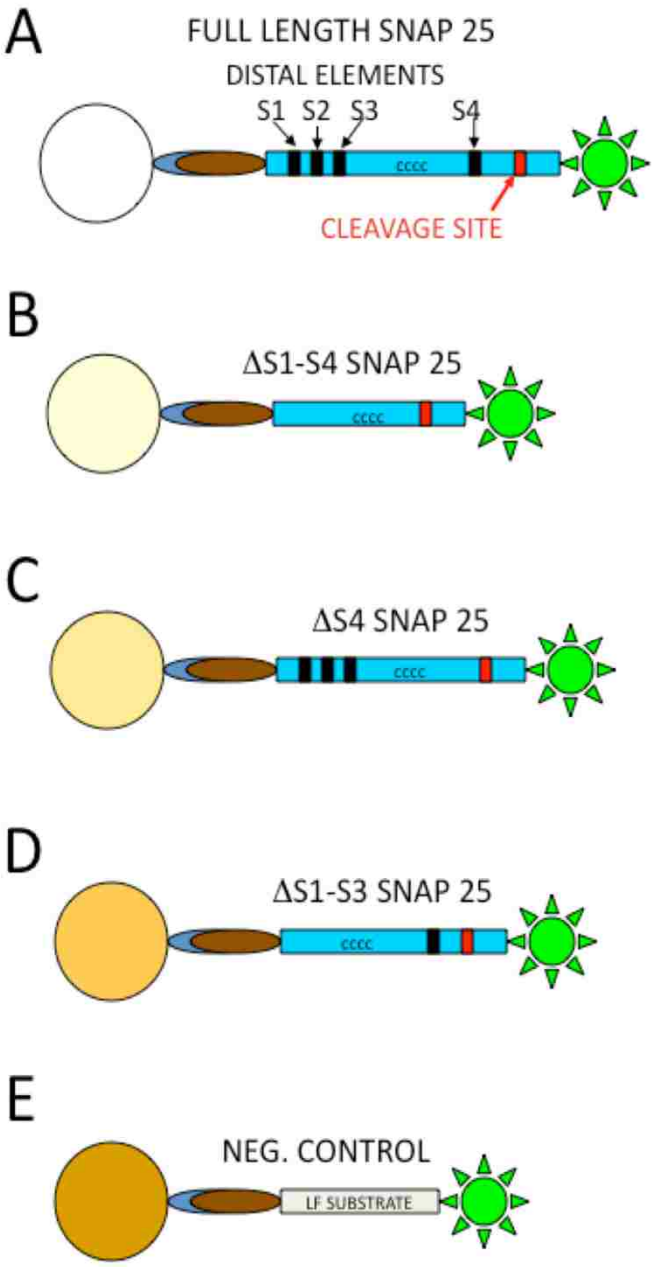

Figure 4.1. Schematic representation of the five-plex substrate system Microsphere populations are represented by different colored circles, the streptavidin by the blue crescent, the biotinylation tag by the brown oval, GFP by the green sun, cleavage site on SNAP-25 by the red square, and distal binding sites by the black gaps. A. SNAP-25 Full Length. B. SNAP-25 ΔS1-S4 (residues 21-59 & 145-155 deleted) containing no distal binding sites C. SNAP-25 ΔS4 (residues 145-155 deleted) containing distal binding sites S1-S3. D. SNAP-25 ΔS1-S3 (residues 21-59 deleted) containing distal binding site S4. E. Lethal Factor cleavage site control substrate was used as a negative control.

run continuously on a flow cytometer and bead sets gated based on size and yellow fluorescence intensity (580/30 nm) to discriminate microspheres bearing each substrate (**Fig 4.2A**). The assay was initiated by the addition of protease and the microsphere bearing full–length SNAP-25 lost fluorescence due to proteolytic cleavage at the fastest rate, followed closely by SNAP-25 ΔS1-S3 **(Fig. 4.2B & 4.2C).** SNAP-25 ΔS4 and ΔS1-S4 showed far less cleavage in the same time frame, with SNAP-25 ΔS4 showing slightly faster fluorescence loss than SNAP-25 ΔS1-S4. (**Fig. 4.2B & 4.2C)** The control LF substrate showed very little fluorescence loss, indicating that the loss on the SNAP-25 substrates is due to specific proteolytic cleavage of the GFP-linked substrate **(Fig 4.2B & 4.2C).**

The rate of specific cleavage increased as a function of BoNTALC concentration (1 to 50 nM), but the relative substrate cleavage profiles remained the same (data not shown). A similar pattern of substrate susceptibility to cleavage was observed in endpoint assays used for compound screening (see below). After a 1 hour incubation with BoNTALC at room temperature, full length SNAP-25 and SNAP-25 ΔS1-S3 were both cleaved to lower fluorescence values than SNAP-25 ΔS4 and ΔS1-S4. (data not shown).

4.3.2 High Throughput Screening of the Prestwick Chemical Library.

One hour endpoint assays were used for library screening, where BoNTALC was added to 20 µl multiplex microsphere assays, with test compounds, contained in 96-well plates and incubated at 25℃. Under these conditions fluorescence loss due to proteolytic cleavage was seen across all 4

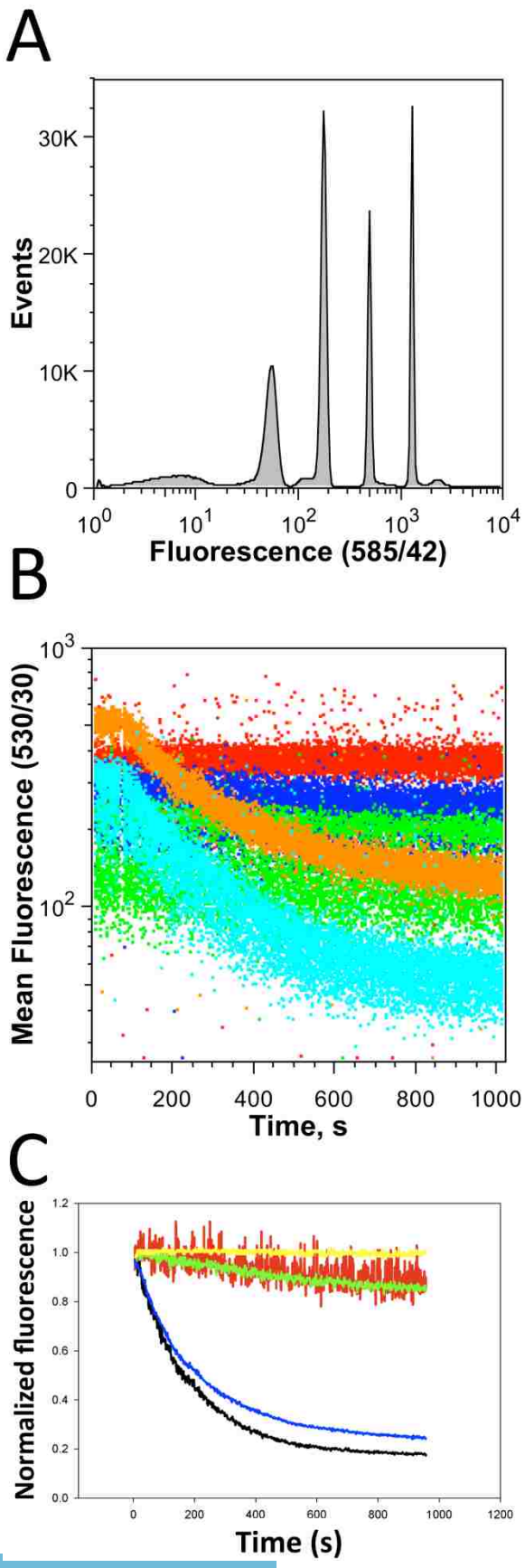

·plex flow
with Botulinum
A Light Chain
ɔn a FACScan
A Multiplex
ʼs. number of
he five distinct
icrospheres. B.
ı data plotted
sphere types

ɜtrate type in
ɜ of total events
-representing
Blue: Full
ɜ GFP Orange:
3 Dark Blue:
reen: SNAP-25
control
vere analyzed
ometry data
ɜ. **C.** Relative
substrate
dition of 25nM
ɔtoxin type A
ta were
ʼeraging mean
ɜ values for the
ɔf data
ACScan flow
ɔ addition of
ɔ and dividing
ean FL1
ıes by that
Substrate types
ack: SNAP-25
SNAP-25 ΔS1-
ɔ-25 ΔS4,
ʼol substrate,
ΔS1-S3.

forms of SNAP-25, with approximately 5% fluorescence loss on the control substrate due to GFP instability or photobleaching (data not shown). Plates were analyzed via the HyperCyt HTS system attached to a Cyan ADP flow cytometer. Z' values were calculated separately for each substrate on every run of individual plates. Data for copies of plates with Z' values below 0.3 were not used to calculate percent inhibition averages or Z' averages. Out of 66 plate runs 7 plate runs were not used due to extremely low or negative Z' values, which were most likely due to instrumental error such as clogs or very low microsphere pickup. For the remaining 59 plate runs, averaged Z' values were calculated along with standard deviations for each substrate used in the screening assay.

SNAP-25 full length gave an averaged Z' of 0.713 with a standard deviation of 0.264. SNAP-25 ΔS1-S3 gave an averaged Z' of 0.890 and a standard deviation of 0.096. SNAP-25 ΔS4 gave an averaged Z' of 0.798 and a standard deviation of 0.142. SNAP-25 ΔS1-S4 gave an averaged Z' value of 0.821 and a standard deviation of 0.136. Representative raw GFP fluorescence data derived from gating of the microspheres for the population bearing the ΔS1-S3 show the results of endpoint assays distributed serially over time (**Fig. 4.3**). As protease activity results in loss of fluorescence the wells that contained negative controls or had non-inhibitory compounds resulted in an approximately ten fold reduction of fluorescence as compared to positive control wells that were inhibited by an addition 1 mM Z^{2+} or lacked protease altogether **(Fig. 4.3).** While in this screen we did not see any experimental wells that inhibited at the level of the positive controls (100%), several wells resulted in partial inhibition, which

indicated a potential inhibitor **(Fig. 4.3)**. Analysis of all of the data showed that 3 compounds inhibited all 4 substrates: Methylene blue (21% to 42% inhibition), Coralyne chloride hydrate (28% to 56% inhibition), and Ebselen (88% to 90% inhibition).

4.3.3 Ebselen inhibits Light Chain across all 4 substrates screened.

The three positive hit compounds from the screen were used in follow up flow cytometry assays to determine concentration-response relationships. Methylene blue and coralyne chloride hydrate gave approximately 40% inhibition at concentrations of 65 µM and 45 µM, respectively (data not shown). Due to poor inhibition at high concentrations these compounds were not pursued further. However, increasing concentrations of Ebselen in the assay resulted in an estimated IC_{50} value of 4.9 µM against SNAP-25 full length with a Hill-Slope of 25 +/- 6. **(Fig. 4.4)**.

4.3.4 *Ebselen does not inhibit the metalloprotease Bacillus anthracis Lethal Factor*

To test if ebselen inhibition is specific to BoNTALC, we used a duplex microsphere assay with the substrate for *Bacillus anthracis* Lethal Factor protease (the negative control substrate in the BoNTALC assay) attached to one microsphere and full-length SNAP-25 GFP attached to the other microsphere. This duplex assay was performed using assay conditions shown to be effective for Lethal Factor protease (LF) activity in a microsphere based protease assay [127] The assay was initiated via the addition of both LF and BoNTALC, except in

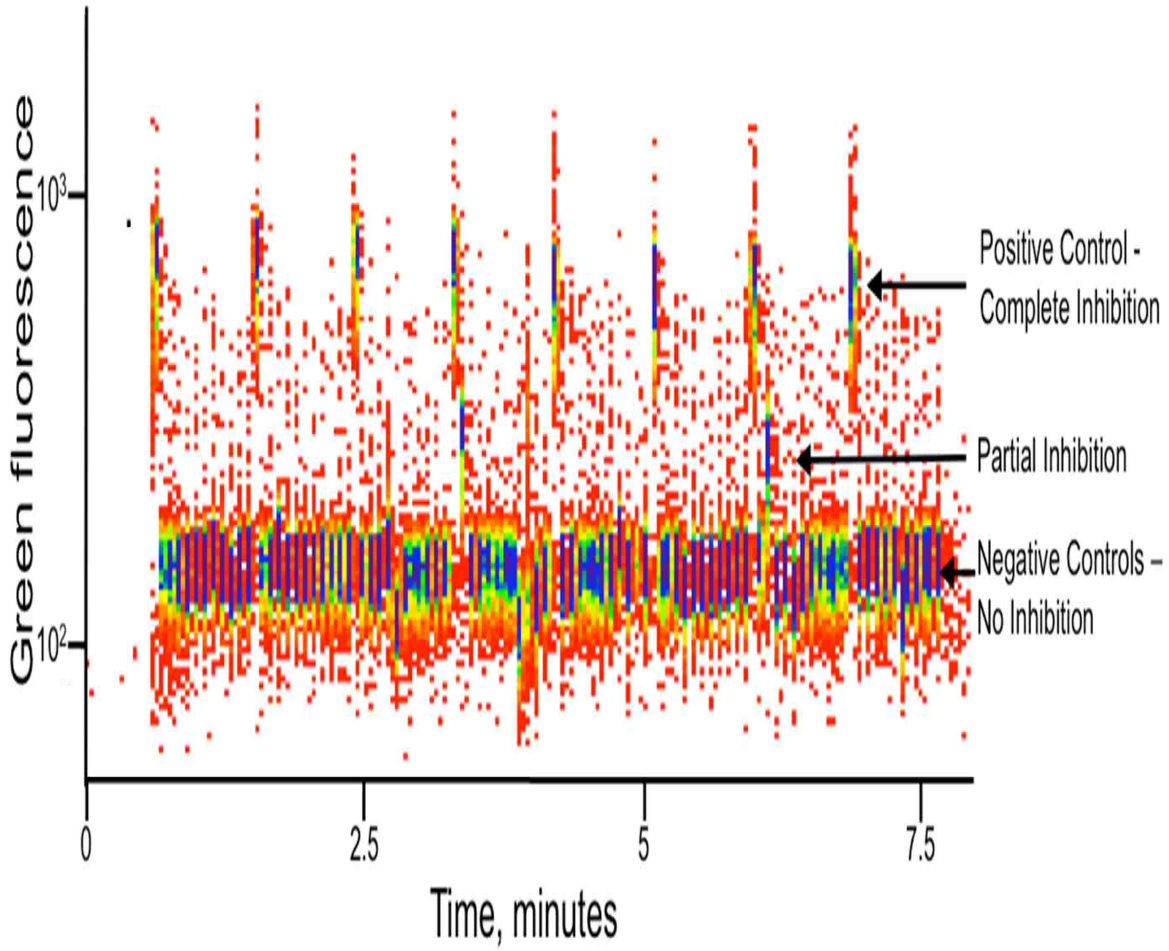

Figure 4.3. Raw data from a Cyan ADP flow cytometer of a 96 well plate for the substrate SNAP-25 ΔS1-S3. Blue clusters of events are from each well. Wells with high green fluorescence (FL1) values are negative control wells at 12 well intervals as defined in the methods section.

the case of controls. Addition of increasing concentrations of ebselen (1 to 1000 µM) demonstrated that concentrations as high as 250 µM did not inhibit LF and 500 µM ebselen only resulted in approximately 30% inhibition after 1 hour of incubation **(Fig. 4.5)**. This is in contrast to a known LF inhibitor, which gave ~90% inhibition of LF at 1 µM after 1 hour **(Fig. 4.5)**. As seen previously, ebselen inhibited the BoNTALC at concentrations between 5 µM and 10 µM (data not shown).

4.3.4 Ebselen inhibits BoNTALC in a peptide based FRET assay

To verify that ebselen is inhibiting the BoNTALC protease and not via some artifact in the SNAP-25 microsphere assay, we used the FRET peptide substrate for BoNTALC (SNAPTide) from List Laboratories (Campbell CA). In the presence of 5 nM of BoNTALC ebselen resulted in an IC_{50} of 18.6 µM with a Hill-Slope of 27 +/- 7 **(Fig 4.6)**.

4.3.5 Inhibition by ebselen is not due to cysteine modification

Ebselen has been reported to be a potent inhibitor of cysteine proteases via cysteine modification that is reversible via the use of reducing agents [160]. To explore if inhibition of BoNTALC is a result of cysteine modification by ebselen either on SNAP-25 or BoNTALC, we specifically attempted to reverse the inhibition of the SNAPtide assay. The SNAPtide FRET peptide does not contain cysteines. This suggests that if cysteine modification was the source of inhibition, a cysteine residue of BoNTALC must be involved. Reversal of inhibition was attempted by addition of 1 mM DTT or 0.05% Beta

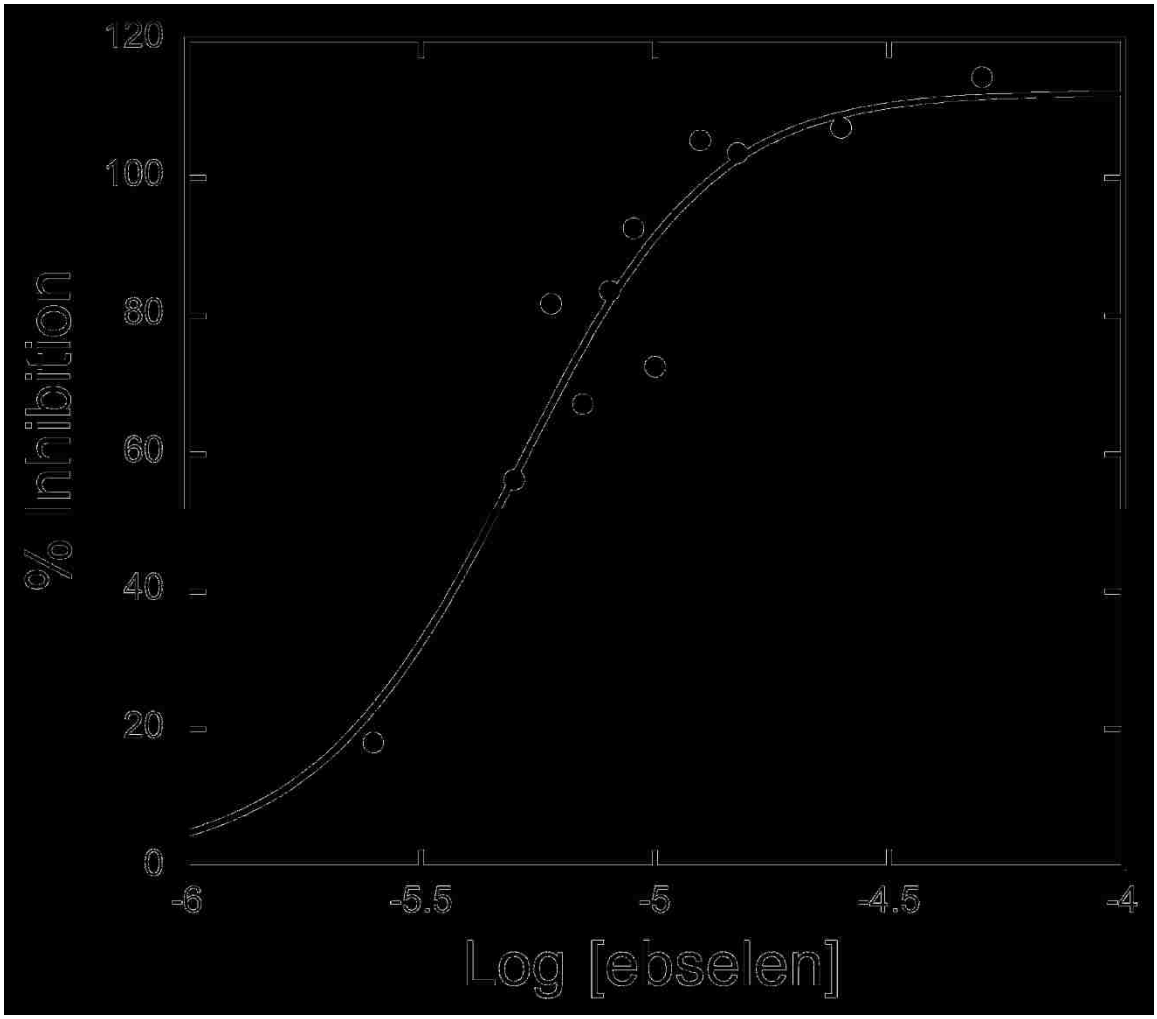

Figure 4.4. Dose response curve for the compound ebselen tested against 5 nm BoNTALC in our microsphere based assay using biotinylated SNAP-25 full length GFP. This data were fitted to a 3 parameter fixed bottom logistic model for a Hill-Slope dose response curve, which was defined as %inh = bottom + ((top – bottom)/ $(1+(x/\log_{10}(IC50))^{hillslope}$). Where the bottom was fixed to the value of the negative control, as the dosing did not extend into the low concentrations, which required the fixing of the bottom parameter to obtain an accurate fit. This fit resulted in an estimate of the $\log_{10}(IC50)$ to be -5.31 +/- 0.05, which estimates the IC50 to be 4.9 µM . The Hill Slope was estimated to be 25 +/- 6 and the fit gave an R^2 of 0.905.

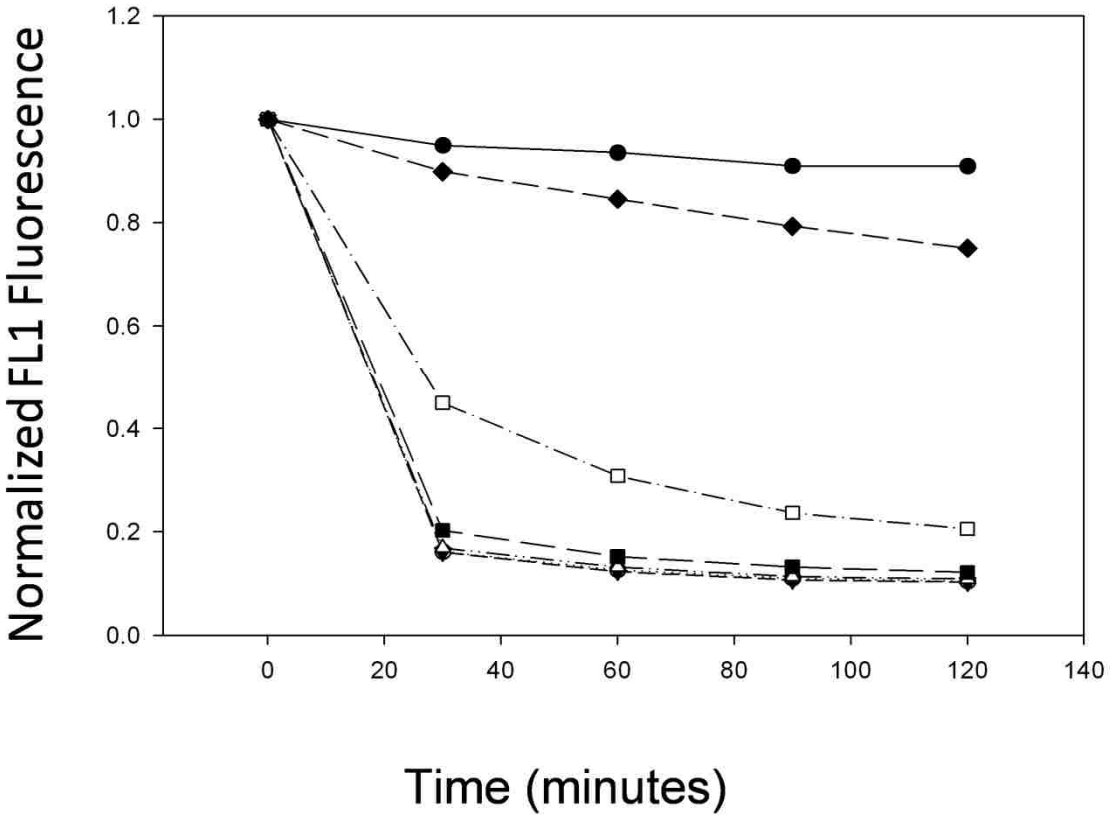

Figure 4.5. Ebselen tested against the *Bacillus anthracis* Lethal Factor metalloprotease in a flow cytometry microsphere based loss of green fluorescence assay. 500 nM Lethal Factor was added to microspheres containing a biotinylated GFP based lethal factor consensus cleavage site sequence and measured on a FACSCAN flow cytometer every 30 minutes. Samples are represented by the following symbols. Closed circles: no lethal factor. Open circles: No ebselen. Inverted closed triangles: 5 μM ebselen. Open Triangles: 25 μM ebselen Closed squares: 250 μM ebselen.Open Squares: 500 μM ebselen Diamonds: 1 μM IN-2-LF, a known lethal factor inhibitor.

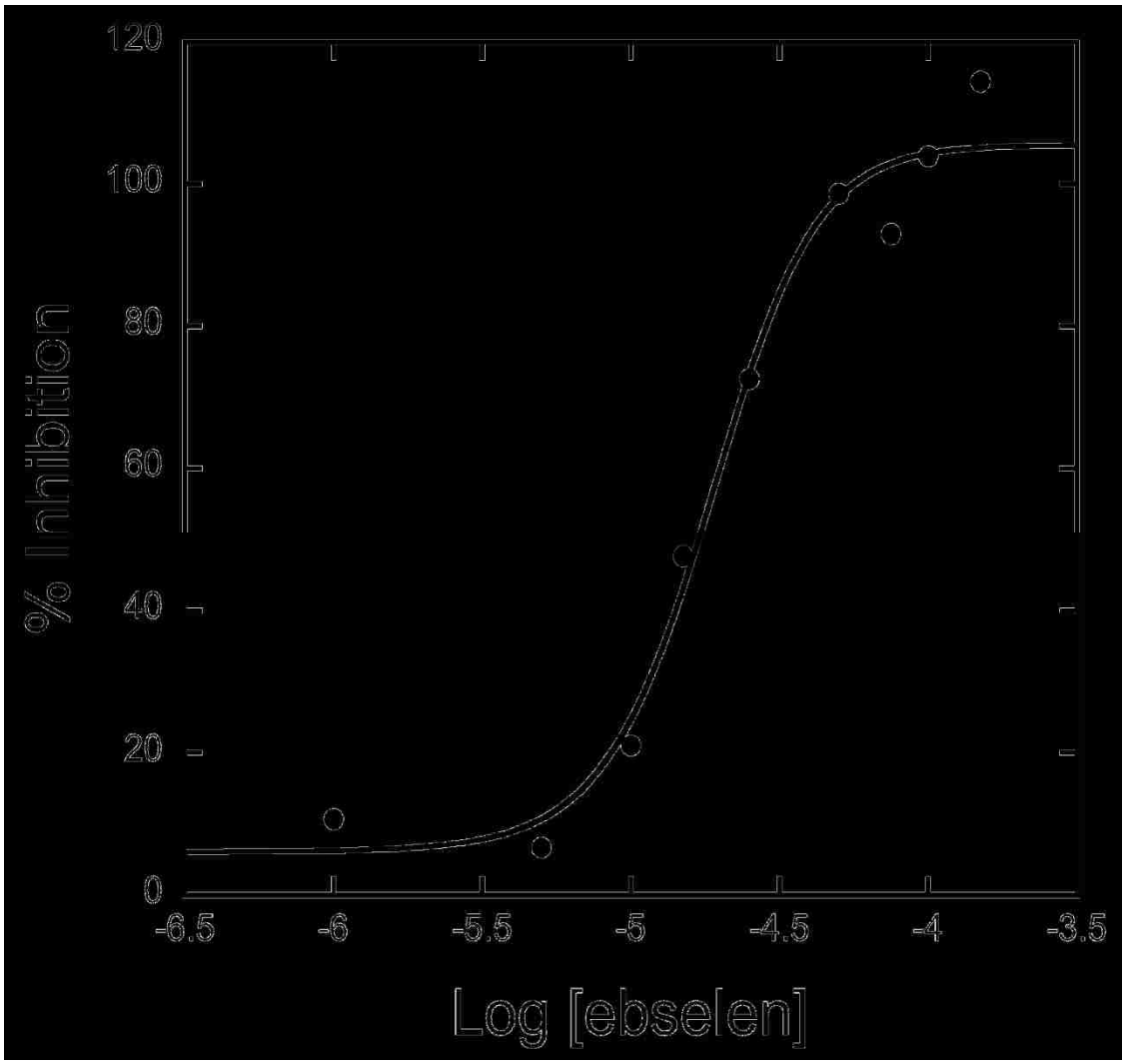

Figure 4.6. Inhibition of 5 nM BoNTALC by ebselen tested with the SNAPtide peptide substrate. Ebselen and 5 µM SNAPtide were added and measured by excitation at 490 nm and emission values were recorded at 523 nm in a fluorimeter 5 nM BoNTALC was added after 60seconds and data collected for 10 minutes after protease addition. This data were fitted to a 4 parameter logistic model for a Hill-Slope dose response curve, which was defined as %inh = bottom + ((top – bottom)/ $(1+(x/\log_{10}(IC50))^{hillslope}$). This fit resulted in an estimate of the $\log_{10}(IC50)$ to be -4.73 +/- 0.05, which estimates the IC50 to be 18.6 µM . The Hill Slope was very abrupt and estimated to be 27 +/- 7 and the fit gave an R^2 of 0.982.

mercaptoethanol to the SNAPtide assay. Neither affected inhibition levels (data not shown) suggesting that inhibition of BoNTALC by ebselen was not due to cysteine modification.

4.4 DISCUSSION

We have developed a multiplex microsphere protease activity assay that enabled screening of BoNTALC against several SNARE motif deletion forms of SNAP-25 in parallel, and resulted in identification of a novel inhibitor. The assay enabled use of full length substrates, a feature that may help to identify small molecule compounds targeting interactions with SNAP-25 that are distant from the cleavage site. The potential for discovery of small molecule inhibitors which interfere with protein-protein interactions between SNAP-25 and BoNTALC has been noted [156], and screening efforts of libraries of compounds known to interfere with such protein-protein interactions have resulted in discovery of BoNTALC inhibitors [161] Such interactions, however, have not been verified and are still hypothetical. [161]. While our current screen has not definitively detected such inhibitors, our five-plex assay to measure cleavage across many structural variants gave results consistent with previous studies that showed a slower rate of SNAP-25 cleavage of substrates lacking the S4 SNARE motif (**Figs. 4.2, 4.3**). This suggests that our assay may be a viable approach for detecting such inhibitors in extended screening of larger compound collections.

The screen of the Prestwick Chemical Library resulted in the detection of ebselen, which inhibited BoNTALC across all four forms of SNAP-25 used. The averaged Z' values, reported for each substrate, are all acceptable for high

throughput screening. Ebselen inhibited 5 nM BoNTALC with an IC_{50} of 4.9 µM for SNAP-25 full-length and 18.6 µM for a peptide based substrate. Because ebselen exhibited similar BoNTALC inhibition on all four SNAP-25 substrates, it seems unlikely to be targeting interactions between SNAP-25 and BoNTALC within the SNARE motifs. Such inhibition would have likely been revealed by differences in the percent inhibition between substrates bearing differing SNARE motifs. However, as ebselen inhibition of LF was not observed at ebselen concentrations 100-fold higher than required for BoNTALC inhibition (**Fig. 4.5**), we postulate that ebselen is acting upon BoNTALC specifically and is not a general Zn^{2+} metalloprotease inhibitor.

While ebselen specifically inhibited BoNTALC at low µM concentations, several aspects of the inhibition were of concern. First, the steep Hill-Slopes obtained from the dose response curves indicate that inhibition may not be occurring through a simple mechanism. One potential concern was that ebselen was causing a solution effect that resulted in loss of BoNTALC activity. However, LF protease activity is unaffected by ebselen (**Fig. 4.5**), making it unlikely that a solution effect is the causing the loss of BoNTALC activity, as LF and BoNTALC require nearly identical buffers for activity. Second, excess Zn^{2+} is expected to be a general metalloprotease inhibitor [24]. Potential concerns about Zn^{2+} contamination causing the inhibitory action of ebselen on BoNTALC, was also addressed by the duplex BoNTALC - LF assay, where both proteases were used simultaneously. If Zn^{2+} contamination were responsible for inhibition it would have likely been seen as an inhibitor of LF in this assay, as the same amount of

potential Zn^{2+} contaminant would be present for both proteases. However, in this experiment BoNTALC is inhibited while LF is not at high concentrations of ebselen (**Fig. 4.5**), which suggests Zn^{2+} is not present at inhibitory concentrations. Third, ebselen has been shown to be a somewhat promiscuous inhibitor, and has been identified as a lead compound in numerous assays. Ebselen has been shown to be an antioxidant and peroxynitrite scavenger [162], that mimics glutathion peroxidase [163]. Ebselen has also been reported to have neuroprotective activity after embolic stroke [164], to attenuate intestinal ischemia/reperfusion injuries [165], to act as antifungal even on fluconazole-resistant yeast cells [166], and even as an antibacterial and antiviral agent [167], among other activities. Ebselen is currently under FDA-approved clinical trials by Sound Pharmaceuticals (as SPI-1005 and SPI-2005) for hearing loss treatment (http://www.soundpharmaceuticals.com/). A recent PubChem search reveals that Ebselen was found bioactive in 70 assays out of 438, of which 39 were confirmatory assasys. One mechanism of inhibition by ebselen has been demonstrated through cysteine modification of papain (a cysteine protease) and other proteins, which is reversible by reducing agents [160, 168]. This known ability of ebselen to modify cysteine residues may be partly responsible for its promiscuity in screening assays. However, the inability to reverse inhibition via reducing agents suggests that ebselen is not inhibiting BoNTALC via oxidation of cysteines. Thus, while there are many interesting aspects to the ebselen inhibition of BoNTALC discovered here, it appears that the inhibition is BoNTALC specific, not based on oxidation of cysteines, and likely not a result of Zn^{2+}

contamination of the ebselen, all of which makes it a potentially interesting BoNTALC inhibitor.

Ebselen is of specific interest as a BoNTALC inhibitor because it is a bio-available compound pre-approved for human use for a variety of purposes. Importantly, the IC_{50} (4.9 µM) of ebselen toward BoNTALC is very good in comparison to other previously reported BoNTALC small molecule inhibitors [78, 91]. This compound has also been shown to have low toxicity in animal studies, and has been administered at levels up to 10 mg/kg in cynomolgus monkeys [169]. Because of its combination of bioavailability and acceptable toxicity level, ebselen may be a useful pharmaceutical for BoNTALC poisoning treatment. Studies are being pursued to investigate its effectiveness in animal models.

This particular assay format also has the distinct advantage of being adaptable to any protease of interest for high throughput screening purposes. Full-length protease substrates can be used to identify small molecules which may interfere with protease substrate interactions leading to specific inhibition of the protease of interest. This assay can also be used for parallel evaluation of multiple proteases, as demonstrated with the dual Lethal Factor/BoNTALC assay in this study. (**Fig. 4.5**.) Screening of multiple proteases against multiple substrates could also lead to discovery of specific inhibitors of closely related proteases and reduce costs of materials and labor in high throughput screening.

4.5 Acknowledgements.

The authors would like to thank Mark Carter and Susan Young for help with instrumentation, Anna Waller for help with data analysis, and Dan Cimino and Megan Dennis for help with subcloning and fluorimetry. We would also like to thank the National Flow Cytometry Resource for funding and support with this work. None of the authors of this work have any conflicting interests in this work.

FundingSources:

This work was supported by the National Flow Cytometry Resource from the National Center for Research Resources, NIH grant RR001315. Additional funding was supplied by a Joint Sciences Technologies Laboratory grant JSTL 26Q4 and by the University of New Mexico Center for Molecular Discovery MH077425 and MH084690 and Cancer Center CA118100

Chapter 5:
Purification of Active Lethal Factor and High Throughput Screening of the Prestwick Chemical Library.

5.1 Introduction

Development of protease assays, with the intention of screening for potential small molecule inhibitors and their use in kinetic analysis requires large quantities of protease. Our botulinum neurotoxin type A light chain assay, with binding site deletions on SNAP-25, uses only 5 nM BoNTALC in the assay. HTS for BoNTALC inhibitors costs approximately 4.3 cents per well, screening in 384 well plates. The potential for finding inhibitors of BoNTALC, particularly the potential for discovery of inhibitors which interfere with protease-substrate binding interactions, justifies the cost. By contrast there are a number of issues related to using commercially available sources of lethal factor as a basis of HTS assays. Lethal factor purchased from List Biological Labs has been observed by our group and others to vary in activity levels from batch to batch. Optimal efficiency in our microsphere based assay requires concentration ranges from 350 nM to 500 nM Lethal Factor. The activity of the LF protease also diminishes over time after reconstitution in buffer. Purchase of quantities of LF for use in high throughput screening for lethal factor inhibitors would be a significant cost, making screening of large chemical libraries expensive.

Purification of the 90 kDa *Bacillus anthracis* lethal factor Zn^{2+} metalloprotease as a soluble active protease by chromatography has been previously done with high yields and relative ease [170]. Due to the high costs of high throughput screening using commercial LF, estimated at 19 cents per well in

384 well plates, and the relatively high amounts of LF used in our microsphere based assay, purification of active LF protease is required to make HTS by this method economically possible.

5.2 Methods

5.2.1 Purification of Lethal Factor

PCR primers were designed to amplify the lethal factor gene for sub-cloning into the plasmid pET20b, which contains a C terminal 6X histidine tag for purification purposes. The lethal factor gene was amplified by PCR from the *Bacillus anthracis* pXO1 plasmid and cloned into pET 20b. However, the lethal factor protein is processed inside *of Bacillus anthracis* to remove the N-terminal signal sequence of 33 amino acids. We therefore performed another round of PCR to remove these 33 amino acids from the open reading frame of the N-terminus of lethal factor. The PCR product was re-cloned into pET 20b, and the resulting plasmid was called LF mature pET 20b. After subcloning and plasmid purification from SCS1 *E. coli* cells, the LF mature pET20b plasmid was transformed into BL21 (DE3) pLysS expression *E. coli* cells. 3 ml cultures were grown overnight in TB media with 50 µg/ml carbenicillin and 34 µg/ml chloramphenicol, transferred into 200 ml cultures of TB with the same concentrations of carbenicillin and chloramphenicol, grown at 37ºC until the OD600 was between 0.6 and 0.8, and then induced with 100 µM IPTG and grown overnight at 30ºC. Cells were harvested by centrifugation at 4,000 rpm for 10 minutes and lysed by sonication; no protease inhibitors were used in this

purification due to the protein of interest being a protease. Cell lysate was spun at 15,000 rpm for 20 minutes to separate soluble protein from insoluble membrane components and possible inclusion bodies. Purification on a Ni-NTA HisTrap column with an imidazole elution gradient, followed by dialysis into 2 L of minimal protease buffer (50 mM HEPES, 100 mM NaCl), yielded a protein of approximately 90 kDa by SDS-PAGE gel, the expected size for lethal factor. The LF preparation was stored at 4ºC with 0.02% sodium azide present to prevent bacterial growth. Flow cytometry assays were performed using the LF15 optimized lethal factor substrate [33] adapted to our previously described lethal factor assay [127]. Microspheres were bound and washed, with 600 µl total volumes used and 100 µl samples run on a FACScan flow cytometer every 30 minutes, as previously described [127]. Prior to lethal factor addition 100 µl of microsphere mix was analyzed as a 0 minute value. After lethal factor addition, 100 µl samples were run on the FACScan every 30 minutes and mean fluorescence values recorded. Fluorescence values were normalized by dividing each time point mean FL1 fluorescence by the 0 minute value.

5.2.2 Screening of the Prestwick chemical library against lethal factor.

Cloning of LF15 GFP was done as previously described in Chapter 4, while cloning of Xa sub GFP was done as previously described in Chapter 2 [127]. Substrate purification, binding to biotinylated microspheres and wash steps were carried out as previously described [127], using 100 µl of Spherotech streptavidin-coated multiplex microspheres for each duplicate plate copy. For screening of

the Prestwick library against Lethal Factor 384 well plates were used, with three plates total containing 880 test compounds. 5 µl of bead mix was added to each well of a 384 well plate by a Beckman Coulter Biomek NX S8 instrument. Negative control wells in columns 2 and 23 with no test compound had an additional 1 µl of bead mix added. Positive control wells in columns 1 and 24, with no protease, had an additional 2µl of bead mix added. Test compounds were diluted 1/100 to a final concentration of 0.01 mg/ml per well by a Beckman Coultor Biomek NX MC instrument. 2 µl of approximately 4 µM purified recombinant Lethal Factor was added to each well, except columns 1 and 24, which were used as positive control wells, by a Biomek NX MC, giving a final concentration of approximately 1 µM lethal factor in each well. Plates were covered with a plate cover and incubated at room temperature on a plate rotator for 2 hours before sampling. Plates were set up in duplicate and screened once each. Screening was carried out using the HyperCyt flow cytometry high throughput screening system connected to a Dako Cytomation CyAn ADP flow cytometer with settings of FS Peak Gain 15, SS Log voltage 300, gain 1.0, FITC Log voltage 700, gain 1.0 and PE Log voltage 700 gain 1.0. Wells were sampled for 1 second sampling times, with approximately 2 µl volume pickup per well, and a 1 second wash step in between sample wells to prevent microsphere carry over between samples. The 1 second wash steps were determined necessary due to the relatively small size of the microspheres used in this particular assay, (2.8 µm diameter Spherotech streptavidin coated pink particle kit) and experiments which showed that approximately 10% of the microspheres were

carried over between samples, compared to 1.5% carry over with wash steps between samples (data not shown). Plates were set up in duplicate and each copy screened once.

Data analysis of the Prestwick library screening was carried out using the IDL based Hyperview program written by Dr. Bruce Edwards. Sample wells were gated for each well of the 384 well plate by number of event peaks, with air bubbles and wash steps in between each sample not gated. Each microsphere was gated based on its median FL2 intensity and median FL1 fluorescence was calculated for each microsphere type for each well of the 384 well plate. Wells with no sample pickup or less than 50 microspheres for a microsphere type were not used in data analysis. Z' values for each microsphere/substrate were calculated using the average median FL1 and standard deviation in FL1 values for positive and negative controls. Using the equation (absolute value (median FL1 positive control – median FL1 negative control control/(3X stdev positive control + 3X stdev negative control)) *100). Percent inhibition was calculated using the formula (100* (averaged median well fluorescence – positive control average median fluorescence/ (negative control average median fluorescence - positive control average median fluorescence)). Copies of plates with Z' values below 0.3 for a particular substrate were not used in averaging data for that substrate. Percent inhibition for each copy of each plate was averaged into an average percent inhibition for each well of each plate in the Prestwick library. Wells with high % inhibition values were chosen for potential follow up work and characterization.

5.3 Results

5.3.1 Purification of the Bacillus anthracis lethal factor

Purified lethal factor was tested in our microsphere based protease assay against the high affinity LF 15 GFP lethal factor substrate [33, 127]. We observed that by quantifying our purified LF by UV_{280} spectroscopy and use of 375 nM LF from our purified stock in comparison to 375 nM LF purchased from List Biological Labs yielded similar amounts of LF 15 GFP substrate cleavage in our microsphere based assay (**Fig. 5.1).**

5.3.2 High throughput screening of lethal factor.

Z' values for high throughput screening of Lethal Factor ranged from 0.73 to 0.89 on different plates, which is in the acceptable range of Z' values. Out of the 880 compounds screend from the Prestwick Library, two compounds gave percent inhibition values against LF above 50%. The compound harmalol hydrochloride dehydrate (**Fig. 5.2),** plate 2 well L3, gave an averaged % inhibition value of 61.9%, whereas the compound pirenperone (**Fig. 5.3**), plate 2 well L4, gave an averaged % inhibition value of 107%. Over 100% inhibition in this assay is obtained by the inhibitor well having higher green fluorescence values than the negative control value with no compound. This increased fluorescence value of pirenperone was also reflected on the control Xa sub

microsphere, which gave a fluorescence value of 130% of the positive control value. Control bead fluorescence values for harmalol hydrochloride dihydrate

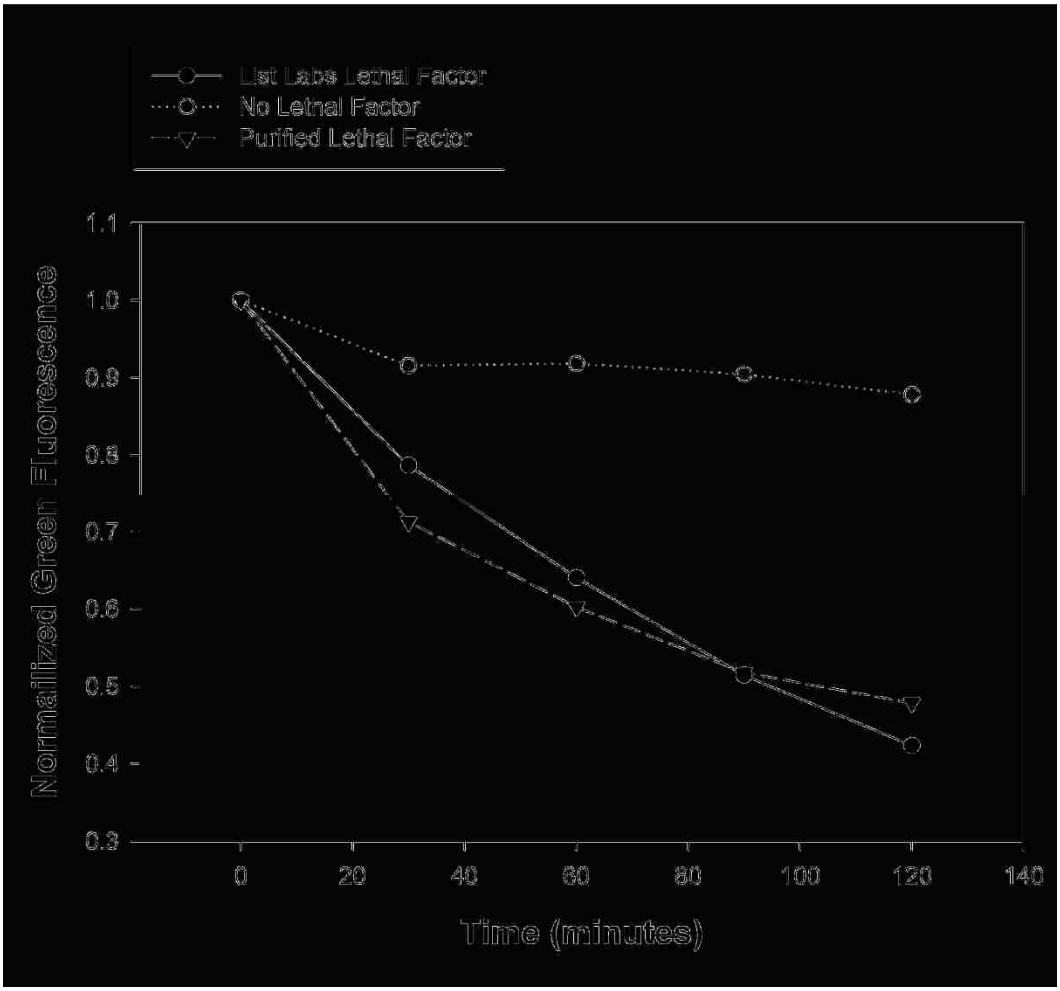

Figure 5.1 Comparison of 375 nM lethal factor obtained from List Biological Laboratories and 375 nM lethal factor purified by Ni NTA Histrap column chromatography in the microsphere based flow cytometry assay. Fluorescence was normalized by dividing each mean FL1 time point value by the 0 minute time point mean FL1 value. Closed circles: List lab LF, open circles: no LF, closed circles: purified LF.

were 91% and 138% on the duplicate copies of the plate, indicating that the control fluorescence is variable between the two duplicate copies of the plate. Nearly complete inhibition of lethal factor proteolytic activity in the presence of these compounds, with end point fluorescence values slightly higher than starting fluorescence values, is consistant with a slightly fluorescent compound which inhibits lethal factor activity.

5.4 Conclusions and Future Directions

The relatively straightforward cloning and purification of Lethal Factor has made the formerly expensive approach of high throughput LFscreening by flow cytometry cost effective. Our recombinant purified LF was as active as the commercially available recombinant lethal factor (**Fig. 5.1**). Due to the costs of library screening with commercially purchased LF and the relatively high amounts our assay uses, we did not perform LF inhibitor screens until we were able to purify active LF ourselves, dramatically reducing the costs of lethal factor screening . While the data shows that 375 nM LF gives efficient cleavage of LF15 GFP from the surface of microspheres, (**Fig 5.1)** 1 µM LF was used in the screen because of reduced activity after prolonged storage, and the presence of several minor co-purified proteins present which could account for approximately 10% of the total protein mass as determined by SDS-PAGE gel electrophoresis (data not shown). These co-purified proteins were of little concern as they did not interfere with the proteolytic activity of LF toward the LF15 substrate and did not cause

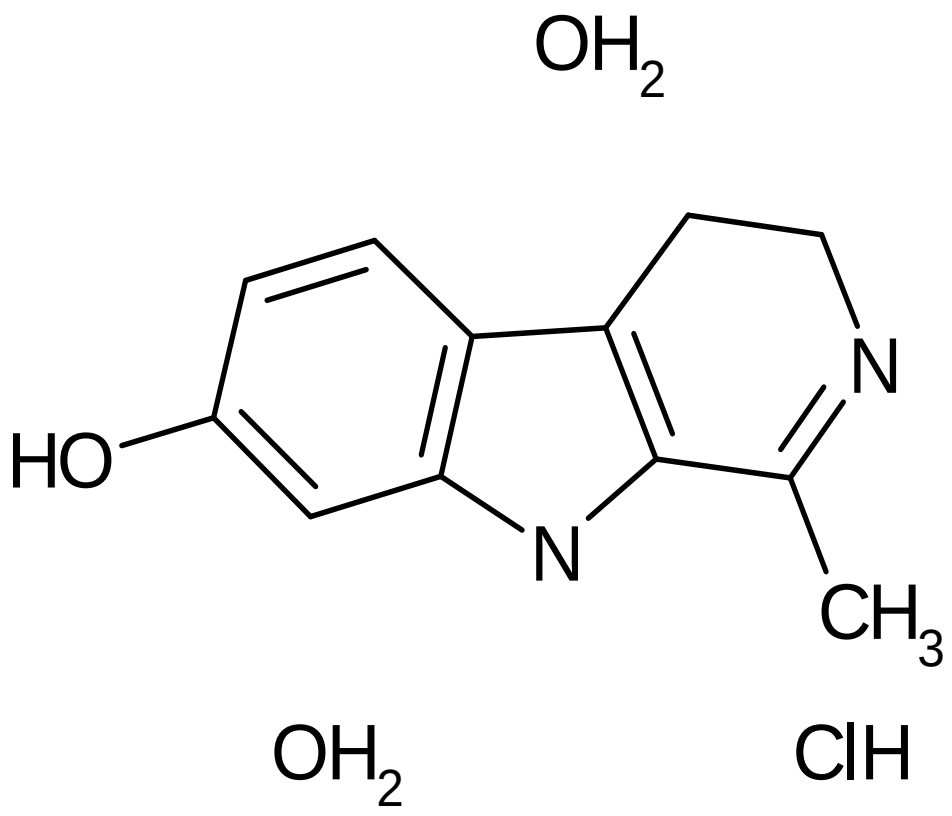

Figure 5.2 Chemical structure of harmalol hydrochloride dihydrate, a potential lethal factor inhibitor.

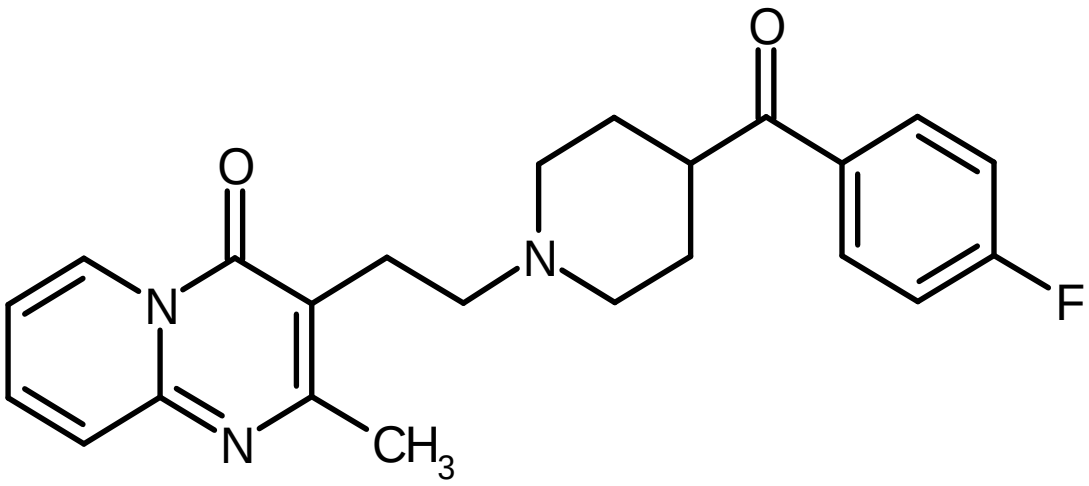

Figure 5.3 Chemical structure of pirenperone, a potential lethal factor inhibitor

loss of fluorescence from the control microsphere in the assay, indicating that they were not non-specific proteases.

High throughputs screening of the Prestwick chemical library yielded two lead compounds, pirenperone (**Fig. 5.3**) and harmalol hydrochloride dehydrate (**Fig. 5.2**). Attempts to obtain these compounds are being made and they will be tested in a dose-response manner to determine IC_{50} values for each of these compounds against lethal factor. There is concern in the observation that these two compounds are located in adjacent wells of the Prestwick chemical library, and that these compounds could have potentially been mixed together during compound dilution steps prior to setting up screening plates. Such concerns will be addressed when compounds are tested individually in a dose-response manner. If only one of these compounds is responsible for inhibition and mixing occurred, the other compound will not give inhibition in the follow up work.

After dose-response work is done in our microsphere based assay, the putative inhibitors will be evaluated in a FRET based assay using LF15 GFP bound to Cy3 streptavidin, or by the use of the MAPKKide FRET peptide available from List Biological Laboratories, in order to verify that these compounds are not interfering with the microsphere attachment chemistry or biotin/streptavidin interactions. A potential cellular based assay to test for the compounds ability to act intercellularly is also being discussed; however, such an assay would need to either express lethal factor intracellularly along with the substrate protein or native map kinase kinase (MKK), or be done on macrophage cell lines with complete lethal toxin, measuring intracellular MKK cleavage by

western blot. The discovery of these two bioavailable compounds, pre-approved for human use does significantly reduce concerns about lead compound toxicity. Animal inhalation anthrax models would be considered if these compounds are able to act intercellularly to inhibit lethal factor activity.

Chapter 6.
High Throughput Screening of the Torrey Pines Combinatorial Library for Botulinum Neurotoxin type A Light Chain Inhibitors.

6.1 Introduction

High throughput screening (HTS) of libraries of chemical compounds typically involves screening a biological target against one individual molecule at a time. Newer approaches are taking advantage of combinatorial chemistry libraries, where numerous chemicals per sample are screened against a target assay of interest in an approach to make drug discovery quicker and more affordable. In this approach mixture-based libraries contain systematically arranged mixtures of compounds with known and unknown positions of chemical modification and diversity [171]. Combinatorial mixture-based libraries have the potential to screen millions of compounds in the same amount of time it would take to screen tens of thousands of compounds one at a time, and use substantially less material [171].

The Torrey Pines Institute for Molecular Studies (TPIMS) combinatorial library is a collection of combinatorialy synthesized chemicals with modifications of 37 chemical scaffold families, consisting of 6,123 sample mixtures representing several million total compounds. In this chemical library each well of a 384 well plate contains between 1,000 and 5,000 distinct compounds. As part of an ongoing collaboration between the University of New Mexico Center for Molecular Discovery and TPIMS we have screened a copy of this combinatorial library against the Botulinum Neurotoxin type A Light Chain multiplex microsphere based assay presented in Chapter 4. For this purpose, the HTS

assay as described for the screening of the Prestwick library was scaled down from 20 µl to 8 µl volumes using 5nM BoNTALC in each well of the assay.

Following the initial screen and subsequent data analysis with TPIMS, families of compounds that showed promising leads as BoNTALC inhibitors were synthesized and sent to our group at the University of New Mexico Center for Molecular Discovery for follow up. These libraries contained less complex mixtures of compounds per well and helped in deconvoluting the data to identify specific compounds and the chemical scaffold modifications responsible for enzyme inhibition. Follow up plates also contained single compounds per well for two particular chemical families. A scaffold plate, which contains the single chemical scaffolds used in the TPIMS library with no chemical modifications was screned as well. Importantly identification of chemical scaffolds without modifications would be used to effectively determine if the chemical scaffold or the modifications done to that scaffold are primarily responsible for inhibition of BoNTALC.

6.2 Methods

6.2.1 Plate setup and high throughput screening.

Substrate purification, binding to biotinylated microspheres and wash steps were carried out as previously described (Chapter 4) using 100 µl of Spherotech streptavidin coated multiplex microspheres for each duplicate plate copy. For screening of the TPIMS library, 384 well plates were used, with 5 ul of bead mix added to each well by a Beckman Coultor Biomek NX S8 instrument.

Positive control wells in columns 2 and 23, with no test compound, had an additional 1 ul of bead mix added; negative control wells in columns 1 and 24, with no protease, had an additional 2 ul of bead mix added. Test compounds were diluted 1/100 to a final concentration of 0.01 mg/ml per well by a Beckman Coulter Biomek NX MC instrument. 2 ul of 0.01 mg/ml BoNTALC was added to each well except columns 1 and 24, which were used as negative control wells, by a Biomek Coulter NX MC. Plates were covered and incubated at room temperature on a plate rotator for 2 hours before sampling. Plates were set up in duplicate and run twice each on the HyperCyt flow cytometry high throughput screening system with 1 second sampling times, with approximately 2 µl volume pickup per well and a 1 second wash step in between sample wells to prevent microsphere carry over between samples. The 1 second wash steps were determined to be necessary due to the relatively small size of the microspheres used in this particular assay, (2.8 µm diameter Spherotech streptavidin coated pink particle kit). Initial studies showed that approximately 10% of the microspheres were carried over between samples when no wash was performed, compared to 1.5% carry over when wash steps were included between samples.

6.2.2 Data analysis.

Data analysis of TPIMS screening was carried out using the IDL Query program written by Dr. Bruce Edwards. Sample wells were gated for each well of the 384 well plate by number of event peaks, with air bubbles and wash steps in between each sample not gated. Each microsphere set was gated based on its median FL2 intensity, and median FL1 fluorescence was calculated for each

microsphere set for each well of the 384 well plate. Compensation of FL2- 7.6% FL1 was used to subtract FL1 spectral overlap into the FL2 channel and separate the FL2 histograms for gating purposes. Samples with less than 100 microspheres for a microsphere type were not used in data analysis. Z' values for each microsphere/substrate were calculated using the average median FL1 and standard deviation in FL1 values for wells in columns 1 and 24, containing no BoNTALC as a positive control, and wells in columns 2 and 23, containing no test compound as a negative control. Using the equation (absolute value [average median positive control fluorescence - average median negative control fluorescence/(3X stdev positive control fluorescenec + 3X stdev negative control fluorescence)] *100). Percent inhibition was calculated using the formula [100* (averaged median well fluorescence – negative control average median fluorescence/ positive control average median fluorescence- negative control average median fluorescence)]. Copies of plates with Z' values below 0.3 for a particular substrate were not used in averaging data for that substrate. % inhibition for each copy of each plate was averaged into an average percent inhibition for each well of each plate in the TPIMS library.

6.2.3 Follow up plate setup and screening.

Follow up plates from TPIMS were set up and run in 96 well format in 20 µl volumes using 5 nM BoNTALC. 50 µl of each spherotech streptavidin coated microsphere set were used to set up 2 copies of each compound plate. Plates were set up by hand as described in screening of the Prestwick chemical library (Chapter 4), with column 1 being used as a positive control with no BoNTALC

and column 12 being used as a negative control with BoNTALC added and no test compound used. Plates were set up in duplicate and screened twice each, with Z' values and % inhibition values calculated as above. Test compounds were diluted 1/10 in follow up plates, making concentrations of compounds 0.1 mg/ml for mixtures of library 1477, the platinum containing compound library, and 0.2 mg/ml for the tertrapeptide compound scaffold family 923. Individual compounds of both the 1477 and the 1644 scaffold families were also diluted 1/10 to a final concentration of 0.2 mg/ml. 10% dimethylformamide (DMF) was added to control wells to control for potential effects of DMF in compound wells on protease activity. Compounds from family 1644 were supplied in DMSO and not DMF, however, 10% DMF was still used as a control in control wells for this family of compounds. Data analysis was done in IDL Query as described above with % inhibition values for each run of each sample plate averaged, and then those two plate copy averages were averaged into a % inhibition value for each compound well. The TPIMS scaffold plate was also diluted 1/10 for sampling in two copies, sampled twice each and averaged as in follow up plates. No DMF was used in control wells of the scaffold plate screening.

6.3 Results and Conclusions

6.3.1 TPIMS combinatorial screen.

Percent inhibition was plotted for each of the SNAP-25 substrates as a histogram with each well showing up as a vertical line and each scaffold family color coded. (**Figs. 6.1- 6.4**). All four substrates showed inhibition by almost all

members of the compound scaffold 1477, a platinum based compound. The particular synthesis of the TPIMS library causes overlap in chemicals in wells and three "hits" are needed to verify activity of one particular compound. The data shows that one particular modification of scaffold family 1477 actually increases activity of BoNTALC, as indicated by negative percent inhibition in three wells (**Fig. 6.1**). A tetrapeptide library, scaffold family number 923, also showed several promising candidates for inhibition of BoNTALC. Surprisingly, the SNAP-25 ΔS1-S3 substrate did not show nearly as much inhibition as observed for the other substrates (**Fig. 6.2**). One possible explanation for this is that the ΔS1-S3 substrate contains only the high affinity S4 SNARE domain for BoNTALC, and cleavage of that substrate may have occurred faster than the inhibition of BoNTALC by the test compounds, as BoNTALC was the last component added to the assay plates. One unexpected result was that for SNAP-25 ΔS4 and SNAP-25 ΔS1-S4 substrates numerous compounds in the library actually improved the cleavage of the substrates from the microspheres. (**Figs. 6.3, 6.4**) This effect was not seen on the SNAP-25 ΔS1-S3 substrate (**Fig. 6.2**) due to the fact that nearly complete fluorescence loss was observed on this microsphere/substrate after 2 hours of incubation regardless of the presence of test compounds. Not all of the substrate fluorescence is normally cleaved off of the other microspheres, especially for the SNAP-25 substrates lacking the S4 SNARE domain, where about 50% fluorescence is still on the microsphere after screening in the absence of test compound. Compounds which increase the activity of BoNTALC would cause loss of additional fluorescence when compared

to wells with no test compounds added. These compounds could be considered activators for BoNTALC, and seemed to have that function across all three of the substrates where fluorescence was not completely cleaved in the absence of test compound.

The finding that this high throughput screen can identify inhibitors of BoNTALC as well as compounds which increase activity is particularly useful in the field of small molecule screening of BoNTALC. As discussed previously, there is currently interest in identifying compounds which can be administered along with BoNTA in order to increase the localized effect of BoNTA as a pharmacological or cosmetic agent while minimizing the risk associated with systemic effects of BoNTA [92]. This assay gives us the ability to identify compounds which increase proteolytic activity as well as inhibit it, as seen for factor Xa in Chapter 2 [127].

Due to the nature of combinatorial chemistry screening with 1,000-5,000 compounds per well, deconvolution of the data requires synthesis and screening of follow up libraries based upon compound mixtures which have been shown to have inhibitory effects. Follow up studies were performed for inhibitory compounds but not for compounds which apparently increased the activity of BoNTALC.

6.3.2 Screening of Follow up Plates

Follow up plates were synthesized by collaborators at the Torrey Pines Institute for Molecular Studies for libraries 1477, 923 and an additional scafold family, 1677, not originally included in the initial screen. These follow up libraries

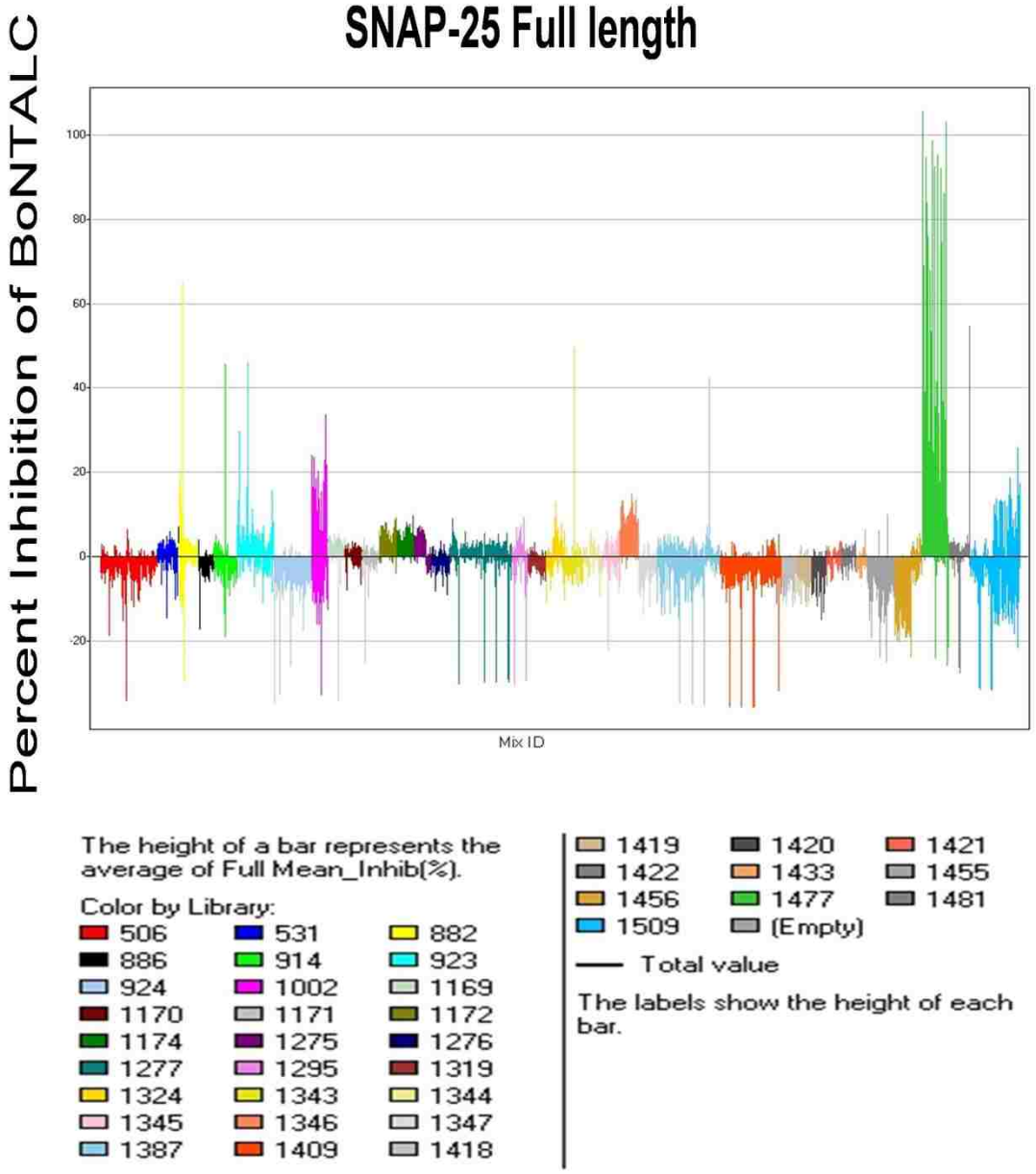

Figure 6.1 Percent Inhibition of Botulinum Neurotoxin type A Light Chain as measured on the microsphere bound multiplexed substrate SNAP-25 full length. Y axis is percent inhibition. Each line represents one well in the screen of the TPIMS library with scaffold families color coded.

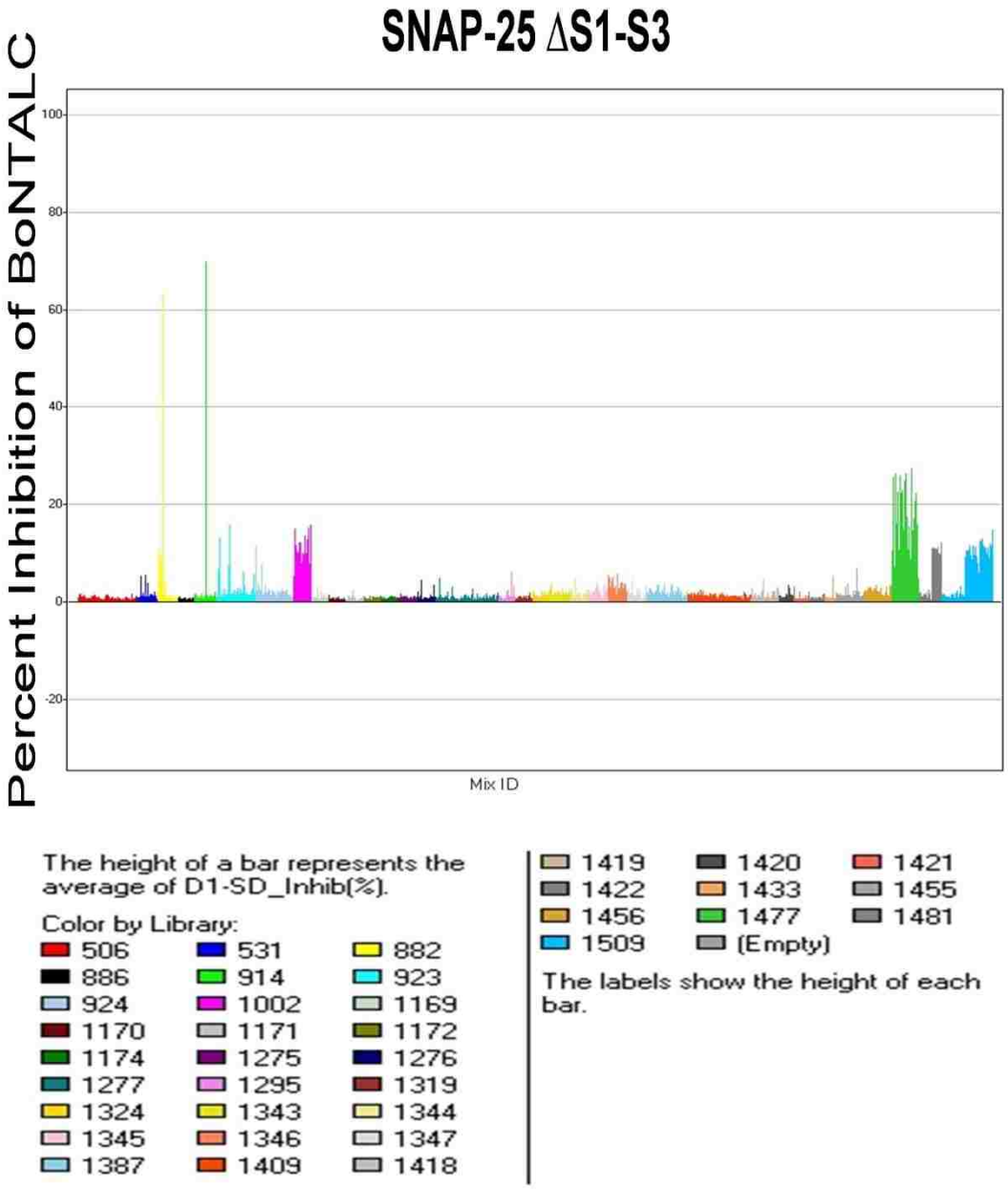

Figure 6.2 Percent Inhibition of Botulinum Neurotoxin type A Light Chain as measured on the microsphere bound multiplexed substrate SNAP-25 ΔS1-S3. Y axis is percent inhibition. Each line represents one well in the screen of the TPIMS library with scaffold families color coded.

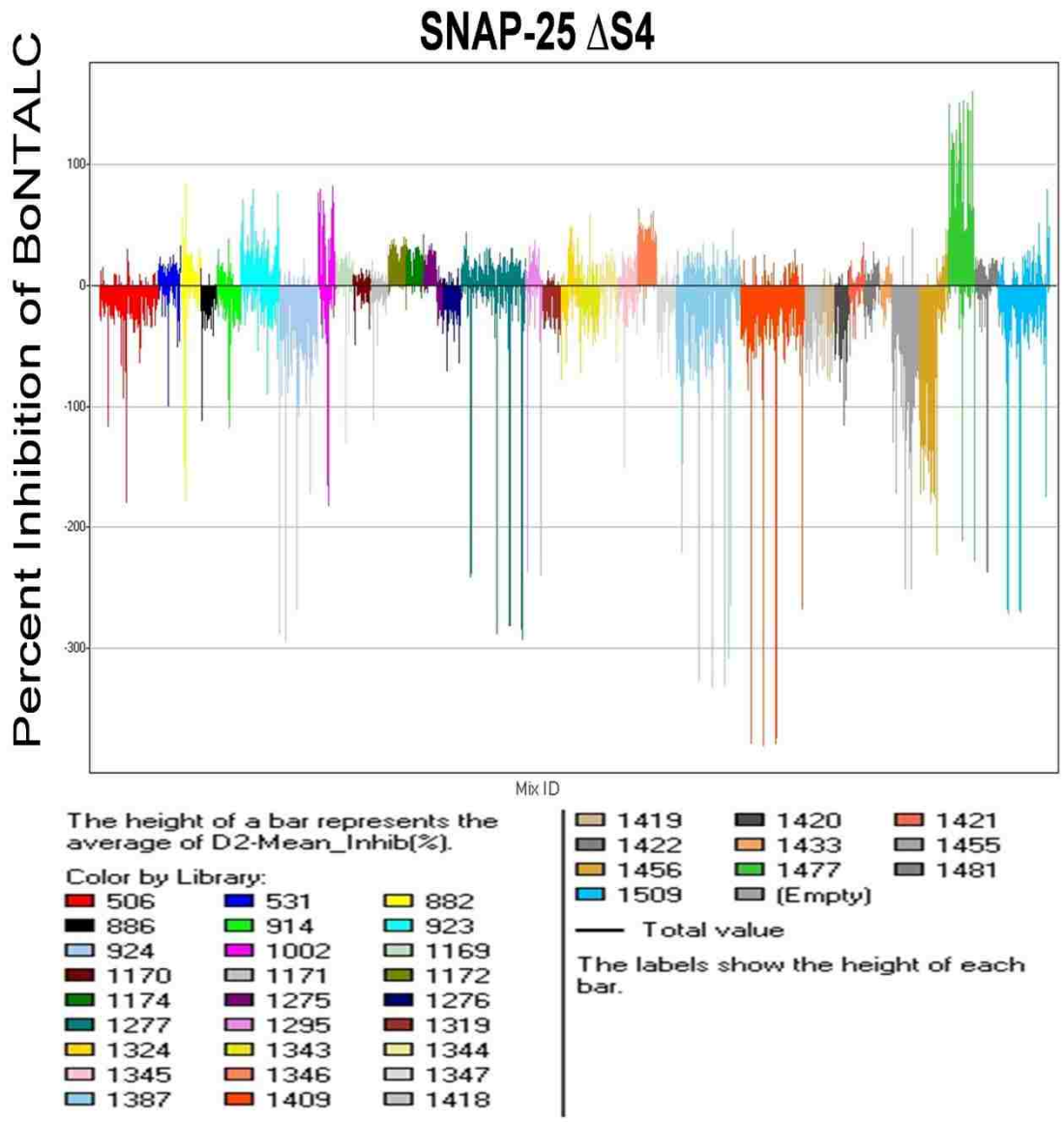

Figure 6.3 Percent Inhibition of Botulinum Neurotoxin type A Light Chain as measured on the microsphere bound multiplexed substrate SNAP-25 ΔS4. Y axis is percent inhibition. Each line represents one well in the screen of the TPIMS library with scaffold families color coded.

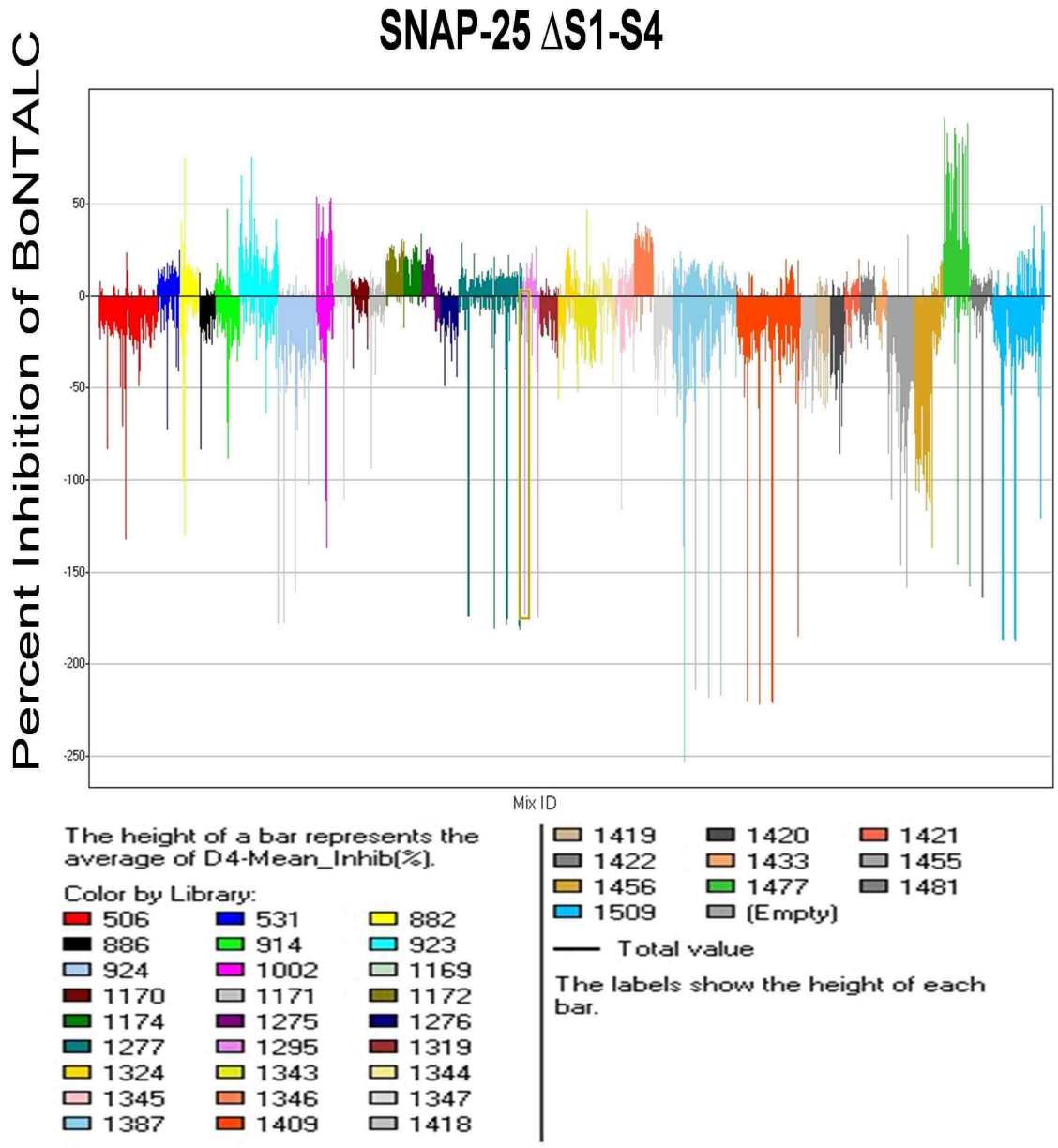

Figure 6.4 Percent Inhibition of Botulinum Neurotoxin type A Light Chain as measured on the microsphere bound multiplexed substrate SNAP-25 ΔS1-S4. Y axis is percent inhibition. Each line represents one well in the screen of the TPIMS library with scaffold families color coded.

contained fewer compounds per well than the initial library, in order to make deconvolution of compounds with inhibitory effects easier to perform. Scaffold family 1477 was screened as mixtures as well as individual compounds. Scaffold family 923, the tetrapeptide scaffold family, was screened as mixtures, and scaffold family 1677 was screened as individual compounds. Follow up libraries were screened in 96 well plate format, with 2 copies of each plate run in duplicate, converted to % inhibition and averaged. Compounds in these plates were also screened at 10 to 20 times higher concentrations than the original TPIMS library. Z' values for SNAP-25 substrates which do not contain the S4 SNARE motif were low for many of the plates, and % inhibition values were often unreliable for these two substrates in the follow us screen as indicated by low Z' values. Therefore % inhibition values for runs of plates with Z' values below 0.3 were deleted for that substrate. % inhibition values for SNAP-25 full length and SNAP-25 ΔS1-S3 substrates, which both contain the S4 SNARE motif, were in close agreement as expected (**Appendix 4**). While the SNAP-25 ΔS4 substrate did not have reliable Z' value data for two plates, the SNAP-25 ΔS1-S4 substrate did have reliable Z' values for several runs. Despite complications in the ΔS4 substrate results, at least one acceptable result was obtained for every compound (**Appendix 4**).

6.3.2 Scaffold family 1477 mixture based follow up

In follow up screening studies of compound 1477 mixtures, increased cleavage of SNAP-25 ΔS1-S4 and SNAP-25 ΔS4 was observed across most compounds when compared to the control well results. This showed up as

negative % inhibition as discussed above. SNAP-25 full length and SNAP-25 ΔS1-S3 showed between 10% and 50% inhibition for most of the 1477 mixture based wells. Of particular note were some wells in which the S4 deletion substrates also showed inhibition. Mixture wells of this type were 1477-004, 1477-006, 1477-011, 1477-16, 1477-039, 1477-047, 1477-048, 1477-052, 1477-053, 1477-054, 1477-069, 1477-154, 1477-155, 1477-164, 1477-167, 1477-168, and 1477-175 **(Appendix 4).** These compounds may be of particular interest in deconvolution and analysis of the follow up library screening due to their property of inhibition of cleavage from the S4 deletion substrates, in contrast to most mixtures of scaffold family 1477 which increased the cleavage of these two substrates.

6.3.3 Scaffold family 1477 individual compound follow up

Individual compounds from the scaffold 1477 series showed inhibition of all four substrates across most of the compounds screened. These individual compounds also generally showed greater % inhibition values than observed in the mixtures from which they were derived. This may have reflected their use at two-fold higher concentration (0.2 mg/ml vs. 0.1 mg/ml in mixtures). Compounds which demonstrated particularly high percent inhibition values, above 40%, on SNAP-25 full length and SNAP-25 ΔS1-S3, were 1477-004, 1477-007, 1477-009, 1477-011, 1477-027, 1477-038, 1477-056, 1477-067, 1477-069, 1477-083, 1477-085, 1477-098, 1477-123, 1477-125, 1477-1271477-139, and 1477-154 (**Appendix 4**). These compounds also generally also displayed inhibition of BoNTALC toward the SNAP-25 ΔS1-S4 and SNAP-25 ΔS4 substrates, whereas

the mixture based compounds seemed to increase cleavage of these substrates while inhibiting cleavage of SNAP-25 full length and SNAP-25 ΔS1-S3. The initial screen of the TPIMS library showed 80% to 100% inhibition on SNAP-25 full length as well as the S4 deletion substrates for numerous wells of mixtures of modified scaffold compound 1477. (**Figs. 6.1, 6.2**) The finding that none of the mixtures or individual compounds of modified compound 1477 gave 100% inhibition suggests that the mixtures in the initial screen may have had an additive, or synergistic effect on inhibition. Further work will be needed to tell if this proposed effect is, in fact, taking place with a large number of compounds.

6.3.4 Tetrapeptide scaffold family 923 follow up

The tetrapeptide scaffold family 923 did not show inhibition values above 30% for any of the mixture based wells screened at 0.2 mg/ml. The initial TPIMS screen showed three wells which gave inhibition values between 30 and 45% on SNAP-25 full length, which would represent one particular peptide family present in three separate wells. On the S4 deletion substrates, high inhibition values were seen for numerous wells of the tetrapeptide library, with several wells giving 100% inhibition. Several wells in the follow up screen did show inhibition values around 15% to slightly above 20% on SNAP-25 full length and SNAP-25 ΔS1-S3, most notably compound mixtures 923-06, 923-07, 923-036, 923-041, 923-044, 923-049, 923-051, 923-052, 923-054, 923-057, 923-058, 923-059, 923-069, 923-075, and 923-095 (**Appendix 4**)

6.3.5 Scaffold 1644 individual compound follow up

Another scaffold, 1644, was not included in the initial screen of the TPIMS combinatorial library, but was included in the follow up screen as a series of individual compounds, screened at 0.2 mg/ml in the BoNTALC assay. All members of scaffold family 1644 showed some inhibition of BoNTALC on the substrates SNAP-25 full length and SNAP-25 ΔS1-S3, the S4 binding site containing substrates. Compounds labeled 1644-033, 1644-041, 034, 1644-042, 1644-036, 1644-013, 1644-007, 1644-015 showed % inhibition values above 75% on the S4 containing substrates, while all of these compounds also showed inhibition on the other S4 deletion substrates (**Appendix 4**). These high inhibition values for compound 1644 make it another attractive target molecule for development of BoNTALC inhibitors, along with compound 1477.

6.3.6 Scaffold plate screening.

As seen by the % inhibition values for many mixtures of scaffold family 1477 in the initial TPIMS library screen, some scaffold chemicals alone with no modifications may cause inhibition. To verify if the scaffolds are causing inhibition themselves rather than modification of the chemical scaffold, the Torrey Pines Institute for Molecular Studies sent us a 96 well plate containing unmodified scaffold chemicals at concentrations of 1 mg/ml and 0.5 mg/ml. Results of scaffold plate screening (**Fig. 6.5**) (**Appendix 4**) show approximately 60% inhibition of cleavage of SNAP-25 GFP full length and SNAP-25 ΔS1-S3 in wells containing either 0.1 mg/ml or 0.05 mg/ml of scaffold 1477 (**Fig. 6.5**).

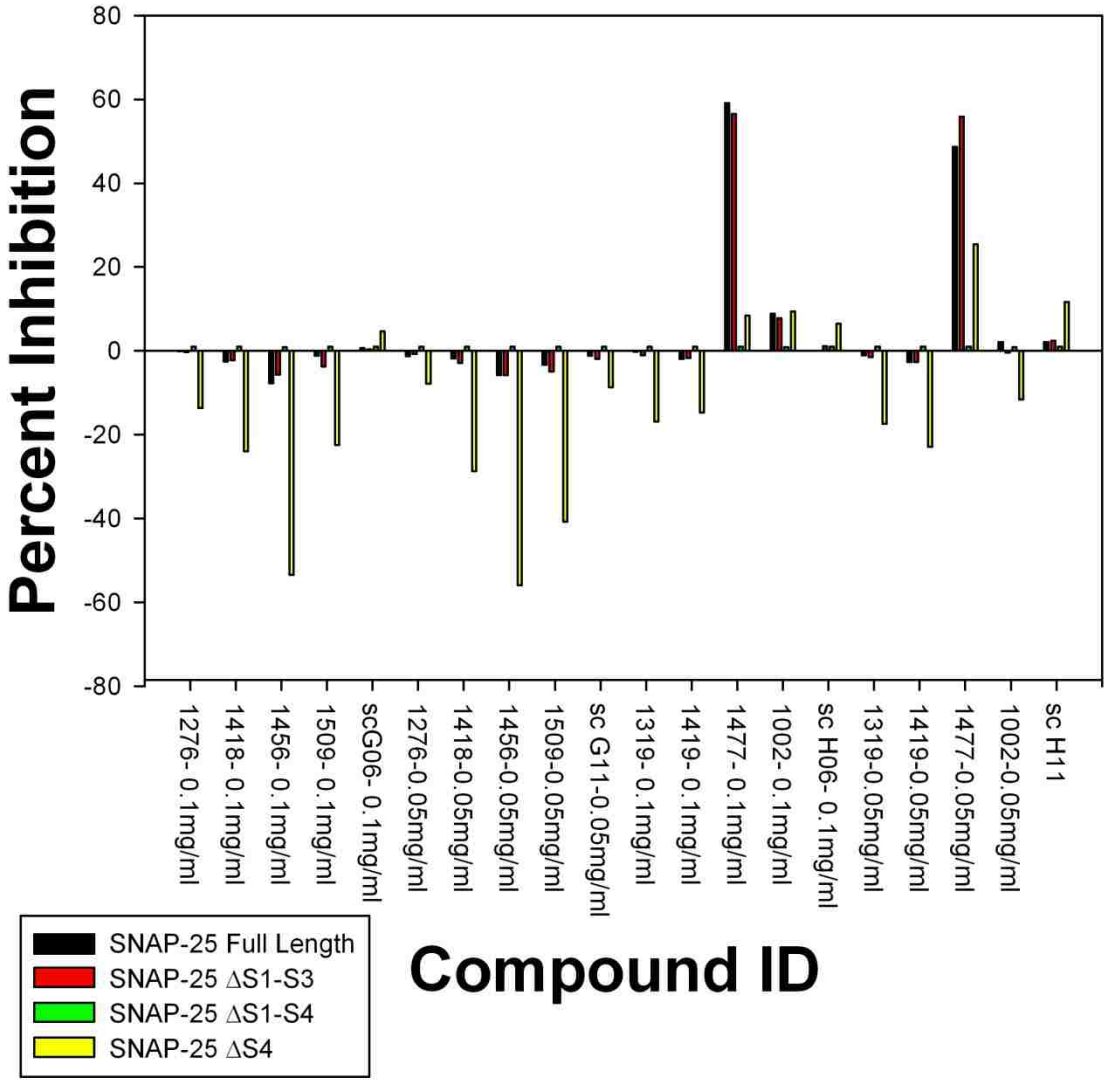

Figure 6.5 Percent inhibition values for compounds in part of the TPIMS scaffold plate which includes scaffold compound 1477. Compound 1477 was present at both 0,1 mg/ml and 0.05 mg/ml in this area of the plate, with both concentrations giving 50% to 60% inhibition on SNAP-25 full length and SNAP-25 ΔS1-S3 substrates. Full plate graphs and numerical percent inhibition values are included in Appendix 4.

This experiment verifies our original assumption that the platinum based scaffold caused inhibition independent of chemical modifications.

6.4 Future Follow up

Further analysis of these follow up screening results is under way at the Torrey Pines Institute for Molecular Studies. After identification of the most potent inhibitors, characterization of IC_{50} values using our microsphere based assay and testing in FRET based assays will be performed. Characterization of modifications of chemical scaffolds which give greater inhibition than the scaffold molecules themselves will be of interest and may lead to identification of particularly potent inhibitors. Once high affinity inhibitors of BoNTALC have been identified and characterized these molecules will need to be tested in cell based models of BoNTALC cleavage of SNAP-25. Compounds which are able to pass freely through cellular membranes and have little to no cellular toxicity in these assays will then be considered lead candidates for animal modeling for BoNTA treatment. Continued work is being done on characterizing chemicals of scaffold families 1644 and 1477.

Chapter 7.
Solution Based Protease Assay Development for Kinetic Analysis

7.1 Introduction

7.1.1 Rationale

In the development of flow cytometry microsphere based protease assays, two major goals were considered. The first was the application of flow cytometry-based high throughput screening (HTS) methodologies, which differ from most current protease assays in the ability to use full length substrates compared to protease cleavage sites alone. This goal has been accomplished, and previously unidentified inhibitors for both *Bacillus anthracis* Lethal Factor and *Clostridium botulinum* type A Light Chain have been discovered. The second goal in the development of these assays was for use in kinetic analysis, particularly toward the goal of identifying the contribution of protease/substrate distal binding or interaction sites toward the overall cleavage rate. Flow cytometry is particularly well suited for this application due its ability to collect and analyze data on a millisecond timescale while continuously analyzing particles one at a time. In flow cytometry every individual particle is analyzed separately in real time, which differs from other methodologies where a change of overall signal is measured. This makes flow cytometry a desirable platform for the study of kinetic measurements as well as HTS. Kinetic measurements of proteases by our microsphere based assay reqires validation by traditional solution based methods, therefore the complications associated with microsphere based methods are discussed here, along with the development of solution based methodologies to validate microsphere based protease kinetics.

7.1.2 Low substrate concentrations in microsphere based protease assays for kinetics.

Due to the fact that our microsphere-based assay makes it difficult to precisely adjust substrate concentrations, as done in traditional Michaelis-Menten kinetics approaches, we instead used a constant substrate concentration and increasing amount of enzyme. Earlier experiments with our microsphere bound substrate, quantified with EGFP standard microspheres, showed that we had bound in the magnitude of 10^5 substrate molecules per microsphere [127]. Varying the number of microspheres would still give us very low total substrate concentrations bound to microspheres, in approximately the low to mid picomolar range. The problem with using a system where [S] <<Km for kinetic measurements is derived and explained in the book Enzymes Second Edition by Robert Copeland [172].

The progress of an enzymatic reaction can be defined by the equation

Eq. 1. $[S]= [S_o]e^{-kt}$

where S is the substrate concentration remaining after time t, S_o is the starting concentration of substrate and k is the observed first order rate constant. By using the following relationships we see where the problem with low substrate concentrations occurs.

Eq. 2. $V_{max} = k_{cat}[E]$

where V_{max} is the maximum enzymatic rate, k_{cat} is the catalytic rate constant and [E] is the enzyme concentration, combined with the central expression for steady-state enzyme kinetics.

Eq.3 $v = \frac{Vmax[S]}{Km \cdot [S]}$

where K_m is the substrate concentration that provided a reaction velocity half of the V_{max} and v is the rate of the reaction over time, otherwise denoted as

Eq. 4 $v = -\frac{d[S]}{dt}$

Because [S]<<Km, the [S] in the denominator of equation 3 can be ignored and using the definition of V_{max} in equation 2, equation 3 can be rearranged to

Eq. 5 $-\frac{d[S]}{dt} = \frac{kcat}{Km}[E][S]$

Rearranging equation 5 and integrating we obtain

Eq. 6 $[S] = [S_o] \exp\left(\frac{kcat}{Km}[E]t\right)$

By using the definition of equation 1 in equation 6 it reduces to

Eq. 7 $k = \frac{kcat}{Km}[E]$

Equation 7 shows that using a known concentration of enzyme, an estimate of k_{cat}/K_m can be made from the observed first-order rate constant when [S]<<Km. This is the situation in the microsphere based protease assay where the substrate is in the low to mid picomolar range. This ratio k_{cat}/K_m is the specificity constant of an enzyme and measures the efficiency of an enzyme to convert substrate to product. Based on this derivation it would be impossible to obtain a K_m or a k_{cat} value alone from the microsphere based kinetics experiments but does allow a specificity constant to be measured instead. To obtain a K_m and k_{cat} value a traditional solution based approach must be taken in which increasing

substrate concentrations are used to reach a saturation rate of V_{max} for a constant enzyme concentration. From a hyperbolic fit a Km can be determined as the concentration at which 50% of Vmax is observed. A k_{cat} value could also be determined as follows. Assuming the following reaction pathway and considering the assumption that rates past catalysis, such as protease and cleaved substrate dissociation, are not rate limiting, we have distinct steps for k_{on}, k_{off} and k_{cat}.

Figure 7.1. Simplified kinetic model for proteolytic cleavage of a substrate (S) by proteolytic enzyme (E) to a product (P) Binding constants kon and koff represent the enzyme substrate binding and release while kcat is the catalytic rate of cleavage.

The rates of k_{off} over k_{on} would yield the binding constant K_d for enzyme substrate binding. If methods were available to pre-bind the protease (E) and substrate (S) to the ES form without catalysis and then activate the enzyme, it would be possible to calculate the k_{cat} from this reaction. These experiments and analysis would be analogous to magnesium jump experiment used to measure kinetic rates and K_d values of DNA and RNA polymerases [173]. It would be be possible to use this method in comparison with samples without pre-binding to determine the Kd of BoNTALC for SNAP-25. A K_m value and a k_{cat} value determined in this fashion in a solution-based assay could validate the k_{cat}/K_m specificity constant observed in the microsphere based assay.

7.1.3 Feasibility of full length protein FRET and substrate protease binding.

Studies using SNAP-25 in a fusion protein with N-terminal cyan fluorescent protein (CFP) and C-terminal yellow fluorescent protein (YFP) expressed intracellularly in the PC12 rat pheochromocytoma derived cell line have shown fluorescence resonance energy transfer (FRET) to occur despite the FRET partners being tethered at the opposite ends of full length SNAP-25 protein [174]. The PC12 cell line stably expresses the synaptotagmin II receptor and is capable of internalizing botulinum neurotoxin through the interaction of the toxin heavy chain with the receptor [175]. BoNTA treatment of PC12 cells transfected with the CFP/YPF SNAP-25 FRET construct was shown to result in an increase in CFP emission at 470nM [174], indicating that CFP/YPF SNAP-25 is cleaved by BoNTALC upon translocation of the light chain into the cytosol after entry into the cell mediated by the heavy chain. Cleavage of SNAP-25 in this system was also verified by Western blot analysis [174]. The efficiency of this system demonstrates that the N and C-terminus of full length SNAP-25 are sufficiently proximal to use in FRET based assays.

We have therefore adapted the same biotinylated SNAP-25 GFP used in microsphere based assays for use in a solution-based FRET assay. This assay is capable of using high substrate concentrations in order to identify the kinetic constants for comparison with microsphere based assays. With the ability to separate the protease/substrate binding steps from the catalytic step such an assay would also potentially allow for the identification of the kinetic contribution of the S1-S3 and S4 SNARE domains to substrate cleavage.

One possibility to achieve protease/substrate binding without catalysis would be to replicate methods used to characterize inhibitory Zn^{2+} binding demonstrated on the metalloprotease carboxypeptidase A. It has been shown that excess divalent metals, especially Zn^{2+}, will inhibit carboxypeptidase A [176]. The proposed mechanism of this inhibition is the formation of a metal hydroxide bond from the catalytic zinc atom in the metalloprotease active site to a zinc ion in solution, which is then stabilized by another active site glutamic acid residue opposite the catalytic zinc [176]. Because the active sites of metalloproteases are conserved, this is likely a mechanism for excess zinc inhibition of all metalloproteases. The catalytic zinc bound to the metalloprotease zinc binding motif, comprised of residues histadine-glutamic acid-any amino acid-any amino acid–histadine (HExxH), is tightly bound and coordinated by multiple negative charges. It may be possible therefore to chelate the inhibitory zinc molecule with EDTA without affecting the tightly bound catalytic zinc, thereby restoring catalytic activity to the metalloprotease. If such mechanism were to inhibit catalytic activity of a metalloprotease but allow protease/substrate binding, it may be possible to pre-bind protease to substrate without catalysis. Addition of EDTA to start catalysis would make it possible to measure differences in fluorescence burst amplitude to calculate a k_{cat} value.

There are two primary concerns in the adaptation of such an assay to kinetics analysis. The first is to verify the specificity constant, k_{cat}/K_m ratio, observed in the microsphere-based assay is consistent with the ratio of k_{cat}/K_m, as observed in a solution-based assay using the same substrate. The second

objective is to determine the kinetic contribution of distal interaction sites for proteases on substrates, which could be accomplished by using the strategy described above. In order to determine these constants, a solution based assay capable of using substrate concentrations high enough to reach V_{max} is necessary to determine Km, while zinc pre-binding would allow determination of the k_{cat}. The use of biotinylated GFP protease substrates in the microsphere based assay may give rates slightly different than cleavage rates of the natural substrates to their proteases due to the relatively large biotinylation tag and GFP attachments. It is therefore desirable to use identical protease substrates in solution based assays to verify microsphere based specificity constant measurements with this approach.

In the work presented here solution based assays have been developed for BoNTALC which would allow substrate concentrations high enough to reach Vmax and determine the Km for BoNTALC on SNAP-25 GFP. The strategy of Zn^{2+} inhibition followed by chelation of inhibitory Zn^{2+} and restoration of proteolytic activity of BoNTALC has also been demonstrated, and appears to lead to a faster initial rate of SNAP-25 GFP cleavage. The assays developed here would allow for measurements of both Km and k_{cat} in solution based assays for comparison to microsphere based assays, and further compliment the study of SNAP-25/BoNTALC kinetics and interactions.

7.2 Methods

7.2.1 GFP quenching by Cy3 streptavidin

Streptavidin (purchased from Pierce scientific) was labeled with Cy3 NHS ester (GE healthcare) as per the manufactures instructions and incubated with our previously described biotinylated SNAP-25 GFP for 1 hour at room temperature in protease buffer (50 mM HEPES, 100 mM NaCl) covered from light. The maximal excitation wavelength of EGFP, 488 nm, directly excites Cy3 at about 15%, therefore we chose to use an excitation wavelength of 450 nm, which only excites Cy3 with about 1 % efficiency. For determination of optimal Cy3 strepatvidin to biotinylated SNAP-25 GFP quenching, 25 nM SNAP-25 GFP (concentraions determined by UV_{280} spectroscopy) was bound with increasing amount of Cy3 streptavidin (concentrations also determined by UV_{280} spectroscopy) and excited at 450 nm in a PTI fluorimeter with slit lengths of 2 nm used with an emission scan between 488 nm to 650 nm performed to determine the ratio of Cy3 streptavidin to biotinylated SNAP-25 GFP for optimal GFP quenching.

7.2.2 FRET based Cy3 streptavidin biotinylated GFP assays.

FRET based protease assays were run for 1 minute after Cy3 streptavidin/biotinylated SNAP-25 GFP binding in a PTI fluorimeter collecting 1 data point per second with slit sizes of 2 nm and excitation at 450 nm and emission at 507 nm recorded. Samples were run in glass cuvettes with a stir bar providing continuous mixing. Emission of EGFP was measured at 507 nm, the peak emission of biotinylated SNAP-25 EGFP, as seen in an emission scan on a PTI fluorimeter. SNAP-25 GFP and deletion mutations were sampled for 55

seconds and BoNTALC was added to the sample at 1 minute with 507 nm emission recorded for 10 minutes after addition. Normalization of fluorescence data for analysis of rates of SNAP-25 deletions was done by averaging the first 55 seconds of 507 nm emission and subtracting that value from each data point after 5 nM BoNTALC addition. Conversion of fluorescence into nM changes for increasing concentrations of SNAP-25 Cy3 streptavidin was done by normalizing the raw fluorescence values as described and dividing by the maximum fluorescence value of the entire 10 minute time course and multiplying by the starting nM concentration of SNAP-25 GFP in the reaction. Normalization of fluorescence data for analysis of rates of SNAP-25 deletions was done by averaging the first 55 seconds of 507 nm emission and subtracting that value from each data point after 5 nM BoNTALC addition.

7.2.3 Non-FRET based SNAP-25 GFP solution based protease assays. (self quenching)

SNAP-25 GFP self-quenching experiments were set up with the desired concentrations of biotinylated SNAP-25 GFP in protease buffer (50 mM HEPES 100 mM NaCl) and run on a PTI fluorimeter collecting 1 data point per second with slit sizes of 2 nm. SNAP-25 GFP was excited at 488 nm and emission read at 507 nm with sample continuously mixed by stir bar in glass cuvettes. 5 nM BoNTALC was added to the SNAP-25 GFP sample after 1 minute and increase in 507 nm emission was monitored for 10 minutes.

7.2.4 Microsphere based LF inhibition by zinc chloride

Microsphere-based LF assays were set up as described previously using biotinylated LF consensus GFP [127]. 25 µl Spherotech streptavidin coated pink particles were used, washed and split into three separate sample tubes in protease buffer. 1 mM $ZnCl_2$ was added to two of the tubes. The no $ZnCl_2$ sample was run on a FACScan flow cytometer with settings described previously [127] for 60 seconds, 365 nM LF was added and sample was run until depleted. One of the $ZnCl_2$ samples was run identically to the no $ZnCl_2$ sample with LF added at 60 seconds, the other had 365 nM LF added prior to running and 2 mM EDTA was added at 60 seconds. Gates were drawn on graphical data using time on the X axis and FL1 green fluorescence on the Y axis with X means for used for time and Y mean FL1 fluorescnece values for each time bin was taken. X means were changed to real time after addition by subtracting 60 seconds from it and Y mean FL1 fluorescence was normalized by dividing by the Y mean for the first 60 seconds. Each data point represents normalized fluorescence for a time binned gate.

7.2.5 Zinc pre-binding and reaction starting of solution-based BoNTALC assays.

Experiments using excess zinc to inhibit the BoNTALC metalloprotease were set up with 5 nM BoNTALC and 1 mM zinc chloride in protease buffer and incubated at room temperature for 10 minutes. Desired concentrations of SNAP-25 GFP were added to the sample, incubated for 30 minutes at room

temperature, and run on a PTI fluorimeter as described above. After 1 minute of 507 nm emission monitoring 2 mM EDTA was added and increase in 507 nm emission was monitored for 10 minutes. Controls for this experiment were set up as described above in the self quenching experiment with 5 nM BoNTALC added instead of EDTA after 1 minute.

7.3 Results

7.3.1 GFP fluorescence quenching by Cy3 streptavidin FRET

Increasing amounts of Cy3 streptavidin were added to 25 nM SNAP-25 GFP to determine maximum quenching effects on GFP by fluorescence energy resonance transfer (FRET). GFP emission at 507 nm was quenched most efficiently at concentrations of 100 nM Cy3 labeled streptavidin, with a corresponding increase in Cy3 emission at 468 nm (**Fig. 7.2**). A similar degree of GFP quenching was seen with the use of 250 nM Cy 3 streptavidin (**Fig. 7.2**), indicating a 4:1 molar ratio was sufficient to produce the maximum amount of GFP quenching.

7.3.2 BoNTALC cleavage of SNAP-25 bound to Cy3 streptavidin leads to loss of FRET and increased 507nm emission.

Addition of BoNTALC to Cy3 streptavidin led to increases in GFP emission at 507 nm at a hyperbolic rate to maximum cleavage (**Fig. 7.3**). According to traditional enzyme kinetics, increasing the amount of substrate in the presence of a constant amount of enzyme should lead to increased initial rates of cleavage.

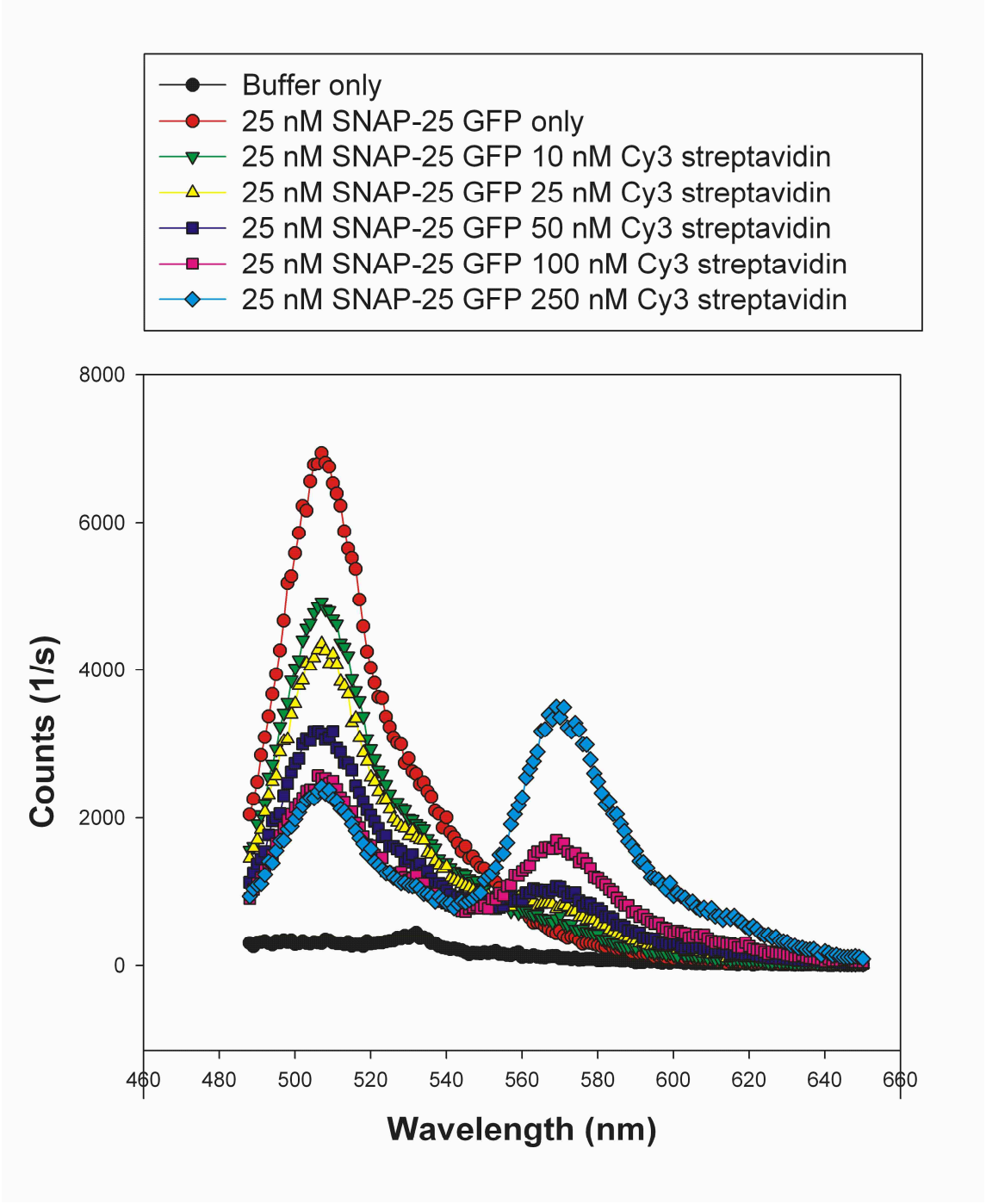

Figure 7.2 Cy3 streptavidin titration onto 25 nM biotinylated SNAP-25 GFP. Excitation was done at 450 nm to avoid direct excitation of Cy3 and emission spectra from 488 nm to 650 nm were collected at 1 data point per nm. Maximum quenching of GFP emission at 507 nm was achieved using a 4:1 ratio of Cy3 streptavidin to SNAP-25 GFP.

This was observed using biotinylated SNAP-25 GFP Cy3 streptavidin (**Fig. 7.3, 7.4**). This indicated that this assay could be used for kinetics analysis to determine the Km for BoNTALC cleavage of SNAP-25 full length. Initial rates of SNAP-25 GFP cleavage, after conversion into units of nM cleaved, were plotted for the first 30 seconds of the reaction to determine if a V_{max} value had been obtained (**Fig. 7.4**). It was observed that SNAP-25 GFP Cy3 neutravidin concentrations up to 300 nM did not reach Vmax and a higher concentration range would be needed. When 5 nM BoNTALC was added to 25 nM concentrations of substrate (**Fig 7.5**), the same relative rates of cleavage occurred across all four of the tested substrates as observed in the microsphere based protease assay. Interestingly, SNAP-25 full length and SNAP-25 ΔS1-S3 had similar rates in this particular assay. However, it appeared that cleavage of full length SNAP-25 went to completion faster than SNAP-25 ΔS1-S3 (**Fig. 7.5**), indicating that the rate of SNAP-25 full length cleavage was faster**.** The two S4 deletion substrates had dramatically lower rates of cleavage than the S4 containing substrates, and did not appear be cleaved to completion in the 10 minute time course analyzed (**Fig 7.5**).

One problem with the solution based FRET assay was non-specific FRET that apparently occurred at substrate concentrations at or above 250 nM This is presumed to be due to intra-molecular FRET. Occurrence of such non-specific FRET was suggested by the finding that after cleavage of high concentrations of SNAP-25 GFP with Cy3 streptavidin, fluorescence intensity failed to reach the same level as that of SNAP-25 GFP in the absence of Cy3 streptavidin (data not

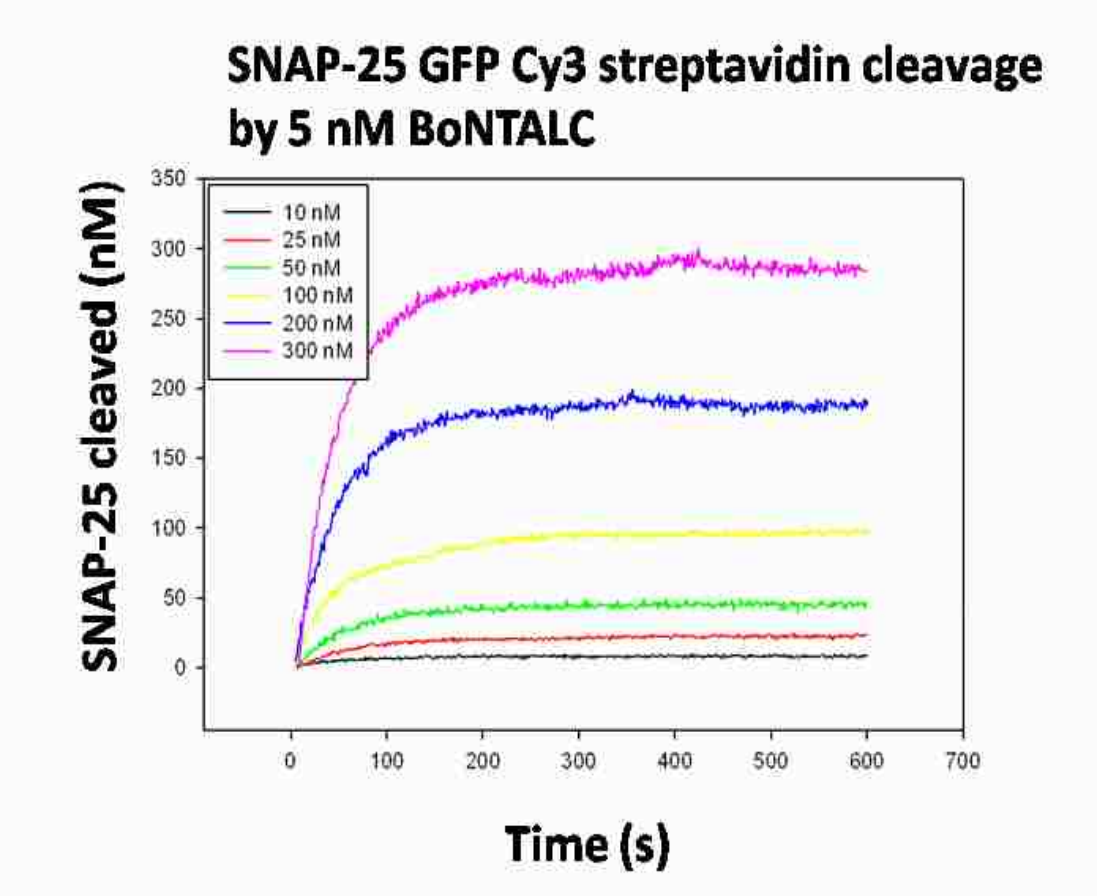

Figure 7.3 Increasing amounts of SNAP-25 GFP bound with 4 times as much Cy3 streptavidin with addition of 5 nM BoNTALC. Samples were run for 1 minute prior to addition of BoNTALC, 5 nM BoNTALC was added and samples run for an additional 10 minutes Fluorescence values were converted into cleaved substrate concentrations by averaging the first 55 seconds of 507 nm emission and subtracting that value from each data point after 5nM BoNTALC addition, dividing by the maximum fluorescence value of the entire 10 minute time course and multiplying by the starting nM concentration of SNAP-25 GFP in the reaction.

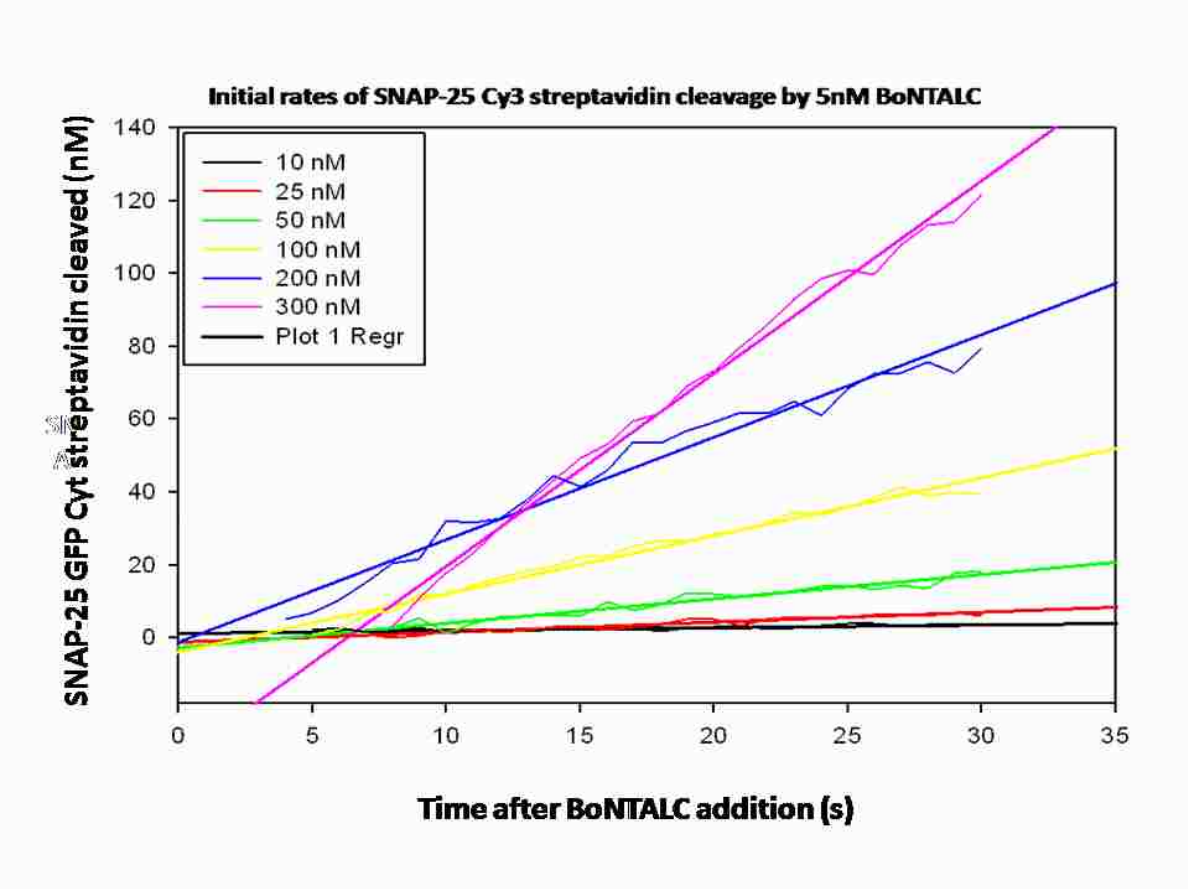

Figure 7.4 Initial rates of SNAP-25 GFP Cy3 streptavidin cleavage by 5 nM BoNTALC. Data has been converted into nM SNAP-25 cleaved as described in methods and liner fits have been performed for the first 30 seconds of data. Saturation rates were not reached in this particular experiment so a K_m value was not determined

shown). This non-specific FRET made it impossible to compare initial rates of SNAP-25 GFP Cy3 streptavidin cleavage at high concentrations to those of lower concentrations. Fortunately, we identified a simpler method based on unique fluorescence properties of GFP in association with this set of substrates as outlined below.

7.3.3 SNAP-25 GFP fluorescence increases without a FRET partner after cleavage by BoNTALC.

During the course of performing SNAP-25 GFP FRET experiments it was observed that in a negative control with no Cy3 streptavidin bound to biotinylated SNAP-25 GFP, addition of 5 nM BoNTALC led to a burst of increased fluorescence similar to that seen in the FRET based assays. These experiments demonstrated comparable kinetics of fluorescence increase without the same magnitude seen in FRET based assays. This increase in 507 nm fluorescence was seen at all concentrations from 5 nM to 1 µM of biotinylated SNAP-25 GFP (**Fig. 7.6**). To test if this decreased GFP emission of biotinylated SNAP-25 GFP was due to the presence of the biotinylation tag or the folding of biotinylated SNAP-25, we examined the behavior of biotinylated LF15 GFP in similar solution based assays. For this purpose 25 nM LF15 GFP was bound to 100 nM Cy3 streptavidin in one sample, and another sample without bound Cy3 streptavidin were both exposed to 500 nM lethal factor. The increase in GFP emission after cleavage without a FRET partner that was seen for biotinylated SNAP-25 GFP was not observed for biotinylated LF15. A loss of FRET was observed in the Cy3 streptavidin containing sample, indicating that LF15 was cleaved in this assay

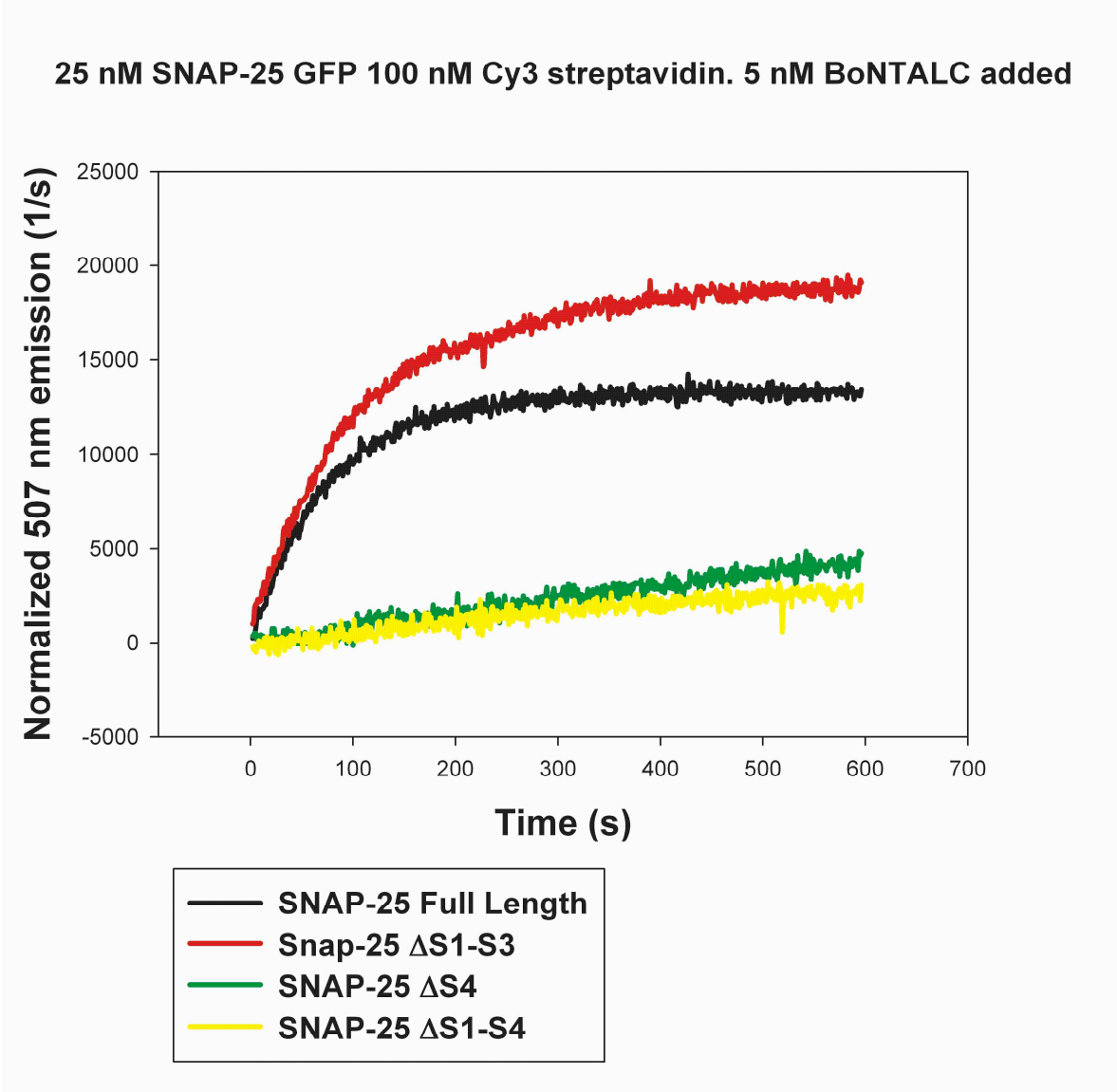

Figure 7.5 25 nM SNAP-25 full length and SNARE motif deletions used in our microsphere based assay bound to 100 nM Cy3 neutravidin and run by fluorimetry with addition of 5 nM BoNTALC. 507 nm fluorescence emission has been normalized as described in methods.

(**Fig. 7.8**). This experiment indicated that GFP quenching was not due to the biotinylation tag alone and was rather a property of biotinylated SNAP-25. We have termed this phenomenon self-quenching, a result of GFP emission being quenched in the presence of biotinylated SNAP-25 by an undetermined mechanism. This self-quenching property was exploited to evaluate kinetic properties of BoNTALC cleavage of biotinylated SNAP-25 GFP.

7.3.4 Zinc inhibition and pre-binding of metalloprotease substrates

Early experiments during development of our microsphere based protease assay showed that the lethal factor metalloprotease was completely inhibited by 1mM zinc chloride. Not only did 1 mM zinc chloride in protease buffer (50 mM HEPES, 100 mM NaCl, 1 mg/ml BSA and 0.025% tween-20) completely inhibit lethal factor, but addition of 2 mM EDTA started the reaction at a slightly faster rate than experiments using protease buffer alone (data not shown). This inhibition was most likely due to the same mechanism of carboxypeptidase A inhibition by divalent metals, as previously reported, in which proteases bound substrates without catalysis [176]. Consistent with such a mechanism, no cleaveage occurred when 100 nM SNAP-25 GFP was combined with BoNTALC that had been pre-incubated with 1mM $ZnCl_2$ in protease buffer for 10 minutes, whereas cleavage was rapidly initiated upon subsequent addition of 2 mM EDTA . This indicates that the hypothesis outlined in the introduction of this chapter was correct such that inhibitory zinc could be selectively chelated by EDTA, sparing the catalytic site Zn so as to allow jump starting of the metalloprotease reaction.

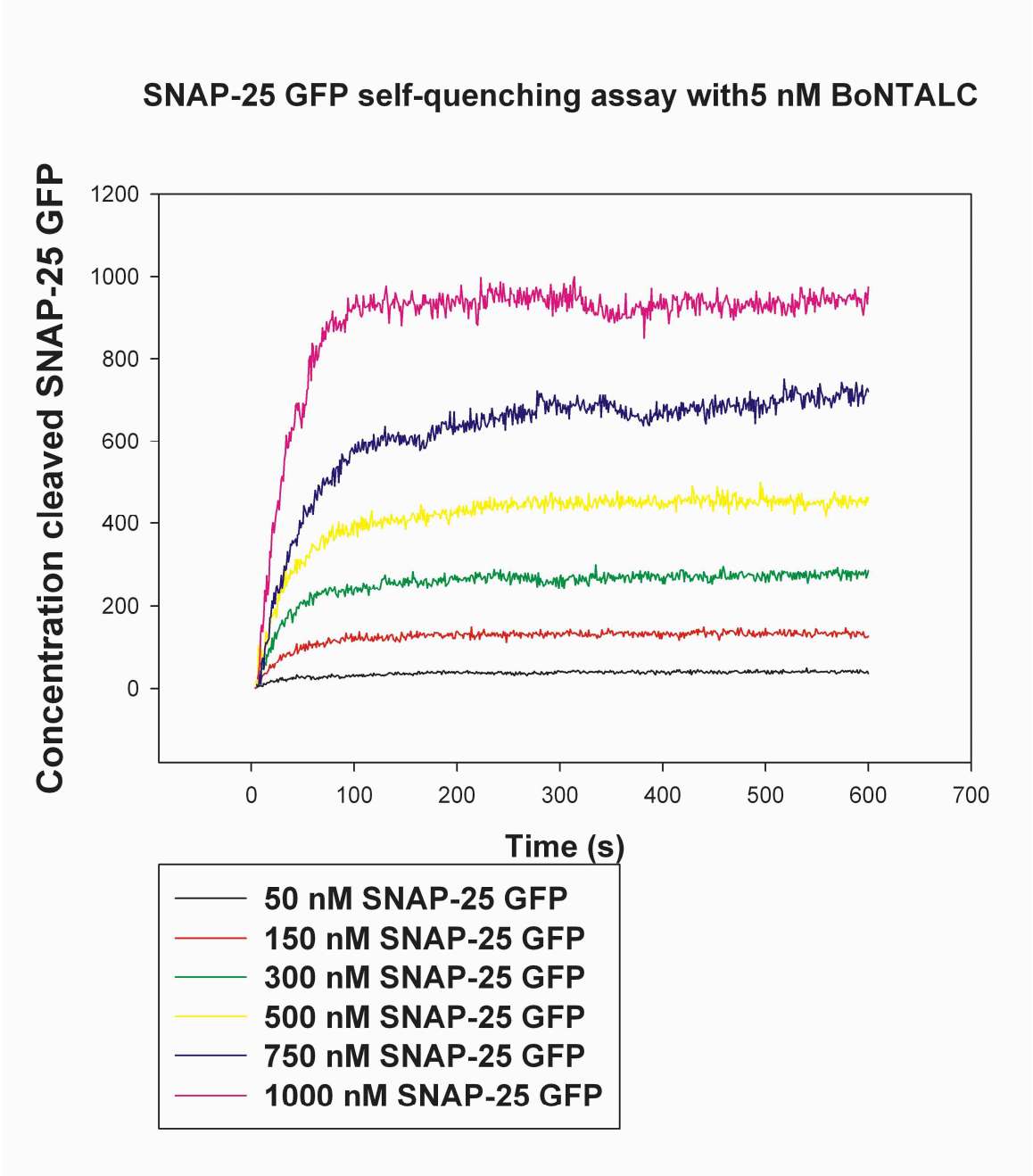

Figure 7.6 SNAP-25 GFP 507 nM emission with no FRET partner after addition of 5 nM BoNTALC. Cleavage of SNAP-25 releases GFP which increases its 507 nm emission after release from biotinylated SNAP-25 GFP. Data was normalized and converted to nM cleaved as described in methods

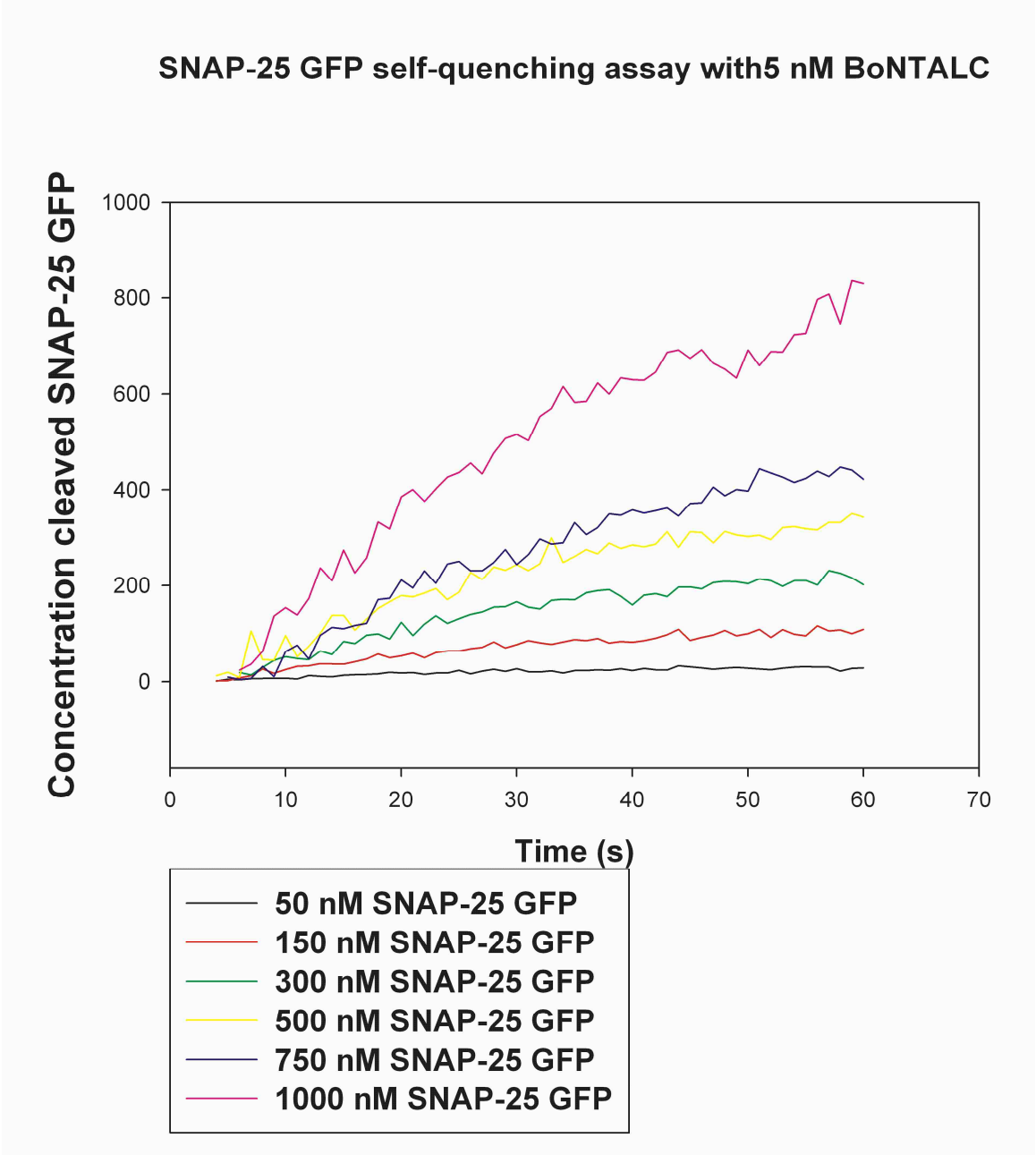

Figure 7.7 Initial rates of biotinylated SNAP-25 GFP cleavage with no FRET partner in the concentration range of 50 nM to 1 µM biotinylated SNAP-25 GFP. Data was normalized and converted to nM cleaved as described in methods. A saturation rate was not reached in the substrate concentrations used in this experiment, therefore a K_m value was not determined.

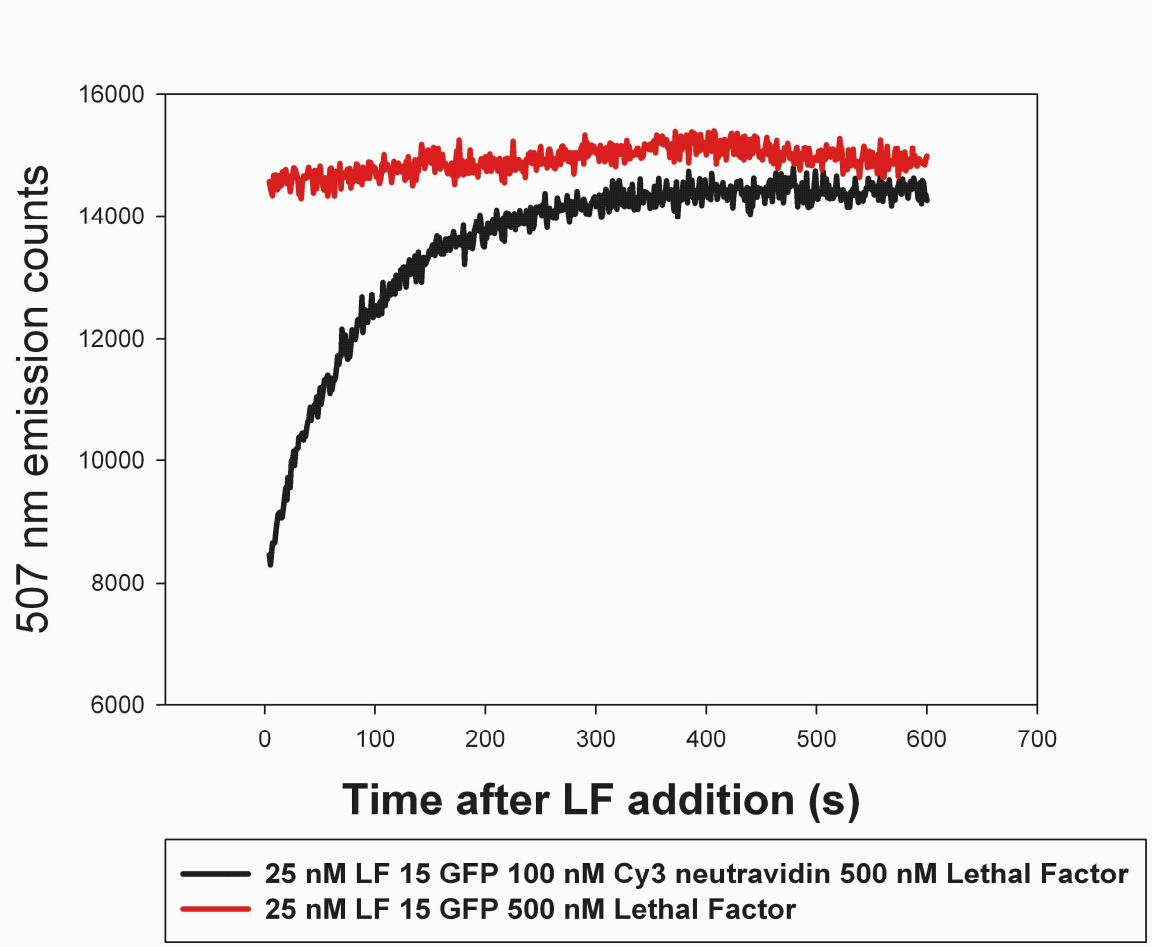

Figure 7.8 Biotinylated LF15 GFP cleaved with 500 nM lethal factor in samples containing Cy3 streptavidin or biotinylated LF15 GFP alone. Excitation was done at 450 nm and emission read at 507 nm.

To examine this further, 5 nm BoNTALC was added to 100 nM SNAP-25 GFP in the absence of $ZnCl_2$ and analyzed on the fluorimeter with the same settings. When comparing these samples we observed a slightly faster increase of 507 nm emissionon the pre-bound sample (**Fig. 7.10**), indicating faster proteolytic cleavage. Taken together These results indicate that BoNTALC may be binding to SNAP-25 GFP in the presence of 1 mM $ZnCl_2$ and chelation of inhibitory zinc starts the reaction from a pre-bound enzyme-substrate (ES) state. We could potentially use this mechanism to separate the kinetic steps of binding from catalysis and calculate a k_{cat} value. More work will need to be done and samples repeated several times in order to validate these promising preliminary findings.

7.4 Discussion and future directions

In the work presented here we have developed a solution based FRET assay to monitor cleavage of SNAP-25 by botulinum neurotoxin type A light chain. This assay uses the GFP quencher Cy3 covalently bound to streptavidn molecules on the N-terminus biotin of our biotinylated SNAP-25 GFP. This assay was also used to demonstrate cleavage of lethal factor consensus sequences by lethal factor in our biotinylated GFP substrates when bound to Cy3 streptavidin (**Fig. 7.8**). The development of solution based protease assays as a compliment to our microsphere-based assays will provide an independent test to validate protease kinetics measurements. These solution based assays can also be used to verify inhibitors discovered by high throughput screening of microsphere based flow cytometry assays.

7.4.1 GFP stability for kinetics only works for SNAP-25 GFP.

The finding that cleavage of biotinylated SNAP-25 GFP by BoNTALC leads to an increase in GFP fluorescence at 507 nm without a FRET partner simplifies the use of this solution-based assay for kinetics work. Because we can eliminate Cy3 streptavidin from this assay and get initial cleavage rates from biotinylated SNAP-25 GFP alone, it will be much easier to use the high concentrations of biotinylated SNAP-25 necessary to reach V_{max} using 5 nM BoNTALC.

We do not completely understand why cleavage of biotinylated SNAP-25 GFP by BoNTALC leads to an increased 507 nm emission from the C-terminal GFP. Our current theory is that the folding of SNAP-25 either causes the orientation of GFP to be quenched by nearby protein, or that the attachment of the rather large biotinylation tag along with SNAP-25 to GFP leads to a slight mis-folding of GFP, consistent with the lower 507 nm emission compared to that after cleavage. This "self-quenching" was not seen for the biotinylated LF15 GFP lethal factor substrate (**Fig. 7.8**), so it is not due soley to the presence of the relatively large biotinylation tag. Whatever the mechanism for this phenomenon, it is a useful tool for the study of kinetic measurement of SNAP-25 GFP cleavage by BoNTALC. Measurements of V_{max} and Km remain to be compared to measurements of those values by FRET based measurements as well using Cy3 streptavidin. The problem of non-specific FRET at high Cy3 streptavidin concentrations can be avoided by setting up control reactions at those

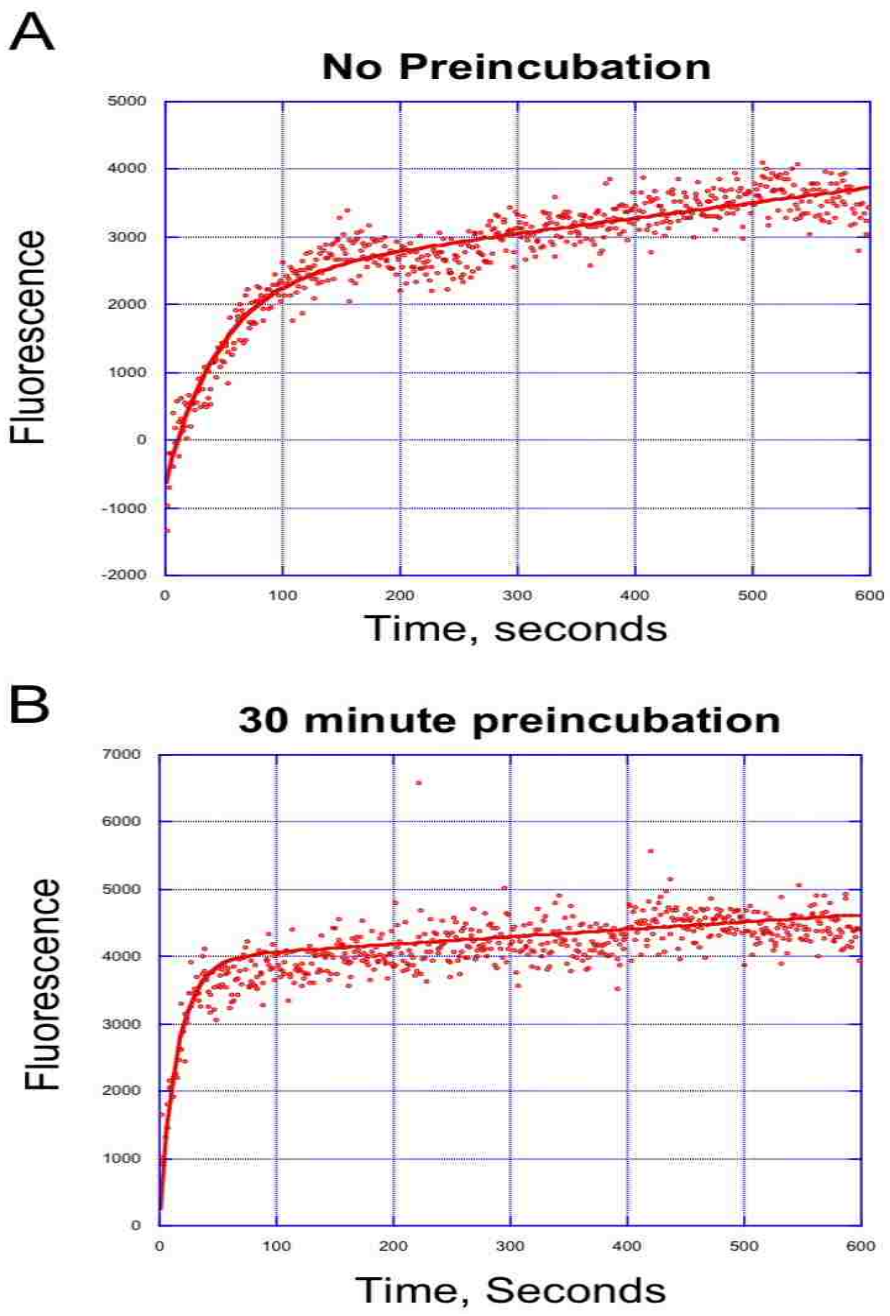

Figure 7.9 Biotinylated SNAP-25 GFP by 5 nM BoNTALC using 100 nM biotinylated SNAP-25 GFP in our self quenching assay. **A.** 5 nM BoNTALC was added to 100 nM biotinylated SNAP-25 GFP. **B.** 5 nM BoNTALC was incubated for 10 minutes with 1mM $ZnCl_2$. 100 nM SNAP-25 GFP was added and incubated for 30 minutes, sample was run for 60 seconds and 2 mM EDTA added to start cleavage. An average of the fluorescence values was for the first 55 seconds was subtracted from subsequent values for both samples.

concentrations in which Cy3 streptavidin is blocked by high levels of free soluble biotin prior to addition of biotinylated SNAP-25 GFP. These controls reveal the maximum value of GFP emission, which can be used to normalize data and calculate initial rates in nM cleaved.

By measuring the V_{max} and K_m values in both FRET-based measurements and in self-quenching assays, a comparison can be made in order to validate the self-quenching method for future use. If self-quenching turns out to be a valid methodology to perform protease enzyme kinetics, our group is looking into ways to adapt it for use in other protease assays. The addition of highly structured and folded protein tags may cause slight mis-folding of GFP and allow us to adapt this system to other protease substrates, which do not seem to exhibit the extent of self-quenching observed by SNAP-25 GFP.

7.4.2 Kinetic constants found in solution based assays will be compared to the specificity constant found in microsphere based assays.

The discovery that zinc inhibition of metalloproteases and pre-binding, and that EDTA addition leads to a faster rate of cleavage than the addition of protease substrate alone, suggests that the proteolytic reaction are initiated from an ES enzyme-substrate complex. Consequently, this can be used to measure the k_{cat} of BoNTALC and therefore can then be used to calculate the Kd for SNAP-25 full length and SNAP-25 ΔS1-S3. By comparison of the rate kinetics for SNAP-25 full length and ΔS1-S3 it should be possible to calculate the kinetic contribution of the S1-S3 SNARE domains on BoNTALC cleavage. Moreover, if we take the K_m from the FRET based and self-quenching experiments and the

k_{cat} from zinc pre-binding methods we should be able to calculate the specificity constant k_{cat}/K_m. Comparison of the specificity constant in solution to that found in microsphere based assays would provide an important validation of microsphere based protease assays with low substrate concentrations.

7.4.3 Future directions

The experiments outlined above to determine and validate kinetic constants of SNAP-25 BoNTALC continue to be carried out, as well as experiments to validate GFP self-quenching as a method to determine these constants. If GFP self-quenching is a valid method of measuring these constants, work will be done to engineer self-quenching properties into protease substrates which are not inherently self-quenching. This will most likely involve sub-cloning of protein motifs which are highly structured and folded into our protease substrates in an attempt to cause GFP to slightly mis-fold. The use of GFP self-quenching could greatly reduce complications with FRET based methods currently used to measure protease kinetics, as well as allow us to use full length substrates containing distal protease interaction elements in such kinetic studies.

Chapter 8.
Conclusions and Future Directions

8.1 Conclusions

8.1.1 Development of a microsphere based protease assay for high throughput screening.

In the work described here, we demonstrate the successfull development of microsphere based protease assays for *Bacillus anthracis* Lethal Factor and *Clostridium botulinum* type A Light Chain. We have demonstrated that these proteases specifically cleave their substrates and that these assays can be evaluated in a multiplex assay format. These assays are capable of being run simultaneously in the same reaction volume, as demonstrated in Chapter 4, and are compatible with small volumes in microplates for high throughput screening. This microsphere based protease assay has been successfully developed and shows promise for adaptation to any future proteases of interest.

8.1.2 Identification of inhibitors of bacterial toxins

In high throughput flow cytomery screening using the HyperCyt system we have identified inhibitors of two different bacterial toxin proteases. The compound ebselen was shown to be an inhibitor of BoNTALC with an IC_{50} value of 6 µM. Two inhibitors of Lethal Factor have also been identified, pirenperone and harmalol hydrochloride dehydrate. Confirmatory studies remain to be done on these two compounds. Numerous potential compounds for inhibiton of BoNTALC have been identified by screening of the TPIMS library, some of which are under continued investigation. The use of microsphere based protease

assays shows promise for additional inhibitor identification of these bacterial toxin proteases through screening of larger and more diverse chemical libraries.

8.1.3 Solution based assay development and use for protease kinetics.

We have developed and implemented solution based FRET assays to verify potential inhibitors discovered through our microsphere based assays. The use of Cy3 streptavidin as a GFP quencher on the same biotinylated GFP substrates used in our microsphere based assays has made these assays easy to perform because we do not need to develop specialized FRET substrates. These assays have verified ebselen as an inhibitor of BoNTALC, as have assays using the SNAPtide FRET peptide from List Biological Laboratories.

The finding that biotinylated SNAP-25 GFP does not require a FRET partner for increased 507 nm emission after cleavage by BoNTALC simplifies these solution based assays even further. However, this “self-quenching” system observed for biotinylated SNAP-25 GFP does not appear to be a general method for protease study since biotinylated LF15 GFP does not produce similar results upon cleavage by LF. Nevertheless it is conceivable that this approach may be used with protein engineering methods to produce similar self-quenching substrates, which would aid in development of additional fluorescence based protease assays.

We have demonstrated the effective use of inhibitory zinc for jump starting cleaveage reactions by metalloprotease, both in microsphere based Lethal Factor assays and in solution based SNAP-25 GFP “self-quenching” assays. These approaches can be used to find k_{cat} and K_m values for BoNTALC to SNAP-

25 GFP. A k_{cat}/K_m value can then be used to verify the specificity constant observed in our microsphere based assay.

8.2 *Continued work in progress.*

8.2.1 Follow up on Lethal Factor inhibitors

We have recently discovered two potential inhibitors of the *Bacillus anthracis* lethal factor from screening of the Prestwick chemical library. Follow up work purifying additional lethal factor and performing dose response curves to determine IC_{50} values for these compounds will be done in the near future. After IC_{50} values are determined in our *in vitro* microsphere based assay, they will be verified in FRET based assays, either using the MAPKKide FRET substrate from List Biological Laboratories or using biotinylated LF15 GFP bound to Cy3 streptavidin. Future assays to determine the potential of these inhibitors in biological systems will be designed for macrophage cell lines challenged with lethal toxin and in animal models of inhalational anthrax.

8.2.2 Follow up on Botulinum Neurotoxin type A light chain inhibitors.

The compound ebselen, which has been shown to be an inhibitor of BoNTALC, shows promise as a lead compound for treatment of Botulinum neurotoxin infection and poisoning. Ebselen is a pre-approved drug for human use and has been given to animals in high doses with no apparent side effects. Ebselen has been patented for numerous uses; however, emergency treatment of botulinum neurotoxin is currently not one of the patented applications. Future

studies using animal models of botulinum neurotoxin poisoning and the potential for the use of ebselen as a treatment will be done. Due to the high biosafety level required for the use of intact botulinum neurotoxin, and the extensive protocols for use of animal models, this work will not be done by our laboratory group. Investigations are underway to identify potential collaborators who are already carrying out such experiments. Information gathered from animal models regarding the effects of ebselen to treat botulinum neurotoxin poisoning will be useful in determining if ebselen has potential as anti-botulinum toxin drug.

8.2.3 TPIMS combinatorial library screening

Collaboration with the Torrey Pines Institute for molecular studies for identification of BoNTALC inhibitors remains ongoing. TPIMS will be sending individual compounds selected from follow up screening results, and dose response curves will be performed in our microsphere based assay, as well as FRET assays. Continued collaboration with the TPIMS group could also potentially include analysis of data for BoNTALC screening already performed to identify compounds which act as activators of BoNTALC.

8.2.4 Determination of kinetic constants fo Botulinum Neurotoxin type A Light Chain to SNAP-25 and SNAP-25 deletion mutants.

Efforts are underway to determine the K_m and V_{max} values for BoNTALC in both solution based FRET assays as well as solution based GFP self-quenching assays. Comparison of values obtained by these methods could validate our SNAP-25 self-quenching method as a way to perform solution based protease

assays. Using zinc inhibition and pre-binding, we will attempt to calculate a k_{cat} value for BoNTALC. Comparison of BoNTALC rates of cleavage on our SNAP-25 SNARE deletions will be performed to determine Kd values for each of the SNAP-25 mutants. Determination of Km and k_{cat} will be used to calculate k_{cat}/Km, the specificity constant, in a comparison to the k_{cat}/Km estimates from our microsphere-based protease assay with low substrate concentrations, predicted by the calculations in Chapter 7. If the specificity constant from our solution-based assays matches that found in our microsphere-based assay, further work using alternative proteases will be done for additional validation.

8.2.5 Continued screening efforts for Lethal Factor and Botulinum Neurotoxin type A Light Chain.

Both Lethal Factor and Botulinum Neurotoxin type A Light Chain assays have been successful in identifying small molecule inhibitors by high throughput screening. These assays use the same protease buffer (50 mM HEPES, 100 mM NaCL, 1 mg/ml BSA and 0.025% Tween-20) and can be run in parallel in the same well of 384 well plates through the use of multiplex microspheres. Using the Xa substrate as a fluorescence control, LF 15 GFP for the LF assay, SNAP-25 full length and SNAP-25 ΔS4 on different sets of multiplex microspheres, we could combine these assays into one for screening purposes. The inclusion of SNAP-25 ΔS4 in this system would also allow us to screen for S4 SNARE-BoNTALC interaction inhibitors. In this assay we would expect to cleave full length SNAP-25 at the same level of SNAP-25 ΔS4 when a small molecule interfering with protease-substrate interactions at the S4 SNARE motif is

encountered. To perform this parallel assay purified Lethal Factor would be added together with commercially available BoNTALC to the assay plates at the same time. We are also attempting to purify BoNTALC in an active form to allow for large scale screening efforts using this duplex bacterial toxin protease assay to identify additional novel inhibitors of either of these toxin based proteases.

8.3 Microsphere based multiplex protease assays for future protease targets.

In the work described here we have developed microsphere based protease assays for the proteases *Bacillus anthracis* Lethal Factor and *Clostridium botulinum* neurotoxin type A light chain. These two specific proteases were selected for two main reasons. First is the current state of interest in high throughput screening for novel inhibitors of these proteases for bio-defense related reasons. Secondly, both proteases have a unique mechanism of specific substrate recogniition through distal interaction regions on their substrates, which contribute to their exceptionally high specificity. Most existing high throughput screening assays for both of these proteases does not allow use of extended substrates containing distal interaction sites, but use relatively small FRET peptides containing the cleavage site alone. We have shown that these proteases cleave their full length protein targets with rates that are faster than protein targets lacking distal binding sites. This observation has implications for the study of protease inhibitors since it raises the possibility to identify small molecules which target protease/substrate interaction sites.

The methodology of flow cytometry and the use of multiplex microspheres for screening these proteases for inhibitors could easily be adapted to other protease targets for multiplex screening in a similar fashion. The ability to design multiplex assays with multiple substrates and also screen against multiple proteases at one time also has the advantage of providing information about the selectivity of particular inhibitors among closely related proteases evaluated in parallel. Multiplexing protease/substrate pairs on current microsphere sets could allow up to 12 targets screened at once. Such an assay would reduce the amount of chemicals and materials, as well as cut down on labor costs as compared to screening each protease target individually. There are currently a great number of proteases under investigation as drug targets, some of which would benefit from the multiplexed high through screening approach developed in this work. Several of the most high-interest proteases involved in disease states, both human and viral, are discussed briefly here, with implications of how such proteases could be developed for assays in HTS such as those described in this work.

8.3.1 Human proteases as drug targets: Matrix Metalloproteases

Improper expression, regulation or activity of human proteases can lead to numerous disease states [1, 2]. There are currently several small molecule drugs on the market which target proteases as well as numerous others in development and testing [1]. One particular problem with small molecule inhibitors of specific proteases involved in disease states lies in the close similarity of other proteases

involved in protease cascades, such as the blood coagulation serine proteases, or the similar structure and close homology of matrix metalloproteases [1]. Small molecules designed to specifically inhibit one improperly regulated protease could potentially inhibit related proteases which are not improperly regulated. This is best exemplified in the inhibition of matrix metalloproteases by small molecules to prevent tumor metastasis and angiogenesis [1, 11].

Matrix metalloproteases (MMPs) are a family of transmembrane and secreted proteases that mediate the arrangement of the extracellular matrix and have multiple signaling activities that are commonly altered during tumorgenesis [11]. Identifying drug targets in multifactorial diseases such as cancer is difficult because of the thousands of potential drug targets [11]. Of all drug targets identified in tumorgenesis and metastasis, proteases represent 5-10% of the potential targets [177]. MMPs were the first proteases considered for small molecule targets for cancer because of their roles in extracellular matrix degradation and processing of angiogenesis promoting factors [1]. Early MMP inhibitors were tested in clinical trials and failed because of severe side effects and lack of clear benefit in blocking tumorgenesis, metastasis and angiogenesis [11]. These inhibitors were mostly broad-spectrum MMP inhibitors and were developed at a time when only a few MMPs had been identified and little was known about their biological relevance and downstream effects [11]. Matrix metalloprotease inhibitors have been considered one of the greatest failures among protease inhibitors discovered to date [1].

Today much more is known about MMPs, with over 20 members of the MMP family and their biological substrates identified [11]. MMPs promote tumor progression not only through extracellular matrix degradation [178, 179] but also through their numerous signaling pathways [180, 181]. While some matrix metallprotease can be considered to be pro-tumorgenic, others are anti-tumorgenic, and their inhibition can actually promote tumorgenesis [11].

MMP1 has been shown to be the second most important gene associated with metastasis of breast cancer to the lung [182]. It has also been shown to have a mutation in the promoter region, which up-regulates its expression in cancer states [183]. MMP2 has also been shown to be up-regulated in patients with malignant breast cancer metastasis to the lungs [182], has high levels of expression in invasive tumors, and is associated with highly invasive cells [178 179]. MMP2 is also known to release chemokines by proteolysis which regulate the inflammatory response [184]. MMP7 is secreted by tumor cells and is involved in pancreatic cancer development [185]. MMP7 also cleaves the FAS ligand, which leads to the resistance to apoptosis seen in cancer cells [186]. While inhibiton of MMP1, MMP2 and MMP7 could potentially lead to reduced tumorgenesis, metastasis and angiogenesis, other MMPs play a protective effect in cancer development, and their inhibition leads to increased tumor development and metastasis. MMP8 has been shown to be an anti-cancer drug target, and its expression levels are inversely correlated with breast carcinoma invasion and metastasis [11]. Similarly, MMP3 has been shown to have a protective effect in tumor development in mice, and MMP3 null mice develop fewer and less

vascularized papillomas than normal mice when treated with 7,12-Dimethylbenz(a)anthracene (DMBA) [187]. Furthermore, MMP12 has also been shown to be a target, in which inhibition would cause adverse reactions. Its expression has been associated with increased survival times in patients with primary colorectal carcinomas [188]. Interestingly, MMP9 has been shown to have both pro and anti-tumorgenic effects, and the current opinion on MMP9 is that inhibition would be useful in treatment of patients with early-stage cancers but detrimental in treatment of patients with advanced stage cancer [11].

The complexity of MMP inhibition and the failure of broad spectrum MMP inhibitors in treatment of invasive tumors illustrate the need for protease assays which could identify specific protease inhibitors that target disease related proteases without inhibiting closely related proteases which might have protective effects for the same disease. A multiplex assay system which could use multiple substrates and multiple proteases in the same high throughput screening assay would be able to efficiently identify such inhibitors. All of the physiologically relevant full length protein substrates for these MMPs have been identified [11] and peptide substrates could be optimized by library display or other optimization methods [3]. Using such a platform could provide better lead compounds for cancer treatment than the broad spectrum MMP inhibitors identified with other “single-plex” approaches.

8.3.2 TACE and ADAMs

Inhibitors have been developed for human proteases implicated in diseases other than cancer. Relatively recently discovered families of proteases

known as ADAMs (a disintigrin and metalloprotease) have been the focus of recent inhibitor development [189]. A target of particular interest has been ADAM 17, otherwise known as TACE (Tumor Necrosis Factor-α Converting Enzyme), which releases tumor necrosis factor-α (TNF), a key cytokine in inflammation [189]. TACE has been shown to cleave TNFα into its soluble inflammatory inducing form at amounts 100-1000 times higher than other proteases known to cleave TNFα [190]. TACE is currently being investigated as a therapeutic target for cancer, arthritis, diabetes and Alzheimer's disease [189]. Inhibitors for TACE have been identified with K_i values as low as 4nM; however, these inhibitors also are known to inhibit MMPs, [189], which, as previously discussed, could have potential undesirable side effects in disease treatment. TACE is also involved in the processing of amyloid precursor protein and its activity has a protective effect against development of amyloid plaques in Alzheimer's disease [189].

8.3.3 Amyloid precursor protein processing by proteases

The amyloid precursor protein (APP) is a transmembrane protein with three specific protease cleavage sites, an α site, a β site, and a γ site. Cleavage of APP at the β site by APP cleaving enzyme (BACE) and the γ site by γ-secretase produces the Aβ peptide fragment, which is the primary component of amyloid plaques that accumulate in Alzheimer's disease [191]. BACE is an aspartic protease which has two homologues, BACE-1 and BACE-2, both of which are drug targets for Alzheimer's disease [192]. Cleavage of the α exosite, in the middle of the Aβ fragment by TACE, and potentially by a closely related protease, ADAM 10, is thought to have a protective effect in Alzheimer's disease, whereby it

funnels peptide cleavage products toward the non-amyloidognic pathway [189]. Another protease, Caspase-3, cleaves the adaptor protein GGA3, which is required for BACE lysosomal degredation, and thereby stabilizes BACE, leading to elevated Aβ generation. An assay which would be capable of finding inhibitors of BACE, Caspace-3, and γ-secretase that do not inhibit TACE or ADAM-10 all in one screening platform would be of great benefit for discovery of therapeutics for Alzheimer's disease.

8.4 Viral Proteases as drug targets.

Studies have indicated that viral proteases are a requirement in the life cycle of numerous viruses, either through the cleavage of large viral precursor proteins into functional products, or through the processing of structural proteins necessary for viral assembly [6 193]. Processing of polyproteins by virally encoded proteases is a characteristic of numerous viruses in infectious disease, including HIV, West Nile virus, herpesvirus, human cytomegalovirus, poliovirus, rhinovirus, and coronaviruses such as SARS-CoV [193]. The processing steps of many of these viruses are highly coordinated and regulated, often requiring either viral or human cell co-factors to efficiently process viral pro-proteins into enzymatically active and structural proteins [194]. One of the most significant challenges in developing drugs which target viral proteases is finding drugs which are highly selective to viral proteases and will not inhibit host cellular proteases [193].

8.4.1 HIV-1 protease inhibition.

One of the first major viral proteases targeted for pharmaceutical inhibitors is the HIV-1 protease. The HIV-1 protease is an aspartic acid protease which is autocatalytically released from one of the two HIV-1 polyproteins which are translated after infection [6]. The HIV-1 protease contains structurally defined substrate binding cavities, which are ideal for binding of small molecules and inhibition of the protease [193]. Studies on the HIV-1 protease using colorimetric and FRET based methodologies for high throughput screening of small molecule inhibitors have established several paradigms for the study of protease inhibition by small molecules [193]. Currently, nine HIV-1 inhibitors have been approved for human use by the food and drug administration, many of which are used in drug cocktails along with HIV reverse transcriptase inhibitors to effectively slow the disease progression [193]. The success of HIV protease inhibitors which slow viral processing and disease progression exemplifies the potential for pharmaceuticals targeting viral proteases.

8.4.2 Picoronaviruses

Picornaviruses are amongst the most well understood family of viruses in terms of their molecular biology, and cause numerous diseases such as hepatitis A and rhinovirus, for which there currently are no effective antiviral therapies available [193]. They represent one of the largest families of medically important human pathogens. The enterovirus sub-family is associated with a variety of clinical syndromes such as upper respiratory tract illness; aseptic meningitis, encephalitis, hand, foot and mouth disease and myocarditis [6]. The picoronavirus proteases 2A and 3C process the viral pro-proteins, along with cleaving several

host cellular proteins, to help promote their own replication cycle [195]. The picoronavirus proteases 2A and 3C are cysteine proteases; however, they have an overall folding structure similar to trypsin-like serine proteases [193]. Due to the large number of illnesses caused by picoronaviruses, and the lack of non-vaccine therapeutics, development of pharmaceuticals to combat these viruses is a topic of great current interest. The unique structure, and the essential role for viral protein processing of the 2A and 3C proteases leads them be considered excellent targets for anti-viral therapies, and inhibitor discovery [193].

8.4.3 Flaviviruses

Another family of viruses in which proteases are currently under investigation as drug targets is the flavivirius family, which includes the Yellow Fever virus, Dengue fever virus, Japanese encephalitis virus, Tick-bourne encephalitis virus, Hepatitis C virus, and West Nile virus. Yellow fever virus and Dengue fever virus are the leading cause of hemorrhagic fever and related mortality worldwide, with numerous treatments under investigation. [193]. West Nile and Dengue fever viruses produce a pro-protein in which the non-structural NS2B and NS3 proteins are removed from the pro-protein by an autocatalytic process and heterodimerize to form a serine protease required for processing of the rest of the pro-protein [193]. Lack of any efficient preventative measures or therapies for West Nile or Dengue fever makes the viral NS2B/NS3 protease an attractive target for small molecule inhibitor therapies. The Hepatitus C flavivirus encodes two proteases required for viral pro-protein processing, the NS2/3 metalloprotease, the only known metalloprotease in viral processing, and the

NS3/4A serine protease [193]. These proteases are currently under investigation as anti-viral therapies for hepatitis C. The NS3/4A inhibitor BLIN 2061 has been reported to be a specific and potent inhibitor with demonstrated anti-hepatitis C activity in human trials [196]. Additional inhibitor discovery for proteases of flaviviruses continues to be a topic of current research and may lead to pharmaceuticals which combat these viruses through inhibition of proteases,

In summary, proteases are critical to numerous viral processing events and life cycles, implicated in human disease. Drug targeting of these proteases and high throughput screening of small molecule libraries is an emerging field which has led to development of therapeutics for diseases such as HIV, hepatitis C and malaria. Most of the discovered anti-viral protease inhibitors are specific to viral proteases, even though many are closely related to human cellular proteases required for physiological processes. The successful development of protease inhibitors that limit viral processing and infection has in part validated targeting of proteases as drug targets for the treatment of numerous diseases, and has potential for the discovery of additional pharmaceuticals of this class.

8.5 Development of protease assays of interest into a flow cytometry HTS system.

Our laboratory group is currently in the process of extending our microsphere based protease assay to the study of proteases of Dengue virus and the hepatitis C virus. The protease component of Dengue virus NS2B-NS3 has been cloned and shown to have specific proteolytic activity in preliminary FRET assays. The protease component of hepatitis C is also being cloned.

Cloning and purification of a protease of interest for high throughput screening will be beneficial, especially because these particular proteases are not currently commercially available. Initial assays will be done by expression of the viral capsid substrates as biotinylated GFP fusion proteins, and high throughput screening will be carried out using the HyperCyt flow cytometry screening system to identify potential protease inhibitors. Additional work is also being done to express these proteases and their substrates intracellularly. Assays of this type will help in follow up assays of lead compounds to test their membrane permeability. Thus, our microsphere based protease assay originally designed for screening of Lethal Factor and BoNTALC has the ability be adapted to a variety of proteases of interest and in screening applications to identify inhibitors.

8.6 Summary of this work and Future Directions

In summary of the work presented here, we have developed a microsphere based protease asay capable of using full length protease substrates and being run in multiplex. This assay has led to the discovery of ebselen, an inhibitor of botulinum neurotoxin type A light chain with an IC_{50} value in the low µM range. We have also discovered two potential inhibitors of the *Bacillus anthracis* Lethal Factor protease, which are under on-going investigation. A collaboration with the Torrey Pines Institute of Molecular Discovery has identified several poteintial inhibitors of BoNTALC, as well as numerous potential activators of this protease. Work in progress in our laboratory will identify IC_{50} values for several inhibitory compounds discovered in

the screening of the TPIMS combinatorial library. We have also developed the solution based techniques of GFP "self-quenching" and inhibitory zinc pre-binding, which will allow us to determine the kinetic parameters Km and k_{cat} for BoNTALC This information can be used to verify the specificity constant of this protease suggested by results obtained in our microsphere based assay.

The microsphere based flow cytometry assay developed and described in this work has the potential to be adapted to any site-specific protease of interest for screening of libraries of chemical compounds for protease inhibitors. Currently this work is being done to adapt this microsphere based assay to the viral processing proteases of Dengue virus and Hepatitus C. The potential for discovery of specific inhibitor for proteases in disease could have a great deal of impact in the development of pharmaceuticals to treat a variety of diseases.

List of Appendix

Appendix 1 Identified inhibitors of the Bacillus anthracis Lethal Factor

Compound	Structure	Affinity	Reference
IN-2-LF	Hydroxamate containing peptide with sequence AcGYβARRRRRRRRRVLR-Hydroxamate	Ki 1 nM	Tonello (2002)
Neomycin B	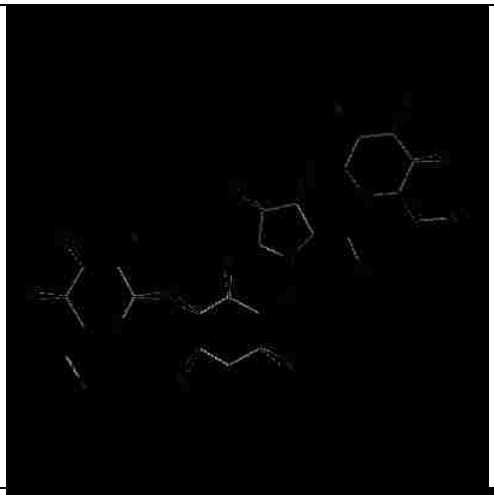	Ki 7 nM	Lee (2004)
Aminoglycoside Compound 1	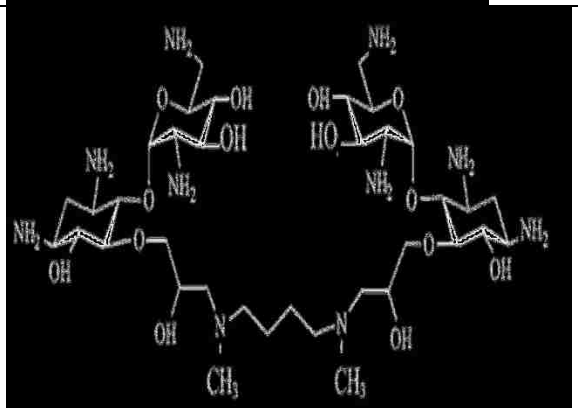	Ki 14.1 nM	Lee (2004)
Aminoglycoside Compound 2	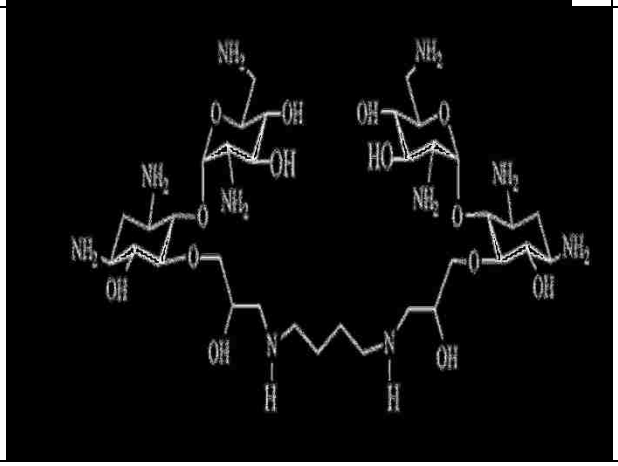	Ki 14.4 nM	Lee (2004)

Aminoglycoside Compound 3	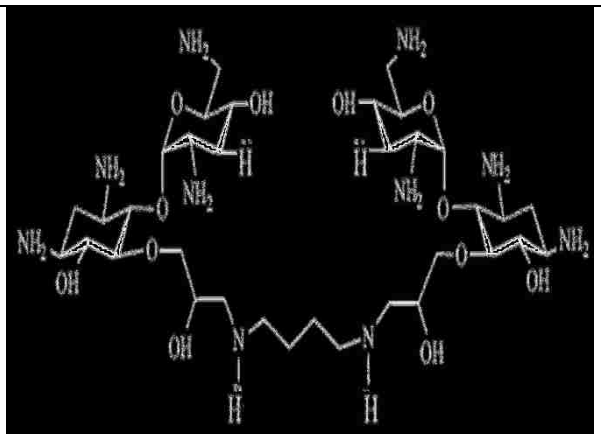	Ki 28.5 nM	Lee (2004)
Modified Neomycin B	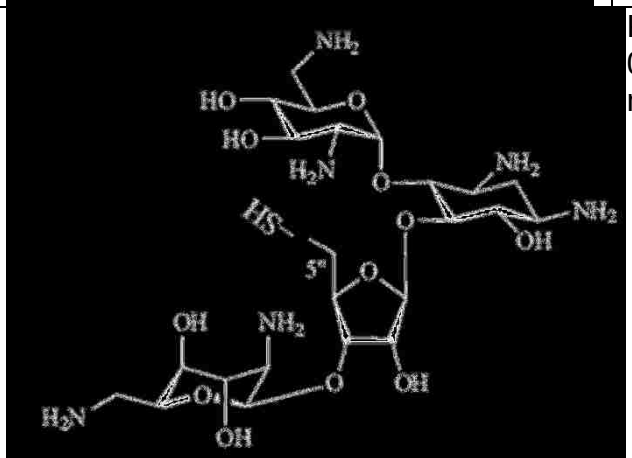	Ki 0.2 nM	Fridman (2005) Best Modification
Modified Neomycin B	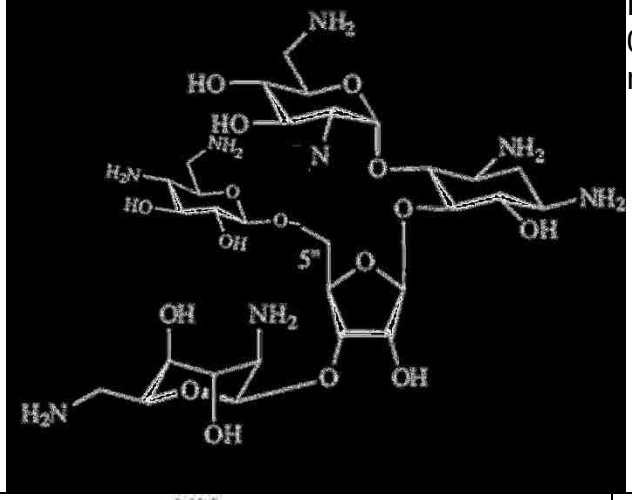	Ki 0.5 nM	Fridman (2005) More modified NeomycinB inhibitors In paper.
Neamide	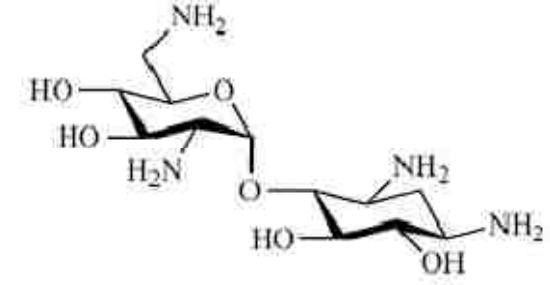	Ki 42.9 µM	Jiao (2006)

guanidinylated 2,5 dideoxystreptamine derivitave of neamide	 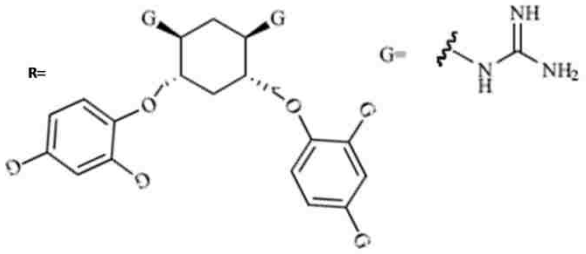	Ki 65 nM	Jiao (2006) Best modification. More modified Neamine derivatives in paper.
Polyamine Spermine		Ki 900 nM	Dalkas (2008)
NCS 12155	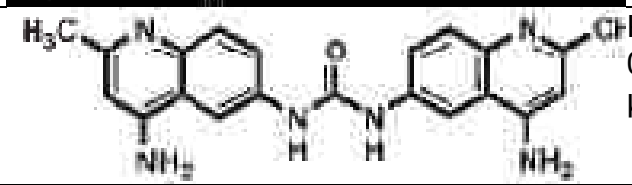	Ki 0.5 µM	Panchal (2004)
Ilomastat (GM6001)	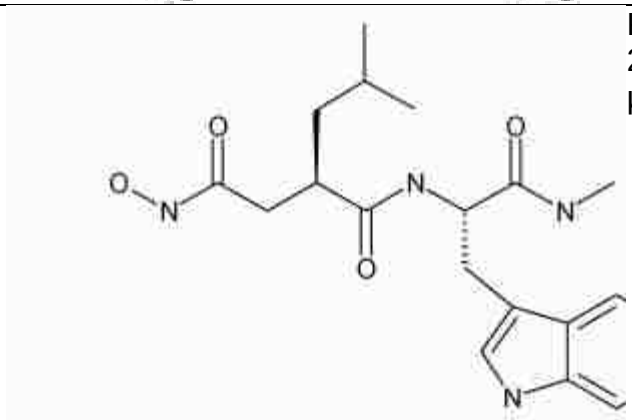	Ki 2.1 µM	Turk (2004) Dalkas (2008)
Chemically modified tetracycline 300	Not available	Ki <7 µM	Kocer (2005)
Chemically modified	Not available	Ki <7	Kocer (2005)

tetracycline 308		µM	
Drug-like inhibitor 1	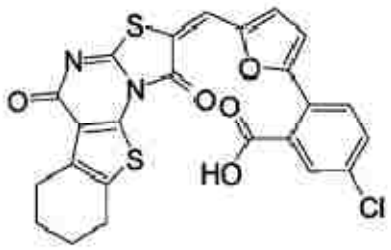	Ki 0.8 µM	Schepetkin (2006)
Drug-like inhibitor 2	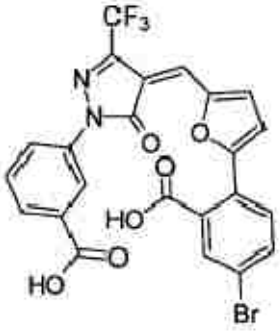	Ki 1.6 µM	Schepetkin (2006)
Drug-like inhibitor 3	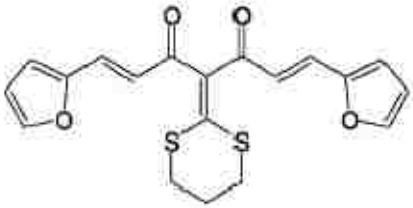	Ki 2.7 µM	Schepetkin (2006)
Drug-like inhibitor 4	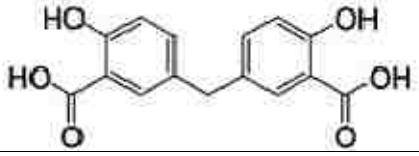	Ki 2.4 µM	Schepetkin (2006)
Drug-like inhibitor 5	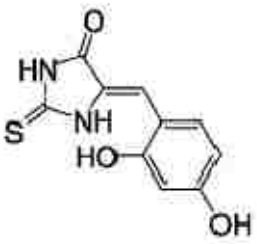	Ki 1.1 µM	Schepetkin (2006)
Drug-like inhibitor 6	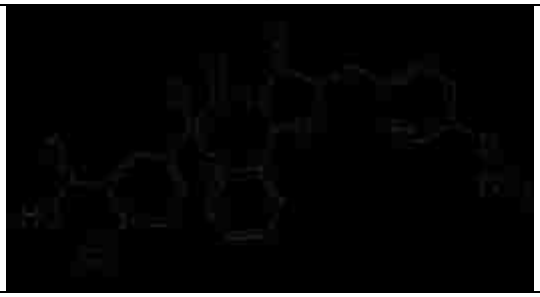	Ki 2.5 µM	Schepetkin (2006)

Drug-like inhibitor 7	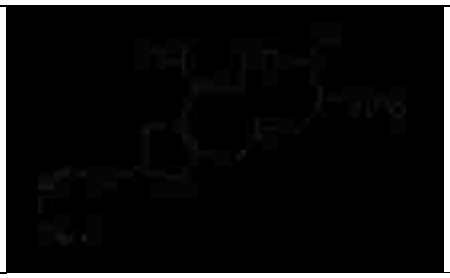	Ki 2.9 µM	Schepetkin (2006)
Drug-like inhibitor 8	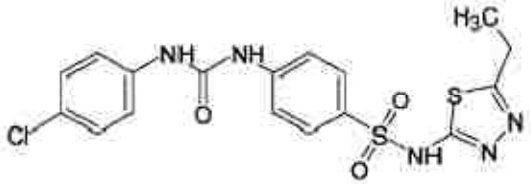	Ki 0.9 µM	Schepetkin (2006)
Drug-like inhibitor 9	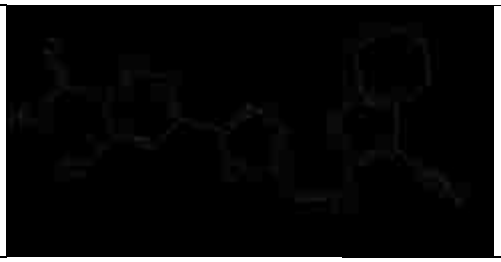	Ki 2.4 µM	Schepetkin (2006)
Drug-like inhibitor 10	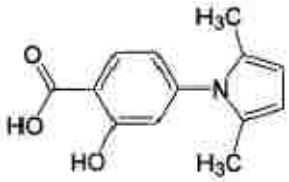	Ki 1.5 µM	Schepetkin (2006)
Drug-like inhibitor 11	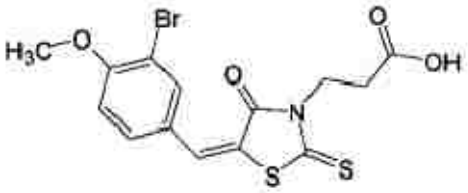	Ki 3.3 µM	Schepetkin (2006)
Drug-like inhibitor 12		Ki 3.1 µM	Schepetkin (2006)
Drug-like inhibitor 13	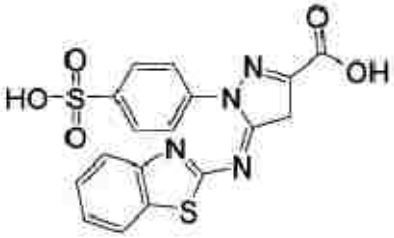	Ki 4.2 µM	Schepetkin (2006)

Drug-like inhibitor 14	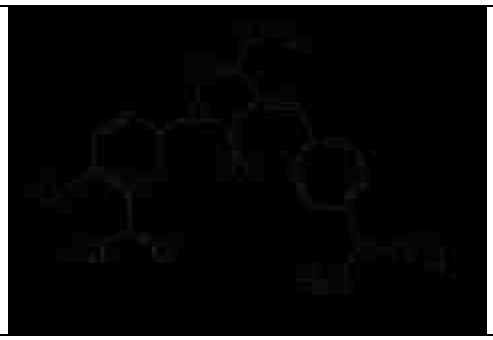	Ki 0.9 µM	Schepetkin (2006)
Drug-like inhibitor 15	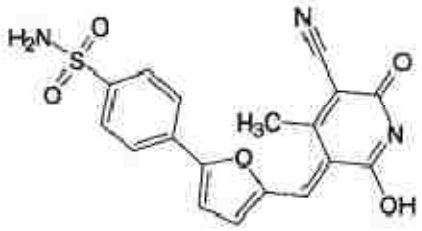	Ki 5.4 µM	Schepetkin (2006)
Drug-like inhibitor 16	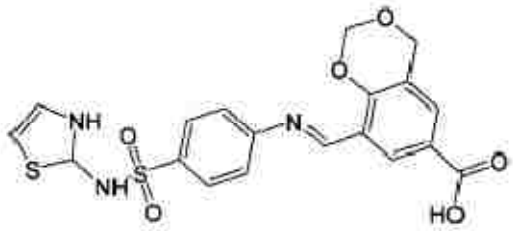	Ki 1.8 µM	Schepetkin (2006)
Drug-like inhibitor 17	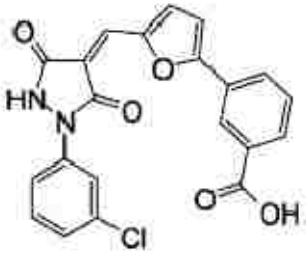	Ki 7.2 µM	Schepetkin (2006)
Drug-like inhibitor 18	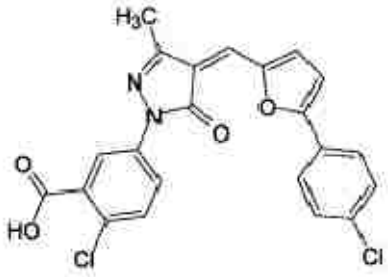	Ki 2.1 µM	Schepetkin (2006)

epigallocatechin-3-gallate (EGCG)	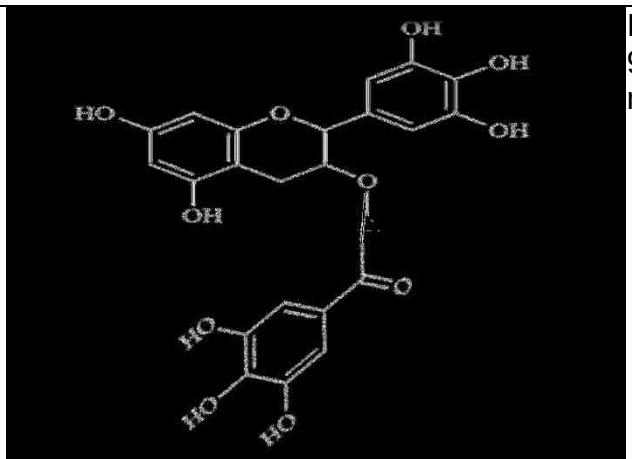	IC_{50} 97 nM	Dell'Aica (2004)
Sulfonamide compound 1	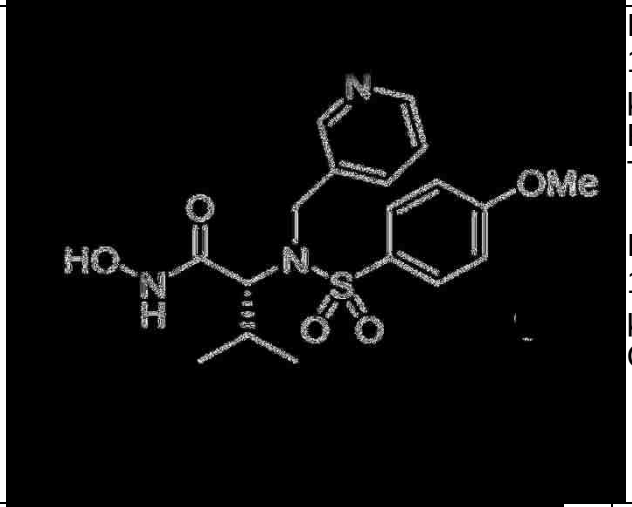	IC_{50} 1.2 µM FRET IC_{50} 12 µM Cell	Xiong (2006)
Sulfonamide compound 2	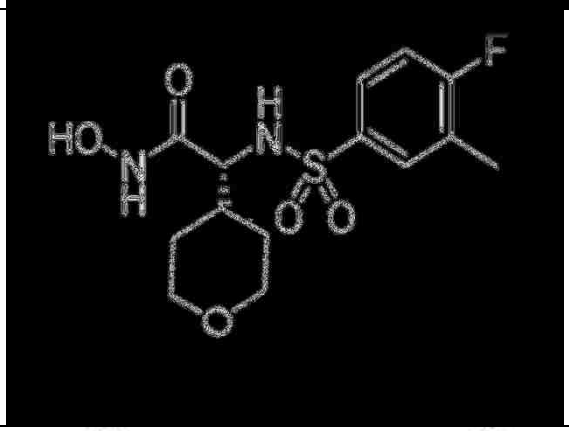	IC_{50} 54 nM FRET IC_{50} 210 nM Cell	Xiong (2006) Best modified compound.
DS-998	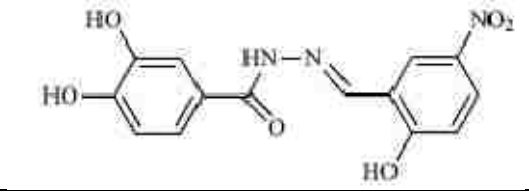	Ki 1 µM	Min (2004)

BI-9B9b	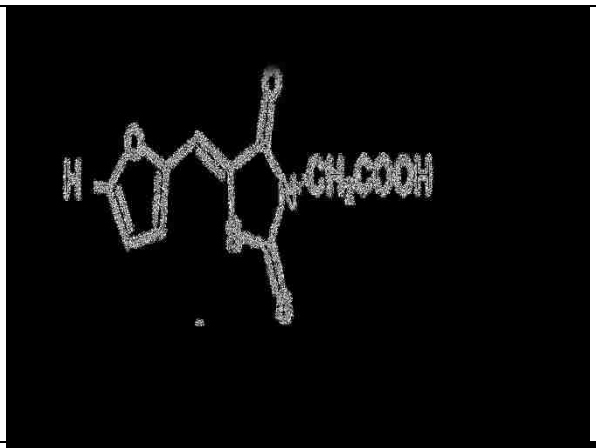	IC_{50} 140 µM	Forino (2005)
BI-MFM3	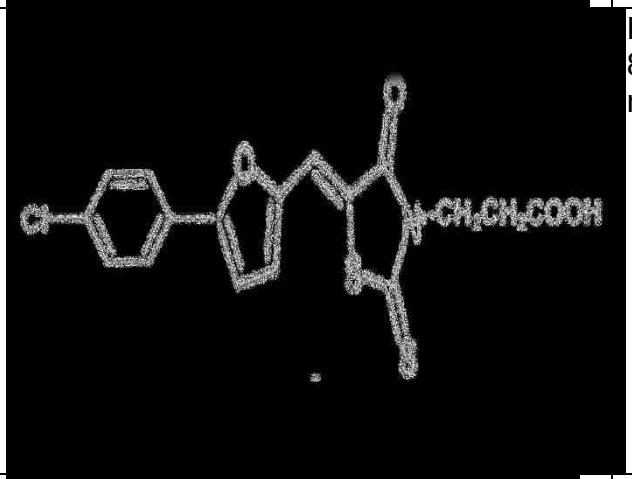	Ki 800 nM	Forino (2005) Best derivative of BI-9B9b
BI-11B3	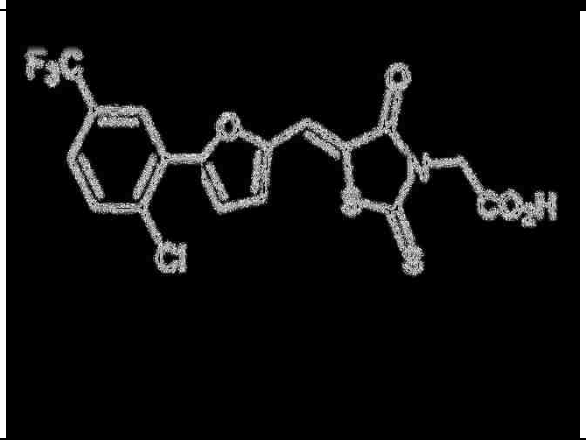	Ki 32 nM	Forino (2005) Best derivative of BI-MFM3

ASDI compound # 100041589	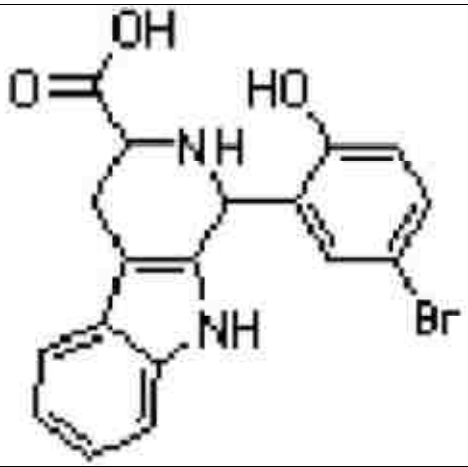	IC_{50} 38.2 µM	Johnson (2007)
ASDI compound # 100045637	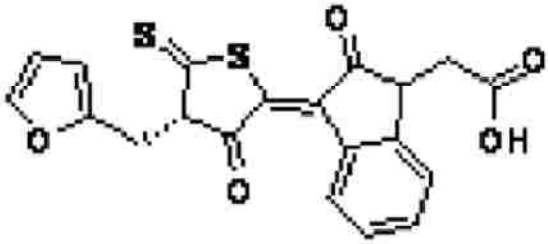	IC_{50} 38 µM	Johnson (2007)
ASDI compound # 10005658	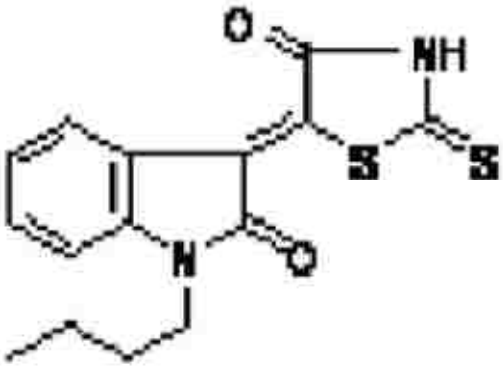	IC_{50} 10 µM	Johnson (2007)
ASDI compound #100088569	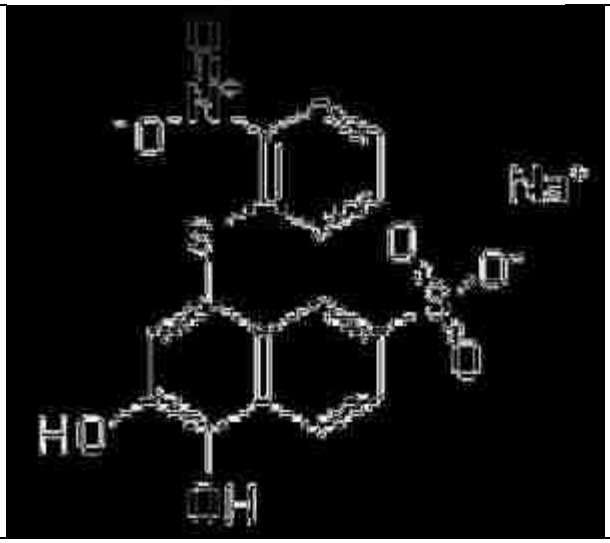	Ki 2.11 µM IC_{50} 5.89 µM	Johnson (2007)

ASDI compound # 150008092	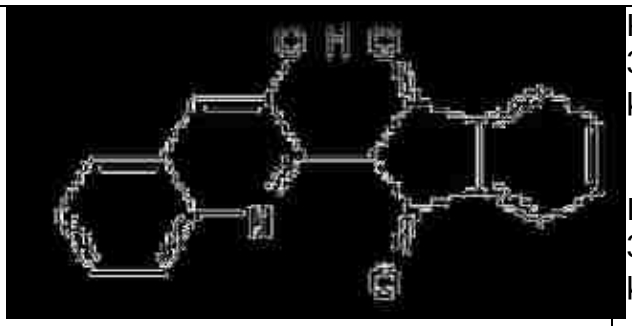	Ki 3.79 µM IC_{50} 3.89 µM	Johnson (2007)
ASDI compound # 150016121	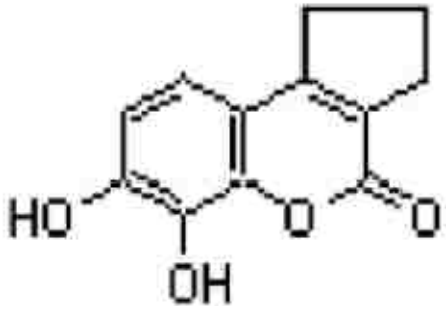	Ki 0.57 µM IC_{50} 1.70 µM	Johnson (2007)
N-oleoydopamine (OLDA)	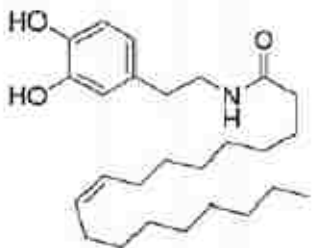	Ki 3 µM IC_{50} 15 µM	Gaddis (2007)
Hydroxylated N-oleoydopamine	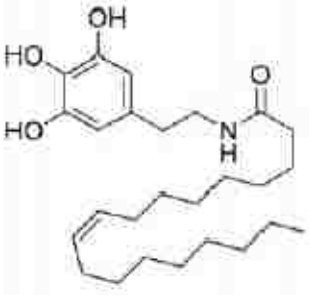	Ki 1.7 µM IC_{50} 13 µM	Gaddis (2007)

Appendix 2 Identified inhibitors of the Botulinum Neurotoxin type A Light Chain

Inhibitor	Structure	Affinity	Reference
Peptide	Sequence CRATKML	Ki 2 µM	Schmidt (1998)
Peptide	Sequence RRGC	Ki 157 nM	Kumaran (2008)
Peptide	Sequence RRGL	Ki 660 nM	Kumaran (2008)
Peptide	Sequence RRGI	Ki 786 nM	Kumaran (2008)
Peptide	Sequence RRGM	Ki 845 nM	Kumaran (2008)
mercapto-3-phenylpropionyl-peptide mpp-RATKML	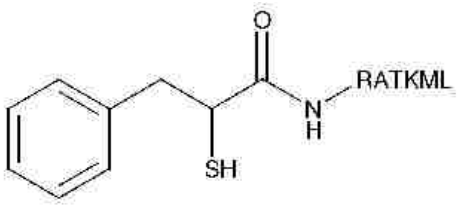	Ki 0.3 µM	Schmidt and Stafford (2002)
L-arginine hydroxamic acid.	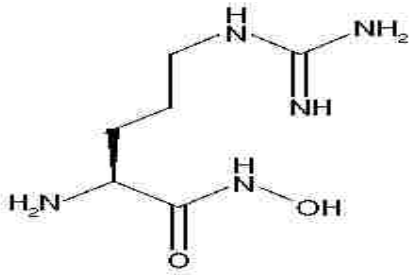	Ki 60 µM	Boldt (2006)
4-chlorocinnamic hydroxamate	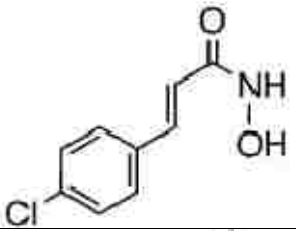	IC_{50} 15 µM	Boldt (2006)
2,4,dichlorocinnamic hydroxamate	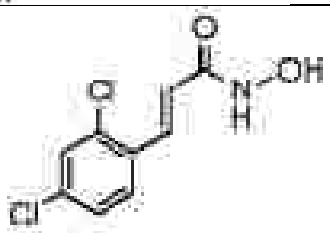	IC_{50} 0.41 µM Ki 300 nM	Boldt (2006)

NSC240898	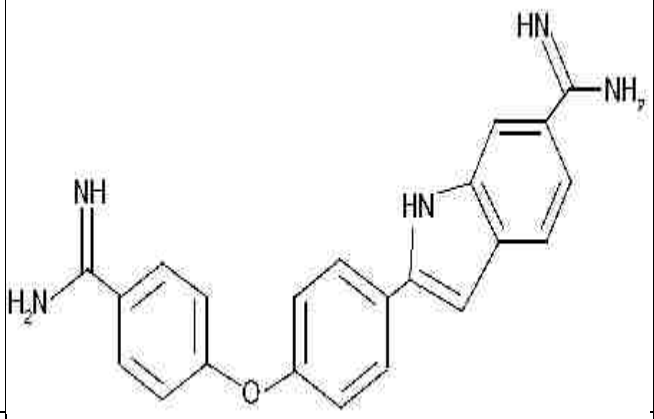	Ki 10 µM	Burnett (2007)
CaDA	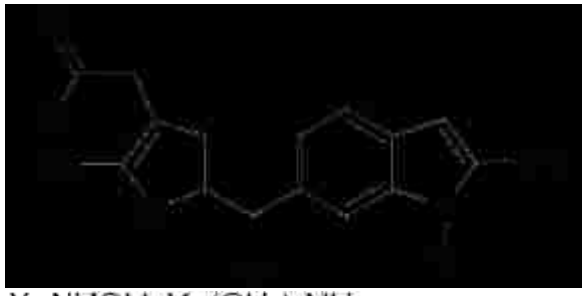 X=NHOH, Y=$(CH_2)_4NH_2$	Ki 12 µM X=OH 3.8 µM	Park (2006) Tang (2007)
Furan Rhodanine derivative	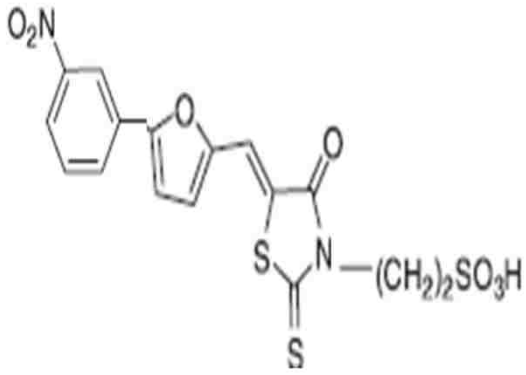	IC_{50} 9.7 µM	Johnson (2007)
NA-A1B2C10	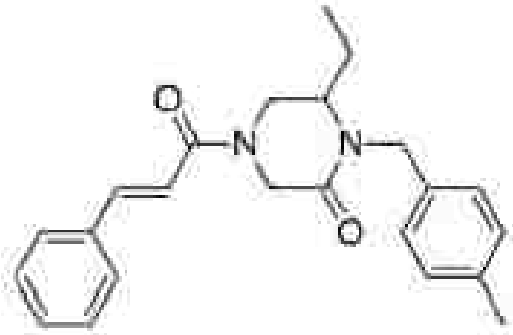	IC_{50} 12.5 µM	Eubanks (2007)

BDIS-A4B11C7	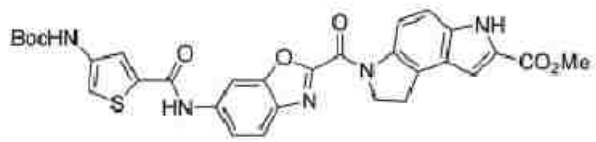	IC_{50} 1.5 μM	Eubanks (2007)
HD4-A2B7	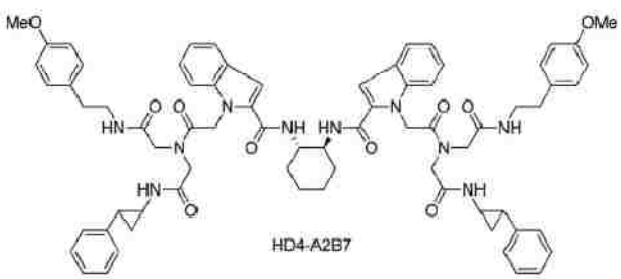	IC_{50} 7.6 μM	Eubanks (2007)
HD4-A3B5	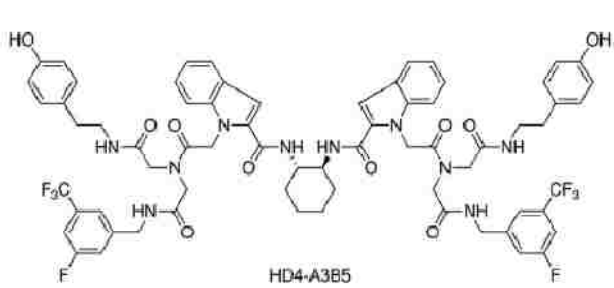	IC_{50} 14.3 μM	Eubanks (2007)
HD4-A4B2	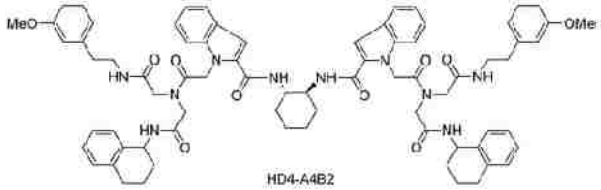	IC_{50} 19.1 μM	Eubanks (2007)
TransPyr1-A1B6C6	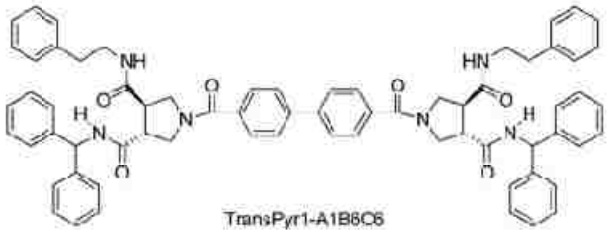	IC_{50} 54.2 μM	Eubanks (2007)
TransPyr1-A6B9C6	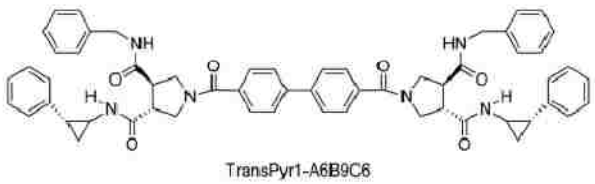	IC_{50} 28.4 μM	Eubanks (2007)
Ebselen	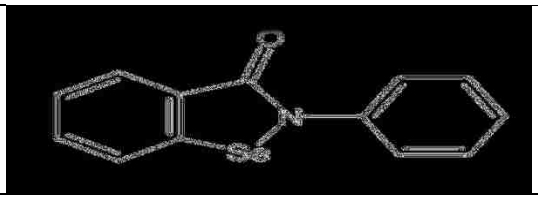	IC_{50} 6 μM	Saunders (2009)

Appendix 3

Adaptation of microsphere based protease assays to full length protease substrates

A.3 .1 Introduction

The demonstration of a multiplex microsphere based protease assay using protease cleavage sites and known inhibitors of specific proteases had demonstrated that we can use this platform for HTS of protease inhibitors. One of the goals of such an assay, however, is to use full length protease substrates in such a system to show the contributions of identified protease/substrate binding sites distal to the protease cleavage sites. Using this approach, it would also be possible to use multiplex microsphere-based flow cytometry high throughput screening with the protease cleavage site, the full length protease substrate, as well as a control substrate in each test well. The thought behind using such a multiplex assay is that an inhibitor which would block protease/substrate binding would reduce the amount of cleavage on the full length substrate to that observed on the cleavage site alone. An observation of this kind may be signifying that the distal interaction element is blocked by such an inhibitor. Our expectation is not that such a distal site inhibitor would not eliminate cleavage of full length substrates altogether, but should greatly reduce the amount of cleavage to that seen on the protease cleavage site alone. Such a compound could be a beneficial addition to a drug cocktail for protease-based toxins, and could be used as an immediate response drug to potential pathogenic bacteria or toxin infection. The use of full length protease substrates could also be extended to other protease systems, where an inhibitor which down-regulates,

but does not completely block protease activity is desirable. Inhibitors which block protease/substrate binding would also tend to be more specific to the protease of interest, because they would most likely not block or inhibit highly conserved protease active sites, and only inhibit the target protease.

A3.1.1 Full Length Lethal Factor Substrates

We have demonstrated the use of a lethal factor consensus cleavage site used in FRET based methodologies [31] to be effective in a microsphere based protease assay using loss of GFP [127]. In development of our microsphere based assay it was observed that the natural cleavage site of MKK2 alone was not cleaved by LF in this assay. Full length MAP kinase kinase 2 (MKK2) was amplified from a plasmid obtained from Open biosystems and subcloned into the ppEGFP plasmid. To compare cleavage of the full length MKK compared to the consensus cleavage site alone, the LF cleavage site in full length MKK2 was also replaced with the consensus cleavage site used in our assay. Our goal to screen for binding site inhibitors, could potentially be achieved by assaying the consensus cleavage site and the full length MKK with the consensus cleavage site together in a multiplex assay.

A3.1.2 Botulinum Neurotoxin type A Light Chain with Full Length SNAP-25.

The substrate for botulinum neurotoxin type A Light Chain (BoNTALC), SNAP-25, is a 25 kDa protein with four identified SNARE motifs which contribute to cleavage by BoNTALC [9]. Previous work has identified the C-terminal SNARE domain, near the BoNTALC cleavage site, to be the most critical SNARE domain in cleavage of SNAP-25 by BoNTALC [71]. Since SNAP-25 is a relatively small

protein, we determined it was likely we would be able to clone it into our bacterial biotinylation/GFP system and be able to express and purify it efficiently from *E.coli*. Comparing the amount of cleavage of full length SNAP-25 against the amount of cleavage in the SNAP-25 cleavage site in a HTS platform could identify compounds which interfere with the SNARE domain BoNTALC protein-protein interactions. Discovery of such compounds could lead to a new class of BoNTALC inhibitors which specifically target BoNTALC and not the conserved metalloprotease active site. In this study we aim to adapt our previously developed microsphere based protease assay to the use full length protein substrates, containing identified distal interaction sites, for both *Bacillus anthracis* lethal factor and *Clostridium botulinum* light chain type A metalloproteases.

A3.2 Methods

A3.2.1 Expression and purification of full length Map Kinase Kinase GFP from bacteria.

The LF cleavage site of MKK2 was replaced with a LF consensus cleavage site previously described [127] by ppEGFP MKK2 plasmid enzyme digestion with restriction enzymes SacI and ApaI. Isolation of the linear DNA was performed by agarose gel electrophoresis gel purification using a Qiagen gel purification kit. Synthetic complimentary 5' phosphorylated DNA oligionucleotides with 5' and 3' ends corresponding to the SacI and ApaI cleavage sites were annealed together, and ligated into the ppEGFP MKK2 plasmid. The resulting plasmid, called ppEGFP MKK consensus full length, encodes the same consensus cleavage site used successfully in our previous assay with the rest of

full length MKK2. Both the ppEGFP MKK2 and ppEGFP MKK consensus full length (MKKCFL) were sequenced to ensure correct open reading frames for both proteins. Plasmids were transformed into BL21 (DE3) pLysS *E. coli* and grown in the same manner as the ppEGFP cleavage site plasmid expression done previously.[127] Expression of biotinylated full length MKK GFP fusion proteins from bacteria proved to be unsuccessful due to low yields.

A3.2.2 Expression of full length Map Kinase Kinase GFP from Sf9 insect cells.

Sf9 insect cells are an efficient system for expression of large proteins. Because our full length biotinylated protease substrates were not efficiently expressed in bacterial systems we decided to use insect cells and the Invitrogen Baculovirus expression system to express these substrates. Unfortunately, insect cell systems do not express the BirA biotin ligase *in vivo*; however, a 15 amino acid sequence of GLNDIFEAQKIEWHE has been identified to be highly effective for *in vitro* biotinylation using purified BirA biotin ligase. [197] The Invitrogen Bac-to-Bac system uses a baculovirus shuttle vector (bacmid) to recombine target protein sequences into a virus for insect cell infection from a starting pFastBac vector, into which our protein sequence of interest was cloned. Since our full length protease substrates will not be biotinylated while expressed, an N-terminal 6XHis vector pFastBacHT was chosen for initial subcloning in order to purify expressed proteins on a Ni-NTA Histrap column. In order to perform *in vitro* biotinylation, we also needed to introduce an N-terminal

biotinylation tag (BT) sequence of the 15 amino acids into the pFastBac vector. This was accomplished by digesting the pFastBacHT plasmid with the restriction enzymes EcoRI and SacI and using 5'-phosphorylated oligioucleotides annealed together containing compatible 5' and 3' ends with the EcoR1 and SacI digestion sites and ligation. MAPKK2 GFP and MAPKK consensus full length coding sequences were amplified by PCR from the ppEGFP MAPKK2 and ppEGFP MKKCFL plasmids with primers containing SacI and NotI in position to conserve the open reading frame. After ligation the resulting plasmids were sequenced to confirm they encoded all of the desired features, all in the correct reading frame for expression.

The plasmids pFastBac HT BT MKK2 GFP and pFast HT BT MKK Consensus GFP were then transformed into DH10Bac competent *E. coli* to create a recombinant bacmid vector, which was purified by Qiagen QIA spin miniprep kit. This recombinant bacmid was then used to generate a P1 baculovirus stock by transfecting Sf9 cells with the Cellfectin III reagent as described below. Cellfectin III reagent from Invitrogen was used to infect 900,000 Sf9 insect cells, as determined on a Coulter counter, in each well of a 6 well tissue culture polystyrene plate with 2 ml of Sf900 II insect cell media containing 1X penicillin/streptomycin (pen/strep) mixture and fetal bovine serum (complete media). Cells were grown at 27°C in a humidified incubator for 1 hour prior to bacmid infection. Two µg of bacmid DNA, calculated by UV260 absorption, added to 100 µl Grace's unsupplemented media with 6 µl of Cellfectin III and incubated at room temperature for 45 minutes. Media was

removed from the 6 wells of the insect cells and each well was washed with 2 ml of Grace's unsupplemented media. 800 µl of Grace's unsupplemented media was added to each well of the 6 well culture plate followed by the DNA bacmid/cellfectin mixture and incubation at 27ºC in a humidified incubator for 5 hours. Media was removed and 2 ml Sf900 II media with pen/strep and fetal bovine serum was put into each well. Cells were grown at 27°C in a humidified incubator for 5 days when signs of infection appeared. Cells were harvested at 5 days post infection by scraping with a rubber policeman, centrifuged at 5,000 RCF and 0.5 ml of the supernatant was used as a P1 baculovirus inoculate stock to infect 2 million Sf9 cells/well in a 6 well plate in complete media. These were grown for 72 hours at 27°C in a humidified incubator and cells collected by rubber policeman, with the media collected as well, centrifuged and stored at 4°C to be used as a P2 innoculate stock. Sf9 cells were seeded into a T-150 tissue culture polystyrene flask and grown to confluence using 25 ml of complete media. At confluence 1 ml of the P2 innoculate stock was added to the cells with fresh media. These P2 innoculated cells were grown for 3 days in a humidified incubator, scraped from the flask and collected. Both the MKK2 GFP and consensus MKK2 GFP Sf9 cells from this infection were visibly green.

A3.2.3 Expression and purification of large scale Map Kinase Kinase GFP from Sf9 insect cells.

To increase yields of expressed protein from baculovirus infected cells, 20 T-150 flasks were seeded with approximately 45 million Sf9 insect cells and

grown for 2 days to approximately 80% confluence. 1 ml of the P2 innoculate stock for MKK2 GFP was added to 10 of the flasks and 1 ml of the P2 innoculate stock for MKK Consensus GFP was added to the other 10 flasks. These flasks were grown at 27°C in a humidified incubator for 3 days, harvested by rubber policeman, and all cells containing each expressed protein type were combined into a single sample in a 50 ml conical Falcon tube. These cells were spun down into a solid pellet, suspended in PBS and frozen. The cells expressing MKK2 GFP were lysed by a dounce, followed by centrifugation at 10,000 RCF for 30 minutes. This yielded visible green fluorescence in the soluble fraction as well as relatively large green inclusion bodies visible by eye. The soluble fraction was purified on a 5 ml Ni-NTA HisTrap column resulting in a large elution peak as measured by UV absorbance at 280 nm. Inclusion bodies were solubilized in 8M urea, vortexed for several minutes, and the membrane components were spun out at 10,000 RCF. The urea/ protein mixture was then put onto a 5 ml HisTrap Ni-NTA column. On-column re-folding of denatured protein was done by running a linear gradient from 100% 8 M urea, 0.5 M NaCl, 20 mM Na_2PO_4, 5 mM imidazole to 0M Urea, 0.5 M NaCl, 20 mM Na_2PO_4, 5 mM imidazole at 1 ml/min over 20 ml. The protein was then eluted by using 0.5 M NaCl, 20mM Na_2PO_4, 300 mM imidazole. Both MKK2 GFP purified from soluble fractions and from inclusion bodies were spun in a 30,000 Mw cutoff filter down to reduce the volume to 2ml of purified protein, and dialyzed against 2 L minimal protease buffer (50mM HEPES, 100mM NaCl). SDS-PAGE analysis showed pure protein bands of the correct molecular weight, with approximately the same

concentration of protein purified from the soluble fraction as that purified from inclusion bodies. The purification process was repeated for the consensus MKK GFP protein.

A3.2.4 In vitro biotinylation of full length MAP Kinase Kinase GFP

In vitro biotinylation was carried out using an *in vitro* biotinylation kit from Avidity (Aurora, CO). To assess how much BirA enzyme was needed to efficiently biotinylate the MKK2 GFP containing the N-terminal biotinylation tag, 4 separate reactions were set up. Each reaction used 500 µl of the pool of MKK2 GFP, 6 µl of biomix A (0.5 M bicine buffer) and 6 µl of biobuffer B(100 mM ATP, 100 mM MgOAc, 500 µM d-biotin). A different amount of BirA enzyme at a stock concentration of 3 mg/ml was used in each reaction. Ten µl, 5 µl, 2 µl and 0.5 µl were added to each reaction separately. Samples were brought up to 600 µl using sterile water and incubated at 30°C for 2 hours and then stored at 4°C. Removal of excess biotin was carried out by separately binding each pool of the biotinylation/protein mix to a 5 ml column containing Q Sepharose and washing with 100 ml of 50 mM Tris and 1 mM EDTA pH 8.3 (binding buffer) at a flow rate of 1ml/min, and eluting with 5 ml 50 mM Tris, 1 mM EDTA, and 1 M NaCl. Q Sepharose was then re-equlibrated using 20ml of binding buffer flowed though at 1 ml/min. Each separate biotinylation reaction was purified on Q Sepahrose separately and spun down to 0.5 ml in an Amicon Ultra Mw 30,000 centrifugation filter unit. SDS-PAGE gel-electrophoresis on all four samples showed that approximately the same concentration of protein was recovered with no retention of the BirA biotin ligase in the protein preparation after Q Sepahrose purification

and removal of free biotin. Protein preps were then dialyzed against 2 L of PBS overnight.

A3.2.5 Microsphere based lethal factor assays.

Spherotech streptavidin coated pink particle kit microspheres were bound with biotinylated GFP substrates, washed, and assays carried out as previously described in Chapter 3 [127]. Three microsphere sets were used in this particular experiment, one for the full length consensus map kinase kinase GFP (MKKCFL), one for the previously described lethal factor consensus cleavage site and a third for the previously described Xa sub control.

A3.2.6 Cloning, purification and analysis of SNAP-25 GFP and SNAP-25 cleavage site GFP against Botulinum Neurotoxin type A Light Chain

The cleavage site of SNAP-25 alone, consisting of amino acids TRIDEANQRATKMLGSG, was cloned into the ppEGFP system using 5'-phosphorylated DNA oligos annealed together and ligated into ppEGFP digested with SacI and HindIII. An N-terminal biotinylated synthetic peptide cleavage site optimized for BoNTALC, previously used in a mass spectroscopy assay [118] was also used in this study, after labeling with Alexa 488, per the manufacturer's instructions, on the C-terminal cysteine for detection of cleavage by BoNTALC (peptide kindly provided by Dr. Jurgen Schmidt).

The SNAP-25 gene, obtained from Open Biosystems, was amplified using PCR primers containing the restriction sites SacI and NotI, and cloned into the ppEGFP plasmid digested with the same enzymes. Protein purification and removal of free biotin was performed as previously described for lethal factor

substrates [127]. SNAP-25 full length was bound to one set of streptavidin coated multiplex microspheres, the SNAP-25 cleavage site to another, and the synthetic biotinylated peptide labeled with Alexa-488 to a third microsphere set. Another microsphere set was used for the previously described control substrate Xa sub [127]. All four microsphere sets were centrifuged and washed three times to remove soluble substrate and combined, then split into 4 separate 600 µl reaction tubes. A 100 µl 0 minute sample was taken from each of the samples and run on the FACScalibur flow cytometer. 364 nM Boutlinum Neurotoxin type A light chain was added to two of the samples, while the other two samples were controls with no BoNTALC added. All 4 were incubated at room temperature and 100 µl samples were run every 30 minutes for 120 minutes. Mean FL1 values were averaged for the two samples and each time point was normalized by dividing the averaged mean FL1 value by the averaged 0 minute sample mean FL1 value

A3.3 Results

A3.3.1 In vitro biotinylation of MKK2 GFP

All 4 biotinylation reactions were recovered at approximately 2 µM protein concentration as determined by UV280 spectroscopy. Each reaction was titrated onto streptavidin-coated microspheres in increasing concentrations of 0 nM, 20 nM, 100 nM, 200 nM and 400 nM and run on a FASCCalibur flow cytometer to analyze binding of biotinylated MKK2 GFP. Duplicate samples where the streptavidin microspheres were blocked with 1 µM biotin for 30 minutes before addition of biotinylated MKK2 GFP protein were used as controls for non-specific

binding. All 4 biotinylation reactions showed relatively similar amounts of specific binding to streptavidin microspheres. (Table A3.1)

This experiment, however, does not take into account potential non-specific biotinylation of this substrate in places other than the specific N-terminal 15 amino acid sequence. Such non-specific binding would still allow the substrate to bind to microspheres, but could potentially interfere with our assay if a biotinylation site were located C terminal to the protease cleavage site in our substrate. This would interfere with our assay because cleavage of the substrate with biotinylation C terminal to the cleavage site would retain fluorescence on the microsphere even after cleavage by the protease.

Biotinylation of consensus full length MKK2 GFP was done using the lowest concentration of BirA tested (0.5 µl of 3 mg/ml in a 600 µl reaction) in an effort to potentially reduce non-specific biotinylation.

A3.3.2 Cleavage of full length LF substrates vs. LF cleavage sites.

To test our hypothesis that full length substrates for proteases containing distal binding elements should be cleaved at a quicker rate and lead to a greater loss of fluorescence in a microsphere based assay, we carried out in a multiplexed reaction as described previously in Chapter 3 [127]. The LF consensus cleavage sequence GFP substrate was attached to one streptavidin coated multiplex microsphere set at a concentration of approximately 50 nM, while the full length consensus MKK2 GFP substrate, using the lowest amount of biotinylation was attached to another streptavidin coated multiplex microsphere

10ul Bir A used in biotinylation reaction

nM MKK2 GFP	Unblocked	blocked with 1µM biotin	corrected
0	16.6	16.6	0
20	260.24	64.3	195.94
100	411.68	129.28	282.4
200	457.75	191.1	266.65
400	498.2	253.94	244.26

5ul BirA used in biotinylation reaction

nM MKK2 GFP	Unblocked	Blocked with 1µM biotin	corrected
0	22.69	22.69	0
20	51.2	30	21.2
100	237.22	41.1	196.12
200	329.9	52.77	277.13
400	402.7	71.18	331.52

2ul BirA used in biotinylation reaction

nM MKK2 GFP	Unblocked	Blocked with 1µM biotin	corrected
0	22.69	22.69	0
20	130.28	30.12	100.16
100	337	58.94	278.06
200	450.53	86.2	364.33
400	541.74	128.24	413.5

0.5ul Bir A used in biotinylation reaction

nM MKK2 GFP	Unblocked	Blocked with 1µM biotin	corrected
0	22.69	22.69	0
20	69.02	27	42.02
100	239.46	39.26	200.2
200	350.09	53	297.09
400	449.3	74.5	374.8

Table A3.1. Mean FL1 fluorescence values of MKK2 GFP bound to streptavidin coated polystyrene microspheres and run on a FACSCalibur flow cytometer after different concentrations of the biotinylating enzyme BirA was used to biotinylate the N terminus of the purified recombinant protein. Biotin was removed by ion exchange chromatrography on Q sepharose followed by dialysis. Corrected value is mean FL1 value with the 1 µM biotin blocked sample subtracted out.

set at a concentration of approximately 100 nM. Our Xa sub control substrate was attached to a third fluorescent microsphere set to measure GFP stability and non-specific fluorescence loss. Addition of 365 nM LF was done to three separate samples while another 3 samples were used as negative controls with no LF added. Fluorescence normalization and graphing of averages was done for each substrate (**Fig A3.1**) Error bars represent one standard deviation of the averaged data. The results show that the full length consensus MKK shows a faster initial rate of cleavage followed by no additional fluorescence loss after the initial 30 minute sample while the consensus cleavage site showed continuous fluorescence loss over 2 hours with a slower initial rate of cleavage (**Fig A3.1**) To additionally show that the full length MKK substrate did not show fluorescence loss after the initial 30 minute time point while the cleavage site alone does 600nM Lethal Factor was used in an additional experiment experiment instead of 365nM. This experiment demonstrates that the LF protease is not losing activity after 30 minutes. As was seen in the normalized data (**Fig. A3.2**), the consensus full length MKK substrate is cleaved at a faster rate than the consensus cleavage site substrate, as expected, but only for the first 30 minutes. After the first 30 minutes the full length substrate microsphere normalized fluorescence values stay relatively steady, with a slight decrease similar to that of the control substrate. The consensus cleavage site substrate continues to lose fluorescence from its microsphere set during the entire 120 minutes of the experiment (**Fig. A3.2**), as was seen using 365 nM LF as well (**Fig. A3.1**) Because these two substrates contained the same lethal factor cleavage site, it would have been

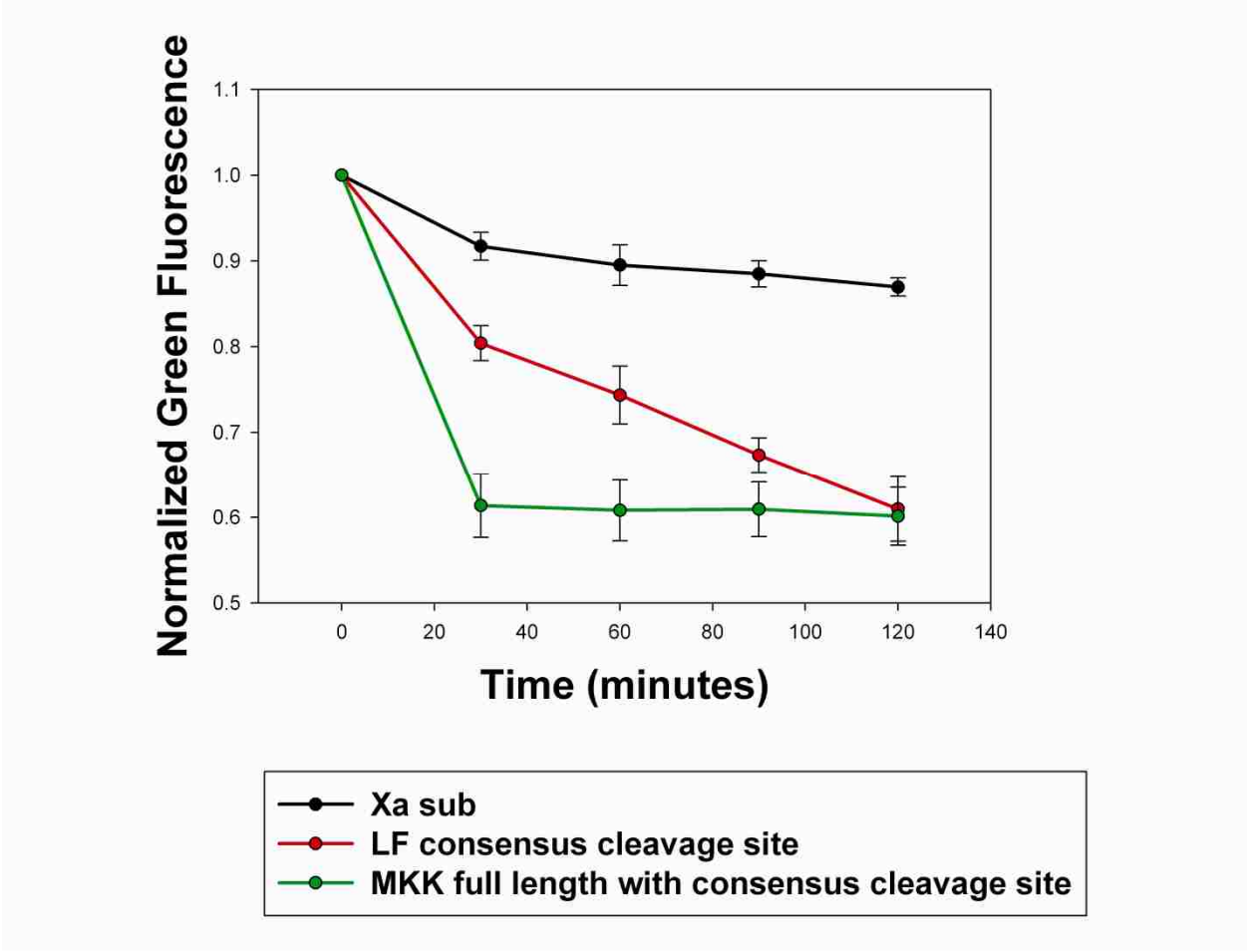

Figure A3.1. Multiplex microsphere based Lethal Factor assay using 364 nM Lethal Factor done in triplicate. Red points are averaged normalized data from the LF consensus cleavage site substrate purified from bacteria and green points are averaged normalized data from the consensus full length MKK GFP substrate purified from Sf9 insect cells followed by *in vitro* biotinylation. Back points are averaged normalized Xa sub control substrate data. Error bars are one standard deviation from triplicate data points. 100 µl sample was collected and run on a FASCSCAN flow cytometer every 30 minutes. Fluorescence was normalized by dividing by the 0 minute time point prior to LF addition.

expected that the full length substrate should continue to lose fluorescence over the entire experiment time course as well. The major difference between the preparation of these two substrates is that the consensus cleavage site GFP substrate was biotinylated *in vivo* by bacterial cells while the consensus full length MKK GFP substrate was biotinylated *in vitro* using the BirA enzyme. This data suggests that the *in vitro* biotinylation of the full length consensus MKK2 GFP is non-specific and biotinylation is occurring C-terminal to the cleavage site. The faster cleavage rate seen in the first 30 minutes most likely represents the higher affinity for lethal factor for the full length substrate, containing the distal interaction site. This increased rate may also be due to Lethal Factor binding to MKKs at the distal interaction site causing a conformational change in either the protease or substrate, leading to more efficient cleavage. The lack of fluorescence loss after that time most likely represents substrate which is cleaved by LF, but stays bound to the streptavidin coated microsphere due to biotinylation C-terminal to the cleavage site. The MKK2 full length GFP substrate with the natural LF cleavage site was tested as well with no apparent cleavage by the LF protease. (data not shown). It has not been determined if this is due to poor affinity, non-specific biotinylation or a combination of both.

One of the goals of this project is to create multiplex protease assays for use in high throughput screening assays to potentially identify inhibitor of protease/substrate interactions, thus identifying new classes of specific protease inhibitors against toxin based proteases. We have been able to show that a full length MKK2 containing a consensus lethal factor cleavage site does in fact have

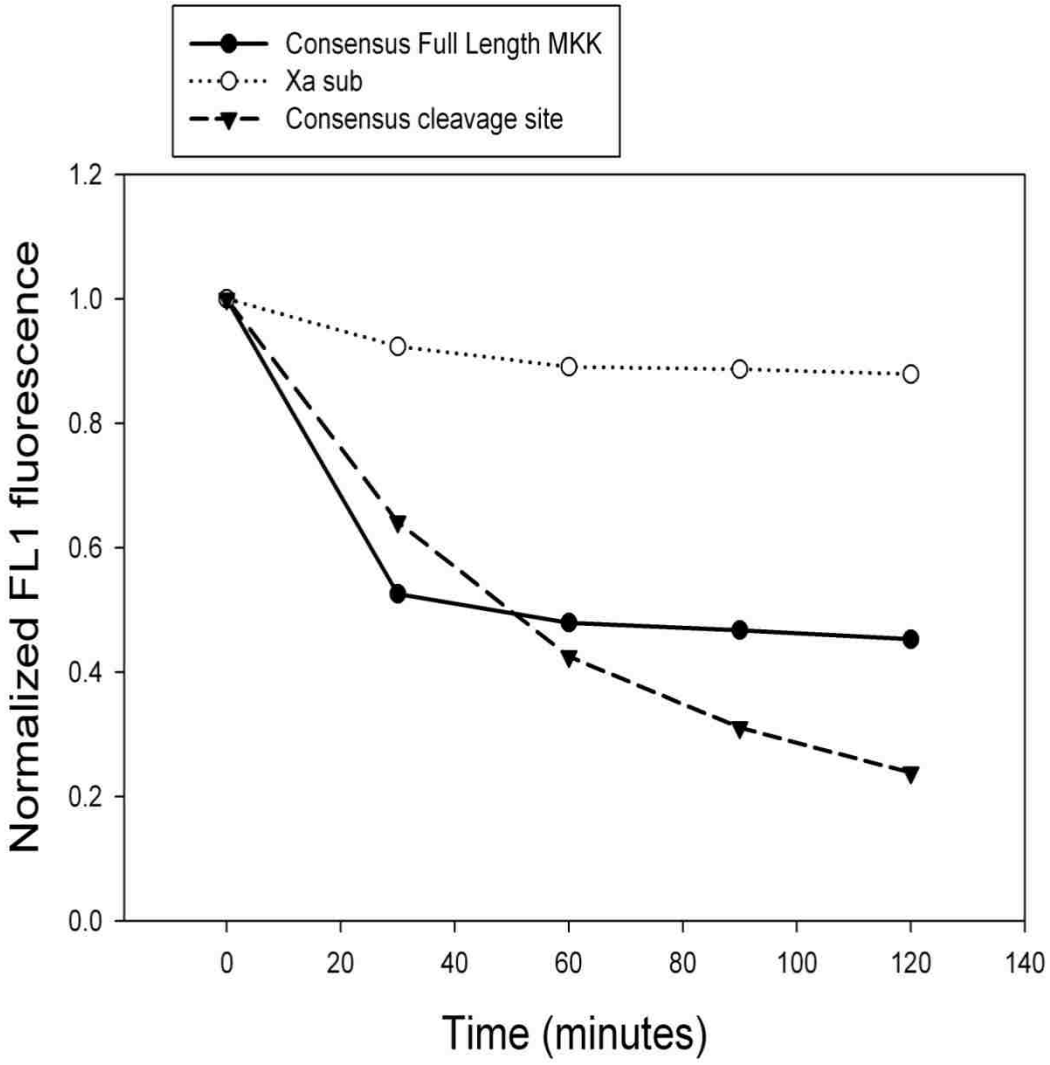

Figure A3.2 Normalized fluorescence of 600nM Lethal Factor added to multiplex microspheres containing Consensus Full Length MKK GFP from Sf9 insect cells with in vitro biontinylation, (closed circles) Consensus cleavage site GFP and Xa sub grown in BL21 DE3 pLysS *E. coli*. 100 µl sample was collected and run on a FASCSCAN flow cytometer every 30 minutes. Fluorescence was normalized by dividing by the 0 minute time point prior to LF addition.

a faster initial rate of cleavage than the consensus cleavage site substrate alone. The observed end point fluorescence, however, would not make this a suitable assay for screening for binding site inhibitors, due to the cleavage site having less normalized fluorescence than the full length substrate at 2 hours, most likely because of non-specific biotinylation of the full length substrate. Binding site inhibitors in such an assay would reduce the amount of cleavage of full length substrate to that of the cleavage site alone, which would not be possible in this assay because the full length substrate does not lose more fluorescence than the cleavage site alone after 1 to 2 hours of incubation. (**Fig. A3.1 and A3.2**) Due to the difficulty of expressing biotinylated full length MKK GFP proteins in bacteria, combined with the labor intensive efforts of expression from Sf9 insect cells, and the apparent non-specific biotinylation of this protein purified from insect cells, we have chosen another toxin based protease to use for a model system in screening for specific protease/substrate binding inhibitors.

A3.3.3 Botulinum Neurotoxin type A Light Chain cleavage of SNAP-25

Biotinylated SNAP-25 GFP was successfully cloned into our pinpoint GFP expression plasmid and expressed in BL21(DE3) pLysS bacteria. Yields of this protein were good, and we were able to purify sufficient quantities to use in microsphere based assays. The botulinum neurotoxin type A light chain cleavage site of SNAP-25 was also cloned and purified in this system. A synthetic peptide of an optimized SNAP-25 cleavage site was labeled with biotin at the N-terminus and Alexa-488 at the C-terminus was included in this assay as well. Upon biotin removal and binding of SNAP-25 full length GFP to a distinct microsphere set,

SNAP-25 cleavage site to another set and the synthetic SNAP-25 cleavage site peptide to a third set with the Xa sub control to a fourth microsphere set, microspheres were washed and set up as previously described [127]. 364 nM Botulinum Neurotoxin type A Light Chain (BoNTALC) was added to the samples after removing and analyzing a 0 minute time point, and 100 µl samples were taken and run on a flow cytometer every 30 minutes. The amount of BoNTALC used was based upon the amount of Lethal Factor used in similar experiments to give cleavage from the surface of microspheres. It was observed that the cleavage site of SNAP-25 alone, both in our biotinylated GFP system and as a synthetic peptide labeled with Alexa-488, did not lose more than 10% fluorescence, while SNAP-25 full length lost 40% fluorescence in the first 30 minutes. (Fig. A3.3) The quick loss of fluorescence by SNAP-25 full length, followed by a relatively stable fluorescence level could have been due to the relatively low starting fluorescence levels on that particular microsphere set, with auto-fluorescence accounting for nearly 50% of the FL1 channel fluorescence in this particular experiment. Further investigation of SNAP-25 full length showed a continuous fluorescence loss over time as seen in Chapter 4.

Due to the fact that little fluorescence loss was seen on the SNAP-25 cleavage site proteins and peptide, and the presence of 4 identified SNARE domains which contribute to BoNTALC cleavage on SNAP-25 itself [9], we decided to make SNARE domain deletions of full length SNAP-25 instead of using the cleavage site (described in Chapter 4). This approach is also technically feasible, since the biotinylated full length SNAP-25 GFP, and SNARE domain

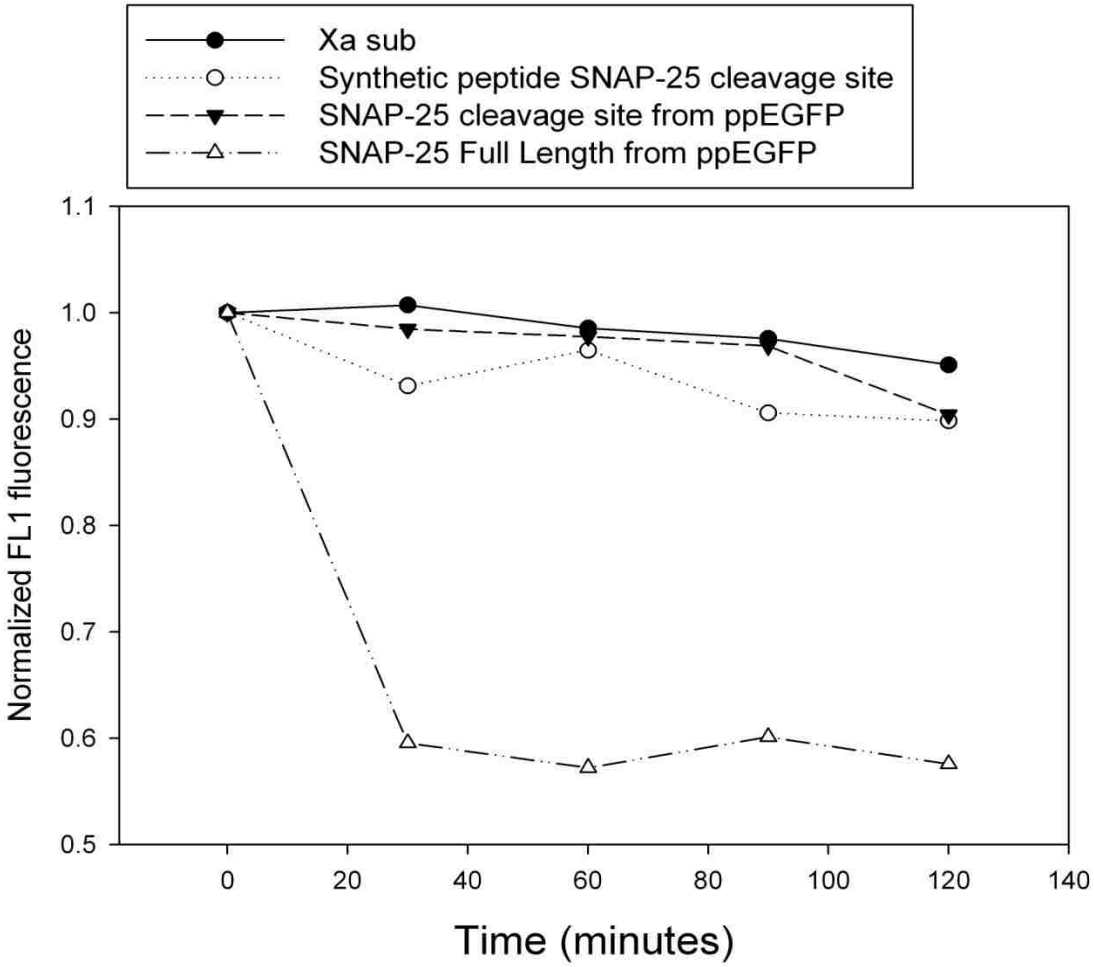

Figure A3.3 Normalized fluorescence of cleavage SNAP-25 Full Length GFP bound microspheres (open triangles) compared to microspheres containing a cloned SNAP-25 cleavage site GFP (closed triangles) and synthetic alexa-488 labeled SNAP-25 cleavage site (open circles) by 364 nM Botulinum Neurotoxin type A Light Chain (BoNTALC) Also included was Xa sub (closed circles) as a fluorescence control. 100 µl sample was taken and run on a FACScan flow cytometer every 30 minutes Fluorescence was normalized by dividing by the 0 minute time point prior to BoNTALC addition.

deletion mutants can all be purified from bacterial systems due to their relatively small size. The use of SNAP-25 and Botulinum neurotoxin type A light chain proves to be a better model system for development of a multiplex microsphere based protease assay to study the effects of deletion of protease/substrate interaction sites due to the fact that deletion of the SNARE domains has an effect on the relative cleavage rates of the substrates, as seen Chapter 4.

Appendix 4 Results of Follow Up Screening of the TPIMS Combinatorial Chemical Library

Graphical representation of the TPIMS follow up screen with all four SNAP-25 substrates graphed as percent inhibition of the botulinum neurotoxin type A light chain protease. Compound ID numbers are from the Torrey Pines Institute for Molecular Studies. Percent inhibition values and Z' values are calculated as described in Chapter 6. Compounds have been grouped according to scaffold family. Scaffold Family 1477 contains both mixtures of numerous chemicals as well as individual compounds with redundancy in naming. Each graph has been labeled as to if they are mixtures or individual compounds. Numerical percent inhibition averages have been included for each well for each substrate at the end of the appendix. Averages are from two copies of each 96 well plate with each copy being screened twice. Substrates with Z' values below 0.3 on any given screen were not used in percent inhibition values. Values of 0 indicate that no reliable data with Z' values above 0.3 were obtained for that particular substrate in either copy of the plate.

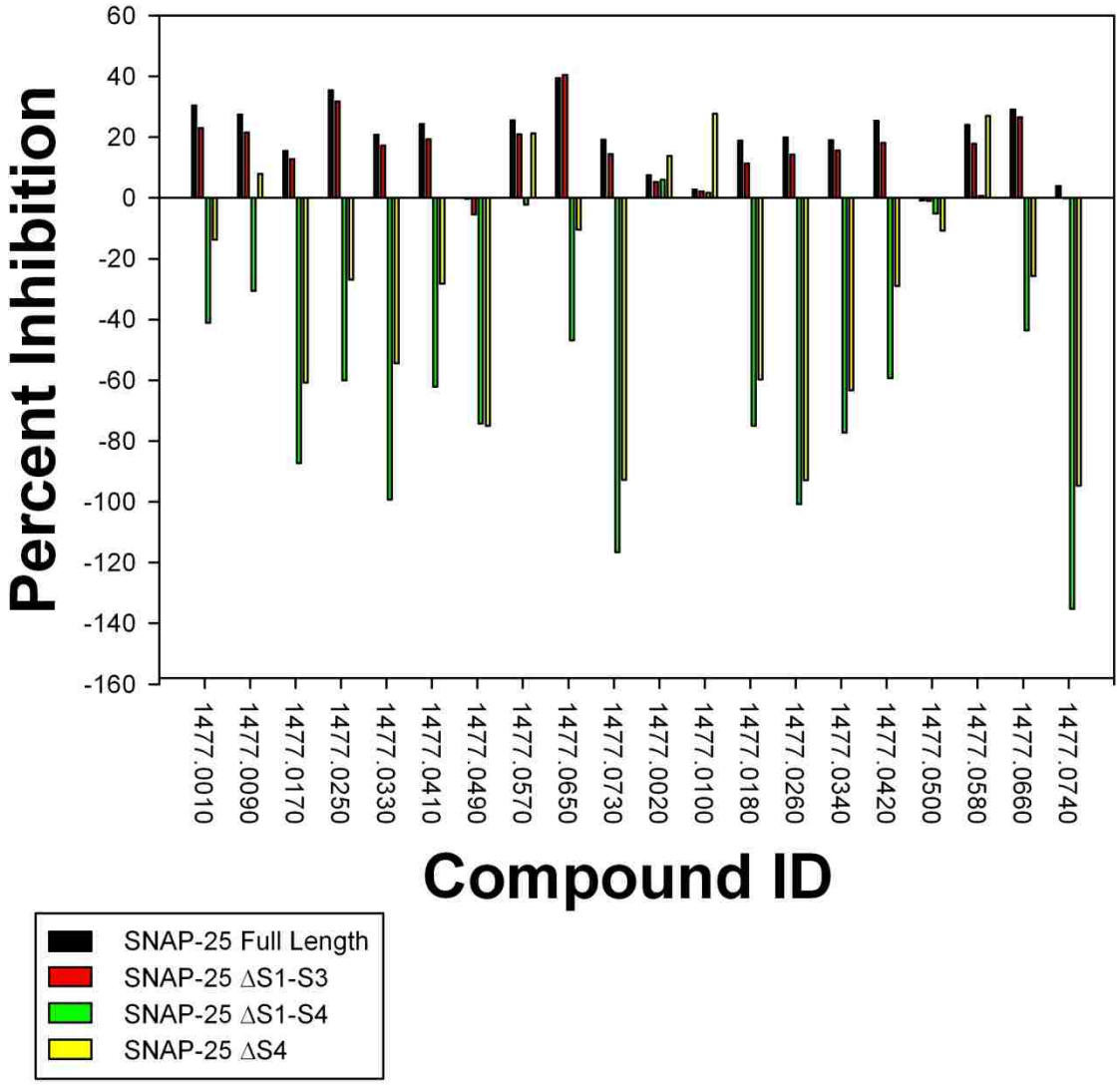

Scaffold Family 1477 mixtures plate 1

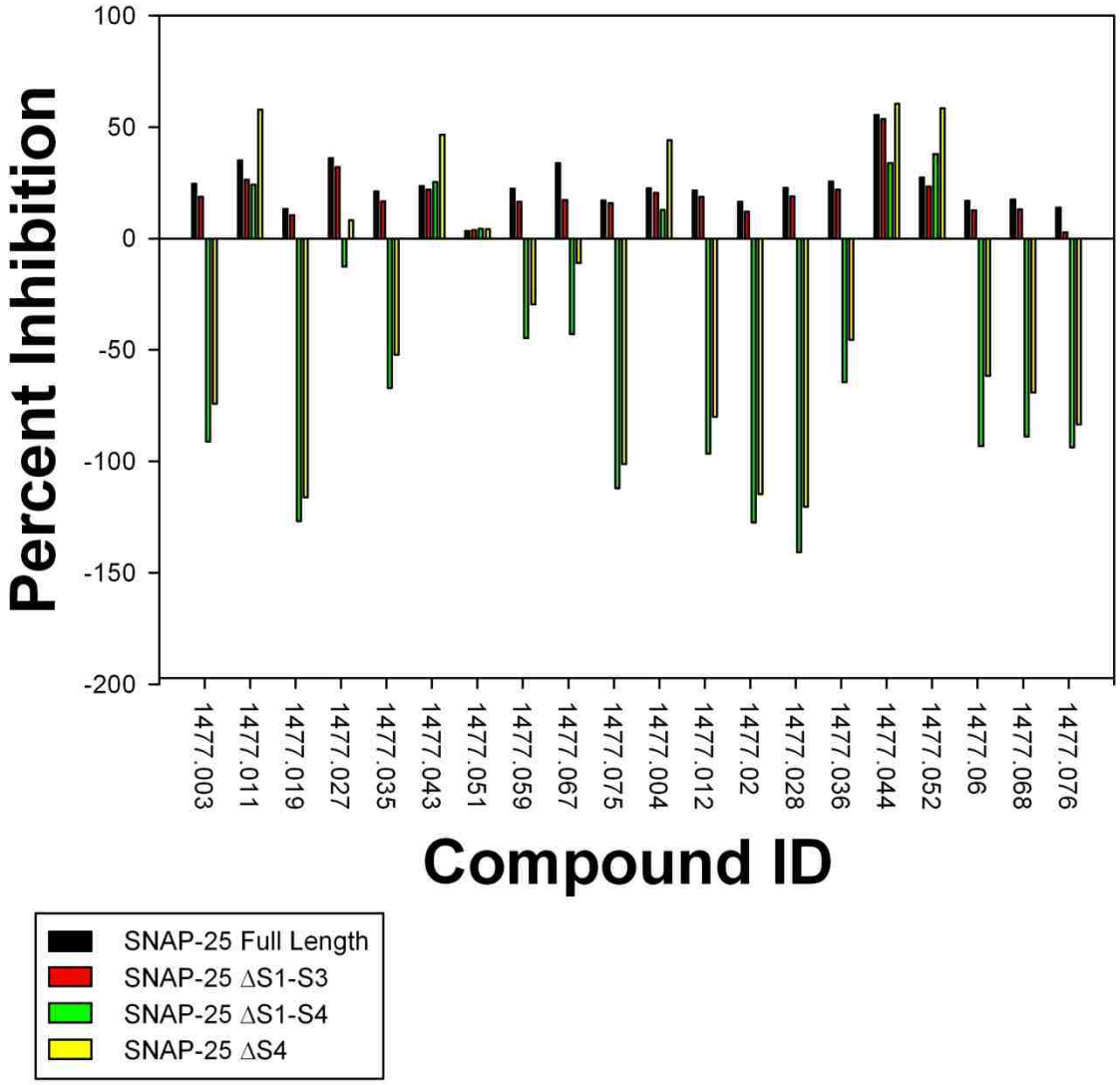

Scaffold Family 1477 mixtures plate 1

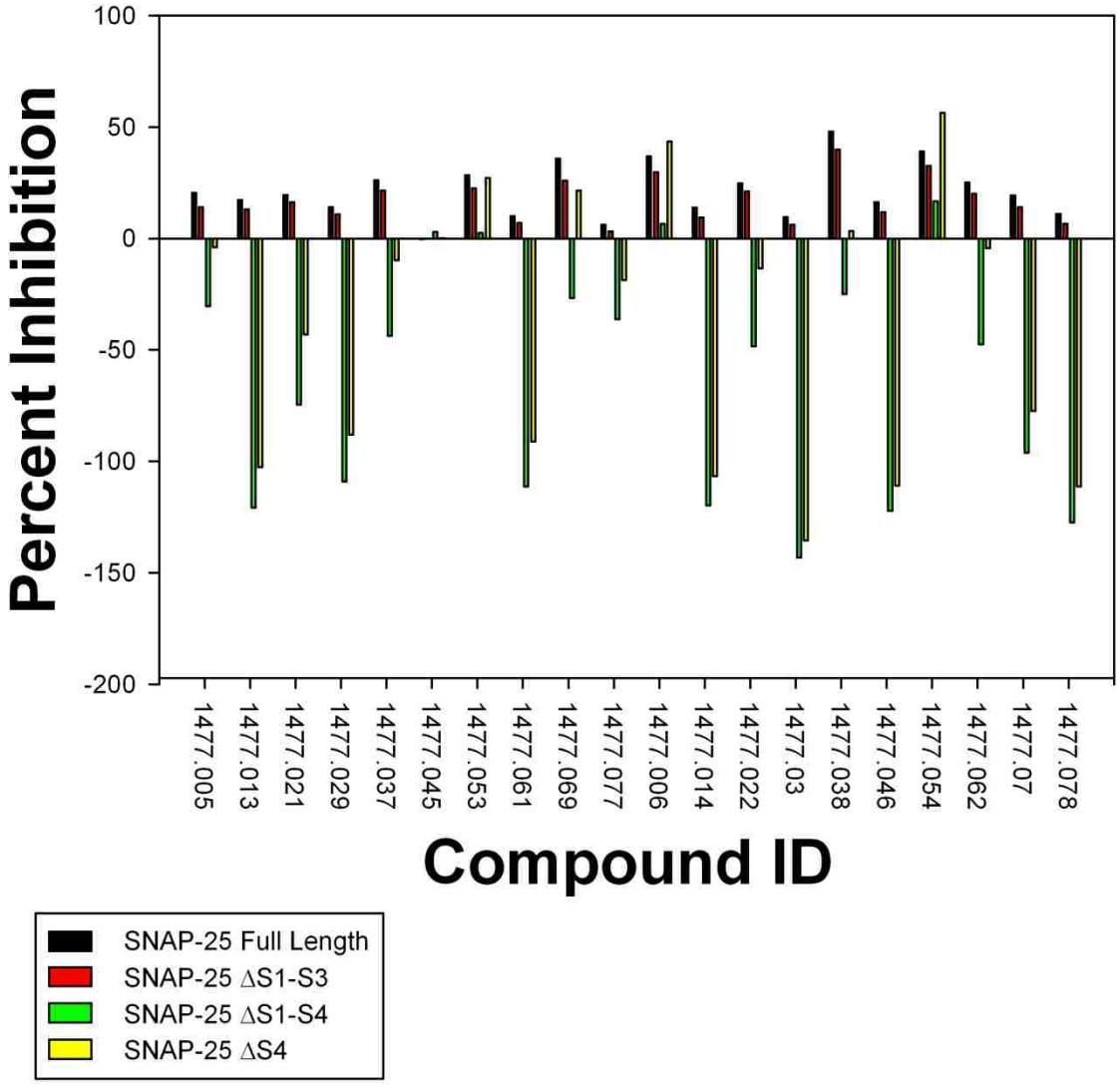

Scaffold Family 1477 mixtures plate 1

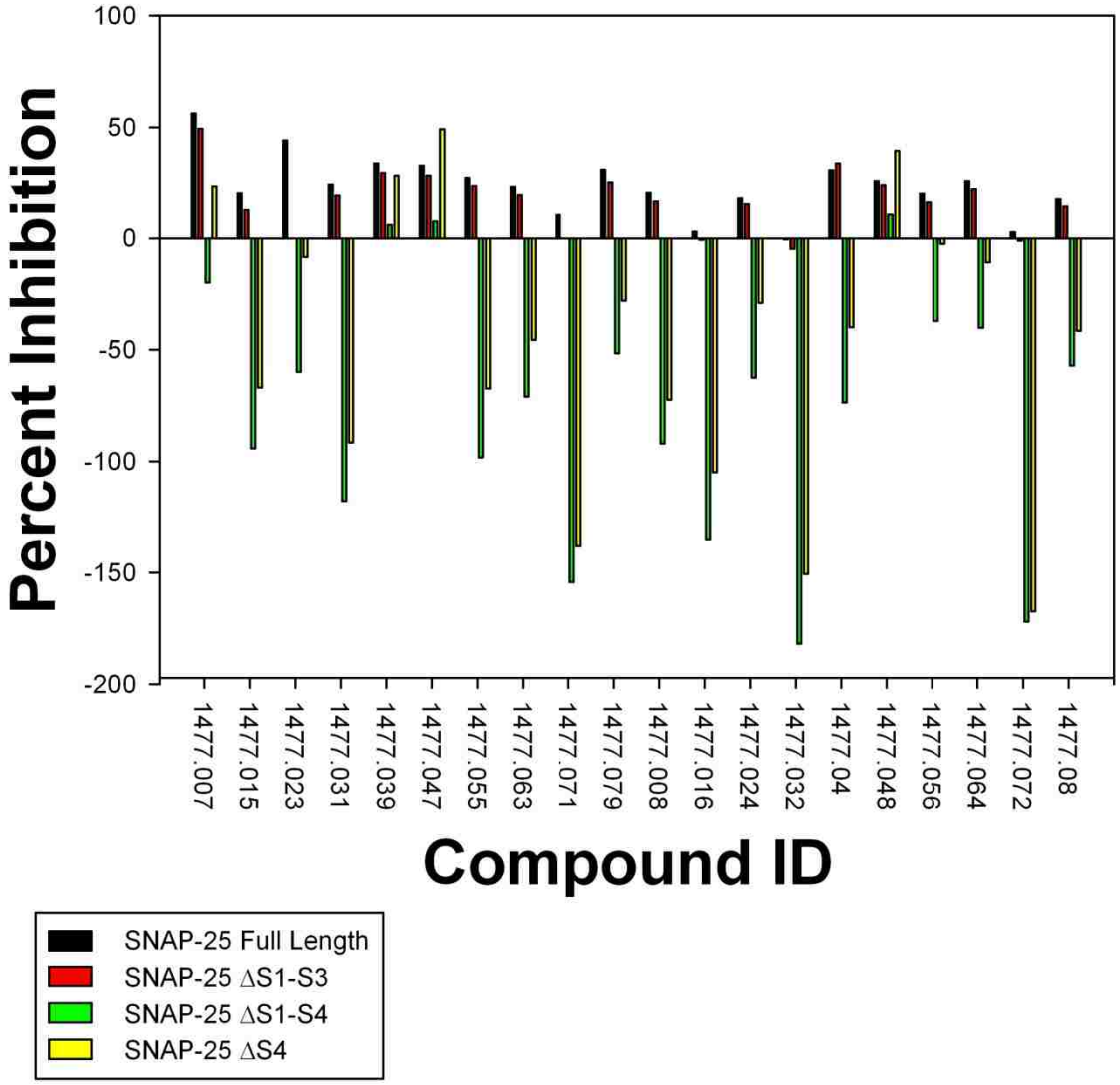

Scaffold Family 1477 mixtures plate 1

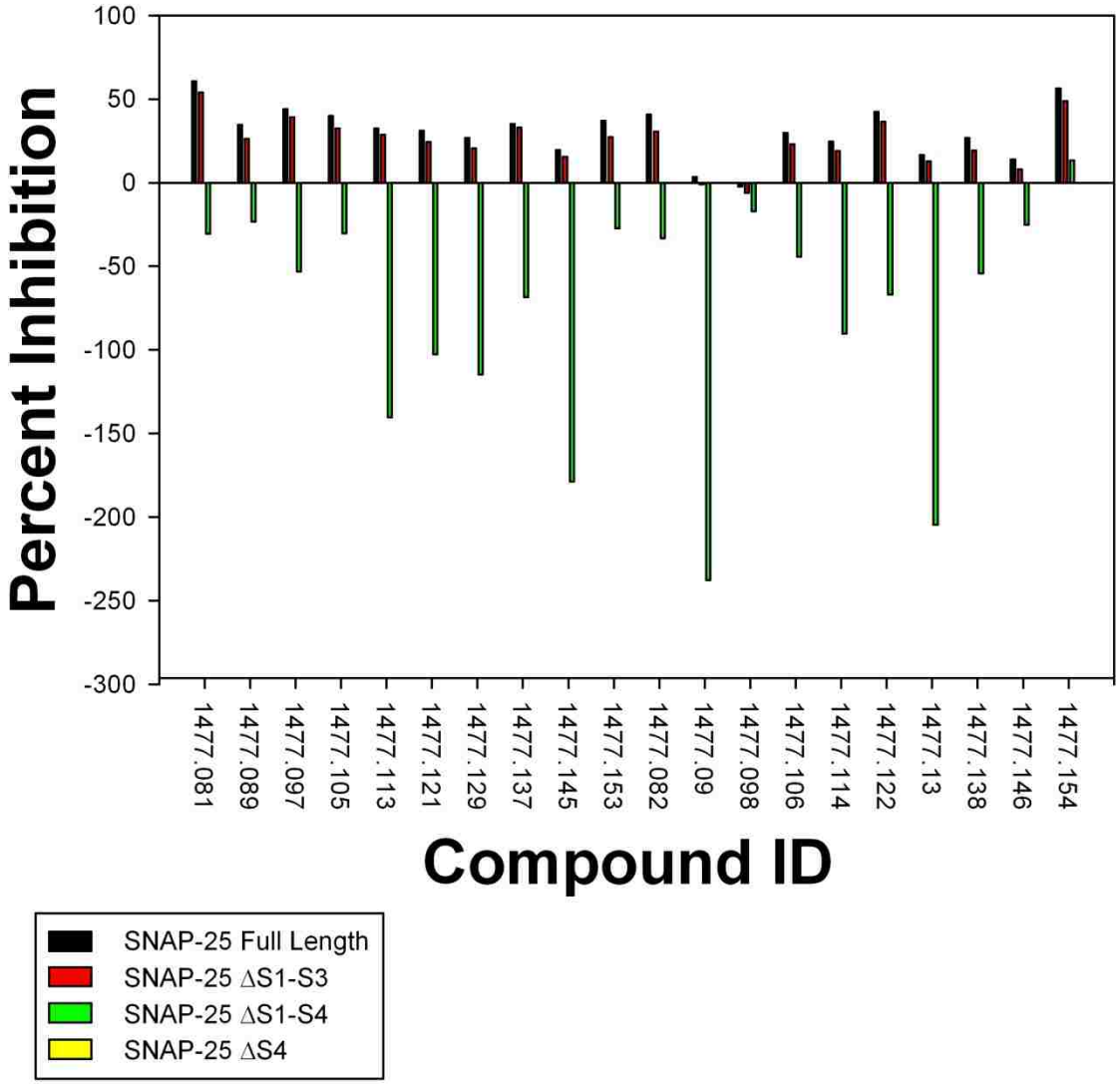

Scaffold Family 1477 mixtures plate 2

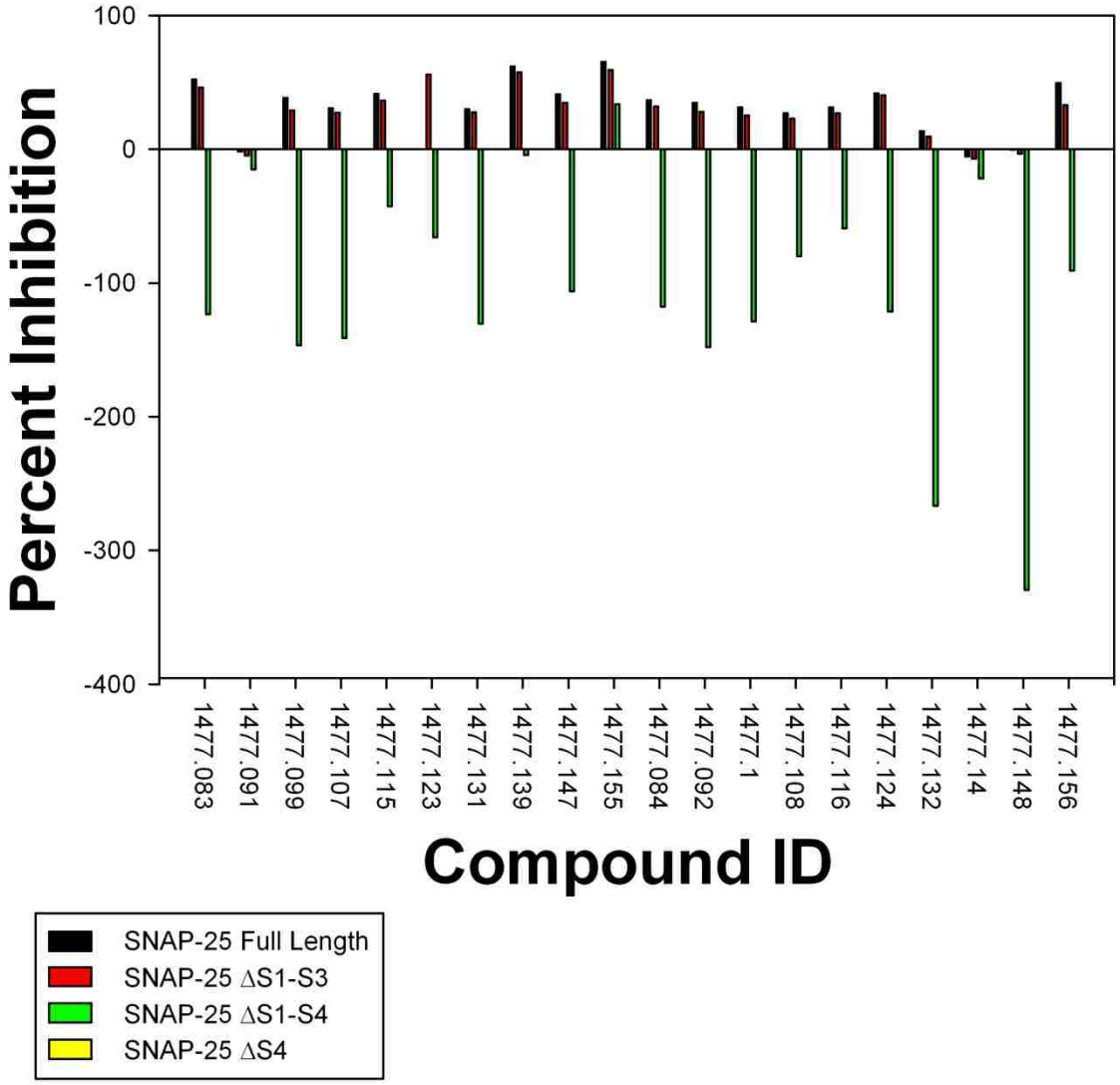

Scaffold Family 1477 mixtures plate 2

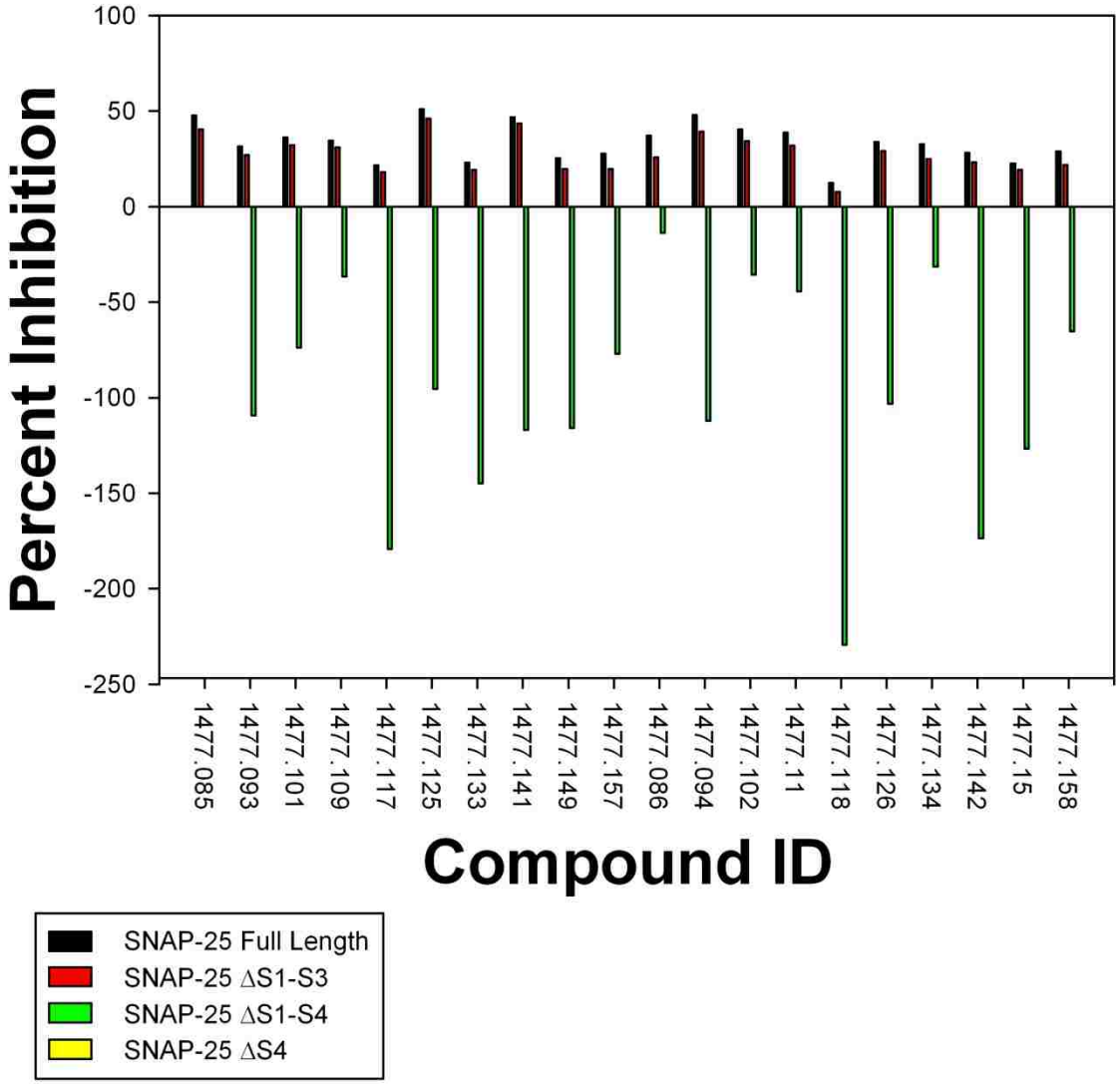

Scaffold Family 1477 mixtures plate 2

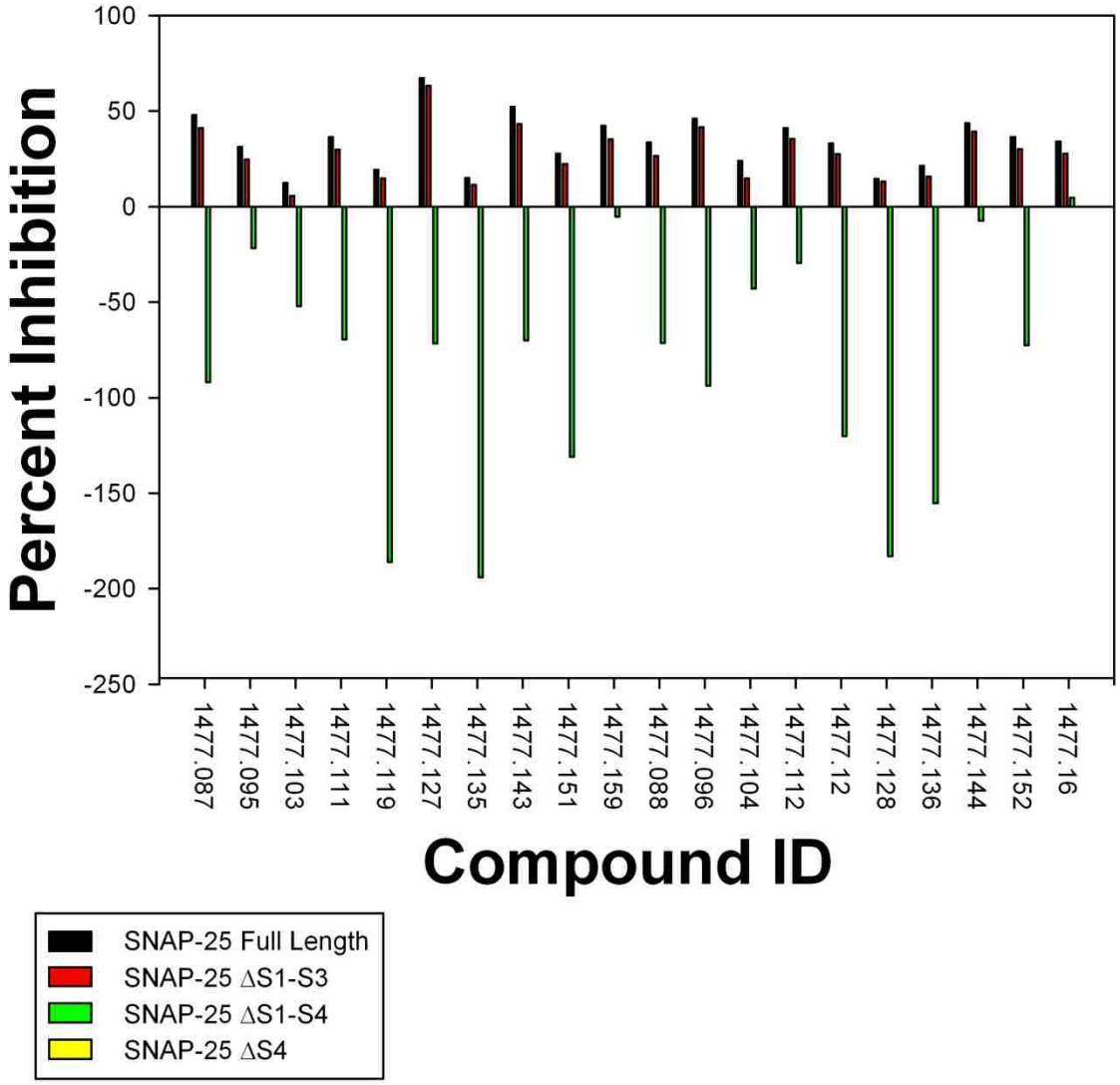

Scaffold Family 1477 mixtures plate 2

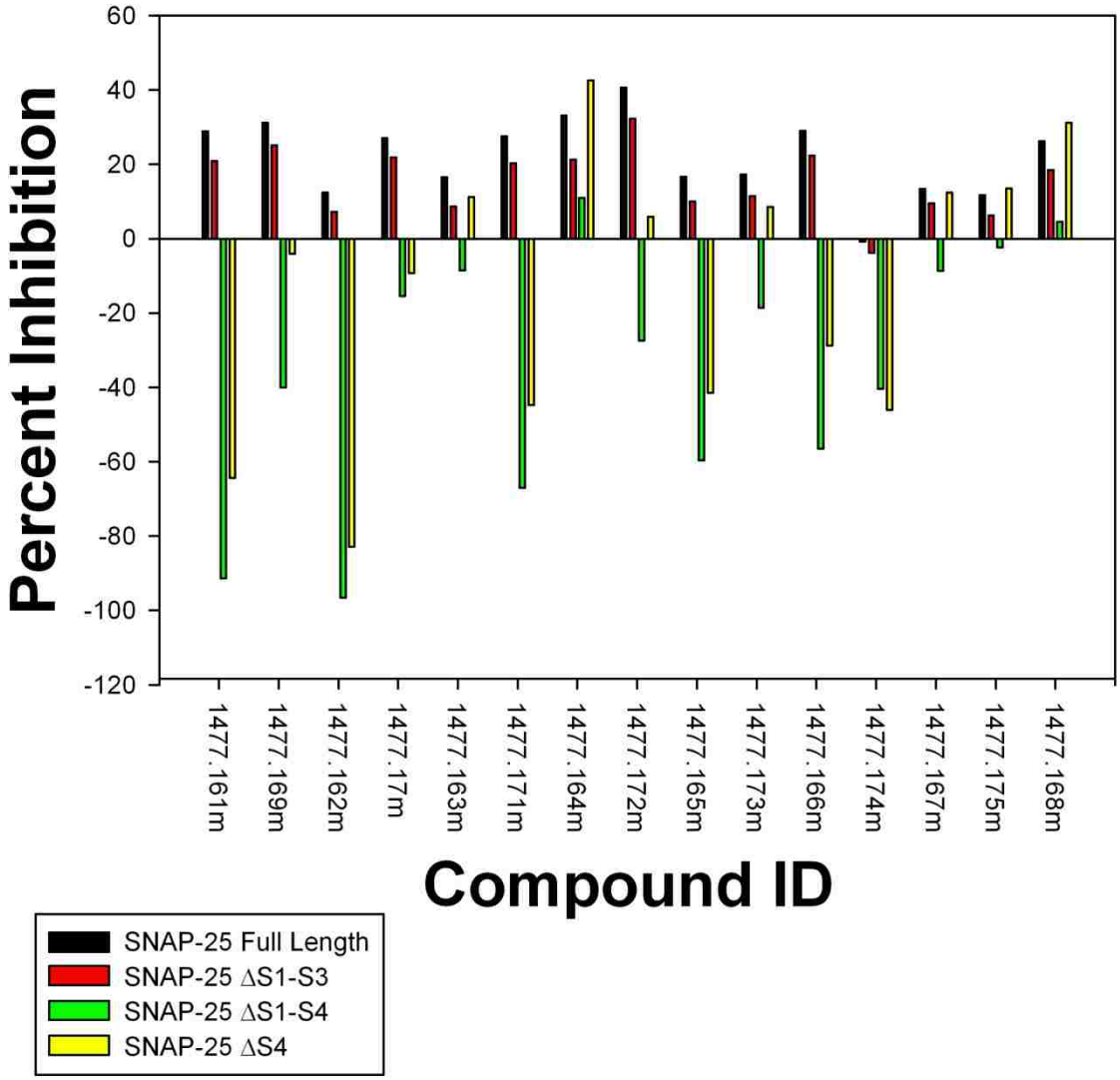

Scaffold Family 1477 mixtures plate 3 (screened with 1477 individual compounds from plate 9 in one 96 well plate. The m after the compound name denotes mixtures)

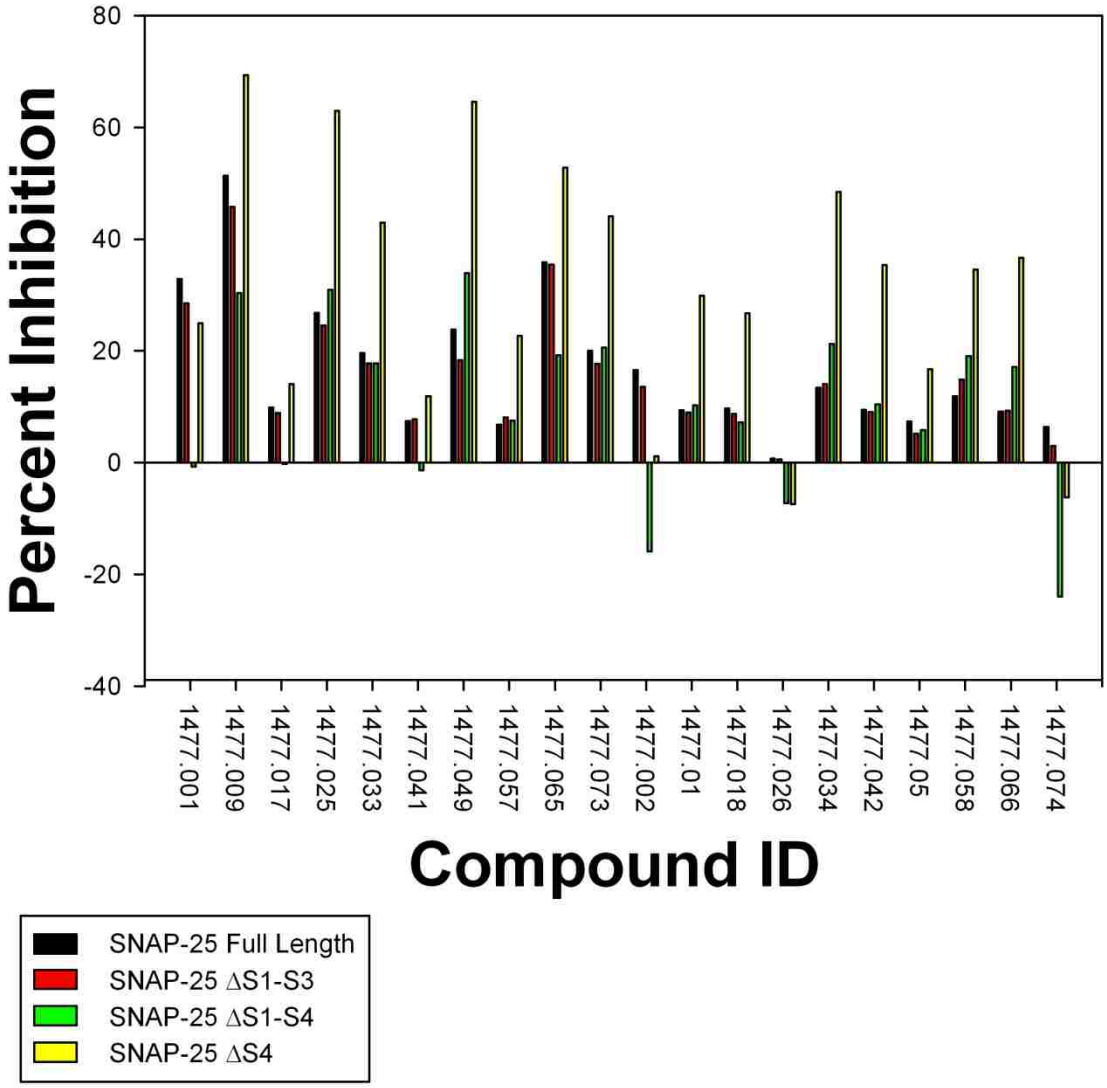

Scaffold Family 1477 individual compounds plate 7

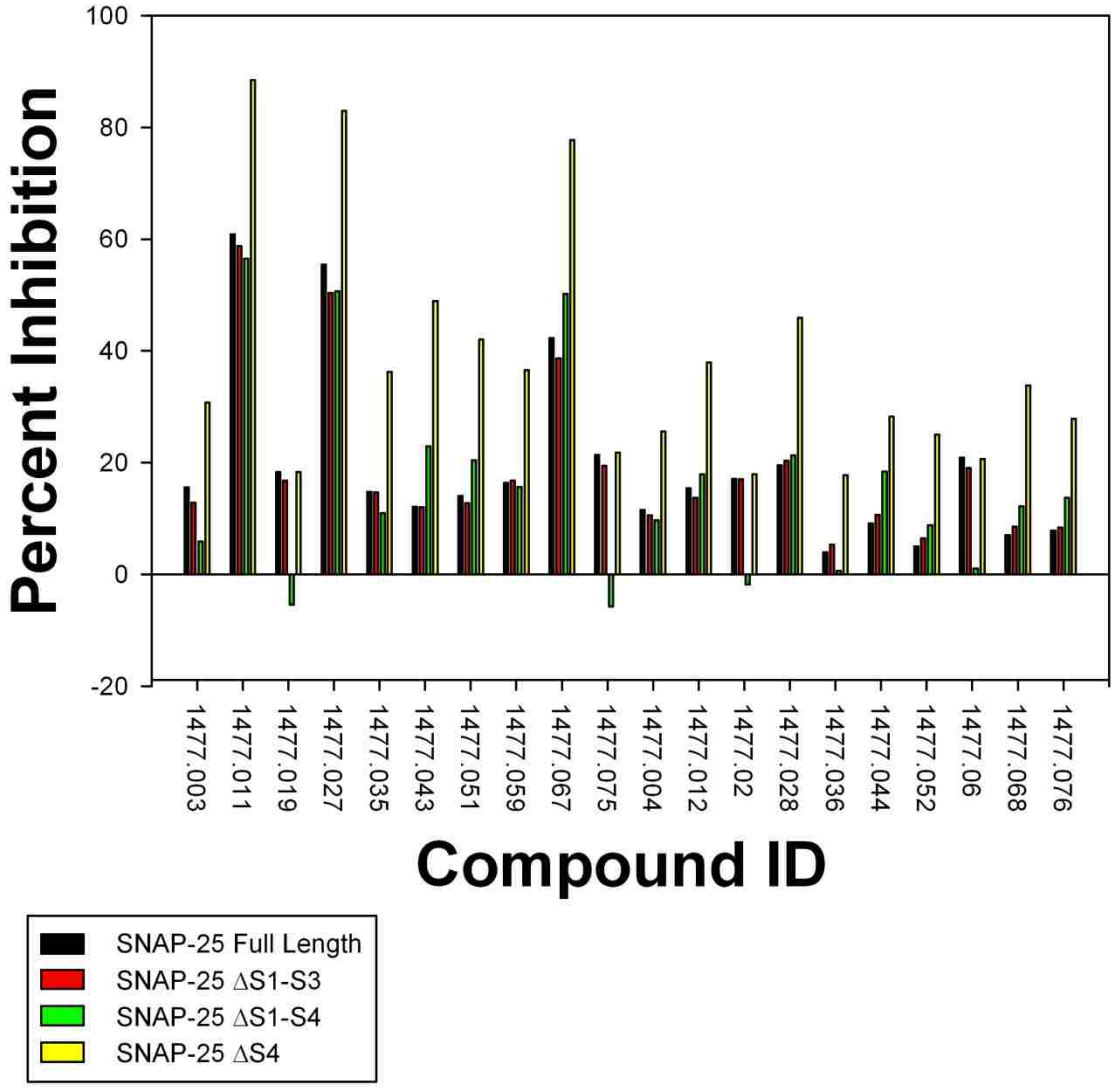

Scaffold Family 1477 individual compounds plate 7

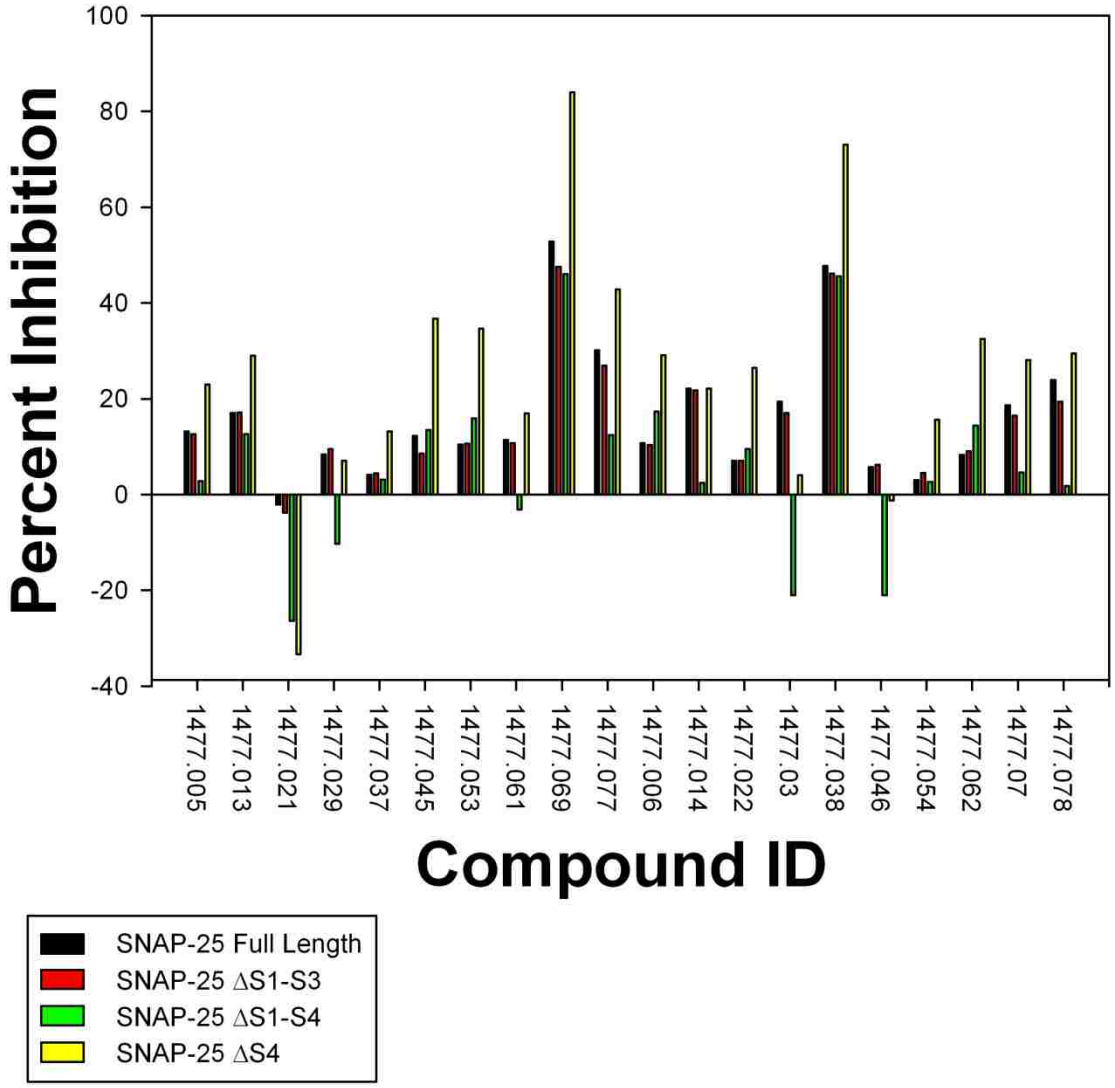

Scaffold Family 1477 individual compounds plate 7

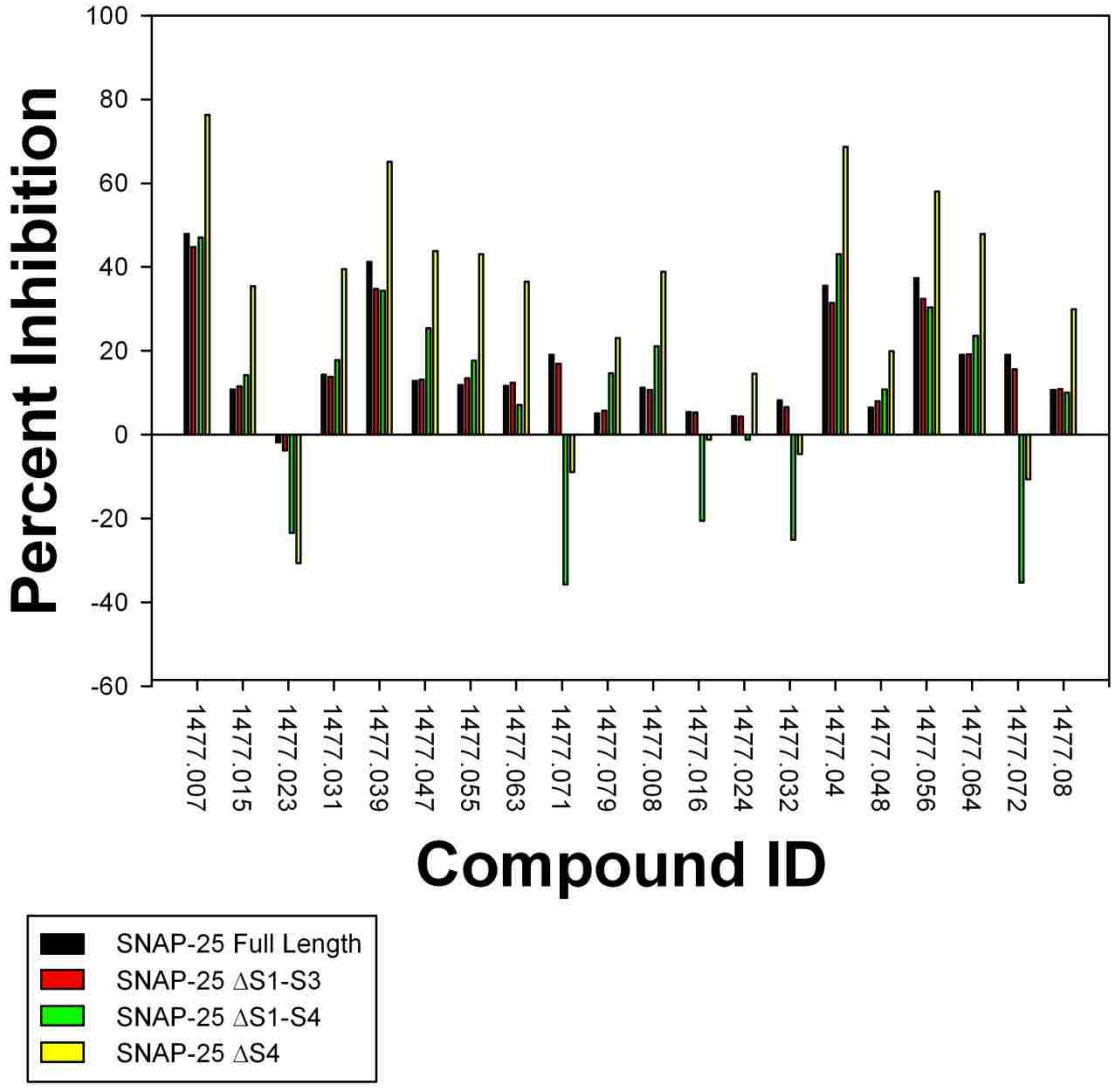

Scaffold Family 1477 individual compounds plate 7

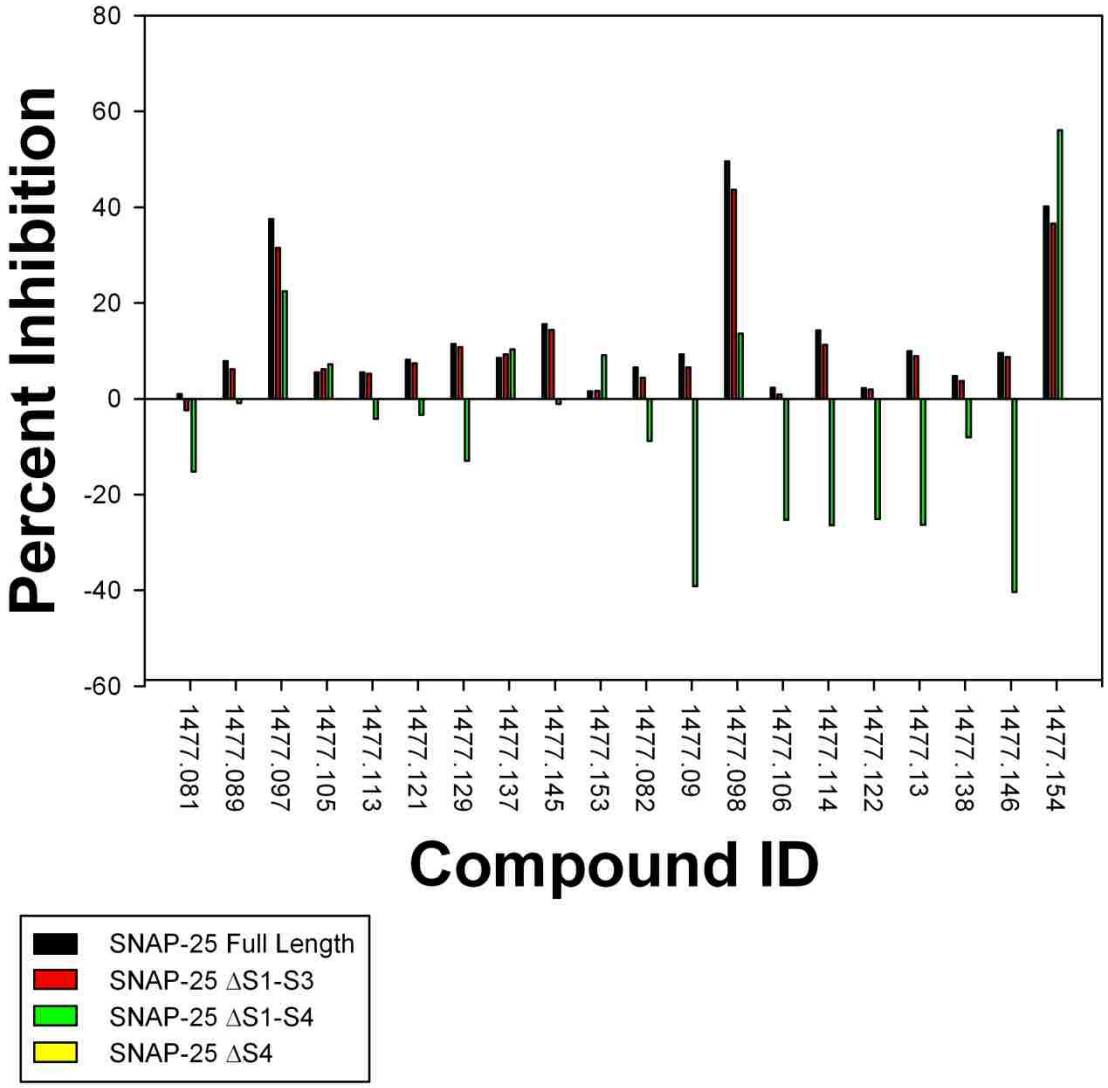

Scaffold Family 1477 individual compounds plate 8

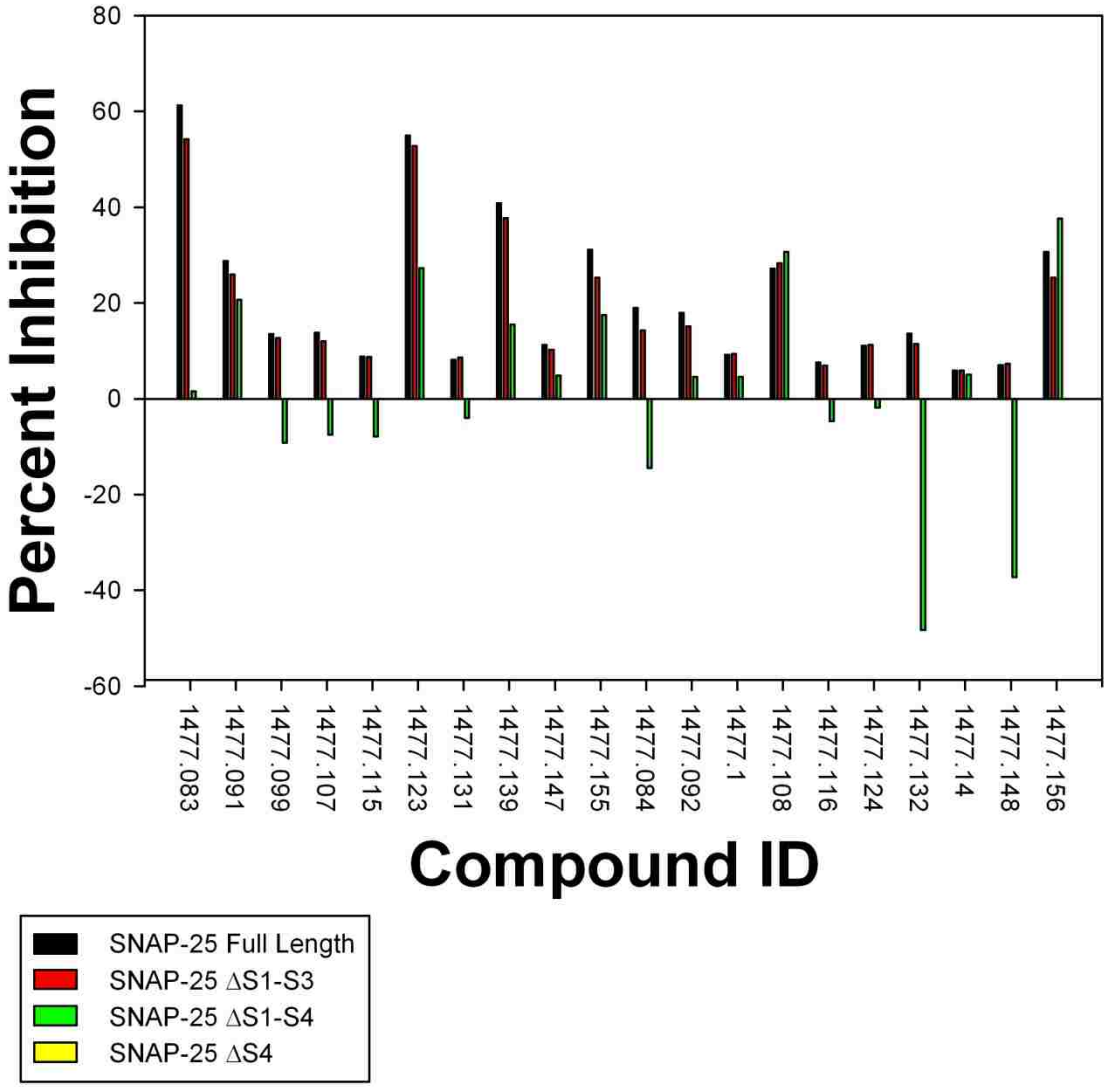

Scaffold Family 1477 individual compounds plate 8

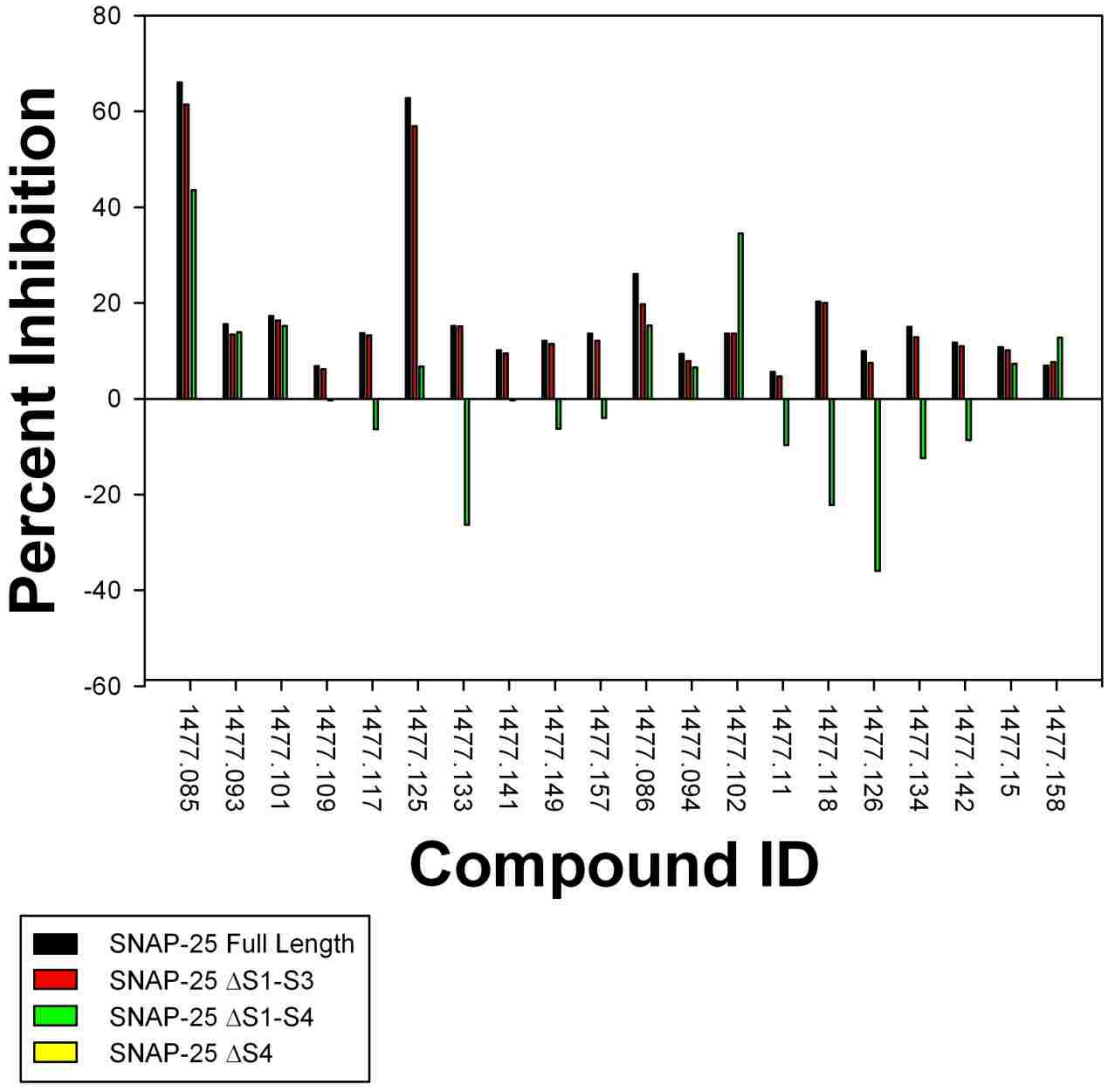

Scaffold Family 1477 individual compounds plate 8

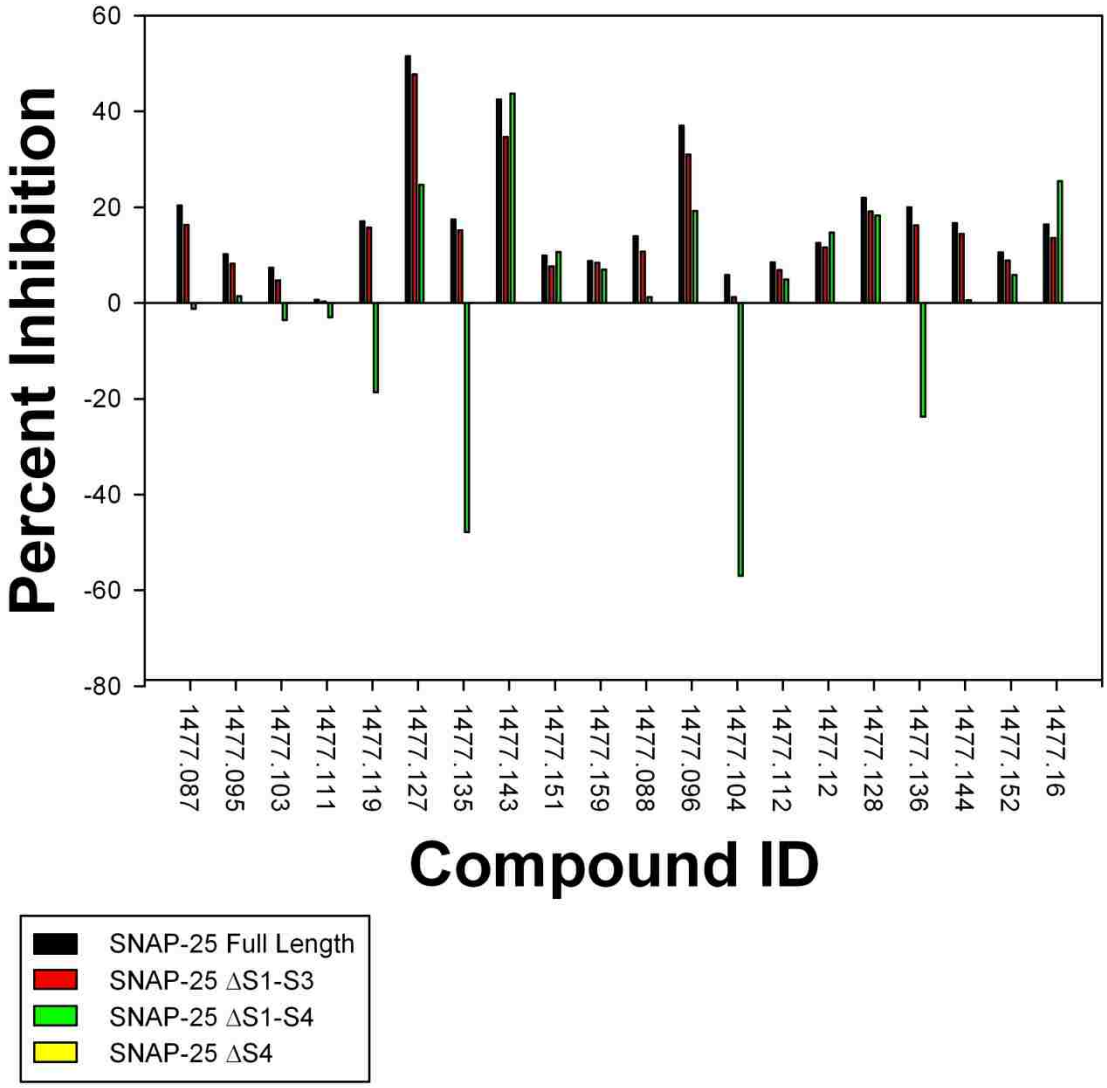

Scaffold Family 1477 individual compounds plate 8

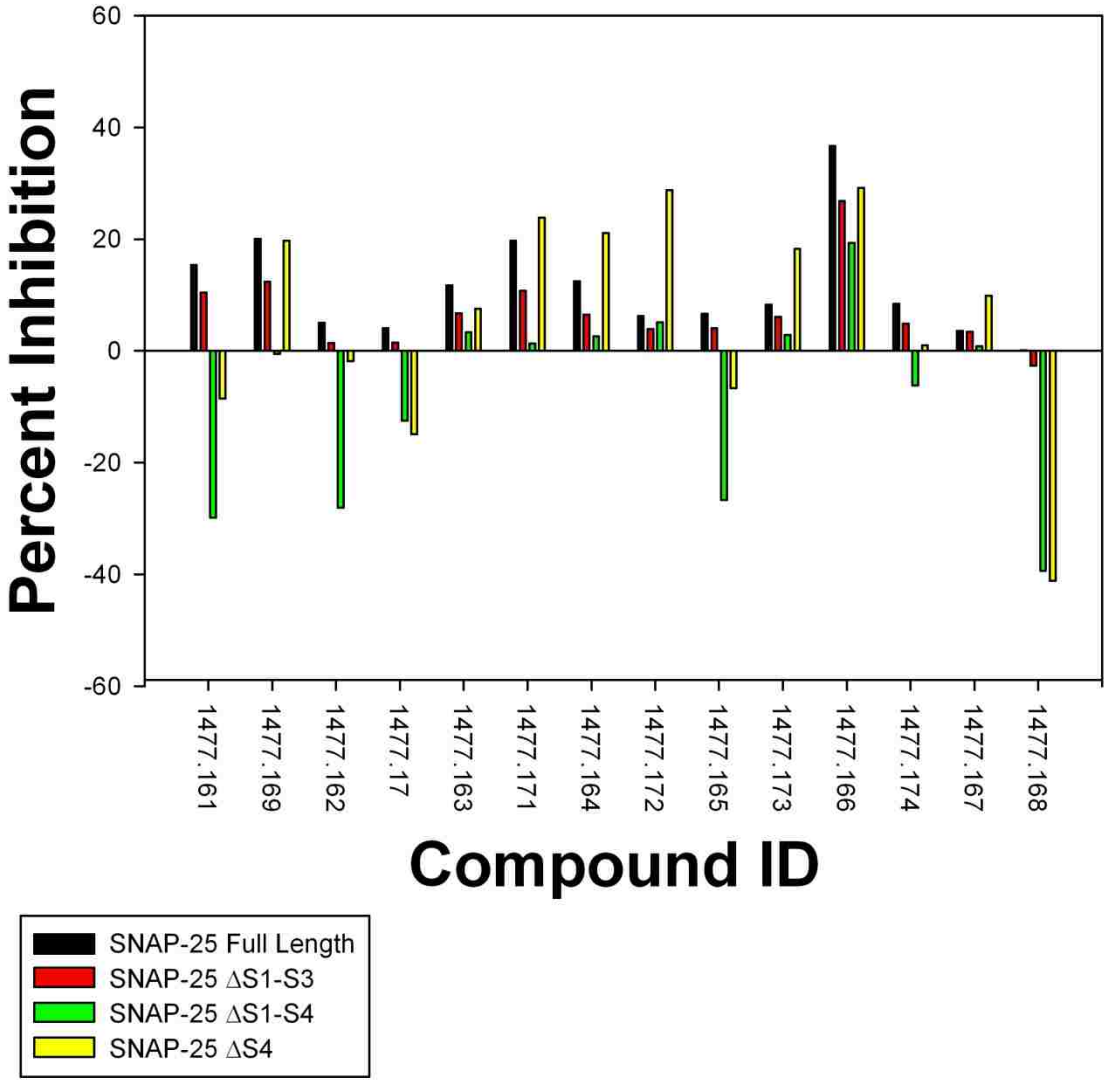

Scaffold Family 1477 individual compounds plate 9

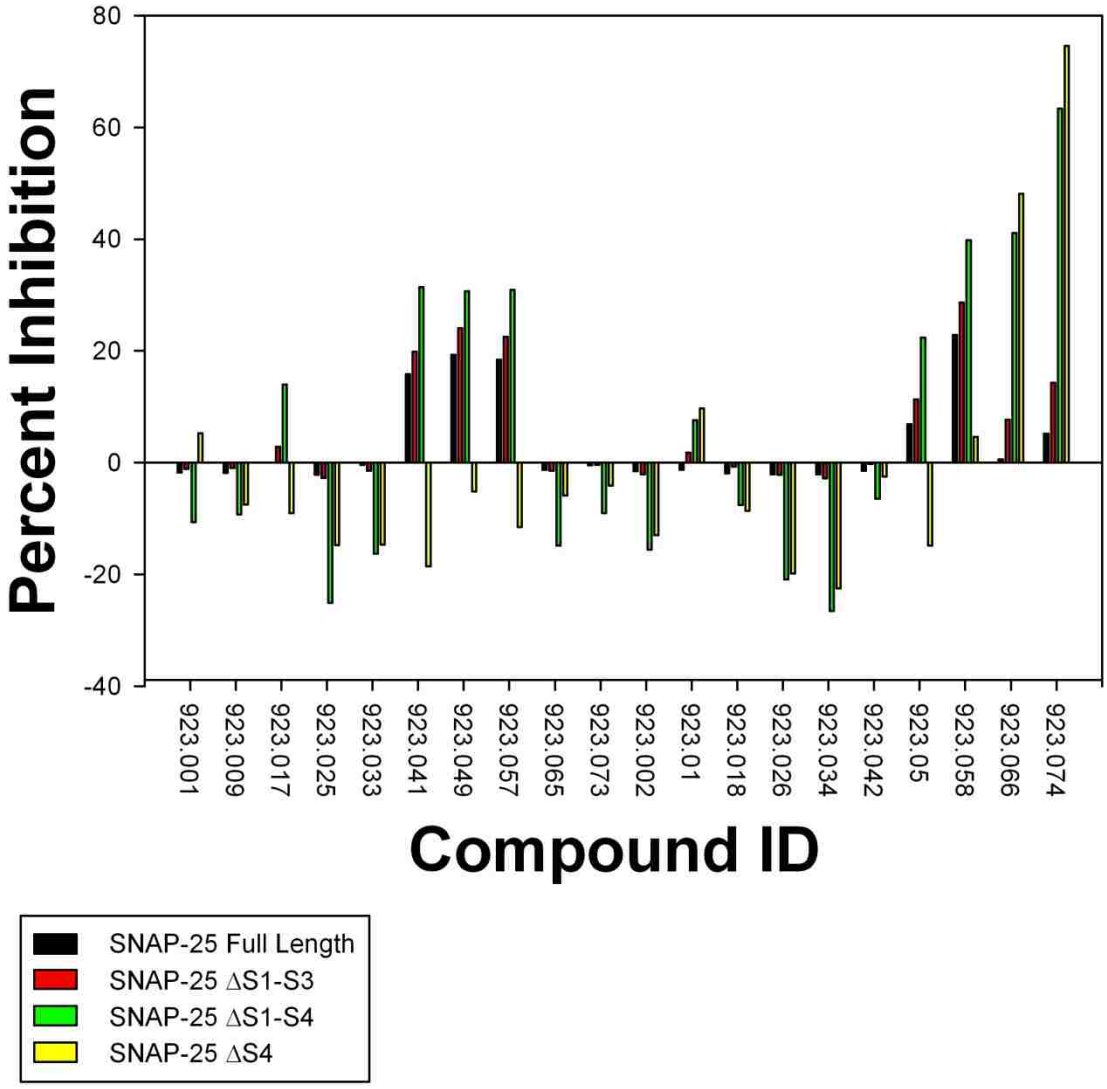

Scaffold Family 923 tetrapeptide mixtures plate 4

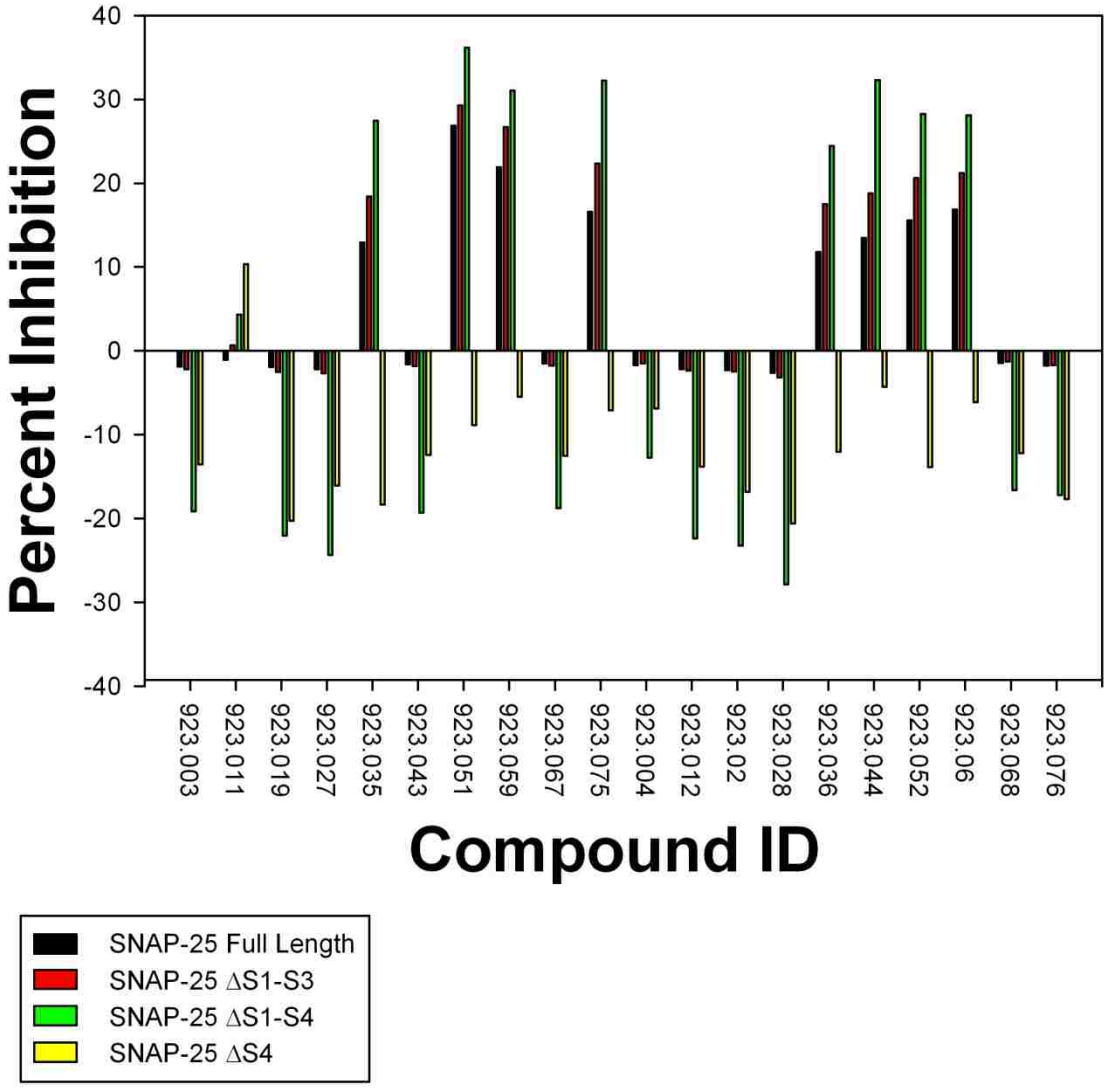

Scaffold Family 923 tetrapeptide mixtures plate 4

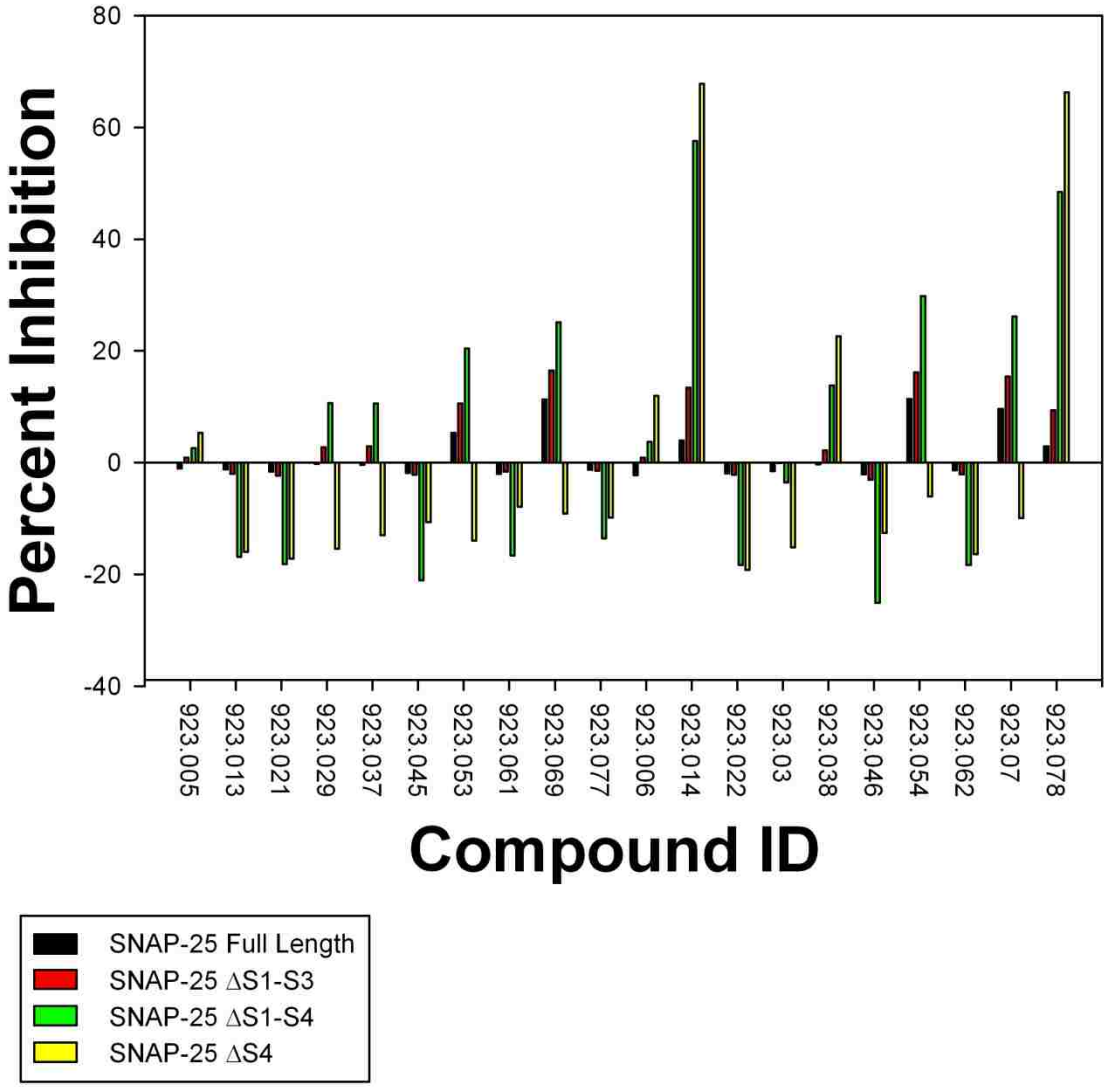

Scaffold Family 923 tetrapeptide mixtures plate 4

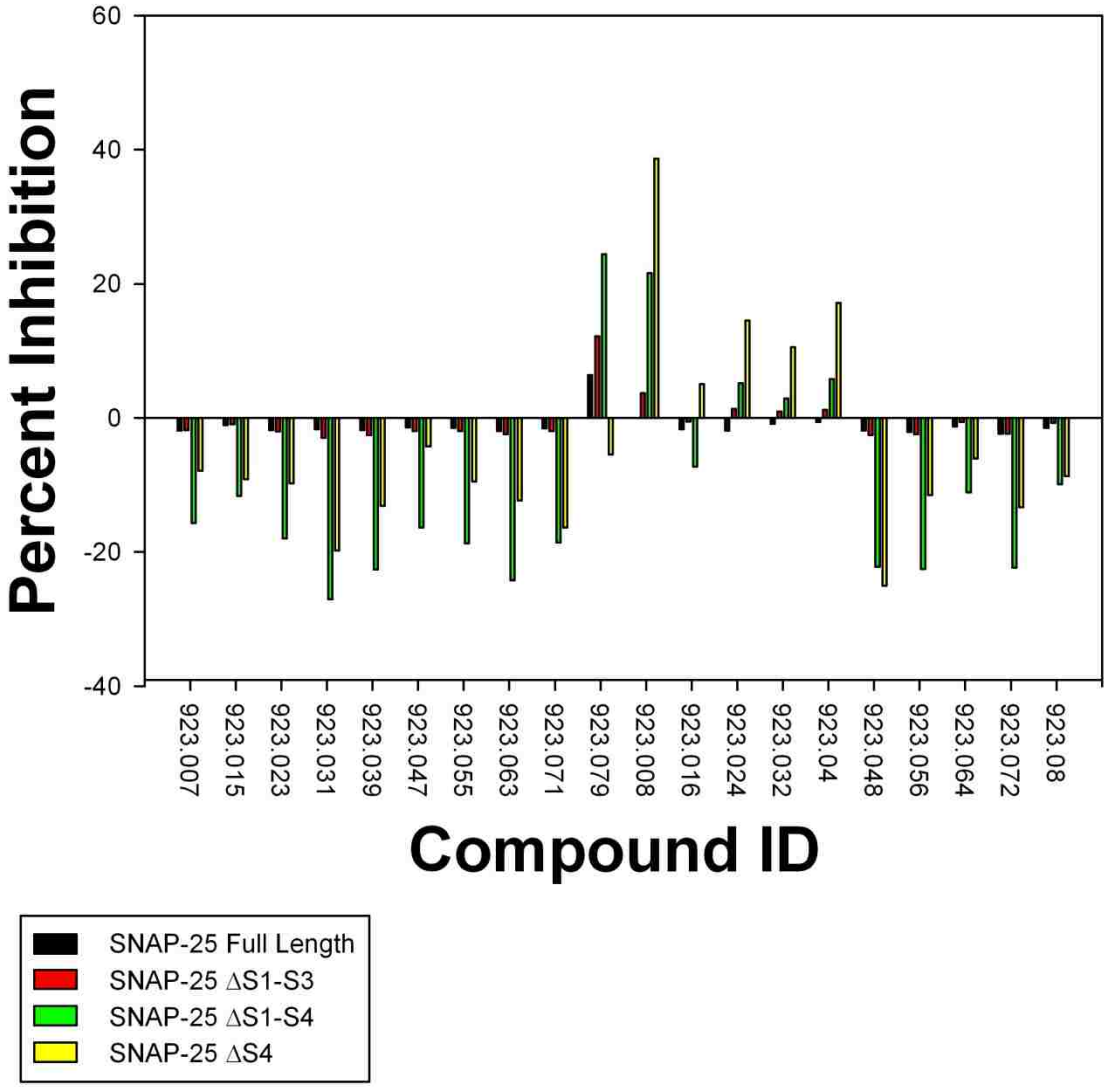

Scaffold Family 923 tetrapeptide mixtures plate 4

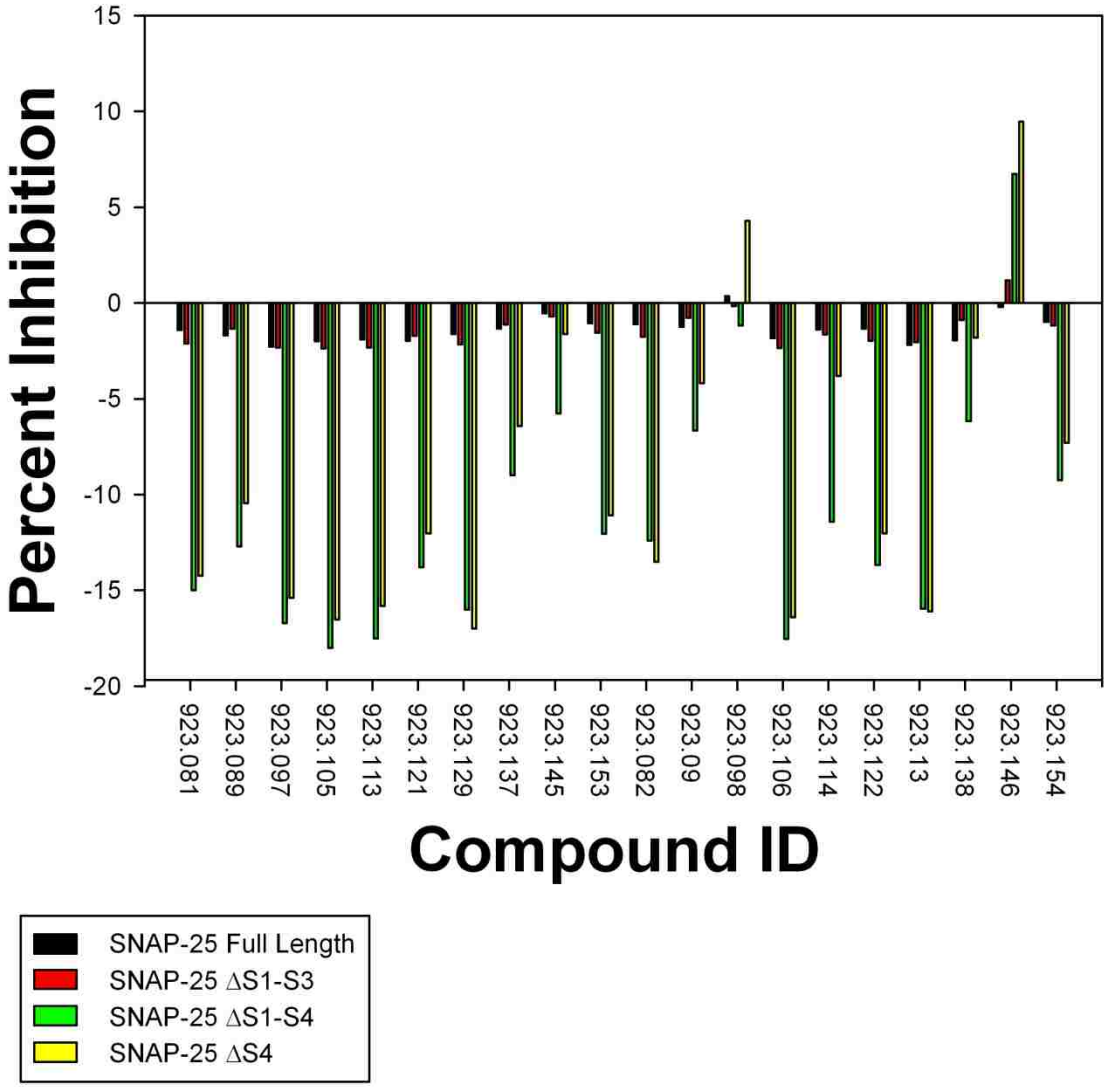

Scaffold Family 923 tetrapeptide mixtures plate 5

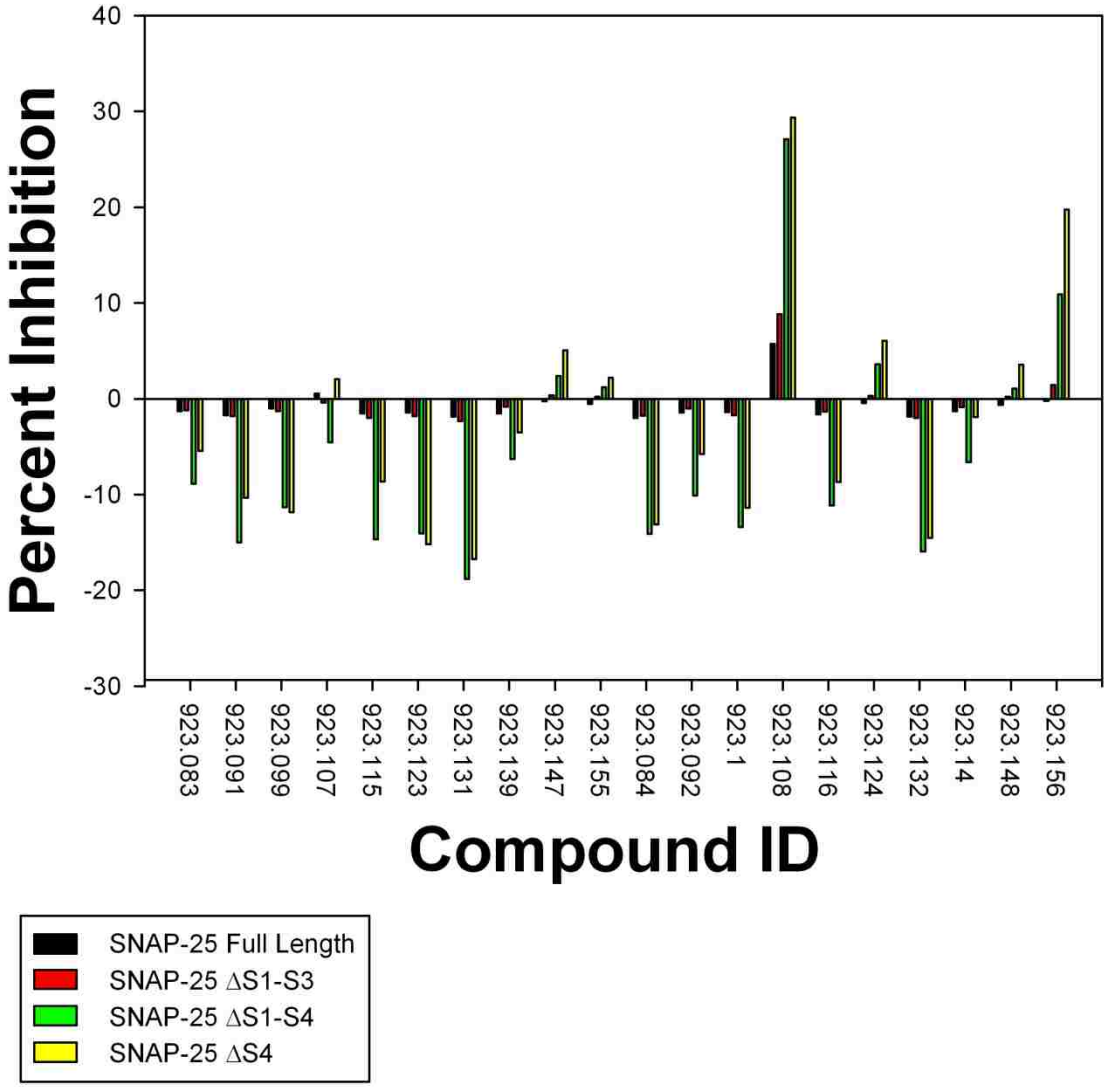

Scaffold Family 923 tetrapeptide mixtures plate 5

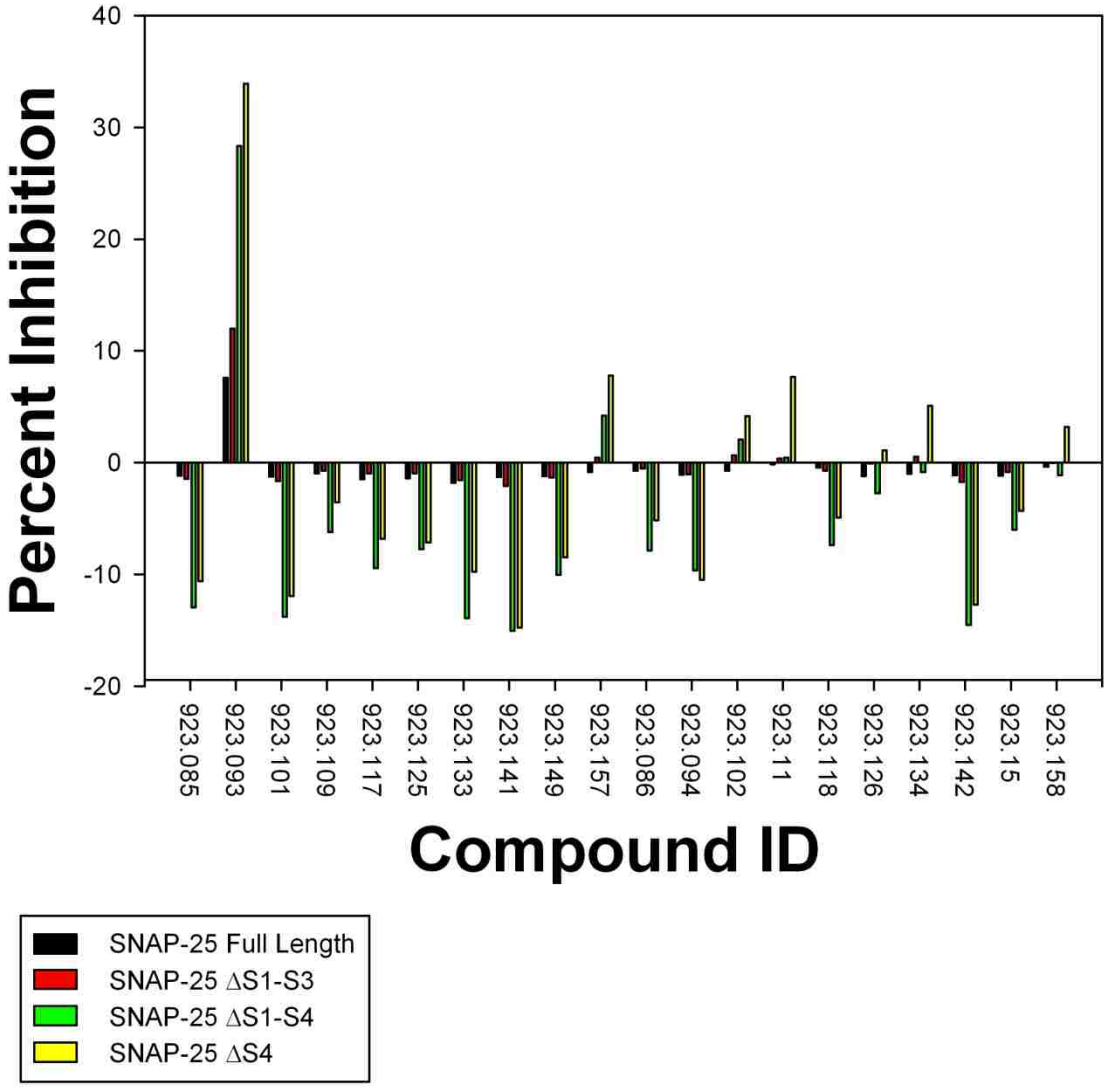

Scaffold Family 923 tetrapeptide mixtures plate 5

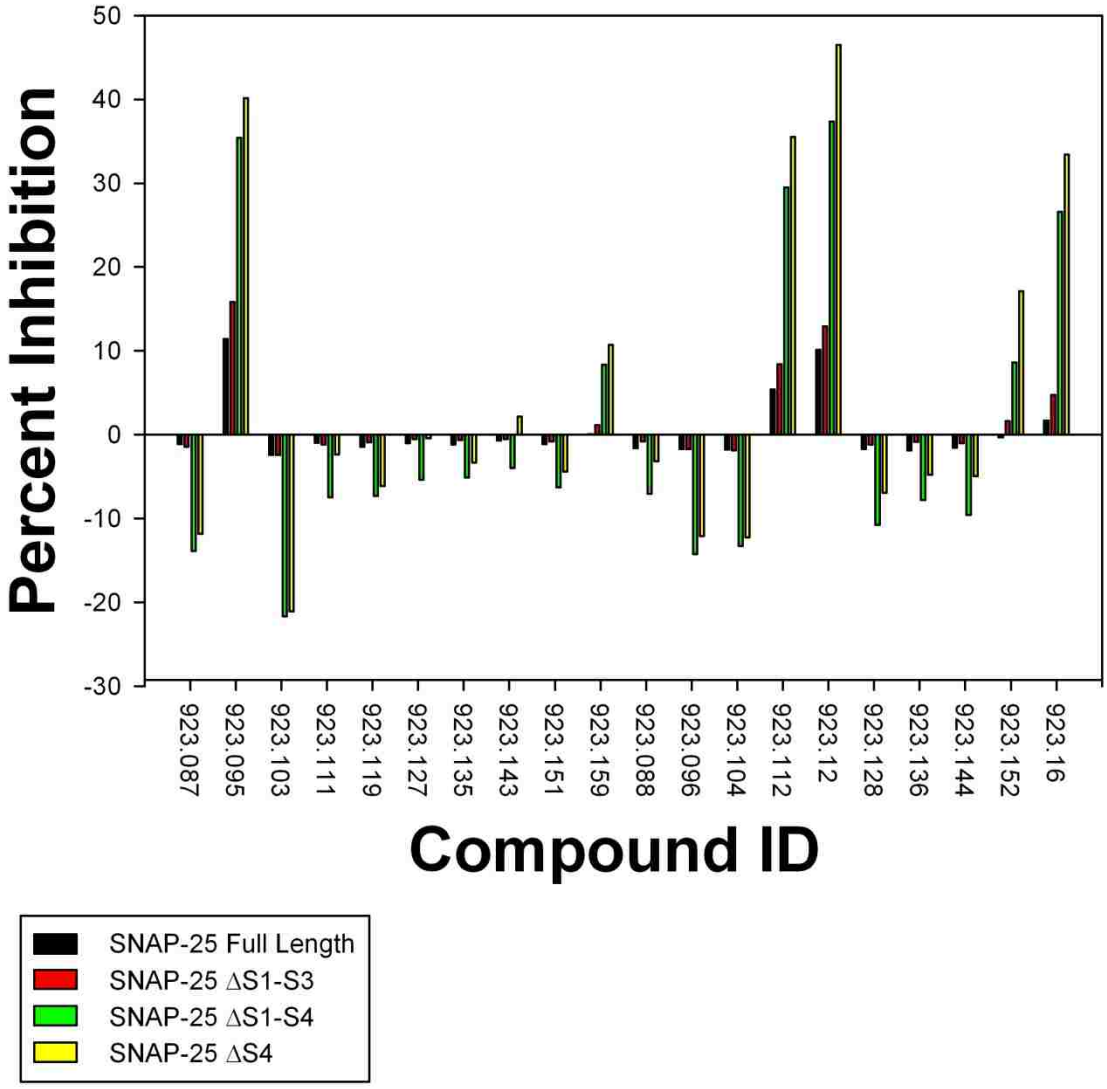

Scaffold Family 923 tetrapeptide mixtures plate 5

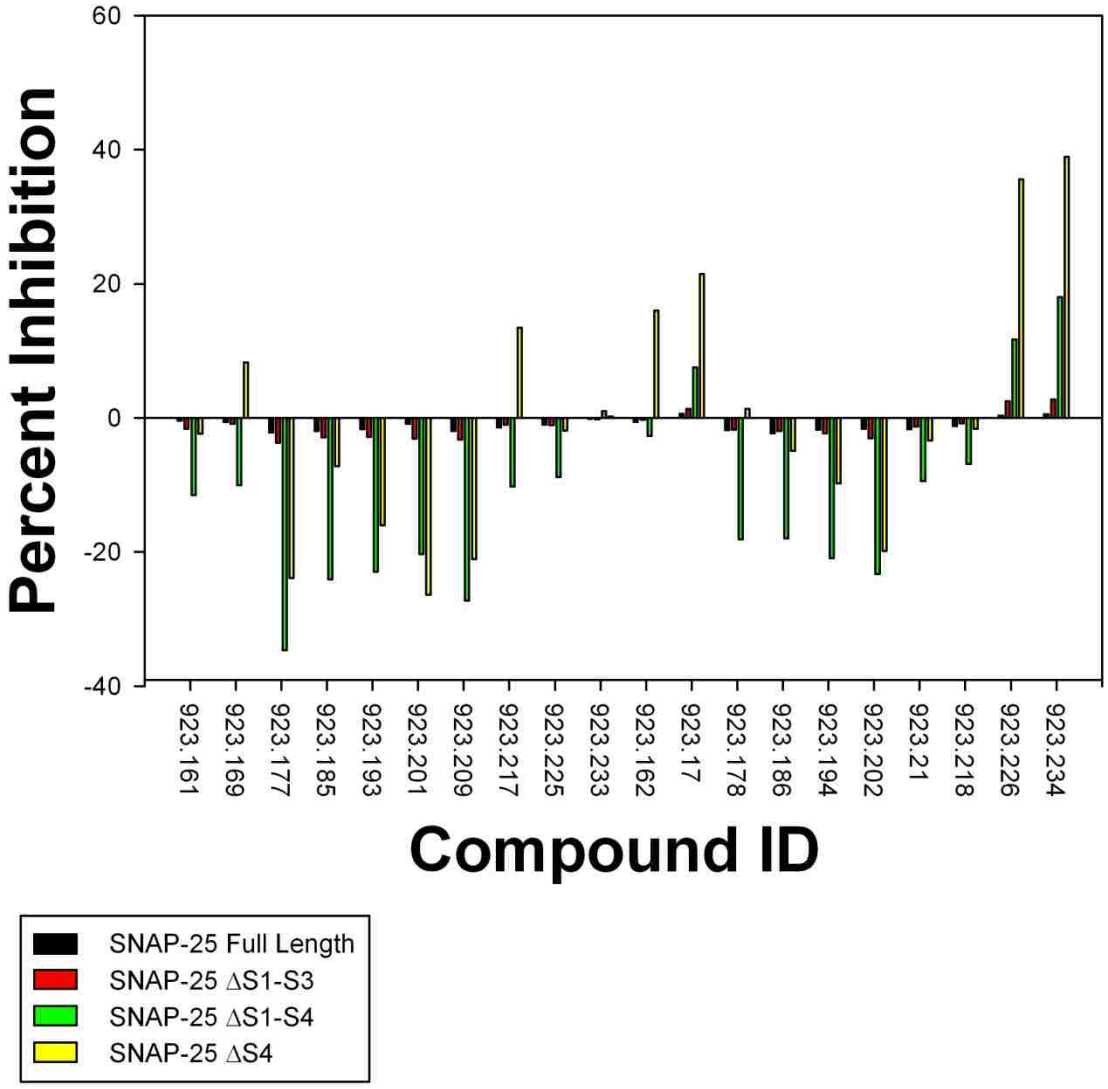

Scaffold Family 923 tetrapeptide mixtures plate 6

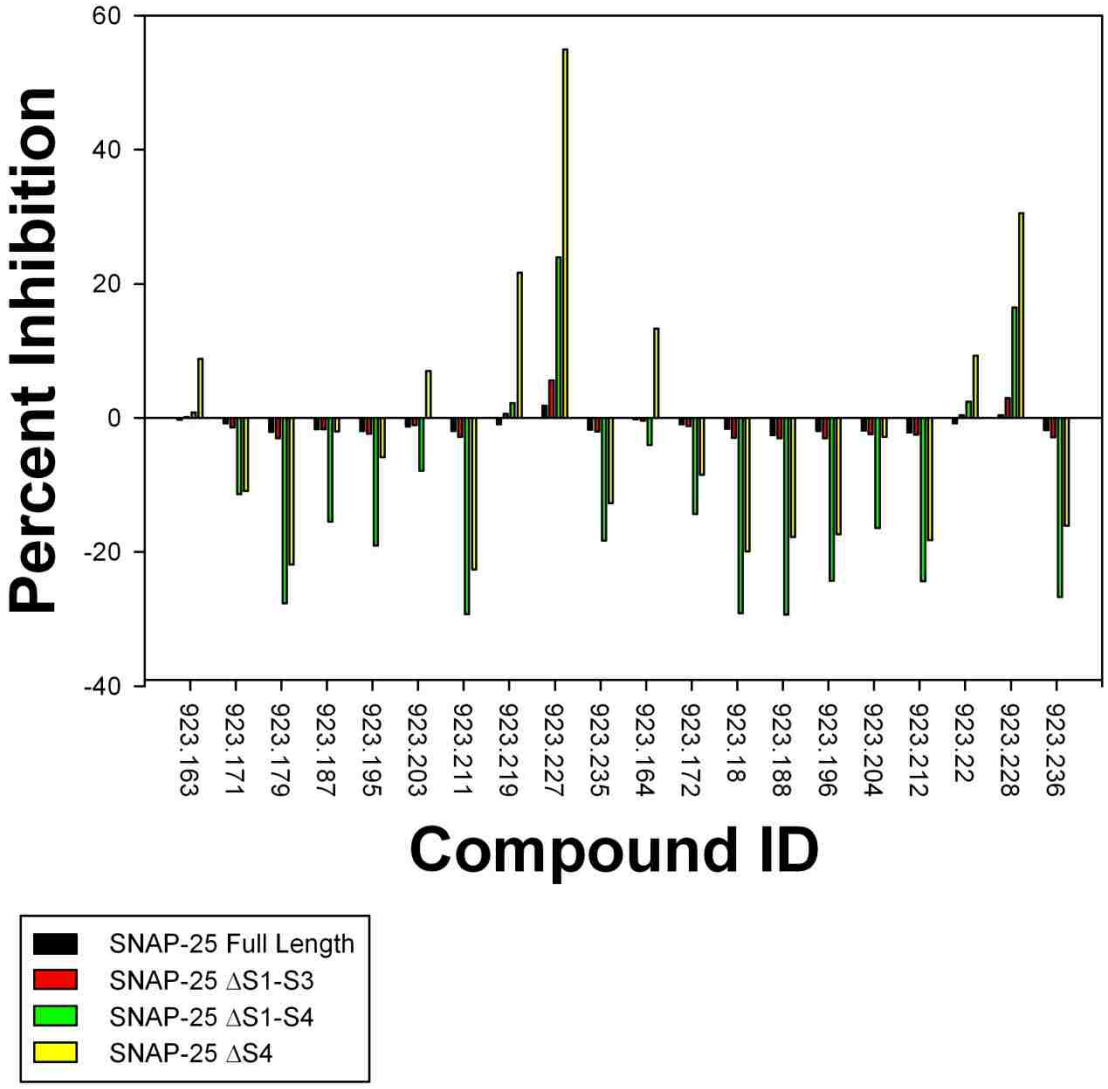

Scaffold Family 923 tetrapeptide mixtures plate 6

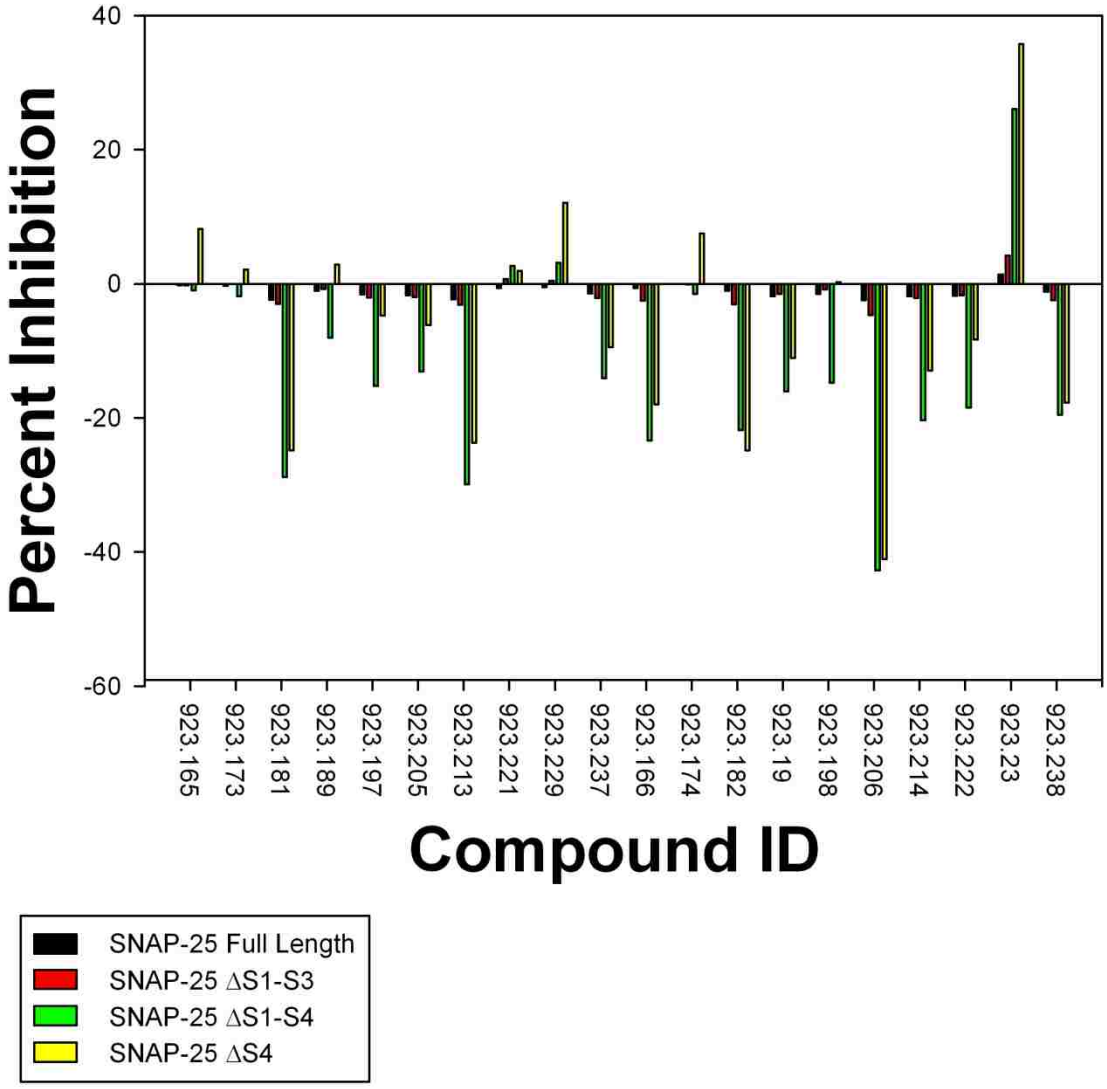

Scaffold Family 923 tetrapeptide mixtures plate 6

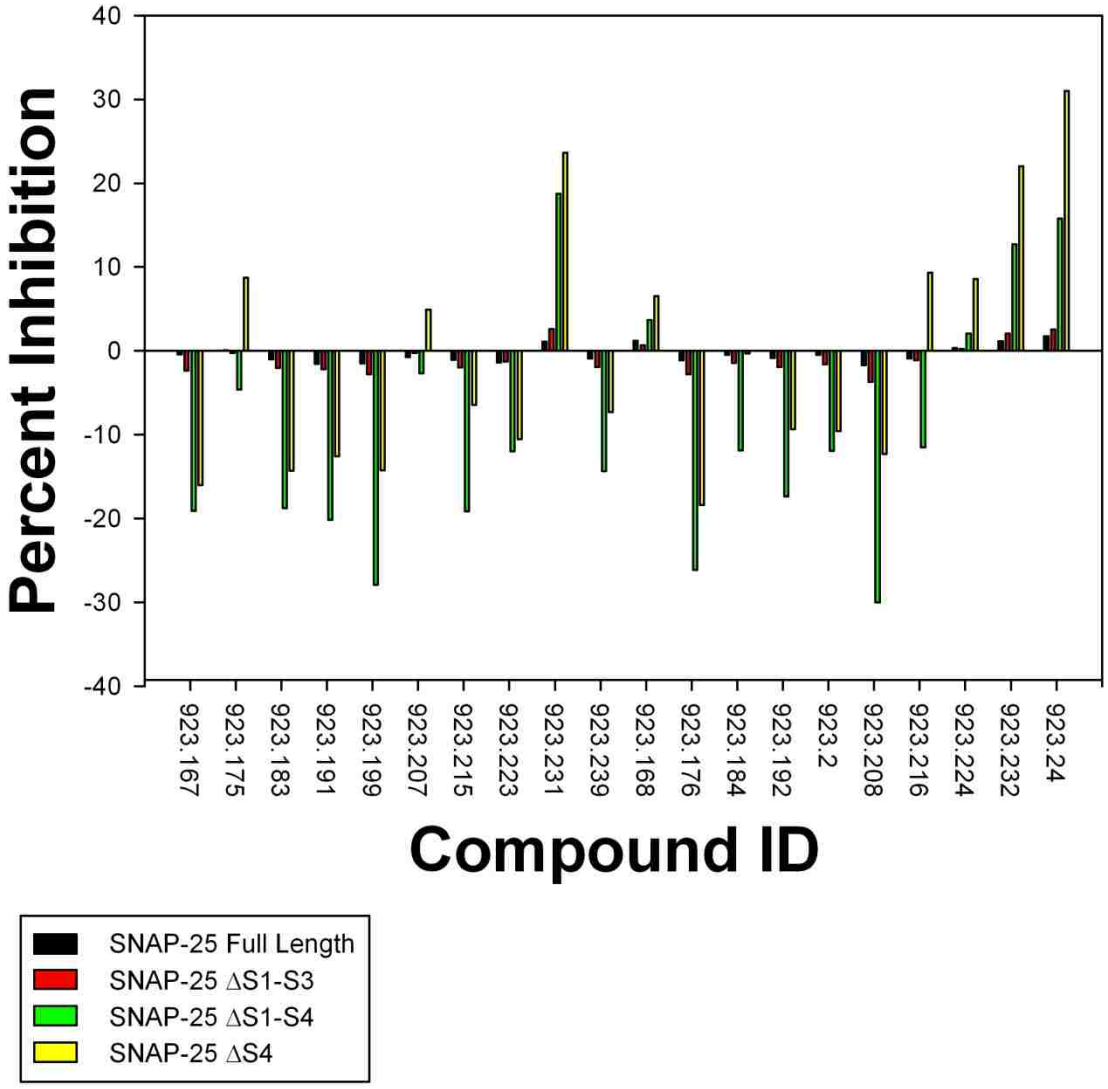

Scaffold Family 923 tetrapeptide mixtures plate 6

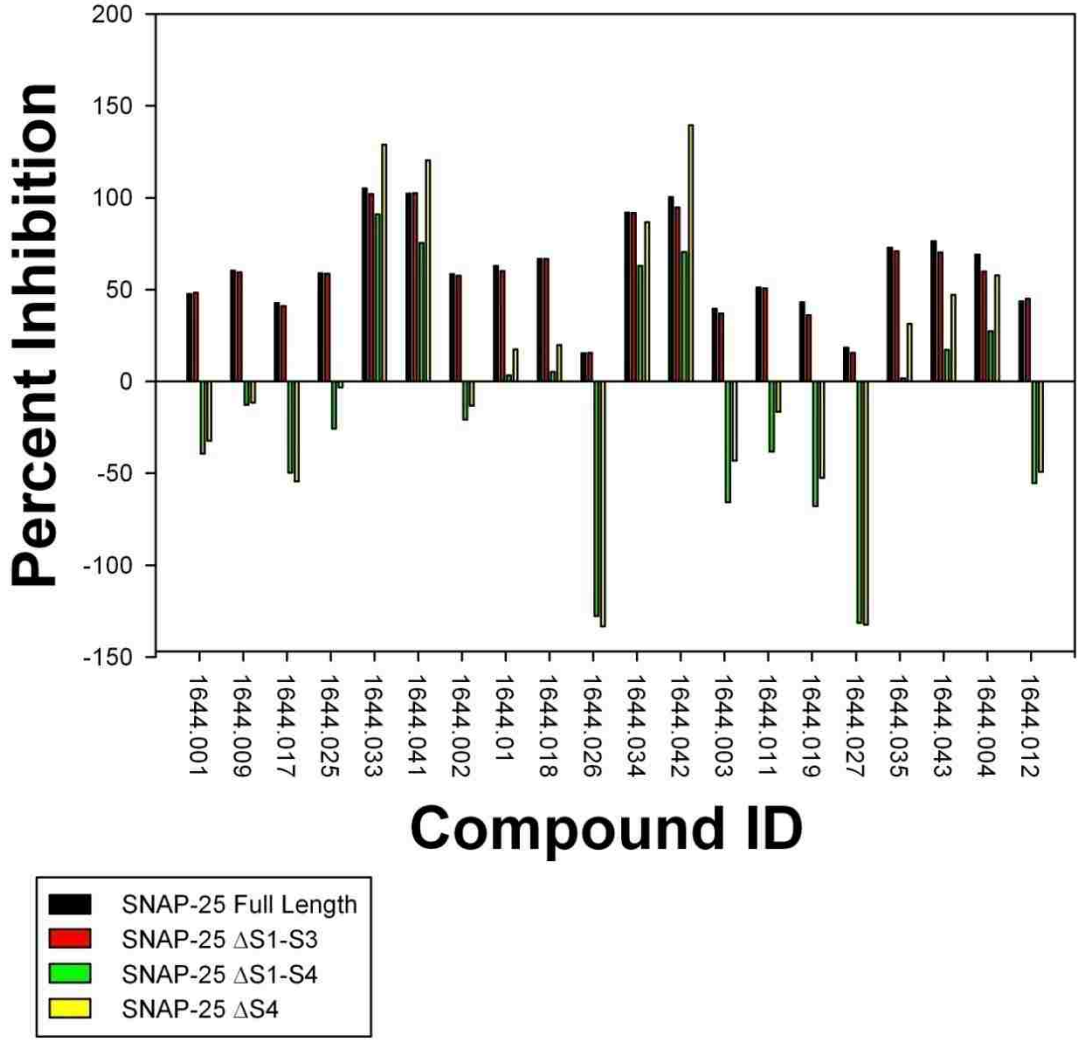

Scaffold Family 1644 individual compounds plate 9

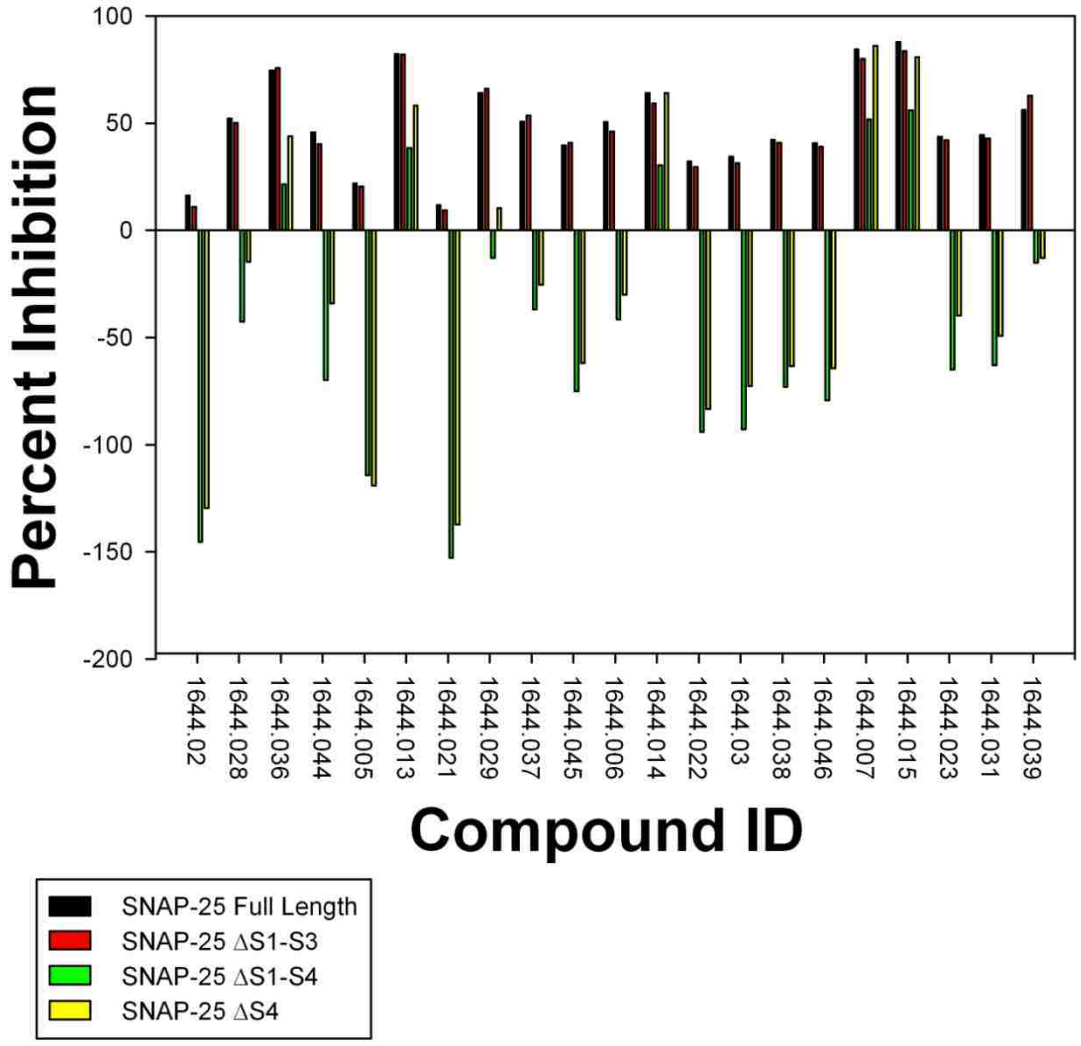

Scaffold Family 1644 individual compounds plate 9

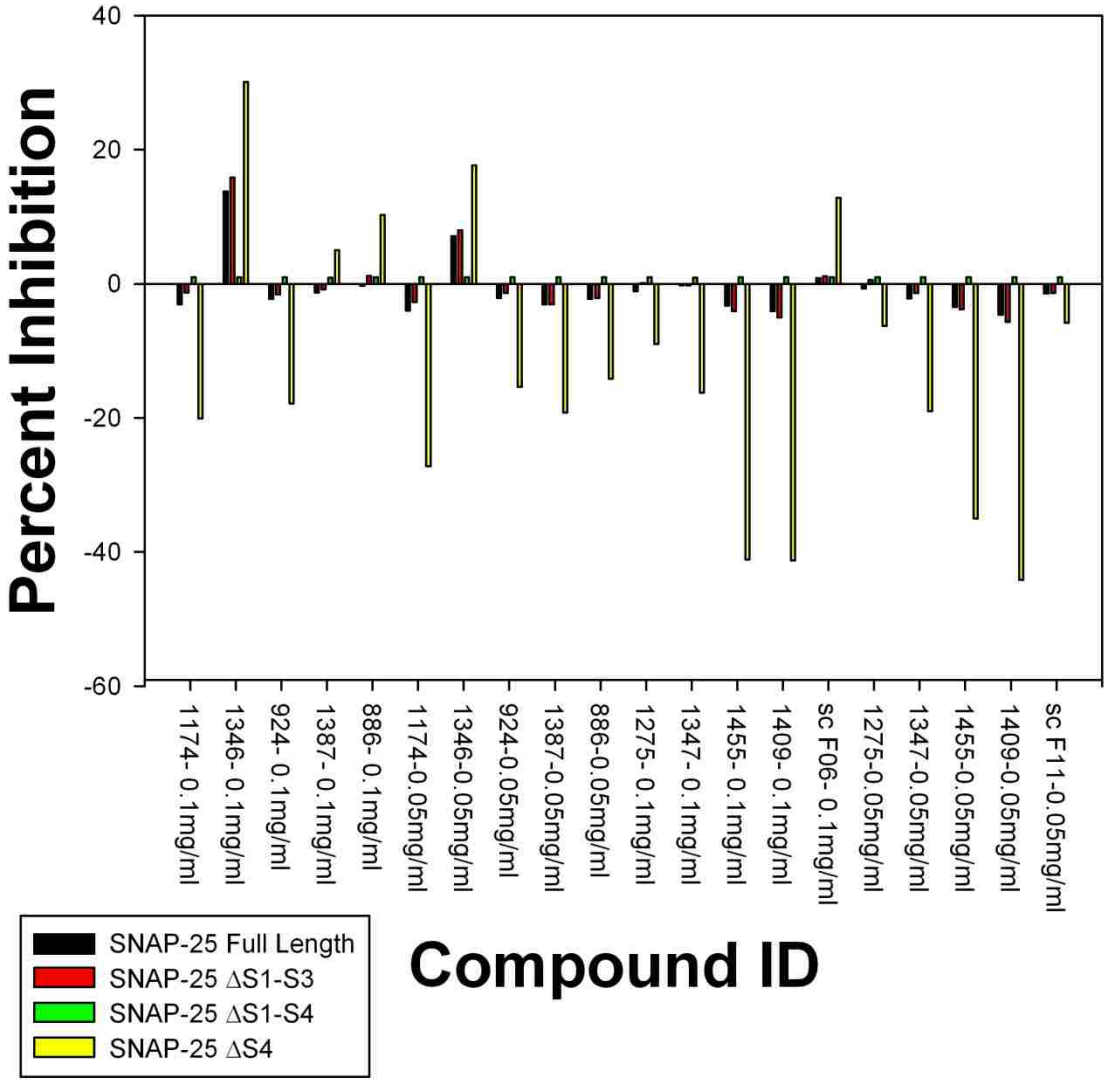

Scaffold plate with unmodified scaffold families.

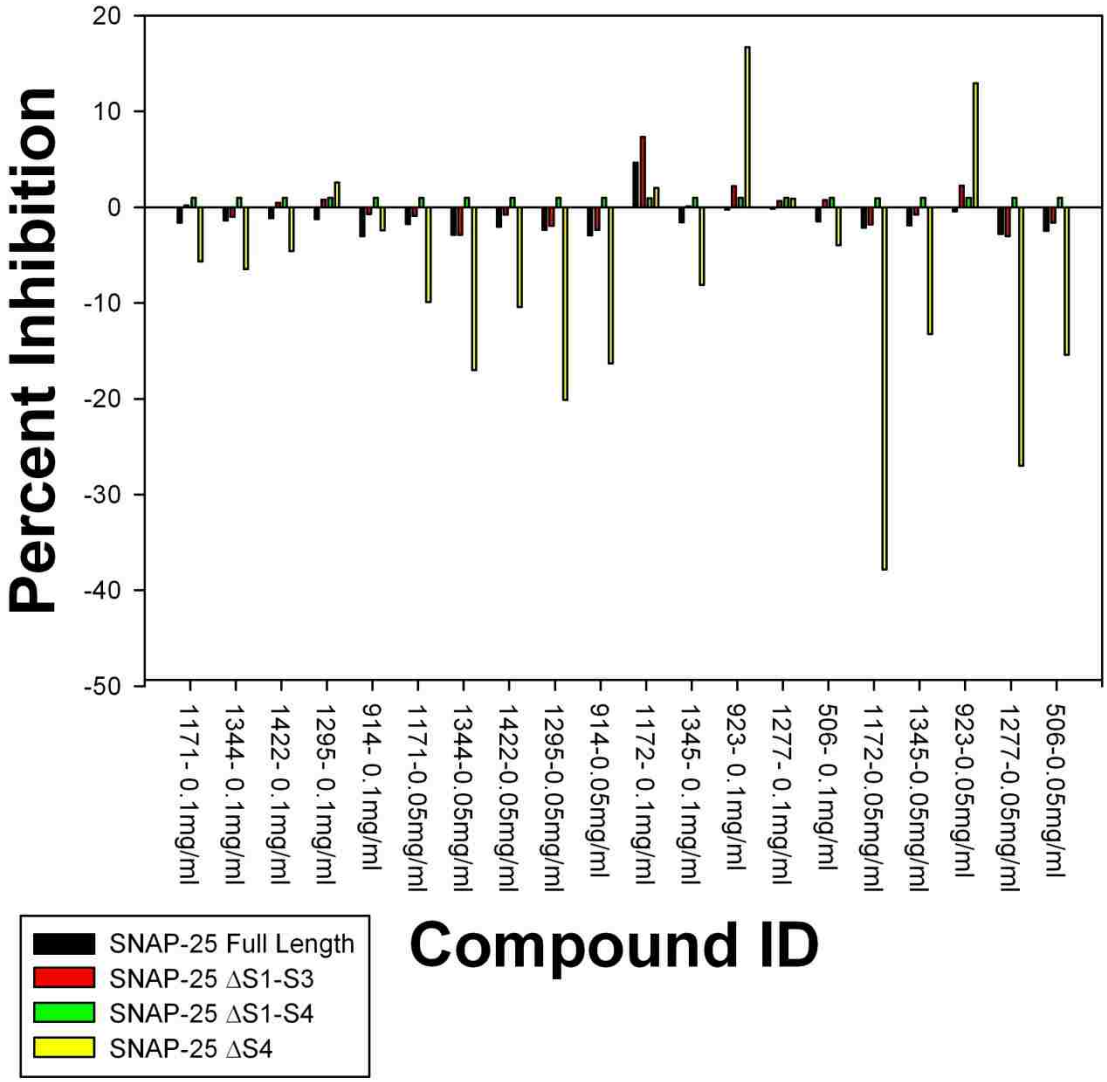

Scaffold plate with unmodified scaffold families.

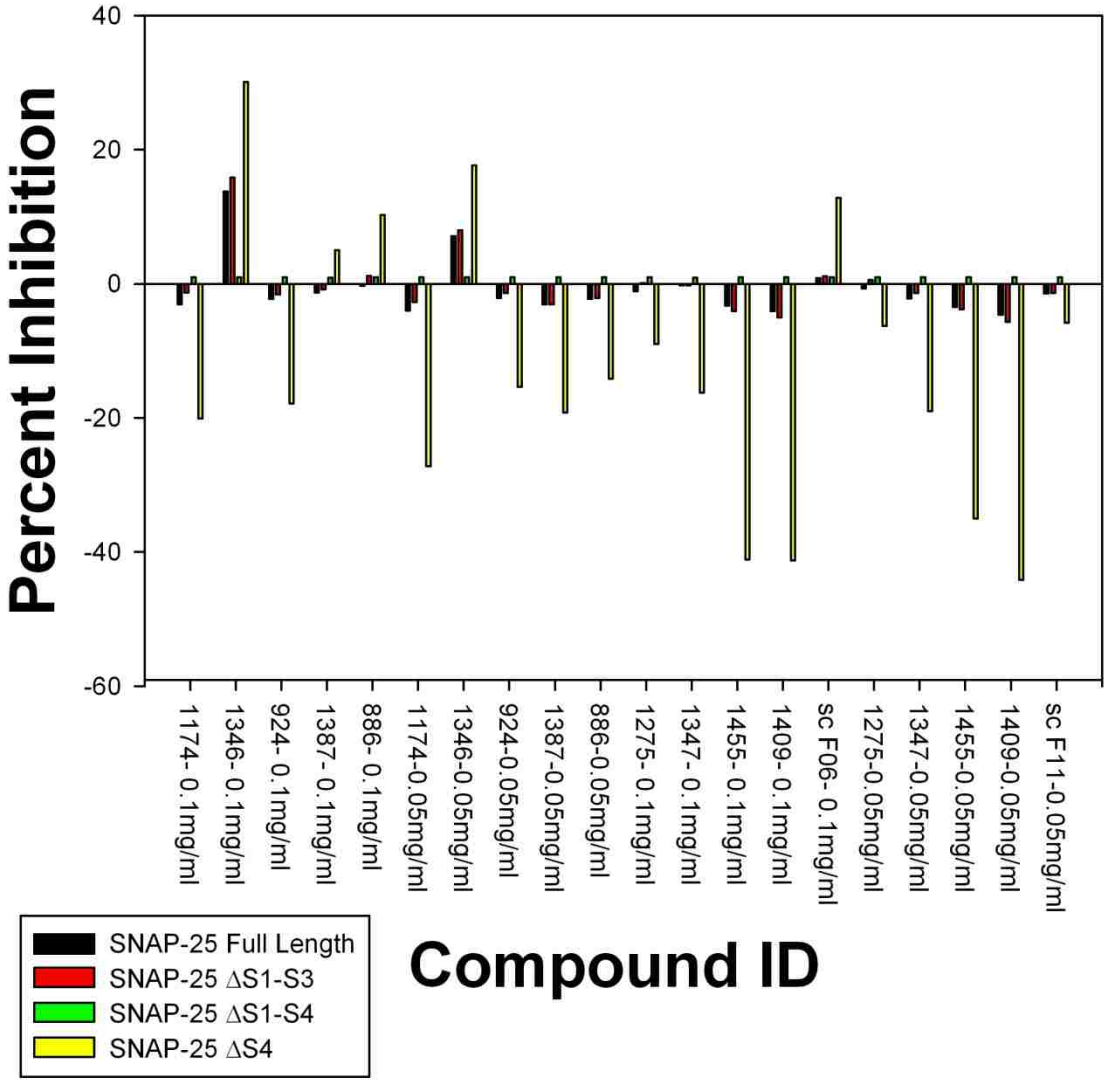

Scaffold plate with unmodified scaffold families.

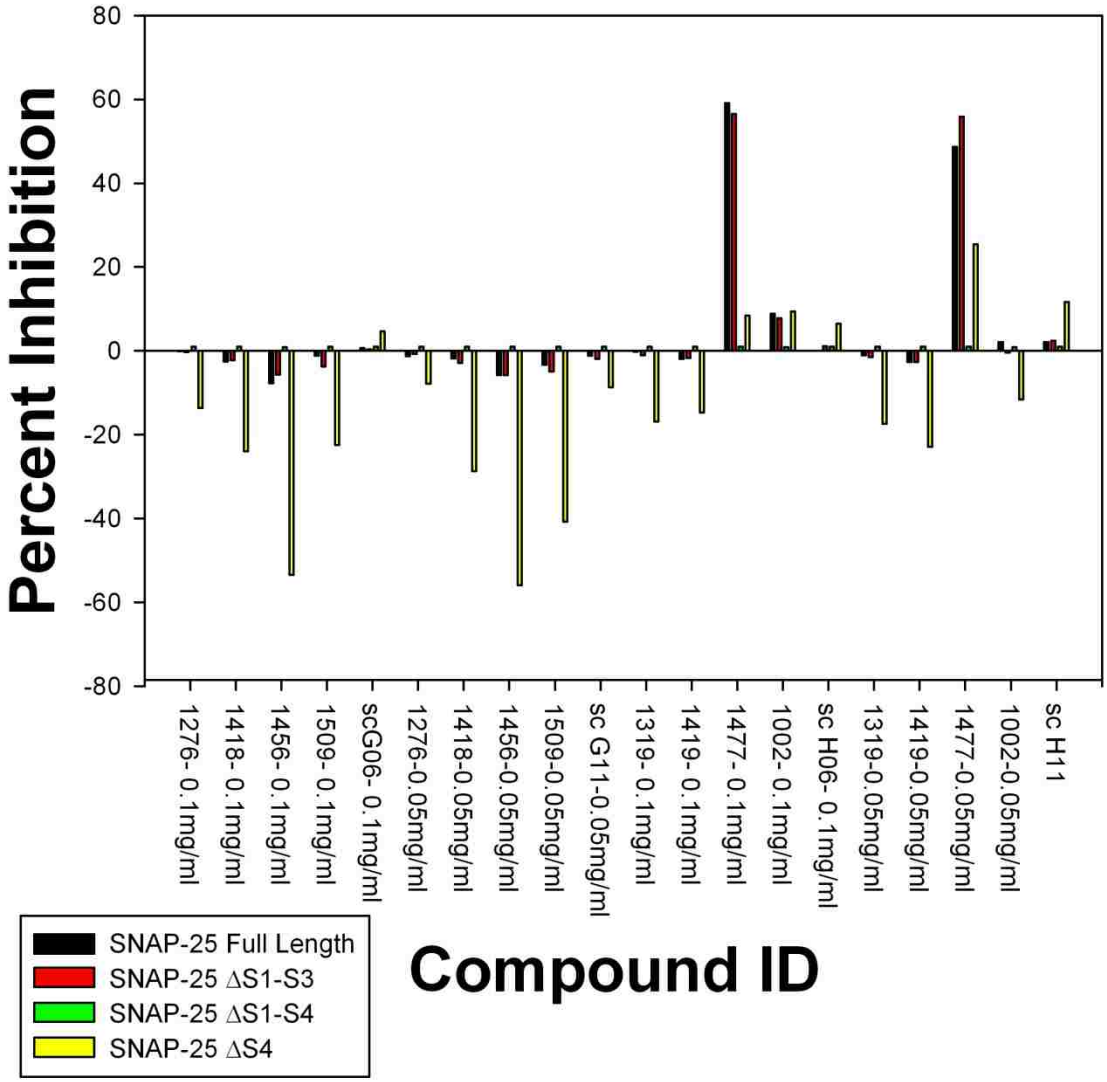

Scaffold plate with unmodified scaffold families.

Numerical Values for each plate

Plates 9 and 3 were combined into one plate. Compound ID numbers with m after them in that plate are mixture based samples from plate 3

	Plate 1					
Cmpd ID#	well	ΔS1-S3	control	ΔS1-S4	ΔS4	Full Length
empty	1	control	1.004603	control	control	control
1477.001	2	23.02654	0.954721	-41.1077	-13.7011	30.34138

1477.009	3	21.43724	0.951919	-30.5484	7.80619	27.46218
1477.017	4	12.75453	0.910962	-87.2189	-60.7035	15.36169
1477.025	5	31.64588	0.944107	-60.0978	-26.9232	35.35905
1477.033	6	17.13617	0.904138	-99.2985	-54.3899	20.76293
1477.041	7	19.27982	0.922824	-62.0314	-28.2289	24.34758
1477.049	8	-5.47676	0.976512	-74.1911	-74.929	-0.31229
1477.057	9	20.96437	0.995464	-2.12878	21.23614	25.43756
1477.065	10	40.41832	0.943566	-46.8487	-10.4909	39.3892
1477.073	11	14.3897	0.860491	-116.544	-92.7674	19.10172
empty	12	control	0.989387	control	control	control
empty	13	control	0.996227	control	control	control
1477.002	14	5.178416	0.98126	6.006361	13.85502	7.497881
1477.010	15	2.042652	0.985048	1.745018	27.71215	2.748228
1477.018	16	11.22651	0.918184	-74.9892	-59.7003	18.79734
1477.026	17	14.3027	0.914173	-100.697	-92.8432	19.79912
1477.034	18	15.61091	0.903563	-77.1843	-63.3464	18.95806
1477.042	19	18.11404	0.923798	-59.3262	-28.9117	25.30943
1477.050	20	-1.01553	0.98886	-5.15647	-10.7987	-0.81902
1477.058	21	17.80597	1.000563	0.565929	27.01755	23.97347
1477.066	22	26.56003	0.930147	-43.553	-25.7514	29.07649
1477.074	23	-0.10528	0.820991	-135.178	-94.6167	3.903056
empty	24	control	0.997376	control	control	control
empty	25	control	1.001592	control	control	control
1477.003	26	18.71651	0.89507	-91.0624	-74.1884	24.41762
1477.011	27	26.33691	1.01929	24.06222	57.864	35.053
1477.019	28	10.38994	0.875047	-126.84	-116.127	13.27558
1477.027	29	31.86838	0.989712	-12.5602	8.070228	35.97494
1477.035	30	16.53645	0.922978	-67.0155	-52.0596	20.98269
1477.043	31	21.8211	1.018152	25.26101	46.60443	23.534
1477.051	32	3.727861	1.004035	4.330956	4.173581	3.375761
1477.059	33	16.35756	0.948305	-44.7369	-29.6106	22.23023
1477.067	34	17.15638	0.960195	-42.8159	-10.9985	33.69973
1477.075	35	15.90113	0.888788	-112.106	-101.09	17.09458
empty	36	control	1.000294	control	control	control
empty	37	control	1.00907	control	control	control
1477.004	38	20.5182	0.986639	12.80737	43.97031	22.54706
1477.012	39	18.62669	0.906089	-96.6035	-80.136	21.45223
1477.020	40	12.07144	0.87253	-127.487	-114.687	16.49173
1477.028	41	18.90189	0.866597	-140.831	-120.369	22.59413
1477.036	42	21.84475	0.912981	-64.5364	-45.6407	25.51937
1477.044	43	53.53016	1.007217	33.76621	60.48312	55.43331
1477.052	44	23.25373	1.033283	37.88106	58.29823	27.41259
1477.060	45	12.61106	0.900277	-93.0411	-61.6367	16.82758
1477.068	46	12.96456	0.901865	-88.981	-69.1307	17.46172
1477.076	47	2.759971	0.903654	-93.7195	-83.4281	13.71994
empty	48	control	0.995754	control	control	control

empty	49	control	1.004991	control	control	control
1477.005	50	14.03195	0.968695	-30.3952	-3.91501	20.55923
1477.013	51	12.97311	0.876151	-120.742	-102.641	17.23614
1477.021	52	16.17008	0.918448	-74.6235	-43.1325	19.50357
1477.029	53	10.68763	0.874105	-108.982	-88.1929	14.04231
1477.037	54	21.51159	0.943789	-43.8197	-9.70379	26.10555
1477.045	55	-0.18729	0.99596	2.873526	0.066333	-0.33214
1477.053	56	22.41021	0.994822	2.564153	27.22541	28.37018
1477.061	57	6.896358	0.867342	-111.249	-91.1537	9.994846
1477.069	58	25.95545	0.991811	-26.6875	21.45913	35.78318
1477.077	59	3.189799	0.964626	-36.3165	-18.6126	6.059668
empty	60	control	0.997644	control	control	control
empty	61	control	0.998084	control	control	control
1477.006	62	29.67286	1.001173	6.553746	43.34206	36.89762
1477.014	63	9.329826	0.858216	-119.735	-106.694	13.72068
1477.022	64	21.07086	0.933602	-48.4146	-13.338	24.68566
1477.030	65	6.117165	0.832675	-143.218	-135.512	9.573229
1477.038	66	39.8062	0.980163	-24.98	3.301508	47.93001
1477.046	67	11.70312	0.868759	-122.237	-110.869	16.13035
1477.054	68	32.49395	1.024117	16.67045	56.45269	39.01694
1477.062	69	20.09117	0.949056	-47.5377	-4.40594	25.1631
1477.070	70	13.93699	0.907505	-96.0764	-77.3727	19.2863
1477.078	71	6.516517	0.86003	-127.425	-111.349	10.95098
empty	72	control	0.98977	control	control	control
empty	73	control	0.993888	control	control	control
1477.007	74	49.30493	0.98589	-19.8245	23.12694	56.21959
1477.015	75	12.60817	0.878304	-94.157	-66.9935	20.07995
1477.023	76	0	0.945143	-59.836	-8.46915	43.95871
1477.031	77	19.05952	0.87194	-117.809	-91.4949	23.82916
1477.039	78	29.65742	0.982796	5.914935	28.2985	33.6822
1477.047	79	28.21882	1.001732	7.57897	49.17721	32.79863
1477.055	80	23.35389	0.868162	-98.2262	-67.4144	27.29546
1477.063	81	19.19878	0.924848	-70.9763	-45.5948	22.76695
1477.071	82	0	0.813657	-154.281	-138.187	10.33847
1477.079	83	24.96302	0.944538	-51.4761	-27.9786	31.00597
empty	84	control	1.002652	control	control	control
empty	85	control	0.996148	control	control	control
1477.008	86	16.45607	0.878088	-91.9423	-72.2895	20.23264
1477.016	87	-0.66733	0.80092	-134.897	-104.95	2.922044
1477.024	88	15.15017	0.909843	-62.5365	-29.0391	17.8288
1477.032	89	-4.66522	0.709137	-181.97	-150.625	-0.47509
1477.040	90	33.86945	0.924228	-73.5986	-39.8937	30.85127
1477.048	91	23.78667	0.998202	10.56904	39.48119	25.80499
1477.056	92	16.00441	0.955548	-36.9645	-2.64685	19.788
1477.064	93	21.89497	0.935943	-40.1514	-10.8037	25.84145
1477.072	94	-1.04714	0.785534	-172.149	-167.386	2.672197

1477.080	95	14.19056	0.922667	-56.9302	-41.5448	17.49611
empty	96	control	0.982477	control	control	control
	Plate 2					
	well	ΔS1-S3	control	ΔS1-S4	ΔS4	Full Length
empty	1	control	0.988369	control	control	control
1477.081	2	54.05166	1.000524	-30.4665	0	60.67453
1477.089	3	26.07121	0.974064	-23.3364	0	34.57713
1477.097	4	39.25946	0.99822	-53.174	0	44.11933
1477.105	5	32.29117	0.988344	-30.3098	0	39.95744
1477.113	6	28.65041	0.910245	-140.323	0	32.30301
1477.121	7	24.25192	0.938403	-102.502	0	31.08232
1477.129	8	20.46905	0.928168	-114.837	0	26.65582
1477.137	9	32.94806	0.969992	-68.4325	0	35.09942
1477.145	10	15.40093	0.883956	-178.864	0	19.60001
1477.153	11	27.28502	0.98874	-27.328	0	37.0505
empty	12	control	0.992824	control	control	control
empty	13	control	1.007461	control	control	control
1477.082	14	30.43023	1.006053	-33.2661	0	40.68845
1477.090	15	-1.03544	0.787894	-237.837	0	3.462704
1477.098	16	-6.0587	0.975781	-16.9975	0	-2.29136
1477.106	17	23.09987	0.98007	-44.2227	0	29.8521
1477.114	18	18.98007	0.944623	-90.2068	0	24.66496
1477.122	19	36.5078	0.954364	-66.961	0	42.32734
1477.130	20	12.90749	0.847941	-204.684	0	16.59866
1477.138	21	19.17931	0.96338	-54.2762	0	26.76599
1477.146	22	7.901442	0.964794	-25.1549	0	13.84869
1477.154	23	48.81655	1.037465	13.28777	0	56.46237
empty	24	control	0	control	control	control
empty	25	control	1.003135	control	control	control
1477.083	26	46.06715	0.989764	-123.412	0	52.30296
1477.091	27	-4.72792	0.978945	-14.9689	0	-1.53258
1477.099	28	29.07729	0.945377	-146.417	0	38.5288
1477.107	29	27.20261	0.919322	-141.037	0	30.52014
1477.115	30	36.32089	0.974786	-42.4742	0	41.57639
1477.123	31	55.91449	0.984364	-65.877	0	#VALUE!
1477.131	32	27.57484	0.920144	-130.559	0	30.05822
1477.139	33	57.45839	0.987822	-4.36625	0	62.04893
1477.147	34	34.72601	0.933278	-106.311	0	41.20751
1477.155	35	59.44089	1.018408	33.58082	0	65.29467
empty	36	control	0.989205	control	control	control
empty	37	control	1.002415	control	control	control
1477.084	38	31.89227	0.947934	-117.71	0	36.74248
1477.092	39	28.10555	0.908361	-148.043	0	34.61644
1477.100	40	25.26499	0.929693	-128.873	0	31.41392

1477.108	41	23.1003	0.948265	-79.7854	0	27.08002
1477.116	42	26.98024	0.96106	-59.1636	0	31.27174
1477.124	43	40.48276	0.927895	-121.377	0	41.65521
1477.132	44	9.583334	0.772414	-266.603	0	13.55453
1477.140	45	-6.9211	0.976228	-21.8961	0	-5.12898
1477.148	46	-3.48036	0.700819	-329.653	0	-0.25114
1477.156	47	32.90047	1.021937	-90.6524	0	49.62151
empty	48	control	0.988217	control	control	control
empty	49	control	0.997909	control	control	control
1477.085	50	40.49897	1.014136	-0.01265	0	47.64969
1477.093	51	27.03499	0.932395	-109.409	0	31.48914
1477.101	52	32.17468	0.95401	-73.7046	0	36.20238
1477.109	53	30.98743	0.977185	-36.6334	0	34.44624
1477.117	54	18.02147	0.884515	-179.354	0	21.4983
1477.125	55	46.04339	0.980288	-95.3663	0	51.00385
1477.133	56	19.09235	0.876759	-144.957	0	22.89045
1477.141	57	43.41619	0.965568	-116.771	0	46.8832
1477.149	58	19.74527	0.930005	-115.873	0	25.31317
1477.157	59	19.6631	0.967647	-77.0834	0	27.81248
empty	60	control	0.981001	control	control	control
empty	61	control	0.99685	control	control	control
1477.086	62	25.91092	0.989116	-13.7793	0	37.08727
1477.094	63	39.18878	0.962281	-112.083	0	47.88772
1477.102	64	34.18431	0.974716	-35.5679	0	40.38503
1477.110	65	31.82687	0.971805	-44.3448	0	38.78338
1477.118	66	7.736591	0.834658	-229.326	0	12.4635
1477.126	67	29.1322	0.948043	-103.162	0	33.6899
1477.134	68	24.86624	0.975548	-31.3913	0	32.74233
1477.142	69	23.2559	0.90528	-173.459	0	28.15406
1477.150	70	19.20072	0.908972	-126.788	0	22.41933
1477.158	71	21.8423	0.976856	-65.2989	0	28.81937
empty	72	control	0.987058	control	control	control
empty	73	control	0.992871	control	control	control
1477.087	74	41.18514	0.970356	-92.0127	0	47.97952
1477.095	75	24.51736	0.98118	-21.7646	0	31.21139
1477.103	76	5.639448	0.947521	-52.2307	0	12.39808
1477.111	77	29.89724	0.953256	-69.5783	0	36.36716
1477.119	78	14.68109	0.862526	-186.047	0	19.2474
1477.127	79	63.1356	1.033035	-71.6214	0	67.0984
1477.135	80	11.38383	0.853428	-194.04	0	14.95489
1477.143	81	43.19911	1.002539	-70.1009	0	52.24456
1477.151	82	22.35532	0.915423	-130.882	0	27.70638
1477.159	83	35.2617	1.014013	-5.34281	0	42.36441
empty	84	control	0.990969	control	control	control
empty	85	control	0.999358	control	control	control
1477.088	86	26.45704	0.944175	-71.5241	0	33.47985

1477.096	87	41.57287	0.952749	-93.8752	0	45.98102
1477.104	88	14.62415	0.970418	-43.0618	0	23.8478
1477.112	89	35.49719	0.976335	-29.3809	0	41.05722
1477.120	90	27.46784	0.923157	-120.232	0	33.11072
1477.128	91	13.1438	0.822999	-182.971	0	14.54707
1477.136	92	15.70932	0.894048	-155.26	0	21.23061
1477.144	93	39.28214	0.992486	-7.43208	0	43.68944
1477.152	94	30.08265	0.965172	-72.5325	0	36.3017
1477.160	95	27.67355	1.020419	4.638274	0	34.04273
empty	96	control	0	control	control	control

	Plate 4					
cmpd ID	well	ΔS1-S3	control	ΔS1-S4	ΔS4	Full Length
empty	1	control	0.96395	control	control	control
923.001	2	-1.12047	0.939908	-10.6497	5.252505	-1.80757
923.009	3	-1.00315	0.930058	-9.25437	-7.47813	-1.82943
923.017	4	2.836436	0.941457	13.93049	-9.02336	-0.0456
923.025	5	-2.7149	0.929534	-25.1213	-14.7813	-2.17943
923.033	6	-1.42383	0.957864	-16.3053	-14.6523	-0.43304
923.041	7	19.8329	0.972505	31.42242	-18.5898	15.8526
923.049	8	24.03715	0.927926	30.70216	-5.19875	19.26508
923.057	9	22.56539	0.946324	30.9335	-11.5359	18.42056
923.065	10	-1.42424	0.955795	-14.8715	-5.86739	-1.29544
923.073	11	-0.36417	0.972163	-9.0671	-4.16056	-0.50542
empty	12	control	0.981674	control	control	control
empty	13	control	0.995757	control	control	control
923.002	14	-2.07571	0.974487	-15.5758	-13.014	-1.54817
923.010	15	1.776055	0.942979	7.5868	9.676471	-1.30808
923.018	16	-0.72919	0.902773	-7.59228	-8.63391	-1.91311
923.026	17	-2.17891	0.942639	-20.9262	-19.8187	-2.11897
923.034	18	-2.79712	0.949006	-26.5782	-22.5105	-2.06372
923.042	19	-0.26151	0.956188	-6.45519	-2.52149	-1.48825
923.050	20	11.32501	0.930332	22.35111	-14.8542	6.86131
923.058	21	28.68306	0.951559	39.81008	4.603412	22.82554
923.066	22	7.653576	0.954064	41.11316	48.09042	0.587422
923.074	23	14.3245	0.959512	63.34675	74.59537	5.153318
empty	24	control	0	control	control	control
empty	25	control	0.997114	control	control	control
923.003	26	-2.19967	0.973596	-19.1282	-13.5552	-1.86823
923.011	27	0.668397	0.964573	4.32539	10.32115	-1.04179
923.019	28	-2.51593	0.944582	-22.0682	-20.3044	-1.92964
923.027	29	-2.70492	0.926822	-24.3742	-16.1044	-2.21264
923.035	30	18.39442	0.944831	27.46553	-18.3091	12.92765
923.043	31	-1.81987	0.954245	-19.3284	-12.4007	-1.61624
923.051	32	29.30431	0.925683	36.18094	-8.84666	26.88222

923.059	33	26.68474	0.942151	31.07287	-5.47962	21.91557
923.067	34	-1.76531	0.942923	-18.7678	-12.5283	-1.49606
923.075	35	22.34622	0.967243	32.25255	-7.10225	16.56911
empty	36	control	0.989284	control	control	control
empty	37	control	0.998978	control	control	control
923.004	38	-1.47392	0.959111	-12.7372	-6.87954	-1.68343
923.012	39	-2.35256	0.952319	-22.384	-13.811	-2.17544
923.020	40	-2.47101	0.937666	-23.2184	-16.8354	-2.31662
923.028	41	-3.19439	0.937951	-27.8467	-20.623	-2.62295
923.036	42	17.47325	0.919682	24.46741	-12.0292	11.76889
923.044	43	18.7729	0.943342	32.29518	-4.31231	13.46634
923.052	44	20.63595	0.954688	28.25363	-13.8552	15.55609
923.060	45	21.21315	0.930432	28.08506	-6.11215	16.86771
923.068	46	-1.26662	0.94717	-16.6266	-12.1734	-1.45735
923.076	47	-1.70435	0.960482	-17.1919	-17.7239	-1.74334
empty	48	control	0.987546	control	control	control
empty	49	control	1.003507	control	control	control
923.005	50	0.858257	0.957375	2.584242	5.281857	-1.0868
923.013	51	-2.01818	0.959062	-16.8414	-16.0204	-1.18811
923.021	52	-2.35625	0.953394	-18.1125	-17.1667	-1.61422
923.029	53	2.766313	0.952952	10.62673	-15.3872	-0.2362
923.037	54	2.859382	0.941553	10.54432	-13.0184	-0.38789
923.045	55	-2.20732	0.956116	-21.0959	-10.6598	-1.83315
923.053	56	10.58223	0.951397	20.39836	-13.9294	5.370328
923.061	57	-1.58953	0.942477	-16.6056	-7.93489	-2.05141
923.069	58	16.42221	0.946719	25.08787	-9.14775	11.2824
923.077	59	-1.41464	0.963835	-13.5664	-9.87203	-1.32261
empty	60	control	0.996852	control	control	control
empty	61	control	1.003098	control	control	control
923.006	62	0.878848	0.963144	3.730838	11.98013	-2.2449
923.014	63	13.40135	0.940597	57.5595	67.76211	3.95424
923.022	64	-2.16988	0.956919	-18.3402	-19.229	-1.9413
923.030	65	-0.09659	0.951085	-3.53234	-15.1454	-1.51851
923.038	66	2.220461	0.956041	13.77957	22.60207	-0.34735
923.046	67	-3.07222	0.967643	-25.1081	-12.6379	-2.07216
923.054	68	16.10605	0.925097	29.8093	-6.05148	11.38493
923.062	69	-2.09894	0.96237	-18.3175	-16.3832	-1.38307
923.070	70	15.40169	0.960119	26.14839	-9.95162	9.631284
923.078	71	9.328164	0.939603	48.4284	66.22989	2.93348
empty	72	control	0.997282	control	control	control
empty	73	control	1.000879	control	control	control
923.007	74	-1.7917	0.957324	-15.6827	-7.86773	-1.88326
923.015	75	-0.92631	0.961307	-11.6691	-9.13439	-1.09001
923.023	76	-2.00028	0.933947	-17.9686	-9.74791	-1.84631
923.031	77	-2.95444	0.940516	-27.0189	-19.8074	-1.67897
923.039	78	-2.5622	0.948386	-22.6241	-13.1404	-1.85512

923.047	79	-1.94361	0.967068	-16.3215	-4.22792	-1.45207
923.055	80	-1.96789	0.928534	-18.6962	-9.4667	-1.50962
923.063	81	-2.45242	0.961498	-24.216	-12.3463	-1.94218
923.071	82	-1.93684	0.95868	-18.5927	-16.3813	-1.55649
923.079	83	12.17758	0.963143	24.379	-5.47319	6.376705
empty	84	control	0.990346	control	control	control
empty	85	control	1.000667	control	control	control
923.008	86	3.709853	0.963065	21.57917	38.69054	0.004731
923.016	87	-0.52884	0.945829	-7.28336	5.000675	-1.68953
923.024	88	1.333656	0.942559	5.156742	14.49763	-1.91064
923.032	89	0.943085	0.935163	2.887721	10.52926	-0.87457
923.040	90	1.219109	0.929834	5.802267	17.14987	-0.64654
923.048	91	-2.55712	0.920664	-22.2223	-25.0487	-1.87193
923.056	92	-2.39878	0.938598	-22.5533	-11.5368	-2.12008
923.064	93	-0.64673	0.932964	-11.1206	-6.10168	-1.27138
923.072	94	-2.33025	0.946185	-22.3499	-13.3259	-2.37314
923.080	95	-0.73235	0.963374	-9.86639	-8.68417	-1.48548
empty	96	control	0	control	control	control

	Plate 5					
cmpd ID	well	ΔS1-S3	control	ΔS1-S4	ΔS4	Full Length
empty	1	control	0.960831	control	control	control
923.081	2	-2.11412	0.953426	-15.0013	-14.2504	-1.42145
923.089	3	-1.3374	0.945086	-12.7238	-10.4423	-1.694
923.097	4	-2.32104	0.923702	-16.7099	-15.3969	-2.29105
923.105	5	-2.3674	0.923187	-18.0089	-16.5228	-2.009
923.113	6	-2.32003	0.937434	-17.5035	-15.8179	-1.91349
923.121	7	-1.72348	0.946382	-13.7979	-12.0364	-1.9743
923.129	8	-2.15891	0.941525	-16.0077	-16.992	-1.62903
923.137	9	-1.12394	0.94411	-8.99674	-6.41497	-1.35373
923.145	10	-0.69771	0.948879	-5.77338	-1.61445	-0.54466
923.153	11	-1.5677	0.963765	-12.0455	-11.0947	-1.05884
empty	12	control	0.984775	control	control	control
empty	13	control	0.99498	control	control	control
923.082	14	-1.76897	0.980579	-12.4107	-13.5171	-1.09914
923.090	15	-0.7758	0.961035	-6.665	-4.20002	-1.24444
923.098	16	-0.16571	0.947248	-1.17194	4.284456	0.353661
923.106	17	-2.34691	0.930104	-17.5376	-16.408	-1.84241
923.114	18	-1.6396	0.910959	-11.412	-3.82049	-1.39427
923.122	19	-1.96529	0.963394	-13.686	-12.0292	-1.3401
923.130	20	-2.04788	0.942738	-15.9606	-16.1064	-2.18295
923.138	21	-0.89411	0.935165	-6.16202	-1.80257	-1.95205
923.146	22	1.167232	0.948867	6.730092	9.4619	-0.20916
923.154	23	-1.16849	0.964194	-9.24784	-7.30343	-0.98316
empty	24	control	0	control	control	control

empty	25	control	0.993578	control	control	control
923.083	26	-1.18951	0.950592	-8.88055	-5.42737	-1.28938
923.091	27	-1.79751	0.962564	-14.9848	-10.3116	-1.73352
923.099	28	-1.28414	0.938097	-11.3018	-11.8285	-1.01731
923.107	29	-0.39758	0.937614	-4.558	2.04922	0.533549
923.115	30	-2.0136	0.909333	-14.6623	-8.62993	-1.52998
923.123	31	-1.81755	0.964733	-14.067	-15.1881	-1.46201
923.131	32	-2.32322	0.945238	-18.8072	-16.7233	-1.88363
923.139	33	-0.81176	0.938085	-6.28311	-3.51959	-1.51786
923.147	34	0.36684	0.94873	2.393146	5.072756	-0.27184
923.155	35	0.195239	0.969026	1.19623	2.16965	-0.53293
empty	36	control	0.985612	control	control	control
empty	37	control	0.994492	control	control	control
923.084	38	-1.75237	0.969877	-14.1032	-13.1239	-2.0279
923.092	39	-1.04141	0.948214	-10.112	-5.7649	-1.45734
923.100	40	-1.69618	0.935645	-13.4106	-11.3798	-1.384
923.108	41	8.830498	0.933686	27.09336	29.33574	5.721909
923.116	42	-1.33428	0.953279	-11.1336	-8.69992	-1.63093
923.124	43	0.286551	0.94131	3.59676	6.069089	-0.45212
923.132	44	-1.98778	0.949352	-15.9229	-14.5464	-1.86196
923.140	45	-0.8588	0.947902	-6.61033	-1.92061	-1.31646
923.148	46	0.198184	0.963368	1.056655	3.541977	-0.63241
923.156	47	1.432165	0.944677	10.88687	19.72922	-0.22806
empty	48	control	0.988211	control	control	control
empty	49	control	1.007089	control	control	control
923.085	50	-1.42918	0.962989	-12.9754	-10.603	-1.15137
923.093	51	11.99326	0.961476	28.31317	33.90607	7.599566
923.101	52	-1.64118	0.944266	-13.8177	-11.939	-1.23887
923.109	53	-0.72272	0.930629	-6.22782	-3.55375	-0.98699
923.117	54	-0.98541	0.96213	-9.44015	-6.81236	-1.49105
923.125	55	-0.96485	0.959941	-7.73152	-7.14295	-1.39428
923.133	56	-1.58877	0.958769	-13.9435	-9.75952	-1.81609
923.141	57	-2.08412	0.974011	-15.0478	-14.7562	-1.28386
923.149	58	-1.31777	0.970438	-10.0283	-8.46923	-1.18884
923.157	59	0.429518	0.956461	4.206361	7.793578	-0.85763
empty	60	control	0.994562	control	control	control
empty	61	control	1.008325	control	control	control
923.086	62	-0.51605	0.975314	-7.87886	-5.16658	-0.71
923.094	63	-1.0616	0.966651	-9.65376	-10.4951	-1.06585
923.102	64	0.65945	0.957118	2.058745	4.140826	-0.70561
923.110	65	0.380923	0.925307	0.428723	7.664332	-0.15035
923.118	66	-0.71907	0.966449	-7.38318	-4.91584	-0.44744
923.126	67	-0.07196	0.967942	-2.75129	1.087465	-1.21117
923.134	68	0.536583	0.948987	-0.84733	5.075288	-1.01833
923.142	69	-1.75105	0.967197	-14.5354	-12.6949	-1.12684
923.150	70	-0.86108	0.956564	-5.99909	-4.3143	-1.18538

923.158	71	-0.04932	0.968093	-1.1368	3.196687	-0.3458
empty	72	control	0.999382	control	control	control
empty	73	control	1.004255	control	control	control
923.087	74	-1.46254	0.973685	-13.8718	-11.8227	-1.11881
923.095	75	15.83291	0.965172	35.41147	40.16345	11.40371
923.103	76	-2.43228	0.946116	-21.6711	-21.0936	-2.42568
923.111	77	-1.20034	0.915135	-7.47811	-2.35465	-0.96811
923.119	78	-0.89485	0.952175	-7.33165	-6.13472	-1.44957
923.127	79	-0.5501	0.955571	-5.35956	-0.44831	-1.00217
923.135	80	-0.64028	0.958715	-5.14063	-3.30926	-1.18463
923.143	81	-0.54922	0.944519	-3.9593	2.185758	-0.71687
923.151	82	-0.83038	0.972213	-6.30477	-4.41354	-1.15007
923.159	83	1.148155	0.958115	8.33195	10.69499	0.032548
empty	84	control	0.986422	control	control	control
empty	85	control	0.992424	control	control	control
923.088	86	-0.83006	0.972539	-7.02961	-3.17346	-1.59308
923.096	87	-1.73824	0.94294	-14.2753	-12.1045	-1.69963
923.104	88	-1.89306	0.941201	-13.2805	-12.2635	-1.79726
923.112	89	8.404841	0.94931	29.5131	35.5012	5.371814
923.120	90	12.92073	0.946682	37.34851	46.50904	10.10211
923.128	91	-1.17792	0.950776	-10.7409	-6.95306	-1.73801
923.136	92	-0.83499	0.951643	-7.80702	-4.77267	-1.8958
923.144	93	-0.9928	0.968357	-9.56828	-4.97798	-1.5457
923.152	94	1.593125	0.955327	8.610157	17.11683	-0.31112
923.160	95	4.751419	0.952527	26.60228	33.42511	1.686729
empty	96	control	0	control	control	control

	Plate 6					
cmpd ID	well	ΔS1-S3	control	ΔS1-S4	ΔS4	Full Length
empty	1	control	0.974294	control	control	control
923.161	2	-1.62303	0.943149	-11.4712	-2.38155	-0.41576
923.169	3	-0.875	0.941476	-10.0178	8.235878	-0.61984
923.177	4	-3.7285	0.953	-34.6717	-23.8633	-2.12723
923.185	5	-2.88766	0.959072	-24.1159	-7.1802	-1.93651
923.193	6	-2.84554	0.959939	-22.955	-16.0038	-1.67749
923.201	7	-3.12955	0.97154	-20.3018	-26.3416	-0.897
923.209	8	-3.19694	0.955523	-27.2221	-21.0366	-1.9456
923.217	9	-1.05096	0.943572	-10.2189	13.44664	-1.44061
923.225	10	-1.0883	0.951734	-8.84239	-1.87673	-1.00225
923.233	11	-0.24004	0.967895	1.021146	0.19699	-0.11827
empty	12	control	0.989903	control	control	control
empty	13	control	1.001411	control	control	control
923.162	14	-0.29881	0.962969	-2.67877	16.00769	-0.59474
923.170	15	1.309039	0.960793	7.536793	21.46332	0.618384
923.178	16	-1.78045	0.952476	-18.1127	1.306101	-1.8219

923.186	17	-1.97478	0.955829	-17.983	-4.89557	-2.30982
923.194	18	-2.30933	0.956682	-20.9095	-9.75813	-1.77827
923.202	19	-3.02839	0.966024	-23.2558	-19.8606	-1.63585
923.210	20	-1.26471	0.948286	-9.42567	-3.37939	-1.7019
923.218	21	-0.79122	0.938606	-6.86298	-1.60891	-1.18406
923.226	22	2.483484	0.93736	11.686	35.56068	0.309931
923.234	23	2.7696	0.934541	18.0395	38.90154	0.542547
empty	24	control	0	control	control	control
empty	25	control	0.99398	control	control	control
923.163	26	0.151108	0.953963	0.819928	8.769598	-0.28579
923.171	27	-1.40153	0.939466	-11.3661	-10.8968	-0.80797
923.179	28	-3.02411	0.946943	-27.6616	-21.8657	-2.08627
923.187	29	-1.66901	0.939389	-15.4795	-2.01895	-1.71795
923.195	30	-2.38629	0.960529	-19.0479	-5.85324	-1.95495
923.203	31	-1.09323	0.950838	-7.87382	6.987085	-1.31763
923.211	32	-2.83753	0.945777	-29.3012	-22.6165	-1.97386
923.219	33	0.570297	0.939333	2.235523	21.66534	-0.95985
923.227	34	5.577363	0.951855	23.9621	54.9269	1.785263
923.235	35	-2.00507	0.962808	-18.3228	-12.7329	-1.78143
empty	36	control	0.983083	control	control	control
empty	37	control	1.000064	control	control	control
923.164	38	-0.39779	0.954554	-4.05857	13.27996	-0.18144
923.172	39	-1.21389	0.955084	-14.3555	-8.47686	-0.92496
923.180	40	-2.94498	0.943794	-29.139	-19.8992	-1.62806
923.188	41	-3.04543	0.948769	-29.3512	-17.7693	-2.53846
923.196	42	-3.00953	0.957878	-24.2954	-17.3394	-1.98081
923.204	43	-2.39087	0.971814	-16.4314	-2.86683	-1.90293
923.212	44	-2.51649	0.950732	-24.3318	-18.2487	-2.15752
923.220	45	0.398675	0.957275	2.4528	9.290464	-0.84422
923.228	46	2.937407	0.947337	16.45025	30.5498	0.425301
923.236	47	-2.88826	0.9737	-26.702	-16.0835	-1.80603
empty	48	control	0.987836	control	control	control
empty	49	control	0.998684	control	control	control
923.165	50	-0.21162	0.955896	-0.97558	8.179882	-0.19519
923.173	51	-0.06665	0.952869	-1.81355	2.126071	-0.32592
923.181	52	-2.98624	0.946693	-28.8365	-24.8189	-2.40275
923.189	53	-0.77191	0.945392	-8.02778	2.886212	-1.03121
923.197	54	-2.0353	0.957962	-15.2109	-4.74609	-1.57133
923.205	55	-1.99002	0.968283	-13.0577	-6.14842	-1.7043
923.213	56	-3.12482	0.95173	-29.9256	-23.7016	-2.2951
923.221	57	0.71898	0.946308	2.652074	1.933479	-0.65584
923.229	58	0.425802	0.950491	3.118199	12.05702	-0.51614
923.237	59	-2.12753	0.971572	-14.0852	-9.46307	-1.45988
empty	60	control	0.998284	control	control	control
empty	61	control	1.006021	control	control	control
923.166	62	-2.54893	0.962008	-23.3868	-18.0136	-0.66075

923.174	63	-0.09488	0.937541	-1.50137	7.504655	-0.00255
923.182	64	-3.04909	0.961526	-21.8505	-24.8799	-1.03623
923.190	65	-1.50278	0.947791	-16.0152	-11.0385	-1.85539
923.198	66	-0.86529	0.957506	-14.7367	0.238071	-1.5171
923.206	67	-4.66656	0.966802	-42.7563	-41.0362	-2.47091
923.214	68	-2.1508	0.954907	-20.3326	-12.9814	-1.83223
923.222	69	-1.69563	0.947769	-18.4576	-8.32304	-1.77918
923.230	70	4.169726	0.949285	26.03784	35.73483	1.344201
923.238	71	-2.4232	0.985452	-19.5629	-17.7101	-1.15403
empty	72	control	0.998275	control	control	control
empty	73	control	1.000444	control	control	control
923.167	74	-2.3735	0.96187	-19.0916	-16.0192	-0.40221
923.175	75	-0.25336	0.933068	-4.63287	8.744029	0.083042
923.183	76	-2.06526	0.959414	-18.7588	-14.3122	-1.02825
923.191	77	-2.21855	0.9533	-20.1903	-12.5674	-1.57302
923.199	78	-2.76093	0.959196	-27.8963	-14.231	-1.50082
923.207	79	-0.28503	0.961434	-2.65852	4.902627	-0.76872
923.215	80	-1.9674	0.963657	-19.1478	-6.4387	-1.07374
923.223	81	-1.2619	0.949491	-12.0084	-10.5464	-1.36315
923.231	82	2.573819	0.948608	18.71075	23.65613	1.071345
923.239	83	-1.92218	0.980645	-14.3434	-7.32357	-0.89099
empty	84	control	0.999717	control	control	control
empty	85	control	0.999396	control	control	control
923.168	86	0.673273	0.952221	3.668984	6.516898	1.182744
923.176	87	-2.76825	0.948313	-26.1232	-18.3881	-1.11367
923.184	88	-1.42887	0.938225	-11.8725	-0.31001	-0.49401
923.192	89	-1.92295	0.954275	-17.3985	-9.37404	-0.85577
923.200	90	-1.62029	0.975371	-11.9288	-9.55853	-0.4952
923.208	91	-3.72549	0.953578	-30.0228	-12.3092	-1.7304
923.216	92	-1.11381	0.942285	-11.5094	9.328141	-0.88173
923.224	93	0.225041	0.958817	2.051767	8.542778	0.311052
923.232	94	2.058982	0.961057	12.72355	22.00628	1.14918
923.240	95	2.551926	0.961707	15.78775	30.99395	1.757415
empty	96	control	0	control	control	control

	Plate 7					
cmpd ID	well	ΔS1-S3	control	ΔS1-S4	ΔS4	Full Length
empty	1	control	0.978475	control	control	control
1477.001	2	28.45259	0.958724	-0.7149	24.94182	32.86009
1477.009	3	45.75903	1.025113	30.37504	69.3114	51.30213
1477.017	4	8.90204	0.963276	-0.24352	14.02285	9.811991
1477.025	5	24.55957	1.017646	30.89676	62.90724	26.78732
1477.033	6	17.74362	0.995594	17.76488	42.90625	19.57779
1477.041	7	7.708962	0.986143	-1.40227	11.84284	7.394823
1477.049	8	18.28725	1.021624	33.9355	64.57955	23.8309

1477.057	9	8.042518	0.981923	7.526232	22.69491	6.740645
1477.065	10	35.47003	1.003411	19.24441	52.81497	35.8276
1477.073	11	17.67491	1.020919	20.62847	44.09485	20.04272
empty	12	control	0.986806	control	control	control
empty	13	control	0.998355	control	control	control
1477.002	14	13.56226	0.949071	-15.9268	1.133856	16.55745
1477.010	15	8.988218	0.994188	10.24739	29.85211	9.388259
1477.018	16	8.758373	0.991594	7.204383	26.7451	9.660732
1477.026	17	0.567759	0.966675	-7.26989	-7.42198	0.717465
1477.034	18	14.06486	1.010248	21.20339	48.44648	13.40321
1477.042	19	9.011033	0.991404	10.3868	35.36857	9.39976
1477.050	20	5.195007	0.979817	5.817338	16.72774	7.318915
1477.058	21	14.84158	1.000932	19.05808	34.55399	11.90852
1477.066	22	9.309136	1.009523	17.07663	36.65966	9.132492
1477.074	23	3.013129	0.93962	-23.9677	-6.21301	6.34474
empty	24	control	0	control	control	control
empty	25	control	0.994255	control	control	control
1477.003	26	12.82444	0.983105	5.866547	30.71505	15.52355
1477.011	27	58.70711	1.097372	56.50356	88.43163	60.82214
1477.019	28	16.78917	0.960788	-5.38166	18.35148	18.27649
1477.027	29	50.37618	1.077878	50.64468	82.99969	55.42259
1477.035	30	14.68196	0.987511	10.92769	36.23982	14.73949
1477.043	31	11.96446	1.000808	22.87658	48.91983	12.10783
1477.051	32	12.74238	0.990558	20.43575	42.06796	14.04502
1477.059	33	16.75557	0.998613	15.66062	36.56555	16.34099
1477.067	34	38.66206	1.067617	50.21026	77.71983	42.2858
1477.075	35	19.40094	0.962634	-5.7792	21.77593	21.35072
empty	36	control	0.989944	control	control	control
empty	37	control	0.996978	control	control	control
1477.004	38	10.53283	1.007004	9.684703	25.58889	11.52387
1477.012	39	13.66725	1.005847	17.89362	37.91569	15.36821
1477.020	40	16.97874	0.95802	-1.77023	17.91448	17.09454
1477.028	41	20.32568	0.997823	21.30598	45.92948	19.48196
1477.036	42	5.346593	0.968685	0.645248	17.7314	3.946312
1477.044	43	10.61802	0.989695	18.36351	28.19581	9.124152
1477.052	44	6.392545	0.983069	8.761745	25.02497	4.95534
1477.060	45	18.99369	0.969943	1.016105	20.62137	20.9069
1477.068	46	8.504743	0.996884	12.18179	33.84915	7.009539
1477.076	47	8.346646	0.997592	13.7435	27.86657	7.844261
empty	48	control	0.98716	control	control	control
empty	49	control	0.999309	control	control	control
1477.005	50	12.5955	0.985688	2.826607	22.96079	13.19183
1477.013	51	17.09139	1.000927	12.56348	28.967	17.00448
1477.021	52	-3.80174	0.971202	-26.4168	-33.3651	-2.05067
1477.029	53	9.500822	0.938867	-10.3307	7.086983	8.402315
1477.037	54	4.38951	0.983332	3.106305	13.20363	4.132357

1477.045	55	8.554646	0.989164	13.48878	36.69821	12.22203
1477.053	56	10.65262	0.993251	15.85921	34.65422	10.45708
1477.061	57	10.69726	0.960166	-3.15515	16.9	11.35243
1477.069	58	47.55692	1.076263	46.0045	83.99011	52.79242
1477.077	59	26.90494	0.985722	12.41787	42.87097	30.14288
empty	60	control	0.991373	control	control	control
empty	61	control	1.004633	control	control	control
1477.006	62	10.37636	1.010161	17.32569	29.07509	10.73432
1477.014	63	21.72429	0.975823	2.413445	22.14246	22.09647
1477.022	64	7.087214	0.988237	9.465104	26.43608	7.077128
1477.030	65	17.036	0.919654	-20.9735	3.983207	19.40909
1477.038	66	46.14106	1.05215	45.51693	72.99945	47.76013
1477.046	67	6.211984	0.936321	-21.0662	-1.24558	5.713129
1477.054	68	4.518597	0.989371	2.576922	15.61256	3.008863
1477.062	69	9.014674	0.995786	14.40399	32.43653	8.255674
1477.070	70	16.41357	0.991059	4.614282	28.06273	18.59359
1477.078	71	19.39854	0.974325	1.769669	29.41475	23.90439
empty	72	control	1.000685	control	control	control
empty	73	control	1.003103	control	control	control
1477.007	74	44.75164	1.054125	47.0461	76.31266	47.91939
1477.015	75	11.56648	1.002929	14.20604	35.44002	10.82939
1477.023	76	-3.76058	0.975721	-23.4415	-30.6222	-1.83684
1477.031	77	13.76564	0.996097	17.7262	39.44987	14.26185
1477.039	78	34.72627	1.04622	34.39093	65.14345	41.19545
1477.047	79	13.18667	1.022213	25.43587	43.84151	12.79555
1477.055	80	13.47702	1.006795	17.67377	43.02489	11.87833
1477.063	81	12.33068	0.99241	7.0747	36.47932	11.64716
1477.071	82	16.8955	0.906152	-35.6926	-8.97275	19.05502
1477.079	83	5.71983	1.007126	14.66375	23.03815	5.091132
empty	84	control	1.007771	control	control	control
empty	85	control	1.003368	control	control	control
1477.008	86	10.65213	1.013355	21.10026	38.87292	11.16488
1477.016	87	5.280515	0.930171	-20.5175	-1.20667	5.417612
1477.024	88	4.255219	0.985696	-1.23673	14.55977	4.411999
1477.032	89	6.572811	0.912831	-25.014	-4.63232	8.158633
1477.040	90	31.4433	1.049454	43.05727	68.6789	35.50839
1477.048	91	7.937621	0.994994	10.73929	19.93834	6.427496
1477.056	92	32.43567	1.04371	30.31094	58.04169	37.37802
1477.064	93	19.09649	1.022394	23.61052	47.92343	19.08149
1477.072	94	15.65969	0.920999	-35.2725	-10.649	19.09527
1477.080	95	10.83227	1.004639	10.05195	29.94715	10.66122
empty	96	control	0	control	control	control

cmpd ID	Plate 8 well	ΔS1-S3	control	ΔS1-S4	ΔS4	Full Length

empty	1	control	0.986862	control	control	control
1477.081	2	-2.44763	0.987077	-15.1745	0	0.98533
1477.089	3	6.188662	0.990959	-0.84984	0	7.884309
1477.097	4	31.47317	1.047347	22.46478	0	37.54732
1477.105	5	6.17975	1.000268	7.193113	0	5.494509
1477.113	6	5.183585	0.981023	-4.15779	0	5.51451
1477.121	7	7.398074	0.984218	-3.37719	0	8.091937
1477.129	8	10.79327	0.977488	-12.9147	0	11.38759
1477.137	9	9.307973	0.99909	10.33631	0	8.496059
1477.145	10	14.34895	0.989132	-1.07212	0	15.60044
1477.153	11	1.611699	0.996812	9.045449	0	1.548754
empty	12	control	0.989946	control	control	control
empty	13	control	1.002972	control	control	control
1477.082	14	4.364317	1.004035	-8.83332	0	6.508059
1477.090	15	6.527766	0.950568	-39.1734	0	9.211436
1477.098	16	43.59762	1.012845	13.59813	0	49.54335
1477.106	17	0.874956	0.970813	-25.2893	0	2.275889
1477.114	18	11.2973	0.988491	-26.434	0	14.2439
1477.122	19	1.920944	0.972913	-25.0727	0	2.193553
1477.130	20	8.866368	0.966134	-26.2819	0	9.925513
1477.138	21	3.677799	0.988779	-8.07325	0	4.787493
1477.146	22	8.719123	0.95424	-40.3481	0	9.546685
1477.154	23	36.55982	1.052107	56.04206	0	40.19211
empty	24	control	0	control	control	control
empty	25	control	1.004522	control	control	control
1477.083	26	54.13632	1.004886	1.562687	0	61.19376
1477.091	27	25.89311	0.999075	20.6662	0	28.71468
1477.099	28	12.62447	0.979012	-9.20038	0	13.55324
1477.107	29	12.01663	0.989845	-7.51304	0	13.80276
1477.115	30	8.708537	0.981385	-7.86529	0	8.801383
1477.123	31	52.71789	1.036319	27.24567	0	54.8951
1477.131	32	8.606281	0.979012	-4.06572	0	8.135596
1477.139	33	37.72763	1.007853	15.48635	0	40.80422
1477.147	34	10.18871	1.006215	4.875001	0	11.2902
1477.155	35	25.24323	1.039251	17.41605	0	31.08793
empty	36	control	0.985277	control	control	control
empty	37	control	1.002719	control	control	control
1477.084	38	14.22301	0.99923	-14.4795	0	18.97463
1477.092	39	15.0721	0.995774	4.588824	0	17.88405
1477.100	40	9.393631	0.983032	4.560895	0	9.191024
1477.108	41	28.28637	1.027806	30.62802	0	27.14873
1477.116	42	6.882541	0.984923	-4.69694	0	7.545192
1477.124	43	11.2945	0.978673	-1.83375	0	11.03453
1477.132	44	11.45677	0.908415	-48.261	0	13.57524
1477.140	45	5.839799	0.989701	5.007302	0	5.892339
1477.148	46	7.269891	0.936447	-37.2104	0	7.058513

1477.156	47	25.24119	1.033916	37.58288	0	30.61613
empty	48	control	0.970146	control	control	control
empty	49	control	0.986247	control	control	control
1477.085	50	61.46745	1.021921	43.52955	0	65.99124
1477.093	51	13.4384	0.999927	13.91758	0	15.61572
1477.101	52	16.37174	1.002304	15.20401	0	17.27618
1477.109	53	6.166806	0.988635	-0.28738	0	6.823479
1477.117	54	13.21016	0.982574	-6.35475	0	13.726
1477.125	55	56.91757	1.004019	6.669935	0	62.75488
1477.133	56	15.13432	0.952493	-26.3145	0	15.20872
1477.141	57	9.433436	0.991012	-0.33196	0	10.15773
1477.149	58	11.44704	0.993935	-6.21998	0	12.13544
1477.157	59	12.06605	0.992193	-3.96701	0	13.61852
empty	60	control	0.984679	control	control	control
empty	61	control	1.000867	control	control	control
1477.086	62	19.74804	1.012626	15.3014	0	26.00671
1477.094	63	7.896077	1.014077	6.530859	0	9.346012
1477.102	64	13.61939	1.001717	34.50639	0	13.60737
1477.110	65	4.620497	0.997455	-9.65943	0	5.63997
1477.118	66	20.03073	0.976963	-22.1936	0	20.31394
1477.126	67	7.449748	0.962839	-35.9536	0	9.895682
1477.134	68	12.81189	0.986657	-12.4203	0	14.97585
1477.142	69	10.96262	0.981477	-8.65094	0	11.73792
1477.150	70	10.12464	1.007381	7.244605	0	10.81571
1477.158	71	7.654162	0.99599	12.71384	0	6.931445
empty	72	control	0.987727	control	control	control
empty	73	control	0.997742	control	control	control
1477.087	74	16.26258	0.985956	-1.2505	0	20.28299
1477.095	75	8.235251	0.995341	1.363727	0	10.13561
1477.103	76	4.718191	0.986984	-3.54937	0	7.365281
1477.111	77	0.262881	0.973719	-3.04508	0	0.682394
1477.119	78	15.69576	0.972985	-18.6627	0	17.02963
1477.127	79	47.72188	1.038144	24.67544	0	51.48948
1477.135	80	15.18348	0.930656	-47.8729	0	17.4188
1477.143	81	34.68786	1.051543	43.69282	0	42.49791
1477.151	82	7.668613	1.019744	10.61696	0	9.844947
1477.159	83	8.359849	1.011227	6.933755	0	8.757967
empty	84	control	0.997707	control	control	control
empty	85	control	1.004931	control	control	control
1477.088	86	10.73174	0.998915	1.267411	0	13.94223
1477.096	87	31.01443	1.026087	19.19863	0	36.97513
1477.104	88	1.229297	0.969453	-56.9829	0	5.844312
1477.112	89	6.884486	0.992457	4.900574	0	8.463748
1477.120	90	11.55073	0.990319	14.70678	0	12.55155
1477.128	91	19.13387	0.996966	18.26407	0	21.94129
1477.136	92	16.17912	0.95994	-23.7478	0	19.91608

1477.144	93	14.41759	0.980517	0.538189	0	16.70035
1477.152	94	8.861581	0.995106	5.800819	0	10.5766
1477.160	95	13.56576	0.988074	25.47061	0	16.39145
empty	96	control	0	control	control	control
	Plates 9 and 3					
cmpd ID	well	ΔS1-S3	control	ΔS1-S4	ΔS4	Full Length
empty	1	control	0.97079	control	control	control
1477.161	2	10.40776	0.937973	-29.8583	-8.5098	15.37709
1477.169	3	12.36008	0.978238	-0.57933	19.75427	20.00382
1644.001	4	48.21155	0.929474	-39.3853	-32.1538	47.50255
1644.009	5	59.31047	0.885729	-12.7056	-11.6012	60.21266
1644.017	6	40.96297	0.91739	-49.6066	-54.4389	42.71646
1644.025	7	58.69622	0.914068	-25.6673	-3.21028	58.78712
1644.033	8	101.9832	1.16805	90.99354	128.768	104.966
1644.041	9	102.3442	1.150197	75.41355	120.2752	102.3183
1477.161m	10	20.90469	0.851794	-91.3109	-64.3585	28.84421
1477.169m	11	25.12452	0.905292	-39.9773	-4.05956	31.21441
empty	12	control	0.984553	control	control	control
empty	13	control		control	control	control
1477.162	14	1.413825	0.959605	-28.0402	-1.81746	5.000478
1477.170	15	1.468267	0.994258	-12.4762	-14.8964	4.022281
1644.002	16	57.34547	0.983633	-20.6485	-13.1639	58.48867
1644.010	17	60.0537	1.01183	3.284739	17.30835	62.96028
1644.018	18	66.53387	0.949571	5.091037	19.75427	66.5318
1644.026	19	15.62192	0.693484	-127.753	-133.252	15.31837
1644.034	20	91.63685	1.112845	62.85043	86.74556	91.75075
1644.042	21	94.60005	1.135843	70.27318	139.401	100.3975
1477.162m	22	7.194623	0.843849	-96.5601	-82.8728	12.40479
1477.17m	23	21.87035	0.942392	-15.4952	-9.29113	27.0506
empty	24	control	0	control	control	control
empty	25	control	0.999823	control	control	control
1477.163	26	6.751083	1.002696	3.364064	7.524629	11.73638
1477.171	27	10.7388	0.992292	1.328368	23.86479	19.71373
1644.003	28	36.96955	0.912471	-65.7306	-43.0246	39.56565
1644.011	29	50.6999	0.944207	-38.0253	-16.561	51.11496
1644.019	30	36.02254	0.802833	-67.8051	-52.5365	43.18402
1644.027	31	15.4738	0.707999	-131.373	-132.335	18.26585
1644.035	32	70.85148	1.003051	1.712246	31.3045	72.75989
1644.043	33	70.14031	0.979212	17.11121	46.99921	76.32179
1477.163m	34	8.639055	0.979703	-8.49947	11.22749	16.4563
1477.171m	35	20.21841	0.879312	-66.992	-44.6892	27.59314
empty	36	control	0.986317	control	control	control
empty	37	control	0.994945	control	control	control
1477.164	38	6.492324	0.98476	2.600475	21.11312	12.44079
1477.172	39	3.895808	0.994874	5.129796	28.75665	6.225743

1644.004	40	59.69608	1.064426	27.4268	57.6322	69.00111
1644.012	41	45.12137	0.920623	-55.2676	-49.1054	43.51643
1644.020	42	10.92898	0.562877	-145.38	-129.651	16.12231
1644.028	43	50.0011	0.967315	-42.6541	-14.6926	52.14967
1644.036	44	75.83938	1.031841	21.38042	43.77194	74.487
1644.044	45	40.16462	0.827097	-69.855	-34.1921	45.75762
1477.164m	46	21.20291	0.995989	10.9439	42.58295	33.15564
1477.172m	47	32.28854	0.94547	-27.4394	5.89401	40.54034
empty	48	control	0.982747	control	control	control
empty	49	control	1.000006	control	control	control
1477.165	50	4.047124	0.967545	-26.6892	-6.70932	6.63561
1477.173	51	6.04963	0.992079	2.874127	18.22557	8.257199
1644.005	52	20.36061	0.734408	-114.15	-119.154	21.75117
1644.013	53	81.99607	1.051983	38.47086	58.17574	82.25863
1644.021	54	9.227452	0.587474	-152.72	-137.261	11.62436
1644.029	55	65.95403	1.046368	-12.9262	10.34424	63.98597
1644.037	56	53.43037	0.949049	-36.8137	-25.3935	50.6239
1644.045	57	40.80887	0.777815	-75.1413	-61.8786	39.52627
1477.165m	58	10.01776	0.915781	-59.7038	-41.4619	16.64545
1477.173m	59	11.39378	0.948499	-18.5707	8.509795	17.25368
empty	60	control	0.990248	control	control	control
empty	61	control	1.005634	control	control	control
1477.166	62	26.78217	1.003341	19.32263	29.13034	36.65366
1477.174	63	4.841745	0.982702	-6.24184	1.002152	8.450358
1644.006	64	46.02418	0.899136	-41.623	-30.0815	50.5177
1644.014	65	59.10986	1.061055	30.24774	64.08674	63.96183
1644.022	66	29.43088	0.809064	-94.1027	-83.3484	32.05398
1644.030	67	31.29431	0.861047	-92.8172	-72.5795	34.36859
1644.038	68	40.87548	0.852224	-72.9729	-63.3733	42.13761
1644.046	69	39.04306	0.774119	-79.4107	-64.2906	40.53872
1477.166m	70	22.34637	0.902847	-56.5093	-28.7227	28.95892
1477.174m	71	-3.7885	0.984951	-40.4151	-46.048	-0.83598
empty	72	control	0.998476	control	control	control
empty	73	control	0.999532	control	control	control
1477.167	74	3.434885	0.983304	0.847671	9.834673	3.541078
SC dmf	75	-3.32508	0.982337	-31.4165	-24.9858	-2.1477
1644.007	76	79.9604	1.098183	51.79869	86.03216	84.40743
1644.015	77	83.67823	1.104215	55.95725	80.80059	87.76785
1644.023	78	42.07046	0.869073	-64.9806	-39.6614	43.67447
1644.031	79	42.91676	0.811299	-62.9866	-49.1734	44.41583
1644.039	80	62.76893	1.045849	-15.0638	-12.8921	56.21318
SC dmso	81	-5.14889	0.969958	-45.851	-51.5174	-2.71487
1477.167m	82	9.487734	0.986237	-8.64956	12.38252	13.38804
1477.175m	83	6.246286	0.987909	-2.35977	13.53754	11.64611
empty	84	control	0.993497	control	control	control
empty	85	control	0.997168	control	control	control

1477.168	86	-2.62224	0.972822	-39.4131	-41.1562	0.121328
SC dmf	87	-2.98656	0.981151	-24.6022	-24.9519	-1.98071
1644.008	88	75.47876	1.044658	26.82205	50.32839	77.64249
1644.016	89	80.89106	1.085246	64.49697	99.28094	89.35378
1644.024	90	61.56984	0.981443	-24.2459	23.69494	61.25882
1644.032	91	79.28081	1.117938	68.94807	93.43789	90.65576
1644.040	92	92.32735	1.118359	62.34649	98.90726	95.02832
SC dmso	93	-6.36826	0.981048	-55.3846	-53.3179	-3.03441
1477.168m	94	18.41254	0.983813	4.550488	31.13464	26.24311
SC dmf m	95	-2.98189	0.992045	-23.2094	-23.8308	-1.45365
empty	96	control	0	control	control	Control

scaffold plate

Cmpd ID		ΔS1-S3	control	ΔS1-S4	ΔS4	Full Length
Empty	1	control	0.999532	control	control	control
1169-0.1mg/ml	2	26.5173	0.938959	51.8423	75.71961	26.59221
1324-0.1mg/ml	3	1.339548	0.975341	-1.75969	9.150718	-0.13128
1420-0.1mg/ml	4	-2.6349	0.957823	-31.271	-22.945	-3.00746
1481-0.1mg/ml	5	-1.1127	0.981829	-4.75423	-1.35882	-0.88853
882- 0.1mg/ml	6	3.577971	0.967715	14.2799	26.63913	1.560792
1169-0.05mg/ml	7	5.454794	0.965323	20.98776	51.6711	4.057314
1324-0.05mg/ml	8	-2.60601	0.981143	-33.4906	-31.9562	-1.83049
1420-0.05mg/ml	9	-3.12037	0.957383	-29.0998	-27.361	-2.99489
1481-0.05mg/ml	10	-1.60348	0.969302	-9.66485	-2.81267	-1.00781
882-0.05mg/ml	11	-0.40574	0.974559	-4.6243	4.524865	-0.37807
Empty	12	control	0.997837	control	control	control
Empty	13	control	1.004094	control	control	control

1170-0.1mg/ml	14	17.59341	0.975787	48.91415	58.74407	14.0877
1343-0.1mg/ml	15	-0.0611	0.951952	-15.5205	2.994368	-1.44288
1421-0.1mg/ml	16	1.17811	0.937067	-9.51297	13.20712	0.469053
1433-0.1mg/ml	17	-1.72523	0.986824	-17.3609	-10.2224	-0.96339
531- 0.1mg/ml	18	5.706018	0.965042	14.70934	43.42125	2.962309
1170-0.05mg/ml	19	-0.11921	0.992633	4.60386	7.327439	-0.81814
1343-0.05mg/ml	20	-1.91177	0.964107	-21.8499	-15.6447	-2.89016
1421-0.05mg/ml	21	-0.7451	0.943646	-11.5303	5.717857	-2.25291
1433-0.05mg/ml	22	-3.71294	0.970422	-31.6039	-26.5897	-3.36155
531-0.05mg/ml	23	-0.96115	0.97933	-19.5995	-6.90513	-1.16913
Empty	24	control	0.996042	control	control	control
Empty	25	control	1.003099	control	control	control
1171-0.1mg/ml	26	0.142838	0.97013	-5.65247	4.289575	-1.63375
1344-0.1mg/ml	27	-0.99205	0.968769	-6.4646	-0.84374	-1.41141
1422-0.1mg/ml	28	0.464108	0.955503	-4.60238	7.440838	-1.16481
1295-0.1mg/ml	29	0.798575	0.969887	2.563032	21.27545	-1.26389
914- 0.1mg/ml	30	-0.73944	0.965916	-2.42435	5.753471	-3.0483
1171-0.05mg/ml	31	-0.92793	0.980775	-9.92342	1.112145	-1.73973
1344-0.05mg/ml	32	-2.8879	0.980025	-17.0243	-18.1653	-2.86969
1422-0.05mg/ml	33	-0.76356	0.960186	-10.433	3.952099	-2.0506
1295-	34	-1.96535	0.9533	-20.1152	-	-2.35022

0.05mg/ml			61		12.6375	
914-0.05mg/ml	35	-2.37404	0.963942	-16.2869	-12.8713	-2.95603
Empty	36	control	0.991011	control	control	control
Empty	37	control	1.002352	control	control	control
1172-0.1mg/ml	38	7.310353	0.911823	2.013995	23.44466	4.659316
1345-0.1mg/ml	39	0.076321	0.958138	-8.09808	-4.66147	-1.58758
923- 0.1mg/ml	40	2.217208	0.972021	16.69517	34.72712	-0.23786
1277-0.1mg/ml	41	0.640474	0.967817	0.884111	11.07784	-0.15471
506- 0.1mg/ml	42	0.753659	0.958796	-3.97382	10.29355	-1.47114
1172-0.05mg/ml	43	-1.81783	0.942627	-37.8256	-26.61	-2.15678
1345-0.05mg/ml	44	-0.76563	0.968299	-13.2715	-4.83422	-1.92042
923-0.05mg/ml	45	2.258132	0.960687	12.92897	26.00657	-0.45843
1277-0.05mg/ml	46	-3.00933	0.955032	-27.0155	-21.7747	-2.81335
506-0.05mg/ml	47	-1.59618	0.973192	-15.4053	-10.0359	-2.47256
Empty	48	control	0.997457	control	control	control
Empty	49	control	0.996406	control	control	control
1174-0.1mg/ml	50	-1.33121	0.941672	-20.064	-5.73658	-3.0983
1346-0.1mg/ml	51	15.84645	0.947347	30.08209	48.14285	13.78266
924- 0.1mg/ml	52	-1.56731	0.978696	-17.8383	-14.0538	-2.24697
1387-0.1mg/ml	53	-0.85936	0.922853	5.019192	12.97974	-1.30112

886- 0.1mg/ml	54	1.18668	1.003986	10.27152	10.35673	-0.33357
1174-0.05mg/ml	55	-2.71092	0.967124	-27.1982	-18.1318	-3.99516
1346-0.05mg/ml	56	7.974711	0.958385	17.67042	38.27886	7.093639
924-0.05mg/ml	57	-1.36493	0.969112	-15.403	-8.59292	-2.13909
1387-0.05mg/ml	58	-3.06893	0.944833	-19.2194	-17.2336	-3.02943
886-0.05mg/ml	59	-2.12235	0.979628	-14.1537	-18.5027	-2.24727
Empty	60	control	0.993143	control	control	control
Empty	61	control	0.995878	control	control	control
1275-0.1mg/ml	62	0.124519	0.950469	-8.96693	-0.34701	-1.1255
1347-0.1mg/ml	63	-0.25143	0.932828	-16.2589	-2.888285	-0.23388
1455-0.1mg/ml	64	-4.04364	0.967719	-41.1428	-40.0946	-3.24044
1409-0.1mg/ml	65	-5.02762	0.987552	-41.2703	-47.874	-4.09442
sc F06-0.1mg/ml	66	1.137978	1.001504	12.83702	12.78326	0.874831
1275-0.05mg/ml	67	0.541574	0.97157	-6.31575	-0.39069	-0.73305
1347-0.05mg/ml	68	-1.37677	0.944664	-19.0079	-11.5658	-2.2023
1455-0.05mg/ml	69	-3.78	0.961539	-35.0294	-32.4076	-3.4752
1409-0.05mg/ml	70	-5.70387	0.971079	-44.1254	-53.4918	-4.61627
sc F11-0.05mg/ml	71	-1.36939	0.984363	-5.80156	-10.7647	-1.42811

Empty	72	control	0.993125	control	control	control
Empty	73	control	1.000806	control	control	control
1276-0.1mg/ml	74	-0.27112	0.960038	-13.6673	-2.43387	-0.07933
1418-0.1mg/ml	75	-2.21739	0.943703	-23.9475	-23.9743	-2.53012
1456-0.1mg/ml	76	-5.66757	0.932456	-53.5173	-45.7175	-7.73592
1509-0.1mg/ml	77	-3.76098	0.954815	-22.5119	-14.3741	-1.21073
scG06-0.1mg/ml	78	0.320843	1.003551	4.633422	-1.81497	0.649175
1276-0.05mg/ml	79	-0.74397	0.971567	-7.8287	-5.91937	-1.22869
1418-0.05mg/ml	80	-2.85827	0.961031	-28.7059	-24.5673	-1.82545
1456-0.05mg/ml	81	-5.7786	0.946678	-55.8849	-57.2195	-5.80786
1509-0.05mg/ml	82	-4.88362	0.946708	-40.7529	-39.1868	-3.33248
sc G11-0.05mg/ml	83	-1.88431	0.983854	-8.66046	-13.6189	-1.09819
Empty	84	control	0.991516	control	control	control
Empty	85	control	0.997365	control	control	control
1319-0.1mg/ml	86	-1.02949	0.95562	-16.8208	-5.04092	-0.14006
1419-0.1mg/ml	87	-1.69681	0.946239	-14.7057	-4.71523	-1.88644
1477-0.1mg/ml	88	56.50049	1.010209	8.40824	52.98798	59.06453

1002-0.1mg/ml	89	7.778126	0.921559	9.387725	26.68214	8.853457
sc H06-0.1mg/ml	90	1.04409	1.005049	6.468006	2.92072	
1319-0.05mg/ml	91	-1.51001	0.959898	-17.3994	-4.63057	-1.01638
1419-0.05mg/ml	92	-2.70402	0.952955	-22.9119	-17.2368	-2.70599
1477-0.05mg/ml	93	55.8264	1.001862	25.41657	65.15101	48.66006
1002-0.05mg/ml	94	-0.41045	0.914934	-11.5875	0.636478	2.014901
sc H11	95	2.332363	0.98195	11.61794	22.01309	2.105061
	96	control	0.980341	control	control	control

List of Abbreviations.

ADAM- a disintigrin and metalloprotease

APP- Amyloid Precursor Protein

BACE- beta-site APP-Cleaving Enzyme

BoNT- *Clostridium botulinum* Neurotoxin

BoNTA-Botulinum Neurotoxin type A

BoNTALC-Botulinum Neurotoxin type A Light Chain

BoNTB- Botulinum Neurotoxin type B

BoNTBLC- Botulinum Neurotoxin type B Light Chain

BSA- Bovine Serum Albumin

CDC- Center for Disease Control

CFP- Cyan Fluorescent Protein

CMG2- Capillary Morphogenesis Protein 2

cAMP- Cyclic Adenosine Monophosphate

DMBA- 7,12-Dimethylbenz(a)anthracene

DMSO- Dimethyl Sulfoxide

DTT- Dithiolthreiotol

EDTA- Ethylenediaminetetraacetic Acid

ERK-Extracellular Signal-regulated Kinases

EF- Edema Factor

ET- Edema Toxin

GABA -Gamma-aminobutyric Acid

GFP/EGFP- Green Fluorescent Protein/ Enhanced Green Fluorescent Protein

HExxH- Zn^{2+} binding domain of metalloprotease consisting of amino acids histadine-glutamic acid-histadine-any amino acid-any amino acid-histadine.

HC- Heavy Chain

HTS- High Throughput Screening

IPTG- isopropyl-β-D-thiogalactopyranoside

JNK- c-Jun N-terminal Kinases

kDa- Kilodalton

LRP6- Low Density Lipoprotein Receptor-related Protein 6

LF- *Bacillus anthracis* Lethal Factor

LFIR- Lethal Factor Interacting Region

LT- *Bacillus anthracis* Lethal Toxin

MAPK- Mitogen Activated Protein Kinases

MKK –Mitogen Activated Protein Kinase Kinases

MMP- Matrix Metalloprotease

PA- Protective Antigen

PA63- Cleaved 63KD Protective Antigen

PA83- Un-cleaved 83KD Protective Antigen

PBS- phosphate buffered saline

PCR- polymerase chain reaction

PTI- photon technology international

SNARE- Soluble NSF Attachment Protein Receptor

SNAP-25- Synaptosome-Associated Protein of 25 Kilodaltons

SV2- Synaptic Vesicle Receptor Protein 2

TACE- Tumor Necrosis Factor-α Converting Enzyme

TB- Terrific Broth

TEM8- Tumor Endothelial Marker 8

TeNT- Tetanus Neurotoxin

TeNTLC- Tetanus Neurotoxin Light Chain

TNFα- Tumor Necrosis Factor Alpha

VAMP-2- Vesicle Associated Membrane Protein-2

YFP- Yellow Fluorescent Protein

References

1. Turk B. Targeting proteases: successes, failures and future prospects. *Nature Reviews Drug Discovery.* Sep 2006;5(9):785-799.
2. Southan C. A genomic perspective on human proteases as drug targets. *Drug Discovery Today.* 2001;6(13):681-688.
3. Diamond SL. Methods for mapping protease specificity. *Current Opinion in Chemical Biology.* 2007;11(1):46-51.
4. Hooper NM. Proteases: a primer. *Proteases in Biology and Medicine.* 2002;38:1-8.
5. Rossetto O, de Bernard M, Pellizzari R, et al. Bacterial toxins with intracellular protease activity. *Clinica Chimica Acta.* 2000;291(2):189-199.
6. Patick AK, Potts KE. Protease inhibitors as antiviral agents. *Clinical Microbiology Reviews.* Oct 1998;11(4):614-+.
7. Vitale G, Bernardi L, Napolitani G, Mock M, Montecucco C. Susceptibility of mitogen-activated protein kinase kinase family members to proteolysis by anthrax lethal factor. *Biochemical Journal.* 2000;352:739-745.
8. Chopra AP, Boone SA, Liang XD, Duesbery NS. Anthrax lethal factor proteolysis and inactivation of MAPK kinase. *Journal of Biological Chemistry.* 2003;278(11):9402-9406.
9. Rossetto O, Schiavo G, Montecucco C, et al. SNARE MOTIF AND NEUROTOXINS. *Nature.* 1994;372(6505):415-416.
10. Breidenbach MA, Brunger AT. Substrate recognition strategy for botulinum neurotoxin serotype A. *Nature.* Dec 16 2004;432(7019):925-929.
11. Overall CM, Kleifeld O. Tumour microenvironment - Opinion - Validating matrix metalloproteinases as drug targets and anti-targets for cancer therapy. *Nature Reviews Cancer.* Mar 2006;6(3):227-239.
12. Moayeri M, Leppla SH. The roles of anthrax toxin in pathogenesis. *Current Opinion in Microbiology.* 2004;7(1):19-24.
13. Guidi-Rontani C, Weber-Levy M, Labruyere E, Mock M. Germination of Bacillus anthracis spores within alveolar macrophages. *Molecular Microbiology.* Jan 1999;31(1):9-17.
14. Guidi-Rontani C, Levy M, Ohayon H, Mock M. Fate of germinated Bacillus anthracis spores in primary murine macrophages. *Molecular Microbiology.* Nov 2001;42(4):931-938.
15. Welkos S, Little S, Friedlander A, Fritz D, Fellows P. The role of antibodies to Bacillus anthracis and anthrax toxin components in inhibiting the early stages of infection by anthrax spores. *Microbiology-Sgm.* Jun 2001;147:1677-1685.
16. Welkos S, Friedlander A, Weeks S, Little S, Mendelson I. In-vitro characterisation of the phagocytosis and fate of anthrax spores in macrophages and the effects of anti-PA antibody. *Journal of Medical Microbiology.* Oct 2002;51(10):821-831.
17. Popov SG, Villasmil R, Bernardi J, et al. Effect of Bacillus anthracis lethal toxin on human peripheral blood mononuclear cells. *Febs Letters.* Sep 11 2002;527(1-3):211-215.

18. Pellizzari R, Guidi-Rontani C, Vitale G, Mock M, Montecucco C. Anthrax lethal factor cleaves MKK3 in macrophages and inhibits the LPS/IFN gamma-induced release of NO and TNF alpha. *Febs Letters.* Nov 26 1999;462(1-2):199-204.
19. Erwin JL, DaSilva LM, Bavari S, Little SF, Friedlander AM, Chanh TC. Macrophage-derived cell lines do not express proinflammatory cytokines after exposure to Bacillus anthracis lethal toxin. *Infection and Immunity.* Feb 2001;69(2):1175-1177.
20. Agrawal A, Lingappa J, Leppla SH, et al. Impairment of dendritic cells and adaptive immunity by anthrax lethal toxin. *Nature.* Jul 17 2003;424(6946):329-334.
21. Hoover DL, Friedlander AM, Rogers LC, Yoon IK, Warren RL, Cross AS. Anthrax Edema Toxin Differentially Regulates Lipopolysaccharide-Induced Monocyte Production of Tumor-Necrosis-Factor-Alpha and Interleukin-6 by Increasing Intracellular Cyclic-Amp. *Infection and Immunity.* Oct 1994;62(10):4432-4439.
22. Obrien J, Friedlander A, Dreier T, Ezzell J, Leppla S. Effects of Anthrax Toxin Components on Human-Neutrophils. *Infection and Immunity.* 1985;47(1):306-310.
23. Loving CL, Khurana T, Osorio M, et al. Role of Anthrax Toxins in Dissemination, Disease Progression, and Induction of Protective Adaptive Immunity in the Mouse Aerosol Challenge Model. *Infection and Immunity.* Jan 2009;77(1):255-265.
24. Young JAT, Collier RJ. Anthrax toxin: Receptor binding, internalization, pore formation, and translocation. *Annual Review of Biochemistry.* 2007;76:243-265.
25. Bradley KA, Mogridge J, Mourez M, Collier RJ, Young JAT. Identification of the cellular receptor for anthrax toxin. *Nature.* Nov 8 2001;414(6860):225-229.
26. Scobie HM, Rainey GJA, Bradley KA, Young JAT. Human capillary morphogenesis protein 2 functions as an anthrax toxin receptor. *Proceedings of the National Academy of Sciences of the United States of America.* Apr 29 2003;100(9):5170-5174.
27. Wei W, Lu Q, Chaudry GJ, Leppla SH, Cohen SN. The LDL receptor-related protein LRP6 mediates internalization and lethality of anthrax toxin. *Cell.* Mar 24 2006;124(6):1141-1154.
28. Turk BE. Manipulation of host signalling pathways by anthrax toxins. *Biochemical Journal.* Mar 15 2007;402:405-417.
29. Pannifer AD, Wong TY, Schwarzenbacher R, et al. Crystal structure of the anthrax lethal factor. *Nature.* Nov 8 2001;414(6860):229-233.
30. Duesbery NS, Webb CP, Leppla SH, et al. Proteolytic inactivation of MAP-kinase-kinase by anthrax lethal factor. *Science.* May 1 1998;280(5364):734-737.
31. Cummings RT, Salowe SP, Cunningham BR, et al. A peptide-based fluorescence resonance energy transfer assay for Bacillus anthracis lethal factor protease. *Proceedings of the National Academy of Sciences of the United States of America.* 2002;99(10):6603-6606.
32. Park JM, Greten FR, Li ZW, Karin M. Macrophage apoptosis by anthrax lethal factor through p38 MAP kinase inhibition. *Science.* Sep 20 2002;297(5589):2048-2051.

33. Turk BE, Wong TY, Schwarzenbacher R, et al. The structural basis for substrate and inhibitor selectivity of the anthrax lethal factor. *Nature Structural & Molecular Biology.* Jan 2004;11(1):60-66.
34. During RL, Li W, Hao BH, et al. Anthrax lethal toxin paralyzes neutrophil actin-based motility. *Journal of Infectious Diseases.* Sep 1 2005;192(5):837-845.
35. Kassam A, Der SD, Mogridge J. Differentiation of human monocytic cell lines confers susceptibility to Bacillus anthracis lethal toxin. *Cellular Microbiology.* Feb 2005;7(2):281-292.
36. Comer JE, Galindo CL, Chopra AK, Peterson JW. GeneChip analyses of global transcriptional responses of murine macrophages to the lethal toxin of Bacillus anthracis. *Infection and Immunity.* Mar 2005;73(3):1879-1885.
37. Paccani SR, Tonello F, Ghittoni R, et al. Anthrax toxins suppress T lymphocyte activation by disrupting antigen receptor signaling. *Journal of Experimental Medicine.* Feb 7 2005;201(3):325-331.
38. Fang H, Xu LX, Chen TY, Cyr JM, Frucht DM. Anthrax lethal toxin has direct and potent inhibitory effects on B cell proliferation and immunoglobulin production. *Journal of Immunology.* May 15 2006;176(10):6155-6161.
39. Reig N, Jiang A, Couture R, et al. Maturation modulates caspase-1-independent responses of dendritic cells to Anthrax Lethal Toxin. *Cellular Microbiology.* May 2008;10(5):1190-1207.
40. Bugge TH, Leppla SH. Anthrax target in macrophages unveiled. *Nature Genetics.* Feb 2006;38(2):137-138.
41. Boyden ED, Dietrich WF. Nalp1b controls mouse macrophage susceptibility to anthrax lethal toxin. *Nature Genetics.* Feb 2006;38(2):240-244.
42. Trombetta ES, Mellman I. Cell biology of antigen processing in vitro and in vivo. *Annual Review of Immunology.* 2005;23:975-1028.
43. Dalkas G, Papakyriakou A, Vlamis-Gardikas A, Spyroulias GA. Low molecular weight inhibitors of the protease anthrax lethal factor. *Mini-Reviews in Medicinal Chemistry.* Mar 2008;8(3):290-306.
44. Waterer GW, Robertson H. Bioterrorism for the respiratory physician. *Respirology.* Jan 2009;14(1):5-11.
45. Chen C, Baldwin MR, Barbieri JT. Molecular basis for tetanus toxin coreceptor interactions. *Biochemistry.* Jul 8 2008;47(27):7179-7186.
46. Chen S, Hall C, Barbieri JT. Substrate recognition of VAMP-2 by botulinum neurotoxin B and tetanus neurotoxin. *Journal of Biological Chemistry.* Jul 25 2008;283(30):21153-21159.
47. Abrahamian FM, Pollack CV, LoVecchio F, Nanda R, Carlson RW. Fatal tetanus in a drug abuser with "protective" antitetanus antibodies. *Journal of Emergency Medicine.* Feb 2000;18(2):189-193.
48. Abrahamian FM. Tetanus: An update on an ancient disease. *Infectious Diseases in Clinical Practice.* Aug 2000;9(6):228-235.
49. Grumelli C, Verderio C, Pozzi D, Rossetto O, Montecucco C, Matteoli M. Internalization and mechanism of action of clostridial toxins in neurons. *Neurotoxicology.* Oct 2005;26(5):761-767.
50. Li L, Singh BR. Structure-function relationship of clostridial neurotoxins. *Journal of Toxicology-Toxin Reviews.* 1999;18(1):95-112.

51. Arnon SS. Botulinum toxin as a biological weapon: Medical and public health management (vol 285, pg 1059, 2001). *Jama-Journal of the American Medical Association.* Apr 25 2001;285(16):2081-2081.
52. Brunger AT, Jin R, Breidenbach MA. Highly specific interactions between botulinum neurotoxins and synaptic vesicle proteins. *Cellular and Molecular Life Sciences.* Aug 2008;65(15):2296-2306.
53. Shukla HD, Sharma SK. Clostridium botulinum: A bug with beauty and weapon. *Critical Reviews in Microbiology.* 2005;31(1):11-18.
54. Dong M, Liu HS, Tepp WH, Johnson EA, Janz R, Chapman ER. Glycosylated SV2A and SV2B Mediate the Entry of Botulinum Neurotoxin E into Neurons. *Molecular Biology of the Cell.* Dec 2008;19(12):5226-5237.
55. Dong M, Yeh F, Tepp WH, et al. SV2 is the protein receptor for botulinum neurotoxin A. *Science.* Apr 28 2006;312(5773):592-596.
56. Cai SW, Kukreja R, Shoesmith S, Chang TW, Singh BR. Botulinum neurotoxin light chain refolds at endosomal pH for its translocation. *Protein Journal.* Dec 2006;25(7-8):455-462.
57. Veit M, Sollner TH, Rothman JE. Multiple palmitoylation of synaptotagmin and the t-SNARE SNAP-25. *Febs Letters.* Apr 29 1996;385(1-2):119-123.
58. Hess DT, Slater TM, Wilson MC, Skene JHP. The 25 Kda Synaptosomal-Associated Protein Snap-25 Is the Major Methionine-Rich Polypeptide in Rapid Axonal-Transport and a Major Substrate for Palmitoylation in Adult Cns. *Journal of Neuroscience.* Dec 1992;12(12):4634-4641.
59. Sudhof TC, Rothman JE. Membrane Fusion: Grappling with SNARE and SM Proteins. *Science.* Jan 23 2009;323(5913):474-477.
60. Fasshauer D, Bruns D, Shen B, Jahn R, Brunger AT. A structural change occurs upon binding of syntaxin to SNAP-25. *Journal of Biological Chemistry.* Feb 14 1997;272(7):4582-4590.
61. Fiebig KM, Rice LM, Pollock E, Brunger AT. Folding intermediates of SNARE complex assembly. *Nature Structural Biology.* Feb 1999;6(2):117-123.
62. Hazzard J, Sudhof TC, Rizo J. NMR analysis of the structure of synaptobrevin and of its interaction with syntaxin. *Journal of Biomolecular Nmr.* Jul 1999;14(3):203-207.
63. Sutton RB, Fasshauer D, Jahn R, Brunger AT. Crystal structure of a SNARE complex involved in synaptic exocytosis at 2.4 angstrom resolution. *Nature.* Sep 24 1998;395(6700):347-353.
64. Ossig R, Schmitt HD, de Groot B, et al. Exocytosis requires asymmetry in the central layer of the SNARE complex. *Embo Journal.* Nov 15 2000;19(22):6000-6010.
65. Fasshauer D. Structural insights into the SNARE mechanism. *Biochimica Et Biophysica Acta-Molecular Cell Research.* Aug 18 2003;1641(2-3):87-97.
66. Lacy DB, Tepp W, Cohen AC, DasGupta BR, Stevens RC. Crystal structure of botulinum neuro-toxin type A and implications for toxicity. *Nature Structural Biology.* Oct 1998;5(10):898-902.
67. Agarwal R, Eswaramoorthy S, Kumaran D, Binz T, Swaminathan S. Structural analysis of botulinum neurotoxin type E catalytic domain and its mutant Glu212 -

> Gln reveals the pivotal role of the Glu212 carboxylate in the catalytic pathway. *Biochemistry.* Jun 1 2004;43(21):6637-6644.
68. Schmidt JJ, Bostian KA. Endoproteinase activity of type A botulinum neurotoxin: Substrate requirements and activation by serum albumin. *Journal of Protein Chemistry.* Jan 1997;16(1):19-26.
69. Foran P, Shone CC, Dolly JO. Differences in the Protease Activities of Tetanus and Botulinum-B Toxins Revealed by the Cleavage of Vesicle-Associated Membrane-Protein and Various Sized Fragments. *Biochemistry.* Dec 27 1994;33(51):15365-15374.
70. Schmidt JJ, Bostian KA. Proteolysis of synthetic peptides by type A botulinum neurotoxin. *Journal of Protein Chemistry.* Nov 1995;14(8):703-708.
71. Washbourne P, Pellizzari R, Baldini G, Wilson MC, Montecucco C. Botulinum neurotoxin types A and E require the SNARE motif in SNAP-25 for proteolysis. *Febs Letters.* 1997;418(1-2):1-5.
72. Vaidyanathan VV, Yoshino K, Jahnz M, et al. Proteolysis of SNAP-25 isoforms by botulinum neurotoxin types A, C, and E: Domains and amino acid residues controlling the formation of enzyme-substrate complexes and cleavage. *Journal of Neurochemistry.* 1999;72(1):327-337.
73. Chai Q, Arndt JW, Dong M, et al. Structural basis of cell surface receptor recognition by botulinum neurotoxin B. *Nature.* Dec 21 2006;444(7122):1096-1100.
74. Schmidt JJ, Stafford RG. A high-affinity competitive inhibitor of type A botulinum neurotoxin protease activity. *Febs Letters.* Dec 18 2002;532(3):423-426.
75. Rupp B, Segelke B. Questions about the structure of the botulinum neurotoxin B light chain in complex with a target peptide. *Nature Structural Biology.* Aug 2001;8(8):663-664.
76. Chen S, Barbieri JT. Unique substrate recognition by botulinum neurotoxins serotypes A and E. *Journal of Biological Chemistry.* Apr 21 2006;281(16):10906-10911.
77. Chen S, Kim JJP, Barbieri JT. Mechanism of substrate recognition by botulinum neurotoxin serotype A. *Journal of Biological Chemistry.* Mar 30 2007;282(13):9621-9627.
78. Willis B, Eubanks LM, Dickerson TJ, Janda KD. The Strange Case of the Botulinum Neurotoxin: Using Chemistry and Bilogy to Modulate the Most Deadly Poison. *Angewandte Chemie-International Edition.* 2008;47(44):8360-8379.
79. Eubanks LM, Hixon MS, Jin W, et al. An in vitro and in vivo disconnect uncovered through high-throughput identification of botulinum neurotoxin A antagonists. *Proceedings of the National Academy of Sciences of the United States of America.* Feb 20 2007;104(8):2602-2607.
80. Kostrzewa RM, Segura-Aguilar J. Botulinum neurotoxin: Evolution from poison, to research tool - Onto medicinal therapeutic and future pharmaceutical panacea. *Neurotoxicity Research.* Dec 2007;12(4):275-290.
81. Schulte-Mattler WJ. Use of botulinum toxin A in adult neurological disorders - Efficacy, tolerability and safety. *Cns Drugs.* 2008;22(9):725-738.

82. Gui D, Rossi S, Runfola M, Magalini SC. Review article: Botulinum toxin in the therapy of gastrointestinal motility disorders. *Alimentary Pharmacology & Therapeutics.* Jul 2003;18(1):1-16.
83. Eccleston KJ, Woolley PD. Botulinum toxin for urogenital conditions. *International Journal of Std & Aids.* Dec 2008;19(12):797-799.
84. Daniel F, De Parades V, Siproudhis L, Atienza P. Botulinum toxin and chronic anal fissure. *Gastroenterologie Clinique Et Biologique.* May 2006;30(5):687-695.
85. Munchau A, Bhatia KP. Regular review - Uses of botulinum toxin injection in medicine today. *British Medical Journal.* Jan 15 2000;320(7228):161-165.
86. Kuhnel TS, Schulte-Mattler W, Bigalke H, Wohlfarth K. Treatment of habitual snoring with botulinum toxin: a pilot study. *Sleep and Breathing.* Feb 2008;12(1):63-68.
87. Ashkenazi A, Silberstein S. Is Botulinum Toxin Useful in Treating Headache? Yes. *Current Treatment Options in Neurology.* Jan 2009;11(1):18-23.
88. Roche N, Schnitzler A, Genet F, Durand MR, Bensmail D. Undesirable Distant Effects Following Botulinum Toxin Type A Injection. *Clinical Neuropharmacology.* Sep-Oct 2008;31(5):272-280.
89. Howell K, Selber P, Graham HK, Reddihough D. Botulinum neurotoxin A: An unusual systemic effect. *Journal of Paediatrics and Child Health.* Jun 2007;43(6):499-501.
90. Royal MA, Pappert EJ, Leong MS. A review of adverse events associated with botulinum toxin type B (Myobloc (R)). *Neurology.* Mar 14 2006;66(5):291-291.
91. Eubanks LM, Dickerson TJ. Investigating novel therapeutic targets and molecular mechanisms to treat botulinum neurotoxin A intoxication. *Future Microbiology.* Dec 2007;2(6):677-687.
92. McAllister LA, Hixon MS, Kennedy JP, Dickerson TJ, Janda KD. Superactivation of the botulinum neurotoxin serotype a light chain metalloprotease: A new wrinkle in botulinum neurotoxin. *Journal of the American Chemical Society.* Apr 5 2006;128(13):4176-4177.
93. Arnon SS, Schechter R, Maslanka SE, Jewell NP, Hatheway CL. Human botulism immune globulin for the treatment of infant botulism. *New England Journal of Medicine.* Feb 2 2006;354(5):462-471.
94. Bigalke H, Rummel A. Medical aspects of toxin weapons. *Toxicology.* Oct 30 2005;214(3):210-220.
95. Sobel J, Tucker N, Sulka A, McLaughlin J, Maslanka S. Foodborne botulism in the United States, 1990-2000. *Emerging Infectious Diseases.* Sep 2004;10(9):1606-1611.
96. Singh BR. Intimate details of the most poisonous poison. *Nature Structural Biology.* Aug 2000;7(8):617-619.
97. Schantz EJ, Johnson EA. Properties and Use of Botulinum Toxin and Other Microbial Neurotoxins in Medicine. *Microbiological Reviews.* Mar 1992;56(1):80-99.
98. Tonello F, Seveso M, Marin O, Mock M, Montecucco C. Pharmacology - Screening inhibitors of anthrax lethal factor. *Nature.* Jul 25 2002;418(6896):386-386.

99. Schwarze SR, Hruska KA, Dowdy SF. Protein transduction: unrestricted delivery into all cells? *Trends in Cell Biology.* Jul 2000;10(7):290-295.
100. Lee LV, Bower KE, Liang FS, et al. Inhibition of the proteolytic activity of anthrax lethal factor by aminoglycosides. *Journal of the American Chemical Society.* Apr 21 2004;126(15):4774-4775.
101. Fridman M, Belakhov V, Lee LV, Liang FS, Wong CH, Baasov T. Dual effect of synthetic aminoglycosides: Antibacterial activity against Bacillus anthracis and inhibition of anthrax lethal factor. *Angewandte Chemie-International Edition.* 2005;44(3):447-452.
102. Jiao GS, Cregar L, Goldman ME, Millis SZ, Tang C. Guanidinylated 2,5-dideoxystreptamine derivatives as anthrax lethal factor inhibitors. *Bioorganic & Medicinal Chemistry Letters.* Mar 15 2006;16(6):1527-1531.
103. Panchal RG, Hermone AR, Nguyen TL, et al. Identification of small molecule inhibitors of anthrax lethal factor. *Nature Structural & Molecular Biology.* Jan 2004;11(1):67-72.
104. Grobelny D, Poncz L, Galardy RE. Inhibition of Human Skin Fibroblast Collagenase, Thermolysin, and Pseudomonas-Aeruginosa Elastase by Peptide Hydroxamic Acids. *Biochemistry.* Aug 11 1992;31(31):7152-7154.
105. Kocer SS, Walker SG, Zerler B, Golub LM, Simon SR. Metalloproteinase inhibitors, nonantimicrobial chemically modified tetracyclines, and Ilomastat block Bacillus anthracis lethal factor activity in viable cells. *Infection and Immunity.* Nov 2005;73(11):7548-7557.
106. Schepetkin IA, Khlebnikov AI, Kirpotina LN, Quinn MT. Novel small-molecule inhibitors of anthrax lethal factor identified by high-throughput screening. *Journal of Medicinal Chemistry.* Aug 24 2006;49(17):5232-5244.
107. Dell'Aica I, Dona M, Tonello F, et al. Potent inhibitors of anthrax lethal factor from green tea. *Embo Reports.* Apr 2004;5(4):418-422.
108. Xiong YS, Wiltsie J, Woods A, et al. The discovery of a potent and selective lethal factor inhibitor for adjunct therapy of anthrax infection. *Bioorganic & Medicinal Chemistry Letters.* Feb 15 2006;16(4):964-968.
109. Shoop WL, Xiong Y, Wiltsie J, et al. Anthrax lethal factor inhibition. *Proceedings of the National Academy of Sciences of the United States of America.* May 31 2005;102(22):7958-7963.
110. Min DH, Tang WJ, Mrksich M. Chemical screening by mass spectrometry to identify inhibitors of anthrax lethal factor. *Nature Biotechnology.* Jun 2004;22(6):717-723.
111. Forino M, Johnson S, Wong TY, et al. Efficient synthetic inhibitors of anthrax lethal factor. *Proceedings of the National Academy of Sciences of the United States of America.* Jul 5 2005;102(27):9499-9504.
112. Johnson SL, Jung D, Forino M, et al. Anthrax lethal factor protease inhibitors: Synthesis, SAR, and structure-based 3D QSAR studies. *Journal of Medicinal Chemistry.* Jan 12 2006;49(1):27-30.
113. Johnson SL, Chen LH, Pellecchia M. A high-throughput screening approach to anthrax lethal factor inhibition. *Bioorganic Chemistry.* Aug 2007;35(4):306-312.
114. Gaddis BD, Avramova LV, Chmielewski J. Inhibitors of anthrax lethal factor. *Bioorganic & Medicinal Chemistry Letters.* Aug 15 2007;17(16):4575-4578.

115. Gaddis BD, Perez CMR, Chmielewski J. Inhibitors of anthrax lethal factor based upon N-oleoyldopamine. *Bioorganic & Medicinal Chemistry Letters.* Apr 1 2008;18(7):2467-2470.
116. Boldt GE, Kennedy JP, Hixon MS, et al. Synthesis, characterization and development of a high-throughput methodology for the discovery of botulinum neurotoxin A inhibitors. *Journal of Combinatorial Chemistry.* 2006;8(4):513-521.
117. Blommel PG, Fox BG. Fluorescence anisotropy assay for proteolysis of specifically labeled fusion proteins. *Analytical Biochemistry.* 2005;336(1):75-86.
118. Barr JR, Moura H, Boyer AE, et al. Botulinum neurotoxin detection and differentiation by mass spectrometry. *Emerging Infectious Diseases.* Oct 2005;11(10):1578-1583.
119. Schmidt JJ, Stafford RG, Bostian KA. Type A botulinum neurotoxin proteolytic activity: development of competitive inhibitors and implications for substrate specificity at the S-1 ' binding subsite. *Febs Letters.* Sep 11 1998;435(1):61-64.
120. Kumaran D, Rawat R, Ludivico ML, Ahmed SA, Swaminathan S. Structure- and substrate-based inhibitor design for Clostridium botulinum neurotoxin serotype A. *Journal of Biological Chemistry.* Jul 4 2008;283(27):18883-18891.
121. Boldt GE, Kennedy JP, Janda KD. Identification of a potent botulinum neurotoxin a protease inhibitor using in situ lead identification chemistry. *Organic Letters.* Apr 13 2006;8(8):1729-1732.
122. Park JG, Sill PC, Makiyi EF, et al. Serotype-selective, small-molecule inhibitors of the zinc endopeptidase of botulinum neurotoxin serotype A. *Bioorganic & Medicinal Chemistry.* Jan 15 2006;14(2):395-408.
123. Tang J. Computer-aided lead optimization: Improved small-molecule inhibitor of the zinc endopeptidase of botulinum neurotoxin serotype A. *PLoS ONE.* 2007;2(E761).
124. Burnett JC, Ruthel G, Stegmann CM, et al. Inhibition of metalloprotease botulinum serotype A from a pseudo-peptide binding mode to a small molecule that is active in primary neurons. *Journal of Biological Chemistry.* Feb 16 2007;282(7):5004-5014.
125. Hines HB, Kim AD, Stafford RG, et al. Use of a recombinant fluorescent substrate with cleavage sites for all botulinum neurotoxins in high-throughput screening of natural product extracts for inhibitors of serotypes A, B, and E. *Applied and Environmental Microbiology.* 2008;74(3):653-659.
126. Johnson SL, Chen LH, Harbach R, et al. Rhodanine derivatives as selective protease inhibitors against bacterial toxins. *Chemical Biology & Drug Design.* Feb 2008;71(2):131-139.
127. Saunders MJ, Kim H, Woods TA, et al. Microsphere-based protease assays and screening application for lethal factor and factor Xa. *Cytometry A.* May 2006;69(5):342-352.
128. Vitale G, Pellizzari R, Recchi C, Napolitani G, Mock M, Montecucco C. Anthrax lethal factor cleaves the N-terminus of MAPKKs and induces tyrosine/threonine phosphorylation of MAPKs in cultured macrophages. *Biochemical and Biophysical Research Communications.* Jul 30 1998;248(3):706-711.

129. Rossetto O, Deloye F, Poulain B, Pellizzari R, Schiavo G, Montecucco C. The Metalloproteinase Activity of Tetanus and Botulism Neurotoxins. *Journal of Physiology-Paris.* 1995;89(1):43-50.
130. Montecucco C, Tonello F, Zanotti G. Stop the killer: how to inhibit the anthrax lethal factor metalloprotease. *Trends in Biochemical Sciences.* Jun 2004;29(6):282-285.
131. Rivera VR, Merill GA, White JA, Poli MA. An enzymatic electrochemiluminescence assay for the lethal factor of anthrax. *Analytical Biochemistry.* Oct 1 2003;321(1):125-130.
132. Kim J, Choi MK, Koo BS, Yoon MY. Development of high-throughput assay of lethal factor using native substrate. *Analytical Biochemistry.* Jun 1 2005;341(1):33-39.
133. Holmes EW, Fareed J, Bermes EW. Automation of Plasma Anti-Thrombin-Iii Assays. *Clinical Chemistry.* 1981;27(6):816-818.
134. Gutierrez OA, Salas E, Hernandez Y, et al. An immunoenzymatic solid-phase assay for quantitative determination of HIV-1 protease activity. *Analytical Biochemistry.* Aug 1 2002;307(1):18-24.
135. Cook ND. Scintillation proximity assay: A versatile high-throughput screening technology. *Drug Discovery Today.* Jul 1996;1(7):287-294.
136. Hirata J, Ariese F, Gooijer C, Irth H. Continuous-flow protease assay based on fluorescence resonance energy transfer. *Analytica Chimica Acta.* Feb 12 2003;478(1):1-10.
137. Deo SK, Lewis JD, Daunert S. Bioluminescence detection of proteolytic bond cleavage by using recombinant aequorin. *Analytical Biochemistry.* May 15 2000;281(1):87-94.
138. Gauglitz G. Optical detection methods for combinatorial libraries. *Current Opinion in Chemical Biology.* Jun 2000;4(3):351-355.
139. StPierre Y, Desrosiers M, Tremblay P, Esteve PO, Opdenakker G. Flow cytometric analysis of gelatinase B (MMP-9) activity using immobilized fluorescent substrate on microspheres. *Cytometry.* Dec 1 1996;25(4):374-380.
140. Sklar LA, Edwards BS, Graves SW, Nolan JP, Prossnitz ER. Flow cytometric analysis of ligand-receptor interactions and molecular assemblies. *Annual Review of Biophysics and Biomolecular Structure.* 2002;31:97-119.
141. Kuckuck FW, Edwards BS, Sklar LA. High throughput flow cytometry. *Cytometry.* 2001;44(1):83-90.
142. Ramirez S, Aiken CT, Andrzejewski B, Sklar LA, Edwards BS. High-throughput flow cytometry: Validation in microvolume bioassays. *Cytometry Part A.* May 2003;53A(1):55-65.
143. Lauer SA, Nolan JP. Development and characterization of Ni-NTA-bearing microspheres. *Cytometry.* Jul 1 2002;48(3):136-145.
144. Gill SC, Vonhippel PH. Calculation of Protein Extinction Coefficients from Amino-Acid Sequence Data. *Analytical Biochemistry.* Nov 1 1989;182(2):319-326.
145. Mock M, Roques BP. Progress in rapid screening of Bacillus anthracis lethal factor activity. *Proceedings of the National Academy of Sciences of the United States of America.* May 14 2002;99(10):6527-6529.

146. Graves SW, Woods TA, Kim H, Nolan JP. Direct fluorescent staining and analysis of proteins on microspheres using CBQCA. *Cytometry Part A.* 2005;65A(1):50-58.
147. Hoffman RA. Standardization and quantitation in flow cytometry. *Methods in Cell Biology, Vol 63.* 2001;63:299-340.
148. Kim J, Kim YM, Koo BS, Chae YK, Yoon MY. Production and proteolytic assay of lethal factor from Bacillus anthracis. *Protein Expression and Purification.* Aug 2003;30(2):293-300.
149. Frank G, Qiu JZ, Somsouk M, et al. Partial functional deficiency of E160D flap endonuclease-1 mutant in vitro and in vivo is due to defective cleavage of DNA substrates. *Journal of Biological Chemistry.* Dec 4 1998;273(49):33064-33072.
150. Tonello F, Ascenzi P, Montecucco C. The metalloproteolytic activity of the anthrax lethal factor is substrate-inhibited. *Journal of Biological Chemistry.* Oct 10 2003;278(41):40075-40078.
151. Barth H, Aktories K, Popoff MR, Stiles BG. Binary bacterial toxins: Biochemistry, biology, and applications of common Clostridium and Bacillus proteins. *Microbiology and Molecular Biology Reviews.* Sep 2004;68(3):373-+.
152. Graves SW, Nolan JP, Jett JH, Martin JC, Sklar LA. Nozzle design parameters and their effects on rapid sample delivery in flow cytometry. *Cytometry.* Feb 1 2002;47(2):127-137.
153. Graves SW, Habbersett RC, Nolan JP. A dynamic inline sample thermoregulation unit for flow cytometry. *Cytometry.* Jan 1 2001;43(1):23-30.
154. Cruz-Munoz W, Khokha R. The role of tissue inhibitors of metalloproteinases in tumorigenesis and metastasis. *Critical Reviews in Clinical Laboratory Sciences.* 2008;45(3):291-338.
155. Johnson EA. Clostridial toxins as therapeutic agents: Benefits of nature's most toxic proteins. *Annual Review of Microbiology.* 1999;53:551-+.
156. Breidenbach MA, Brunger AT. New insights into clostridial neurotoxin-SNARE interactions. *Trends in Molecular Medicine.* 2005;11(8):377-381.
157. Nagase H, Woessner JF, Jr. Matrix metalloproteinases. *J Biol Chem.* Jul 30 1999;274(31):21491-21494.
158. Hase CC, Finkelstein RA. Bacterial extracellular zinc-containing metalloproteases. *Microbiol Rev.* Dec 1993;57(4):823-837.
159. Edwards BS, Kuckuck FW, Prossnitz ER, Ransom JT, Sklar LA. HTPS flow cytometry: A novel platform for automated high throughput drug discovery and characterization. *Journal of Biomolecular Screening.* 2001;6(2):83-90.
160. Nikawa T, Schuch G, Wagner G, Sies H. Interaction of Ebselen with Glutathione-S-Transferase and Papain in-Vitro. *Biochemical Pharmacology.* Mar 15 1994;47(6):1007-1012.
161. Eubanks LM, Hixon MS, Jin W, et al. An in vitro and in vivo disconnect uncovered through high-throughput identification of botulinum neurotoxin A antagonists (vol 104, pg 2602, 2007). *Proceedings of the National Academy of Sciences of the United States of America.* Apr 10 2007;104(15):6490-6490.
162. Bubolz AH, Wu QP, Larsen BT, Gutterman DD, Liu YP. Ebselen reduces nitration and restores voltage-gated potassium channel function in small coronary

arteries of diabetic rats. *American Journal of Physiology-Heart and Circulatory Physiology.* Oct 2007;293(4):H2231-H2237.
163. Schewe T. Molecular Actions of Ebselen - an Antiinflammatory Antioxidant. *General Pharmacology.* Oct 1995;26(6):1153-1169.
164. Takasago T, Peters EE, Graham DI, Masayasu H, Macrae IM. Neuroprotective efficacy of ebselen, an anti-oxidant with antiinflammatory actions, in a rodent model of permanent middle cerebral artery occlusion. *British Journal of Pharmacology.* Nov 1997;122(6):1251-1256.
165. Tunc T, Uysal B, Atabek C, et al. Erdosteine and Ebselen As Useful Agents in Intestinal Ischemia/Reperfusion Injury. *Journal of Surgical Research.* Aug 2009;155(2):210-216.
166. Billack B, Santoro M, Lau-Cam C. Growth Inhibitory Action of Ebselen on Fluconazole-Resistant Candida albicans: Role of the Plasma Membrane H+-ATPase. *Microbial Drug Resistance.* Jun 2009;15(2):77-83.
167. Pietka-Ottlik M, Wojtowicz-Mlociiowska H, Kolodziejczyk K, Piasecki E, Mlochowski J. New organoselenium compounds active against pathogenic bacteria, fungi and viruses. *Chemical & Pharmaceutical Bulletin.* Oct 2008;56(10):1423-1427.
168. Sakurai T, Kanayama M, Shibata T, et al. Ebselen, a seleno-organic antioxidant, as an electrophile (vol 19, pg 1196, 2006). *Chemical Research in Toxicology.* Nov 20 2006;19(11):1557-1557.
169. Handa Y, Kaneko M, Takeuchi H, Tsuchida A, Kobayashi H, Kubota T. Effect of an antioxidant, ebselen, on development of chronic cerebral vasospasm after subarachnoid hemorrhage in primates. *Surg Neurol.* Apr 2000;53(4):323-329.
170. Gupta P, Batra S, Chopra AP, Singh Y, Bhatnagar R. Expression and purification of the recombinant lethal factor of Bacillus anthracis. *Infection and Immunity.* Feb 1998;66(2):862-865.
171. Houghten RA, Pinilla C, Giulianotti MA, et al. Strategies for the use of mixture-based synthetic combinatorial libraries: Scaffold ranking, direct testing, in vivo, and enhanced deconvolution by computational methods. *Journal of Combinatorial Chemistry.* Jan-Feb 2008;10(1):3-19.
172. Copeland RA. *Enzymes : a practical introduction to structure, mechanism, and data analysis*. 2nd ed. New York: Wiley; 2000.
173. Patel SS, Wong I, Johnson KA. Pre-Steady-State Kinetic-Analysis of Processive DNA-Replication Including Complete Characterization of an Exonuclease-Deficient Mutant. *Biochemistry.* Jan 15 1991;30(2):511-525.
174. Dong M, Tepp WH, Johnson EA, Chapman ER. Using fluorescent sensors to detect botulinum neurotoxin activity in vitro and in living cells. *Molecular Biology of the Cell.* Nov 2004;15:103a-103a.
175. Dong M, Richards DA, Goodnough MC, Tepp WH, Johnson EA, Chapman ER. Synaptotagmins I and II mediate entry of botulinum neurotoxin B into cells. *Journal of Cell Biology.* Sep 29 2003;162(7):1293-1303.
176. Larsen KS, Auld DS. Characterization of an Inhibitory Metal-Binding Site in Carboxypeptidase-A. *Biochemistry.* Mar 12 1991;30(10):2613-2618.
177. Drews J. Drug discovery: A historical perspective. *Science.* Mar 17 2000;287(5460):1960-1964.

178. Liotta LA, Tryggvason K, Garbisa S, Hart I, Foltz CM, Shafie S. Metastatic Potential Correlates with Enzymatic Degradation of Basement-Membrane Collagen. *Nature.* 1980;284(5751):67-68.
179. Stetler-Stevenson WG. The tumor microenvironment: regulation by MMP-independent effects of tissue inhibitor of metalloproteinases-2. *Cancer and Metastasis Reviews.* Mar 2008;27(1):57-66.
180. McCawley LJ, Matrisian LM. Matrix metalloproteinases: they're not just for matrix anymore! *Current Opinion in Cell Biology.* Oct 2001;13(5):534-540.
181. Parks WC, Wilson CL, Lopez-Boado YS. Matrix metalloproteinases as modulators of inflammation and innate immunity. *Nature Reviews Immunology.* Aug 2004;4(8):617-629.
182. Minn AJ, Gupta GP, Siegel PM, et al. Genes that mediate breast cancer metastasis to lung. *Nature.* Jul 28 2005;436(7050):518-524.
183. Murray GI, Duncan ME, ONeil P, Melvin WT, Fothergill JE. Matrix metalloproteinase-1 is associated with poor prognosis in colorectal cancer. *Nature Medicine.* Apr 1996;2(4):461-462.
184. McQuibban GA, Gong JH, Wong JR, Wallace JL, Clark-Lewis I, Overall CM. Matrix metalloproteinase processing of monocyte chemoattractant proteins generates CC chemokine receptor antagonists with anti-inflammatory properties in vivo. *Blood.* Aug 15 2002;100(4):1160-1167.
185. Crawford HC, Scoggins CR, Washington MK, Matrisian LM, Leach SD. Matrix metalloproteinase-7 is expressed by pancreatic cancer precursors and regulates acinar-to-ductal metaplasia in exocrine pancreas. *Journal of Clinical Investigation.* Jun 2002;109(11):1437-1444.
186. Fingleton B, Vargo-Gogola T, Crawford HC, Matrisian LM. Matrilysin [MMP-7] expression selects for cells with reduced sensitivity to apoptosis. *Neoplasia.* Nov-Dec 2001;3(6):459-468.
187. McCawley LJ, Crawford HC, King LE, Mudgett J, Matrisian LM. A protective role for matrix metalloproteinase-3 in squamous cell carcinoma. *Cancer Research.* Oct 1 2004;64(19):6965-6972.
188. Yang W, Arii S, Gorrin-Rivas MJ, Mori A, Onodera H, Imamura M. Human macrophage metalloelastase gene expression in colorectal carcinoma and its clinicopathologic significance. *Cancer.* Apr 1 2001;91(7):1277-1283.
189. Moss ML, White JM, Lambert MH, Andrews RC. TACE and other ADAM proteases as targets for drug discovery. *Drug Discovery Today.* Apr 15 2001;6(8):417-426.
190. Mohan MJ, Seaton T, Mitchell J, et al. The tumor necrosis factor-alpha converting enzyme (TACE): A unique metalloproteinase with highly defined substrate selectivity. *Biochemistry.* Jul 30 2002;41(30):9462-9469.
191. Vassar R. Caspase-3 cleavage of GGA3 stabilizes BACE: Implications for Alzheimer's disease. *Neuron.* Jun 7 2007;54(5):671-673.
192. Vassar R. beta-Secretase (BACE) as a drug target for alzheimer's disease. *Advanced Drug Delivery Reviews.* Dec 7 2002;54(12):1589-1602.
193. Hsu JTA, Wang HC, Chen GW, Shih SR. Antiviral drug discovery targeting to viral proteases. *Current Pharmaceutical Design.* 2006;12(11):1301-1314.

194. Dougherty WG, Semler BL. Expression of Virus-Encoded Proteinases - Functional and Structural Similarities with Cellular Enzymes. *Microbiological Reviews.* Dec 1993;57(4):781-822.
195. Ryan MD, Flint M. Virus-encoded proteinases of the picornavirus super-group. *Journal of General Virology.* Apr 1997;78:699-723.
196. Lamarre D, Anderson PC, Bailey M, et al. An NS3 protease inhibitor with antiviral effects in humans infected with hepatitis C virus (vol 426, pg 186, 2003). *Nature.* Nov 20 2003;426(6964):314-314.
197. Schatz PJ. Use of Peptide Libraries to Map the Substrate-Specificity of a Peptide-Modifying Enzyme - a 13 Residue Consensus Peptide Specifies Biotinylation in Escherichia-Coli. *Bio-Technology.* Oct 1993;11(10):1138-1143.